UNIVERSITY OF CALIFORNIA, SAN DIEGO

Insitu Expanding Foam Based Carbon/Epoxy Sandwich Jackets for Column Retrofit

A thesis submitted in partial satisfaction of the requirements
for the degree Master of Science

in

Structural Engineering

by

Alicia Danyeur

Committee in charge:

Professor Vistasp Karbhari, Chair
Professor Yu Qiao
Professor Chia-Ming Uang

2008

The thesis of Alicia Danyeur is approved and it is acceptable in quality and form for publication on microfilm and electronically:

_____

_____

_____

Chair

University of California, San Diego

2008

Table of Contents

List of Symbols

b = width of section

c = neutral axis of section

d = effective depth of member

d_{bl} = diameter of column reinforcement

f'_c = compressive strength of concrete

f'_{cc} = confined concrete strength

f_l = lateral clamping pressure

f_y = yield strength of column reinforcement

f_{uj} = ultimate composite tensile strength of column jacketing system

g = dimension of the gap between the retrofit jacket to the supporting member

t_j = thickness of composite jacket

A = area of cross section

A_s = area of reinforcement

D = diameter of column

E = modulus of elasticity for the non-retrofitted element

E_j = modulus of elasticity for the composite jacketing system

Ie = effective moment of inertia for a cracked concrete section = 0.7 Ig

Ig = gross moment of inertia of a concrete section

L = clear length of column

L_p = length of plastic hinge region

M_y = allowable column moment at first yield

P = gravity point load on column

V_c = shear contribution of concrete

V_y = lateral load at theoretical column yielding

V_{yi} = lateral load at ideal column flexural strength

Δ_p = reference plastic displacement

Δ_y = reference yield displacement

ε_c = maximum concrete compression strain

ε_{cu} = ultimate concrete compression strain in conjunction with a composite jacketing system

ε_{uj} = ultimate composite jacketing strain

ϕ_p = plastic curvature = ϕ_u - ϕ_y

ϕ_y = curvature at first yield

ϕ_u = maximum curvature at probable post-yield

μ = ductility factor

μ_Δ = reference displacement ductility factor

μ_ϕ = reference curvature displacement factor

$\rho = A_s/(b*d)$ = reinforcement ratio

ρ_s = volumetric ratio of concrete confinement

List of Figures

List of Tables

Acknowledgements

I would like to acknowledge Professor Vistasp Karbhari for his support as the chair on my committee. His guidance and patience through this process led to the final completion of this thesis after a long delay.

I would like to acknowledge and thank the Merkel brothers for allowing me the opportunity to test their novel jacketing system as well as the Charles Lee Structural Laboratory staff for all their help and patience during construction and testing on the test columns.

I would also like to acknowledge my classmates and friends who pitched in and helped where they could to make the experience more enjoyable. To my best friend, Loni Hemmings, a special thank you for volunteering so much of your time, support and encouragement throughout the entire process - beginning to end.

ABSTRACT OF THE THESIS

Insitu Expanding Foam Based Carbon/Epoxy Sandwich Jackets for Column Retrofit

by

Alicia Danyeur

Master of Science in Structural Engineering

University of California, San Diego, 2008

Professor Vistasp Karbhari, Chair

With each seismic event, various degrees of damage are imparted to the quake area's superstructures. Concrete columns of these superstructures are often damaged or susceptible to collapse. Those columns exhibiting damage but still functioning under everyday use are structurally assessed. This evaluation considers the degree of remaining capacity the structure still maintains to carry future earthquake loading. Replacement or retrofitting the existing structure is the most common result once these evaluations have been undertaken. The following research consists of the application and testing of a new composite jacketing system proposed for use in this necessary retrofitting of damaged superstructures.

The Highway Innovative Technology Evaluation Center (HITEC) of the Civil Engineering Research Foundation (CERF) has instrumented a process in which composite jackets may be tested to determine their effectiveness as a retrofit option. Using these HITEC evaluation guidelines for "FPR Composite Wrap Durability Evaluation", testing was conducted to assess the response of a novel, fabric-expansive foam sandwich panel jacket. This involved the construction and testing of 6 concrete columns and a structural response model to evaluate the material and its behavior. The new system performed well on square shear, circular and square continuously reinforced flexure and the circular lap spliced reinforced flexure columns, but failed due to inadequate ductility increase on the square lap spliced column and unexpected failure mechanism in the circular shear column.

1. Seismic Retrofitting

1.1 Introduction

The use of fiber reinforced polymer (FRP) composite systems for the rehabilitation of civil structures has been shown to be an efficient option for renewal in a number of cases related to the aging and structurally deficient structural components and systems throughout the country. Due to the material's lightweight nature, high specific strength and specific stiffness, corrosion resistance and intrinsic adaptability, as well as its flexibility for application in the field, there has been increased use and further development of such systems, especially in the area of seismic retrofit.

With each seismic event, the vulnerability of the existing superstructures to catastrophic failures are increasingly recognized and acknowledged. The 1989 Loma Prieta and the 1994 Northridge earthquakes each exposed the inadequacies of design and construction procedures used in reinforced concrete columns with the occurrence of various modes of structural collapse. The need to resolve the structural deficiency of these lifeline elements has become vital. Replacement of each of these deficient superstructures with new construction would be extremely expensive and time intensive. In the light of the extreme lack of funds necessary to replace all deficient structural elements, retrofitting has become the economic solution of choice. To retrofit, according to the Merriam-Webster Dictionary, "is to furnish with new parts not available or considered unnecessary at the time of manufacturing" [1]. Consequently, understanding what is deficient with the existing superstructure construction is necessary to appropriately reduce the presented seismic risk by means of retrofitting.

The origin of support column inadequacies is rooted in the design practice of the civil engineering field prior to 1971. These insufficient design procedures were based on elastic design principles, which overestimated a column's stiffness and underestimated induced seismic deflections. When the 1971 San Fernando earthquake occurred and caused extensive damage,

common design practices were reviewed. In a research report submitted after the quake by Paul C. Jennings, one of the obvious support column deficiencies was reported. "...the extent of the failures in the central columns was aggravated by the inadequate ties. Only one of the lapped ties on Column 1 was found to have yielded and fractured. The other ties became ineffective when the concrete shell outside the reinforcement cage cracked and spalled" [2]. Figure 1-1 is the picture of the Column 1 noted in the quotation and Figure 1-2 and Figure 1-3 are additional pictures representing this failure type.

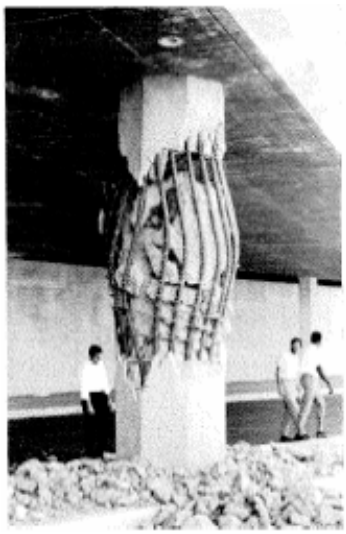

Figure 1-1: Foothill Freeway Column Failure [2]

Figure 1-2: Foothill Freeway Column Failure [2]

Figure 1-3: Foothill Freeway Column Failure [2]

From studying the failures caused by the 1971 San Fernando earthquake, improvements were made to the standard design codes upon the recommendation in report FHWA/RD-81/081 published by the Federal Highway Administration [3]. These design code changes incorporated the inelastic behavior of a column undergoing seismic loading, which is necessary for energy dissipation. This modification in the design approach reduced the occurrence of brittle failures observed in those columns calculated under the elastic design method. Revisions in the amount of column confinement ties and the length of vertical reinforcement lap splice were also

established based on the encountered column failures [4]. Examples of the failure types based on which codes were revised, to avoid continued deficiencies, are shown in Figure 1-4 and Figure 1-5.

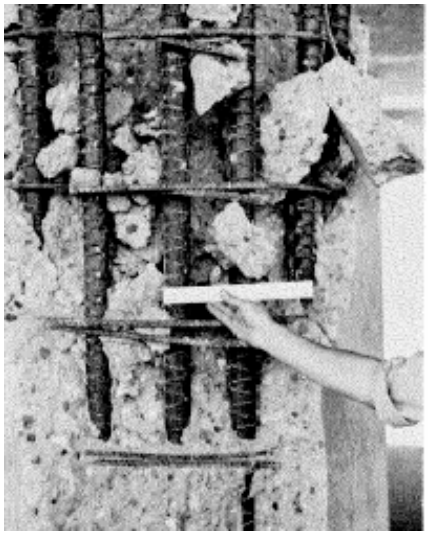

Figure 1-4: Failure Due to Inadequate Confinement Ties [2]

Figure 1-5: Failure Due to Inadequate Lap Splice Length [5]

Most of the subsequent column and superstructure failures experienced since the 1971 San Fernando quake have been on structures designed pre-1971 with the superseded design specifications. With the knowledge that these inadequately designed support columns are in service and lack the adequate confinement ties, lap splice length and ductility (ability to deform after initial yielding), the crucial retrofit regions can be properly addressed if strengthening is found to be necessary. Today though, bridge columns are often built integrally with the superstructure. This design approach allows engineers to rely on plastic hinging of a controlled region within the column to dissipate seismic energy. This is accomplished by good detailing and provision of sufficient shear or confinement reinforcement to increase ductility and to minimize seismic-related damage [6].

1.2 Need for Retrofit

The known existence of aging and inadequate superstructures have caused the formation of new design committees and created new legislation in many regions of high seismic activity in order to address the potential earthquake hazards. In the United States, The National Earthquake Hazards Reduction Program (NEHRP) is the governmental plan, which Congress established in 1977 under Public Law 95-124, The National Earthquake Hazard Reduction Act, acknowledging the seismic hazards present on a national scale [7]. This long-term program is intended to diminish the seismic risks to life and property throughout the United States. NEHRP is managed under the shared umbrella of the Federal Emergency Management Agency (FEMA), National Institute of Standards and Technology and the United States Geological Survey (USGS). According to the FEMA website, "nationwide, at least 39 states are considered at risk from moderate to great earthquakes. In fact, earthquakes have struck various areas of the United States, including Alaska and the Central and East Coast states "[7]. Figure 1-6 shows the level of seismic risk for the continental United States according to the USGS.

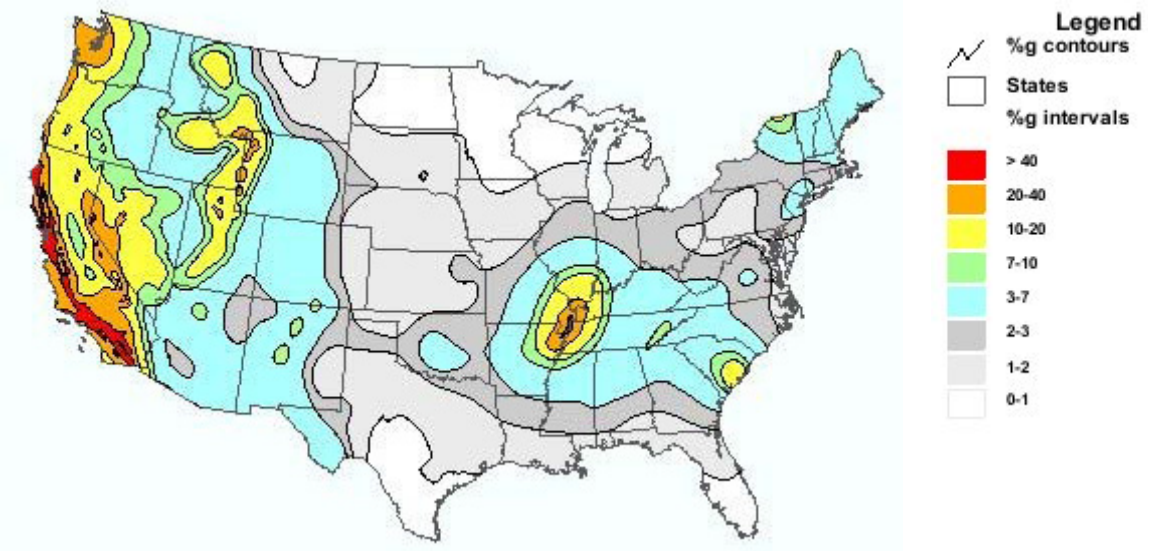

Figure 1-6: 2008 USGS National Seismic Hazard for the Continental United States [8]

Because of the prevalence of notable seismic activity in California, the data on the structural deficiencies of support systems have been more rigorous, and is readily available. This does not imply that other states are not at risk (as noted in the seismic hazard map in Figure 1-6), but that data and research has been more plentiful on structures in the state of California. This abundant data and research presented by Priestley, Seible, Innamorato, Hegemier, Chai, Reynaud, Karbhari, Pantelides, Gergelely, Tang, Lam and others has lead to numerous structural retrofit technologies implemented throughout the state [9][10][11][12][13][14][15][16]. This was partially initiated through the Seismic Safety Retrofit Program which was established in the state of California under emergency legislation SB 36X, after the 1989 Loma Prieta earthquake [17]. This act acknowledged the extent of deficient structural integrity of some of the state's superstructures and opened the door to determine the exact extent of these unsafe conditions. In the years since the program was initiated, over 1,200 publicly owned bridges in the state of California alone have been seismically retrofitted including the San Diego – Coronado, Carquinez, Benicia-Martinez, Richmond-San Raphael, and Vincent Thomas bridges. [18]

Even though the bulk of California's public superstructures high seismic hazards have been addressed, this does not eliminate all earthquake risk within the state. Today, many privately owned structures, such as parking garages and local and county bridges have a high probability for collapse if a seismic event were to occur. With the adoption of the FEMA 273 guidelines [7] as well as the regional California ATC 40 Guidelines [19] for seismic retrofit, a means for the private sector to adopt retrofit strengthening standards is presented.

The United States is not the only country to be proactively addressing the need for superstructure strengthening. Japan, Canada, New Zealand and various European and Middle Eastern countries are also establishing seismic strengthening protocols as well as actively researching retrofitting options. In a 2000 report by Kazuhiko Kawashima, a brief summary of the need for seismic strengthening, the design parameters, and existing applications of retrofit

procedures in Japan were presented. He states that "because of the unsatisfactory performance of highway bridges in the 1995 Hyogo-ken nanbu (Kobe) earthquake, the Japanese Design Specifications of Highway Bridges were revised in 1996" [20]. This has had a similar effect on the retrofit effort in Japan that the 1989 Loma Prieta had on efforts in California. After the Hyogo-ken nanbu earthquake, some 29,400 concrete column piers were retrofitted throughout Japan [20].

In Europe and Canada, code and publications are being produced to address the need for seismic retrofitting of existing structures with the European FIP: Management, maintenance and strengthening of concrete structures [21] and the Canadian Highway Bridge Design Code [22].

1.3 Retrofit Procedures

To date various retrofit methods have been developed and tested worldwide. Retrofit methods developed vary from base isolation to jackets used for confinement of concrete as a means of enhancing ductility. The following are brief summaries of the currently available retrofitting systems.

1.3.1 Base Isolation System

A non- passive approach to seismic retrofitting is the application of base isolation. This is not a strengthening option and has been used in large buildings and concrete superstructures such as bridges. In base isolation a "building or structure is decoupled from the horizontal components of the earthquake ground motion by interposing a layer with low horizontal stiffness between the structure and the foundation. The isolation system does not absorb the earthquake energy, but rather deflects it through the dynamics of the system" [23]. Figure 1-7 is a simple schematic for a concrete column base isolation system.

Base isolation is a very effective retrofit solution that typically only requires construction

at the base of a structure. Many historical buildings in the Northern California bay area such as Oakland City Hall have used base isolation technology for seismic upgrading. The relatively limited application is due to the small percentage of structures where base isolation is feasible. Among viability issues are the consideration of system location, the construction and installation sequence, need for temporary support and bracing of the structure, jacking methods, and the monitoring of settlements [23].

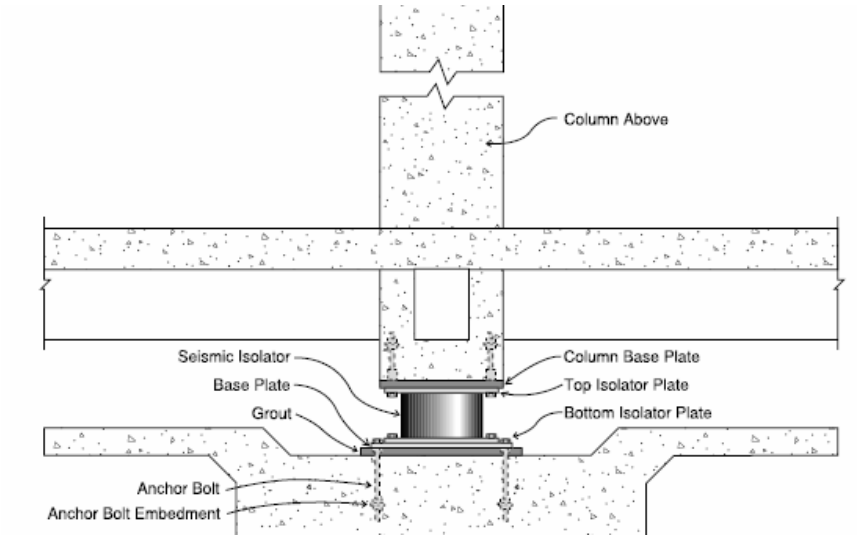

Figure 1-7: A Simple Base Isolator Assembly [24]

Base isolation has been used as well on multiple bridges such as the seismic retrofit of the suspended structure of the Vincent Thomas Bridge in Long Beach Harbor, California. Retrofit details introduced on the bridge included a viscous damper type of base isolators. A base isolation retrofit of the Golden Gate Bridge, North Viaduct in San Francisco, California was performed with lead-rubber isolation bearings. Viscous fluid damper type of base isolation was used to control uplift of the lift-span towers for the Sacramento River Bridge in Rio Vista. These are just a few of the ways base isolations retrofit systems have been implemented as a form of seismically upgrading existing structures [17].

1.3.2 Steel Jackets

The most referenced research with analysis concerning steel jacketing as a means of column retrofitting was compiled by Chai, Priestley and Seible [10]. Steel jacketing was found to be a very effective method of seismic retrofitting by increasing shear strength, flexural capacity and ductility of piers and columns. The procedure involves two half steel shell plates, 12.5 to 25 mm (0.5 to 1 inch) larger than the column radius, being positioned around the area to be retrofitted and subsequently the plates are site-welded together. The gap between the completed steel jacket and concrete column is then filled with concrete grout.

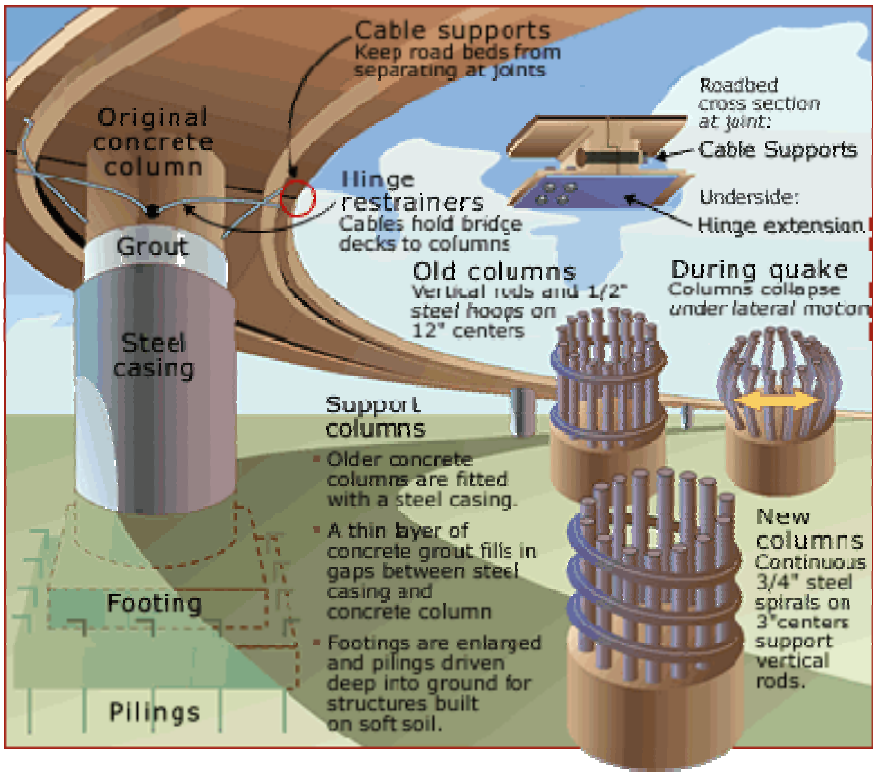

Figure 1-8: Diagram Illustrating Column Retrofit by Caltrans [25]

This steel jacketing retrofit system is designed to supply passive confinement as means of strengthening and the level of confinement depends on the hoop strength and stiffness of the steel jacket [25]. The lateral confining pressure is activated as the concrete attempts to expand laterally due to high axial compression strains. Therefore, the steel jacket does not theoretically function until the concrete column it encases beings to dilate by releasing lateral pressures it can no longer support into the surrounding jacket [10].

Figure 1-9: Welding of Steel Jacket for a Caltrans Strengthening Project [26]

Figure 1-10: Completed Steel Jacket Column Retrofit [27]

Steel jacket strengthening is not without its problems. Placement and construction of heavy steel plates is not simple. Welding the jacket seams together is a time intensive and costly procedure. The integrity of the seam welds is also a concern. Quality control of field welding is difficult to ensure and expensive to inspect but because the performance of the jacket is dependant on the quality of the welded connection, field assessment of weld quality during construction is necessary and critical. Figure 1-9 illustrates the scale of work for the welding of

the jacket's seams on a typical column. Once completed as in Figure 1-10, corrosion of the exposed steel also becomes an additional concern.

Construction and long term viability are not the only concerns when discussing steel jacketing. The impact the jacketing system has on the performance of the superstructure as a whole must be considered. The behavior of the bridge itself under a seismic event can be drastically altered due to the increase in stiffness the steel jacket has added to the retrofitted columns. Research has shown that a steel jacket retrofitted column exhibits a higher stiffness and an increase in lateral load carrying capacity with increasing displacement levels due to the isotropic nature of the steel. Both stiffness and capacity increases are not sought for in bridge columns retrofits since typically higher seismic force levels are transmitted to adjacent structural elements [18]. Analysis of additional structural elements may need to be reviewed beyond just analyzing deficient concrete columns because of this force transfer. This form of retrofit may cause problems areas in other structural components where none was present before column strengthening.

1.3.3 Concrete Jackets

Reinforced concrete jacketing is another option for seismic retrofit of substandard columns, especially when it is important to preserve the appearance and aesthetics of the columns. This option though, is only viable when increase in column size is acceptable since the concrete jacket option typically adds additional thickness to the original column than the other retrofitting options. Such concrete jacket retrofit measures aim to ensure stable flexural response by improving the capacity of non-ductile failure modes and by providing efficient confinement to the plastic hinge regions.

Concrete jacketing systems have the advantage of various application procedures. Traditional cast-in-place construction with reinforcing cages is one form of construction as well

as shotcrete application. In California, Caltrans has utilized shotcrete constructed concrete jackets (concrete mixture that is projected by a high velocity pressure spray to a surface) to encase an inadequate column with additional reinforcement. This is not the only method of strengthening with concrete, though. Figure 1-11 shows the installation of a pre-cast concrete shell jacket and Figure 1-12 displays the installation of a pour-in-place concrete jacket.

Figure 1-11: Installation of a Pre-Cast Concrete Shell Jacket [26]

Figure 1-12: Installation of Poured- in-Place Concrete Retrofit Jacket [29]

The concrete jacketing retrofit process has seen some level of use in the state of California. It has not been the primary means of retrofit when compared to the other alternatives, due to the additional surface area it adds to a retrofitted structure where clearances and tolerances are quite tight. The bond between the new and old concrete surfaces is also a concern in how well the retrofitted column will perform. As with steel jacketing, the increased stiffness of the overall structure also becomes a concern [10].

1.3.4 Fiber Reinforced Polymer Composite Jackets

Composite jacket systems are a modern advancement within retrofitting technology that has been aggressively researched and developed [9][10][11][12][13][14][15][16]. With the

numerous processing and application options with composite materials, FRP retrofit systems can vary from project to project. This is not a novel approach to strengthening deficient structures and is a viable option along side traditional materials and methods. The Federal Highway Administration, Caltrans and other states' department of transportation have adopted retrofit procedures and qualifications for composite strengthening systems. Some agencies have also prepared guidelines on design and application techniques for composite strengthening systems. Caltrans has released a design memo to designers for composite strengthening [30] and the American Concrete Institute (ACI) released ACI-440.2R-02: Design and Construction of Externally Bonded FRP Systems for Strengthening Concrete Structures which presented guidelines for composite retrofit design and construction [31].

Even though composite jacketing systems are common in the retrofit arena, there is still room for growth. Much of this is due to the variability within the fabric and adhesive components which comprise a composite system. Each component combination has its positive and negative aspects. Unlike traditional materials with limited application procedures and mechanical property variability, composites are more adaptable with variations in materials as well as processing procedures.

1.3.4.1 Composite Jacket Materials

Composite strengthening systems tend to be identified by their material components and processing type (i.e. carbon fiber reinforced epoxy with wet lay-up). Identifying the material components is critical due to the inherent framework of what makes a composite. A composite is an engineered material which consists of combining two or more constituent materials with considerably different physical or chemical properties and remains separate and distinct on a macroscopic level within the finished product [32]. The two categories of constituent materials

are matrix and reinforcement or filler. At least one component of each is required to form a composite material [32].

The matrix material surrounds and supports the reinforcing materials by keeping their relative positions. Most composites produced use a polymer matrix material often called a resin. There are many different types of polymers available with the most common being polyester, vinyl ester, epoxy, phenolic, polyimide, polyamide, and polypropylene. These resins have good mechanical properties and adhere well, both of which are important for seismic retrofitting application on civil structures [32].

The reinforcement material imparts its unique mechanical and physical properties to the composite to enhance the matrix. With regards to material variations, there are differences in reinforcement type. The reinforcement type can be a variety of materials such as glass, carbon and aramid.

Fiber architecture in a fabric, layer orientation and layer quantity, differ between system types as well [32]. Since the composites are non-homogenous, the resulting properties will be a combination of the properties of the constituent materials. Different types of loading may call for different components of the composite since the physical properties of the composite are generally not isotropic. This is a benefit of composite materials as they can be constructed to exhibit the best qualities from each of the constituents that neither constituent possesses singularly [32].

1.3.4.2 Composite Jacket Application Techniques

In order to increase speed of installation of column jackets, to reduce maintenance, and to improve durability, different types of advanced composite column jacketing systems have been researched and developed, ranging from hand lay-up of glass or carbon fabrics to winding of tow and adhesive bonding of pre-manufactured layered glass or carbon shell systems

[9][10][11][33][34]. These methods can generically be differentiated into six basic types: wet winding of tow, the use of wet lay-up procedure using fabric, automated winding of prepreg tow followed by curing of the composite wrap at elevated temperatures, the adhesive bonding of prefabricated shell segments, fabrication of the jacket using the resin infusion process, and the use of cables or prefabricated strips wound under tension around the column and anchored at ends [35].

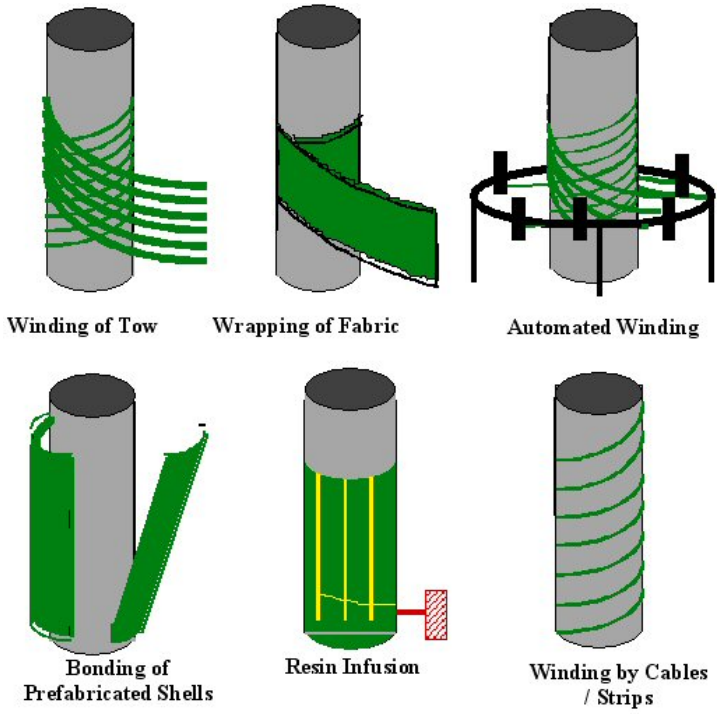

Figure 1-13: Types of Composite Application Techniques [13]

The winding of tow process is where fiber is taken through a resin bath to impregnate the tow with resin and is then wound around the column. The winding is done through mechanical means and can result in fairly uniform jackets. The wrapping of fabric process essentially is a modification of the winding of the tow process with the replacement of the individual tow by fabric. The fabric is wet out with resin and is applied to column. The fabric wet out can be either

done manually through the use of rollers and squeegees or through the use of an impregnator [35].

The automated winding process uses a pre-preg tow material with the winding process. In terms of lay-down, for tow and tape the process is automated and the fabric process is manual. For prefabricated shells, the sections are fabricated in a factory and are adhesively bonded in the field to form the jacket. This method is comparable to the fabrication of steel shells which are installed using field welding [35].

The resin infusion process involves dry fabric applied manually and then resin is infused using vacuum. This method allows for placement over irregular geometries without having significant patching. The last method, involves the use of cables or prefabricated strips, wherein confinement is achieved through additional external placement of reinforcement over the height of the column in the form of composite cables or prefabricated strips. The method of winding with cables mimics the conventional use of steel cables for external helical confinement.

It should, however be noted that as with all composites the final performance of the system depends intrinsically on the choice of constituents and the details of the processing steps used. Whether using a carbon-epoxy tow with an automated process of application to a column or an aramid-epoxy fabric wrapped around a deficient column, each will have it own structural retrofitting capabilities and may perform differently. Understanding the basic mechanics of a composite jacket can be further refined by looking at specific design parameters with regard to retrofitting concrete columns.

1.4 Retrofit Design Variables

Strengthening of deficient concrete columns requires the evaluation of specific design parameters in order to properly achieve a prescribed level of load carrying capabilities. Being aware of the existing column's structural weaknesses from studying past failures, the following

issues become the main design concerns for a seismic retrofitting jacket design. These main design variables for retrofitting a deficient column structure are column ductility, concrete confinement and lap splice clamping, and shear strength [9].

1.4.1 Column Ductility

Conventional reinforced concrete design acknowledges the need for structural ductility by setting limits on the amount of reinforcement incorporated within the element and its required confining transverse reinforcement [36]. An element's ductility or toughness refers to its ability to dissipate energy and deform without the occurrence of severe structural degradation or a brittle failure. Ductility is measured by relating ultimate drift (deflection) to an idealized estimate of yield drift. This drift measurement is affected by a combination of structural components: the amount and yield strength of longitudinal reinforcement, axial load of a member, concrete properties and concrete confining pressure [13].

Figure 1-14: Non-ductile Column Failure [37]

Figure 1-15: Non-Ductile Column Failure [37]

Lack of structural ductility will typically produce a failure mechanism in the plastic hinge region of an element as seen in Figures 1-14 and 1-15. Deficient columns were typically designed without any consideration of the structure's ductility. These columns tend to have a ductility level range of 2-3, which is well below the needed ductility for seismically loaded bridge columns. These low ductility levels can result in high concrete strains in the plastic hinge region of the column, which as noted above, do not have the adequate confinement pressure necessary to prevent the concrete from critically degrading [12]. A composite strengthening method designed to provide additional concrete confinement will therefore, improve the column's ability to deflect and in turn increase its ductility.

In order to determine if a column is deficient, its material properties and its as-built condition require assessment. This analysis will help to determine the existing column ductility level and the necessary retrofit ductility required to bring the column's capacity to a safe level. A plastic collapse analysis procedure should be implemented for performing an as-built column analysis.

On the basis of the plastic collapse analysis, the necessary plastic rotation ϕ_p of the plastic hinge region of the column can be determined. Equations 1.1 through 1.4 are used to determine the plastic curvature ϕ_p and the resulting plastic rotation of a concrete column.

$$\phi_p = \phi_u - \phi_y \qquad \textbf{(Equation 1.1)} \text{ [38]}$$

$$\phi_y = \frac{M_y}{EI_e} \qquad \textbf{(Equation 1.2)} \text{ [38]}$$

$$\phi_u = \frac{\varepsilon_c}{c} \qquad \textbf{(Equation 1.3)} \text{ [38]}$$

$$\phi_p = \frac{\phi_u}{L_p} \qquad \textbf{(Equation 1.4)} \text{ [12][38]}$$

Relating the plastic curvature to the required column plastic rotation also requires the determination of the column's plastic hinge length. For the existing column, this plastic hinge length can be simply taken as 20% of the overall column height [38]. With the calculations for the column's theoretical rotations, the probable displacements can be determined from the Equations 1.5 and 1.6.

$$\Delta_y = \frac{\phi_y L^2}{3} \qquad \textbf{(Equation 1.5)} \text{ [38]}$$

$$\Delta_p = (\phi_u - \phi_y) L_p (L - \frac{L_p}{2}) \qquad \textbf{(Equation 1.6)} \text{ [38]}$$

The probable yield and ultimate rotation and ultimate displacements are applied to Equations 1.7 and 1.8, such that the theoretical column ductilities can be determined.

$$\mu = \phi_u / \phi_y \qquad \textbf{(Equation 1.7)} \text{ [12] [38]}$$

$$\mu = \Delta_u / \Delta_y \qquad \textbf{(Equation 1.8)} \text{ [12] [38]}$$

By determining the ductility levels of an as-built column, the design for strengthening the areas of deficiency that cause low ductility can now be addressed. The following sections outline available theoretical design procedures developed from extensive research for composite jackets. Each design variable addresses an area causing insufficient ductility of as-built columns.

1.4.2 Concrete Confinement

Conventional reinforced concrete design requires the use of horizontal hoops or transverse reinforcement ties to provide adequate core confinement. Confinement is critical to ensure the flexural capacity of the member can be developed without deterioration under

repetitive loading [39]. This confinement is essential to prevent the longitudinal tensile reinforcement bars from buckling and/or lateral expansion of the column concrete. Without sufficient concrete confinement, failures such as those seen in Figure 1-16 and Figure 1-17 may occur.

Figure 1-16: Lack of Confinement Failure [37]

Figure 1-17: Lack of Confinement Failure [37]

To provide adequate confinement a column requires ties (or hoops) that are typically installed at a specified spacing. The required compressive pressure the hoops must provide to the column core is what controls the transverse reinforcement spacing. In deficient structures, these ties are spaced too far apart and cannot provide adequate core compression forces, consequently permitting confinement failure mechanisms to occur [4]. This failure is seen with a mushroom like collapse of the concrete member and tends to be located in the plastic hinge regions of the column.

An external jacketing system should have confinement abilities to be able to provide lateral support of the longitudinal reinforcement, enhance concrete strength and deformation capabilities as well as prevent concrete spalling [9]. The retrofit jacket would basically behave as

an externally applied hoop reinforcement system. The necessity to properly model the confinement behavior of the FRP jacket is because the confining pressure provided by the FRP jacket increases continuously with the lateral strain of the concrete. This lateral strain increase is due to the linear elastic stress-strain behavior of FRP [16].

Research on deficient as-built circular concrete columns retrofitted composite material strengthening jackets indicate that the confinement effectiveness is more efficient than with steel jackets [12][16][33][40][41][42]. With composite reinforcement materials such as glass and carbon fiber, which have basically a linear stress-strain relationship up to failure, there is no increasing damage, and successive cycles to the same displacement result in constant rather than escalating hoop strains.

Displacement ductility based design relates the volumetric ratio required to provide adequate concrete core confinement to the plastic deflection and curvature. With the plastic curvature and deflection identified above in Equation 1.4 and 1.6, the ratio of confinement required of the jacket is defined in Equations 1.9.

$$\rho_s = \frac{4t_j}{D'} \qquad \textbf{(Equation 1.9)} \text{ [12] [16] [40] [41]}$$

Significant research has been published related to this already and with t_j being the required minimum jacket thickness, Table 1-1 presents examples of research formulae derived through experimental testing and evaluation for minimum jacket thickness as well as ultimate concrete compression strain of the column with a composite jacketing system.

Table 1-1: Required Jacket Thickness for Column Confinement of Circular Columns

Researchers	Jacket Thickness, t_j	Ultimate Concrete Compression Strain, ε_{cu}
Priestly, Seible, Calvi [12]	$t_j = \frac{0.1(\varepsilon_{cu} - 0.004)Df'_{cc}}{f_{uj}\varepsilon_{uj}}$	$\varepsilon_{cu} = 0.004 + \frac{2.5\rho_s f_{uj}\varepsilon_{uj}}{f'_{cc}}$
Seible, Priestly, Hegemier, Innamorato [9]	$t_j = 0.009\frac{D(\varepsilon_{cu} - 0.004)f'_{cc}}{\phi_f f_{uj}\varepsilon_{uj}}$	$\varepsilon_{cu} = 0.004 + \frac{2.8\rho_s f_{uj}\varepsilon_{uj}}{f'_{cc}}$
Pantelides, Gergely [15]	$t_j = 2[\frac{0.09D_e(\varepsilon_{cu} - 0.004)f'_{cc}}{\phi_f f_{uj}\varepsilon_{uj}}]$	*Not Available*

In order to determine the thickness of a required composite jacket, the compressive strength of the confined concrete must be first established. Substantial research has been presented on the formulation of models for determining this essential concrete strength component and examples are presented in Table 1-2.

Table 1-2: Column Required Jacket Thickness for Column Confinement

Researchers	Confined Concrete Strength, f'_{cc}
ACI-440 [42]	$f'_{cc} = f'_c[2.25\sqrt{1 + 7.9\frac{f_1}{f'_c}} - 2\frac{f_1}{f'_c} - 1.25]$
Fardis, Khalili [43]	$f'_{cc} = f'_c(1 + 4.1f_r)$
Cusson, Paultre [44]	$f'_{cc} = f'_{co} + 2.1f'_{co}(\frac{f_1}{f'_{co}})^2$
Karbhari, Gao [45]	$f'_{cc} = f'_{co} + 3.1f'_{co}\nu_c\frac{2t}{d}\frac{E_{com}}{E_c} + \frac{2\sigma_t t}{d}$

1.4.3 Lap Splice Clamping

A lapped splice is where two rebar are adjacent to each other and lapped for a specified length in order to develop a mechanical bond necessary for transfer of tension forces to the surrounding concrete. It is expected that these side by side bars develop a response that is

comparable to that of a single bar. Standard reinforced concrete design calls for the proper development of column reinforcement in order to acquire a specified strength needed to transfer induced forces from reinforcement to concrete [39]. This is accomplished with the force transfer through a mechanical bond. Transferring this force from the bar into the concrete adds tensile forces to the concrete causing concrete cracking (concrete has low tension capacity). Figure 1-18 illustrates this force transfer. Without proper reinforcement detailing, the concrete cracks will begin to degrade under cyclic (seismic) loading. If this concrete fracturing is not halted and continues, it will lead to spalling (breaking away of a section of concrete) of the concrete as the mechanical bond is destroyed. The loss of concrete will prevent further force transfer and lead to a lap splice failure. When sufficient confinement hoops are added to the lapped bars, compression forces are produced to prevent the dilation of the cracks, creating a clamping effect [36].

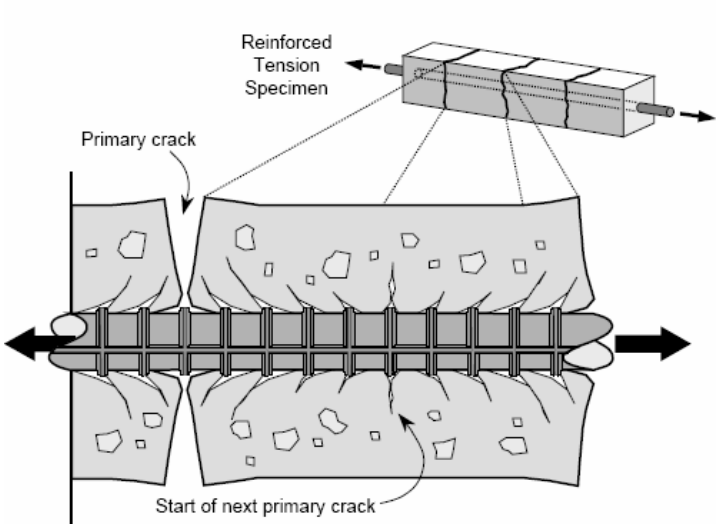

Figure 1-18: Concrete Force Transfer Illustration [36]

The issue with deficient columns is typically at the starter bars (foundation rebar continued into the column for a specified length to connect the two structural elements) where earlier construction practices typically placed rebar splices. This is now known to be one of the worst locations for reinforcement splices. As the longitudinal bar stresses exceed the bond strength of the concrete due to externally applied tension loads, the short starter bars can pull free from the column. Priestley and Seible wrote in *Seismic Design and Retrofit of Bridges,* that "Lap splices in plastic hinge zones, such as the base of columns should not be used...even if very long splice lengths are used" [12]. As splitting resistance governs the level of bond stress that concrete can sustain, confinement provided by an external jacketing can enhance the clamping pressures required to maintain a certain level on bond stress between the reinforcement and concrete [9].

Extensive research has found that deficient concrete columns are vulnerable to pre-mature brittle failure due to bond deterioration, but appropriately retrofitted columns will significant improve column performance with enhanced hysteretic response and increased ductility. The bond slip in lap spliced rebars can cause a gradual degradation of the load carrying capacity of a retrofitted column after the required ductility is developed; however, this bond deterioration is a gradual process and stress redistribution can be developed after the starter bars slip [9][12][33][41].

After a column begins cracking under applied tensile loading, a potential splitting failure at the surface may develop. If cracking has developed, a continuance to splice failure can be inhibited if adequate clamping pressure is provided across the fracture surface by a composite confinement jacket. Knowledge of the long term strength characteristics of the jacketing material under sustained stress should be understood for the determination of composite jacketing design requirements. Strength of E-glass and aramid fiber reinforced composites degrade under sustained loads, therefore it is very important that the effects of passive and active confinement be

low [12]. Table 1-3 provides examples of research driven equations for determining the concrete compressive strength for lap splice confinement.

Table 1-3: Required Jacket Thickness for Lap Splice Column Confinement in Circular Columns

Researcher	**Jacket Thickness, t_j**
Seible, Priestly, Hegemier, Innamorato [9]	$t_j = 500\frac{D(f_l - f_h)}{E_j}$
Pantelides, Gergely [15]	$t_j = 2[\frac{D_e(f_l - f_h)}{2\varepsilon_j E_j}]$
Haroun, Elsanadedy [41]	$t_j = \frac{1000D}{E_j}$

In order to establish the required thickness of a composite retrofit jacket, the lateral clamping pressure of the confined concrete must be determined as well. Results of extensive research on the lap splice confinement concur for the design model for lateral clamping pressure. The resulting lateral clamping pressure is given in Equation 1.10.

$$f_l = \frac{A_s f_{sy}}{[\frac{p}{2n} + 2(d_b + cc)]L_s} \qquad \textbf{(Equation 1.10)} \text{ [9] [12] [28] [41]}$$

As both column confinement and lap splice clamping strengthening procedures involve lateral pressure on concrete to provide additional confinement reinforcement, it should be noted that these two strengthening variables are not additive. This is due to the fact that lap splice clamping and concrete confinement will occur on opposite sides of the column; therefore, the more stringent of the two design requirements will govern the required strengthening jacket thickness [12].

1.4.4 Column Shear Strength

Traditional reinforced concrete design allocates specified shear strength for an element based on its concrete strength and transverse reinforcement properties. A portion of the specified shear strength is assumed to be provided by the concrete and the remainder by the shear reinforcement. The additional shear reinforcement restrains the growth of inclined cracking [39]. With no, or inadequate reinforcement, a shear failure can occur, which is characterized by lack of ductility, very small deflections, and providing little or no warning before failure. In short concrete columns, such as those in Figure 1-19 and Figure 1-20, a high shear to moment ratio and outdated flexure design makes them highly prone to failure [12]. Current design procedure attempts to ensure that a ductile flexure failure occurs before an element shear capacity is even reached by setting minimum design requirements on shear reinforcement [12].

Figure 1-19: Column Shear Failure [37]

Figure 1-20: Column Shear Failure [37]

The shear strength on concrete column is the result of a blend of mechanisms involving concrete compression shear transfer, aggregate interlock along inclined flexure-shear cracks and truss mechanisms making use of horizontal tie reinforcement. Knowing that these shear mechanisms work together in a complex fashion it is not surprising that shear failure is brittle and involves rapid strength degradation [12]. Strengthening columns for deficient column shear becomes important in turning a brittle failure into a ductile one that provides significant warning of impending failure. Table 1-4 is a selection of equations used to determine the required thickness of a composite jacket necessary to strengthen a column in shear. Each equation is similar with the variables and coefficients presented in a different configuration.

Table 1-4: Required Jacket Thickness for Shear Strength of Circular Column

Researchers	**Jacket Thickness, t_j**
Seible, Priestly, Hegemier, Innamorato [9]	$t_j = \dfrac{\frac{V_o}{\phi_v} - (V_c + V_s + V_p)}{\frac{\pi}{2} 0.004 E_j D}$
Hegemier [28]	$t_j = \dfrac{159}{E_j D}\left[\dfrac{V_o}{\phi} - (V_c + V_s + V_p)\right]$
Xiao, Wu, Martin [34]	$t_j = \dfrac{2}{\pi} \dfrac{\frac{1.5V_o}{\phi_s} - (V_c + V_s + V_p)}{f_{jd}(D-c)\cot\theta}$ Where θ = angle of truss mechanism

1.5 Thesis Objective

The reason for undertaking this study was to assess a new and novel FRP alternative for seismic strengthening of inadequate concrete columns. The performance of accepted strengthening methods may not be a concern since they function well within the predefined set of

strengthening parameters, yet they may not be cost effective enough for wide use in areas with lower seismic risk. Cost benefit analysis in these areas is very different than those where established strengthening procedures are already in use. An effective retrofit option which reduces seismic risk for a minimal cost has yet to be implemented. This research focuses on a retrofit option that uses a jacketing system with inexpensive materials and an innovative construction technique in order to provide a potentially rapid and cost effective means of seismic retrofitting.

Before the multiple retrofit methods in the above section had been accepted and established as strengthening options, numerous research projects were conducted which included component testing and analysis. This extensive set of prior research allowed for the establishment of performance standards required of an applied system. The procedures for the requisite product scrutiny by laboratory experimentation have been standardized by various agencies to streamline this transition of research to field application. The established HITEC protocol, assessment and validation of composite seismic strengthening procedures was used as the benchmark for the evaluation of the sandwich system investigated in this study [27].

Chapter 2 will outline the design requirements for jacketing testing methods and procedures as well as summarize the test method utilized for this research. Chapters 3, 4 & 5 will present the experimental test results for the new jacketing technique and materials used within this research. Chapter 6 will summarize the experimental test results and present an analysis of the jacketing system with a list of strengths and weakness and will provide conclusions for the research as well as a summary of potential future work and applications possible with the researched jacketing system.

2. Test Methods and Procedures

2.1 Definition of Parameters

Focused testing and analysis allows for the establishment of performance standards required of an applied retrofit system. Controlled element experimentation and the resulting assessment of performance are essential in order to determine if a system is appropriate for field implementation. The details of testing procedures required for column retrofit systems are predicated by the mechanisms of failure that the system must prevent in a seismic event. The most common types of failure are due to: brittle collapse under shear loading, inadequate concrete confinement, inadequate bar buckling restraint, and lap splice failure. The minimum level of testing necessary for a new system should consequently include loading conditions typical for inducing these failure modes in a non-strengthened element.

As part of necessary testing requirements to provide a means of validating that the common failure mechanisms have been mitigated, all retrofitted concrete columns are expected to be able to dissipate energy through the development of controlled inelastic rotations in the column's plastic hinge regions. This is measured in terms of ductility. A basic definition for structural ductility is an element's ability to displace inelastically through repeated loading cycles without considerable degradation of the element's strength or stiffness [4]. Within the civil engineering discipline, ductility is commonly defined as the ratio of deflection at a given response level to deflection at yield response as shown in Figure 2-1 [38].

Although the ductility ratio defined in Figure 2-1 refers to resulting element displacements, curvature ductility ratios, relating to maximum and yield curvatures, are also used as a measure of structural ductility. Curvature of a structure may be represented differently from element to element due to the direct relationship of the structure's reinforcement with its applied axial load.

Figure 2-2 illustrates the ductility definition in terms of curvature and a column's bending capacity (moment).

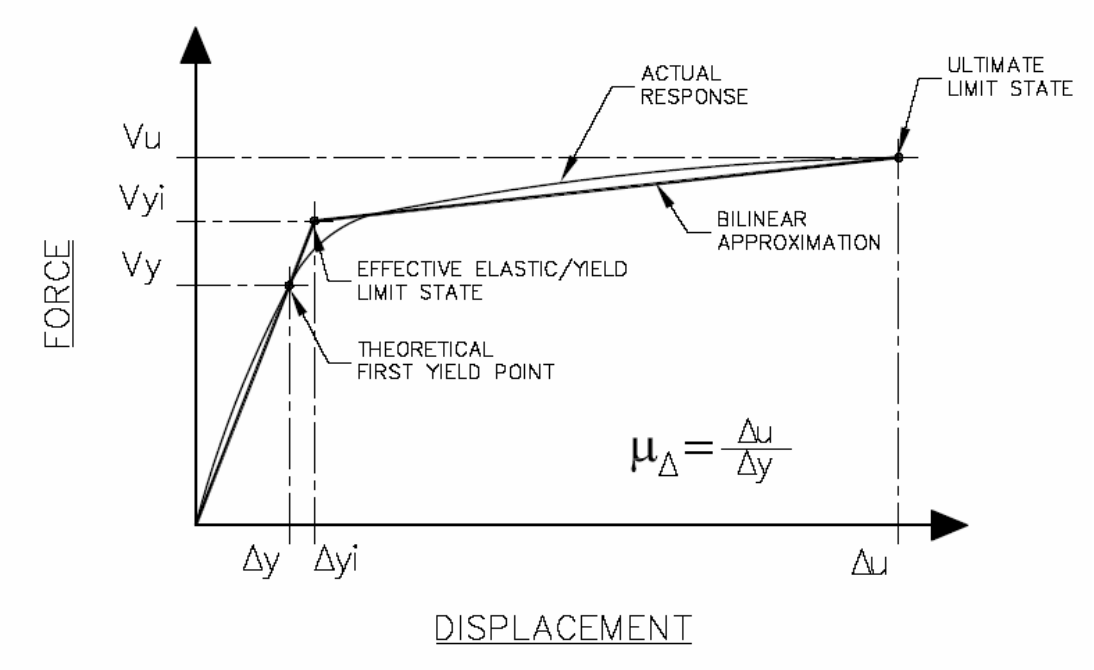

Figure 2-1: Definition of Displacement Ductility [38]

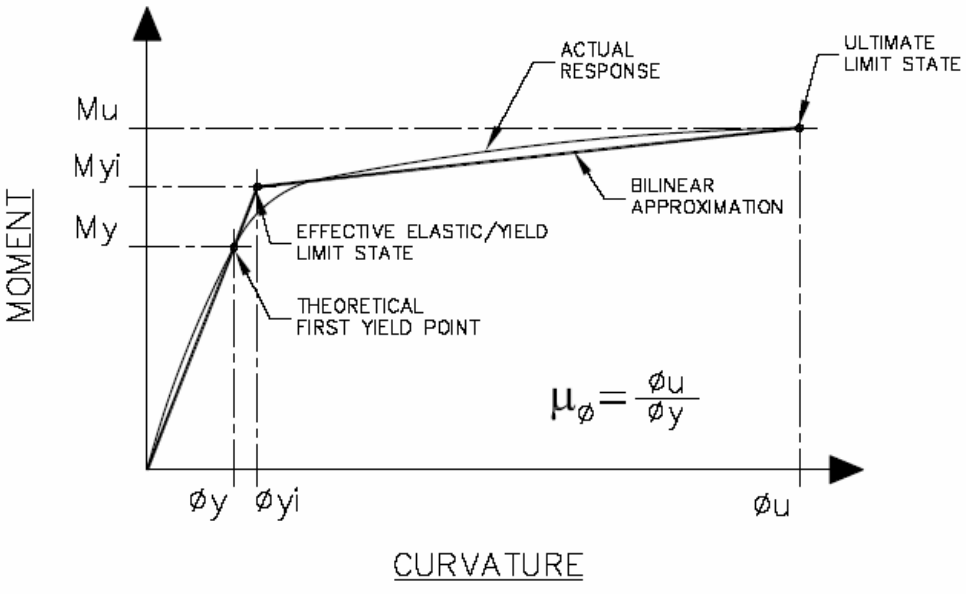

Figure 2-2: Definition of Curvature Ductility [38]

Figure 2-3 shows the relationship of the column's axial load to its allowable moment capacity. Figure 2-3 also illustrates that increasing axial loading on the column beyond its balanced state will reduce the column's moment capacity. This decrease in bending capacity will affect a column's ultimate curvature and will lead to a decrease of the structure's curvature ductility. The ultimate limit state value is determined at the point when the column capacity drops lower than a defined & pre-determined effective yield capacity. The effective yield limit state is defined from the experimentally measured first theoretical yield point which is extrapolated by moment curvature analysis with a concrete strain of 0.5% [38].

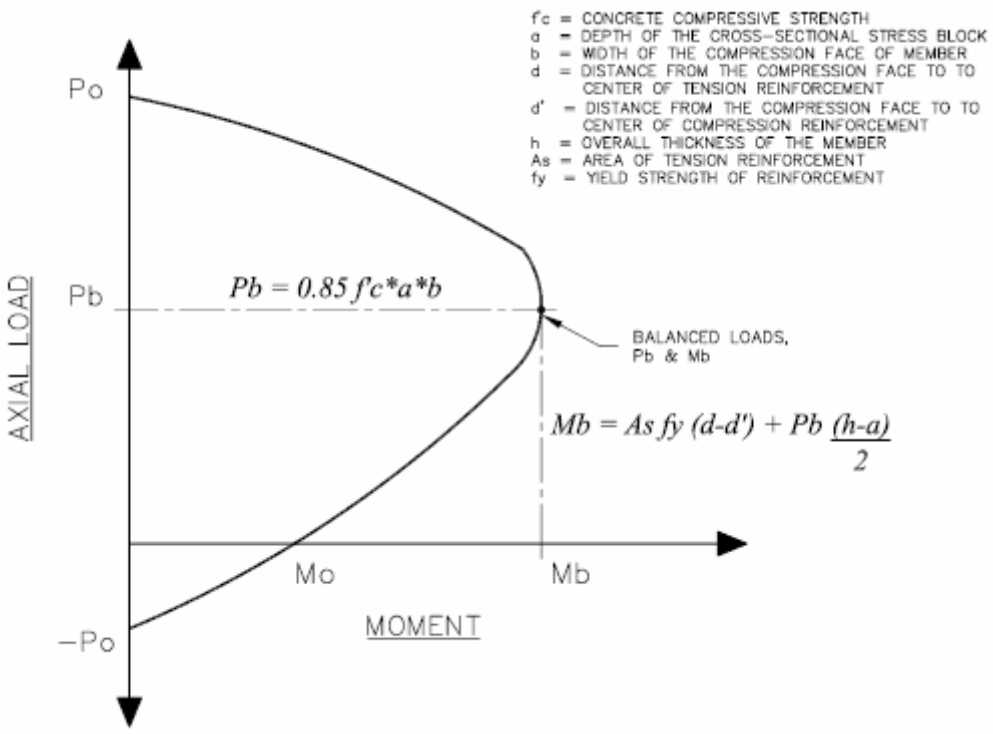

Figure 2-3: Column Interaction Diagram [38]

In a column, the balanced axial load, as well as the balanced column moment, is

determined when the maximum strain at the extreme compression face of concrete reaches 0.003 simultaneously with the first instance of yield strain of the tension reinforcement. The equations given in Figure 2-3 are further defined in ACI 318-05 design requirements [39]. A strengthening system design requires ductility calculation to be based on both of the above measurements: displacement and curvature. In each of the ductility definitions, an ultimate limit state is established on the top right of the Figures 2-1 and 2-2 labeled level ϕ_u and Δ_u respectively.

The cyclical testing procedures required for testing can, however, result in premature low cycle fatigue failure of the column's reinforcement under large repetitive displacements/curvature needed to determine base ductility. This is due to the large amount of energy introduced into the system to produce the large displacement/curvature cycles. The required cycles are necessary though, to establish the column's stability during its hysteretic response. The experimental testing sequences can be used to establish that the retrofitted system is structurally sound. This is accomplished by ascertaining that the test column has attained the set criteria determined by the governing protocol during its testing.

2.2 Testing Protocol

With parameters for ductility defined, a testing protocol is needed to determine ductility limits and requirements for a viable retrofit system. Various procedures were reviewed as part of this investigation. Within the United States alone, a number of organizations have published standardized test procedures for concrete structures retrofitted with composite strengthening systems. The following is a brief synopsis for three such testing protocols.

2.2.1 University of California - Irvine: FHWA A/CA/UCI-99-01 [6]

Results for a structural assessment and qualification-testing program are described in a report by the University of California - Irvine. This program was conducted to assess pre-

qualification requirements for alternative column casings for seismic retrofit for the California Department of Transportation (Caltrans). The report also included a summary of experimental and analytical studies of the composite jacketed retrofitted concrete test columns on the basis which the resulting qualification-testing program was then developed.

The test criteria developed called for the construction of multiple half scale concrete bridge columns, using both circular and square configurations. Flexure columns with lap splice reinforcement were used to evaluate the composite jackets for the enhancement of lap splice clamping and shear columns with continuous reinforcement were used to assess the suitability of the composite jackets for shear enhancement.

Table 2-1: Test Column Matrix

Column Geometry	Shear	Flexure (Lap Splice)
As Built: Circular	2	2
As Built: Square	1	2
Retrofitted: Circular	3	7
Retrofitted: Square	6	4

Table 2-1 lists the breakdown of the column types tested by reinforcement layout and column configuration. Each of the columns had a defined reinforcement ratio, $\rho = 2.2\%$, with 6 mm diameter (#2) horizontal hoop reinforcement spaced uniformly at 12 cm (5 in) center to center with 35 MPa (5000 psi) nominal concrete strength. Each element was cyclically tested using a loading regime given in Table 2-2.

The overall testing procedure was introduced as means of determining the performance of a FRP retrofit system. The resulting test criterion was then implemented to show that the performance of FRP strengthening systems can be predicted by the presented standard analysis of moment-curvature analysis.

Table 2-2: Test Column Loading Matrix

Load	Displacement	Number of Cycles
0.25 H_y		3
0.50 H_y		3
0.75 H_y		3
1.00 H_y	Δ_1	3
	1.0 Δ_y	3
	1.5 Δ_y	3
	2.0 Δ_y	3
	3.0 Δ_y	3
	4.0 Δ_y	3
	5.0 Δ_y	3
	6.0 Δ_y	3

H_y = the first yield lateral load capacity
Δ_1 = the average of the measured displacements corresponding to H_y
Δ_y = the yield displacement determined from the ratio of column's lateral load capacity vs ideal ateral load capacity * Δ_1

2.2.2 International Code Council Evaluation Service [46]

Under the International Code Council (ICC) an Evaluation Service was established to set testing criteria and evaluate products tested within an accepted test criteria. ES report AC125 – Interim Criteria for Concrete and Reinforced and Un-Reinforced Masonry Strengthening using Fiber-reinforced Polymer (FRP) Composite Systems is the criterion which "establishes the minimum requirements for the issuance of ICC-ES evaluation reports on fiber-reinforced composite systems used to strengthen concrete and masonry structural elements" [46]. The report lists the required information needed, the necessary qualification tests, the mandatory quality control and the process for a final report submittal.

Within the 11-page report, definitions, system design criteria and minimum acceptable strengthening requirements are all outlined. For flexural columns, the column configuration is required to be able to induce flexural limit states or failure modes with the extremes of

dimensional, reinforcing and strength parameters considered. For shear columns, the column specimens are required to be constructed to induce shear limit states or failure modes. Extremes of the dimensional, reinforcing and compressive strength parameters are required to be taken into consideration. Testing for both the flexural and shear columns for seismic application are required to conform to Figure 1 in document, which is reproduced in tabular form below in Table 2-3.

Table 2-3: Test Column Matrix

Load	Displacement	Number of Cycles
0.25 H_y		1
0.50 H_y		1
0.75 H_y		1
1.00 H_y	μ	1
	1.0 μ	3
	1.5 μ	3
	2.0 μ	3
	3.0 μ	3
	4.0 μ	3
	6.0 μ	3
	8.0 μ	3
	10.0 μ	3

H_y = the first yield lateral load capacity
μ = displacement ductility level defined relative to yield or crack displacement

The limits state used to determine first yield (Hy) is to be based on material properties and an extreme concrete fiber compression strain of 0.003 for the flexural columns and only based on material properties for the shear columns.

The report states that the listed acceptance criterion was issued in order to provide guidelines for the evaluation of alternative systems where the codes do not provide requirements for testing and determination of structural capacities, reliability and serviceability. The report not only addresses concrete columns, but concrete beams, walls, slabs as well as masonry structural

elements.

2.2.3 Highway Innovative Technology Evaluation Center Procedure [11]

The University of California – San Diego, under contract with the Highway Innovative Technology Evaluation Center of the Civil Engineering Research Foundation published a report TR-2001/11 – FRP Composite Wrap Durability Evaluation. This criterion "outlines requirements for structural evaluation and testing of FRP composite wrap systems for seismic retrofit of columns" [11]. The report lists the required test procedure and criteria of a system for the purpose of structural evaluation. This protocol was used earlier to assess 4 different composite retrofit systems. Within the submitted report, a system design criteria and minimum acceptable strengthening requirements are outlined.

The report lists the minimum specimen testing requirements as presented in Table 2-4 for reinforcement layouts as well as column geometries. A set of criteria for evaluation of the strengthening system after cyclic testing is also presented. Ductility limit states are utilized to provide a standardized testing procedure tailored to each test column with a different cross section and/or reinforcement layout.

Table 2-4: Test Column Matrix

Column Geometry	Shear	**Flexure** (Continuous)	**Flexure** (Lap Splice)
Circular	1	1	1
Square/Rectangular	1	1	1

Figure 2-4 presents the recommended loading history per the HITEC testing protocol [11]. In the "Load Control" segment of the column testing scheme, load levels are based on the experimental column's theoretical yield force level, Vy. Load cycles are stepped at 25% increments of Vy, with each step being a full push-pull cycle. The concluding load-control cycle displacements, Δ_{y1} and Δ_{y2}, under an applied force of 1.0 Vy are used to establish the effective

yield deflection of the specimen according to Equation 2.1. This effective yield measurement is necessary in calculating the retrofitted column's final ductility.

$$\mu = 1 = \Delta_{yi} = \left(\frac{|\Delta_{y1}| + |\Delta_{y2}|}{2}\right) \frac{V_{yi}}{V_y} \quad \textbf{(Equation 2.1)} \text{ [11]}$$

The subsequent testing sequence to ascertain the specimen's ductility is completed in displacement control. This repetitive sequence phase requires that three full push-pull cycles be completed at each level. These levels are stepped displacement increments of the calculated Δ_{yi} per Equation 2-1 with $\mu = 1 = \Delta_{yi}$. These increments should be no larger than 1.5 times that of the previous level in order to ensure column stability [11].

Because of the properties of reinforced concrete are mainly based on dimensions and concrete to reinforcement ratios, the size of the testing element is critical in being able to adequately model the behavior of a full-size field element. Small scale testing does not produce satisfactory results for analyzing column ductilities because it is also difficult to scale down all the components of reinforced concrete without compromising the structural response of the material. Previous laboratory experiments have shown that a minimum 1/3 scale test element is necessary to provide appropriate experimental results for laboratory testing [9]. This scale also allows for the ease of scaling the column's reinforcement. Column reinforcement and detailing in test specimens should reflect the reinforcement deficiencies that are present in the field structures that are in present need of strengthening. Table 2-5 lists the parameters for the necessary "as-built" characteristics of a test column for a qualified experimental specimen.

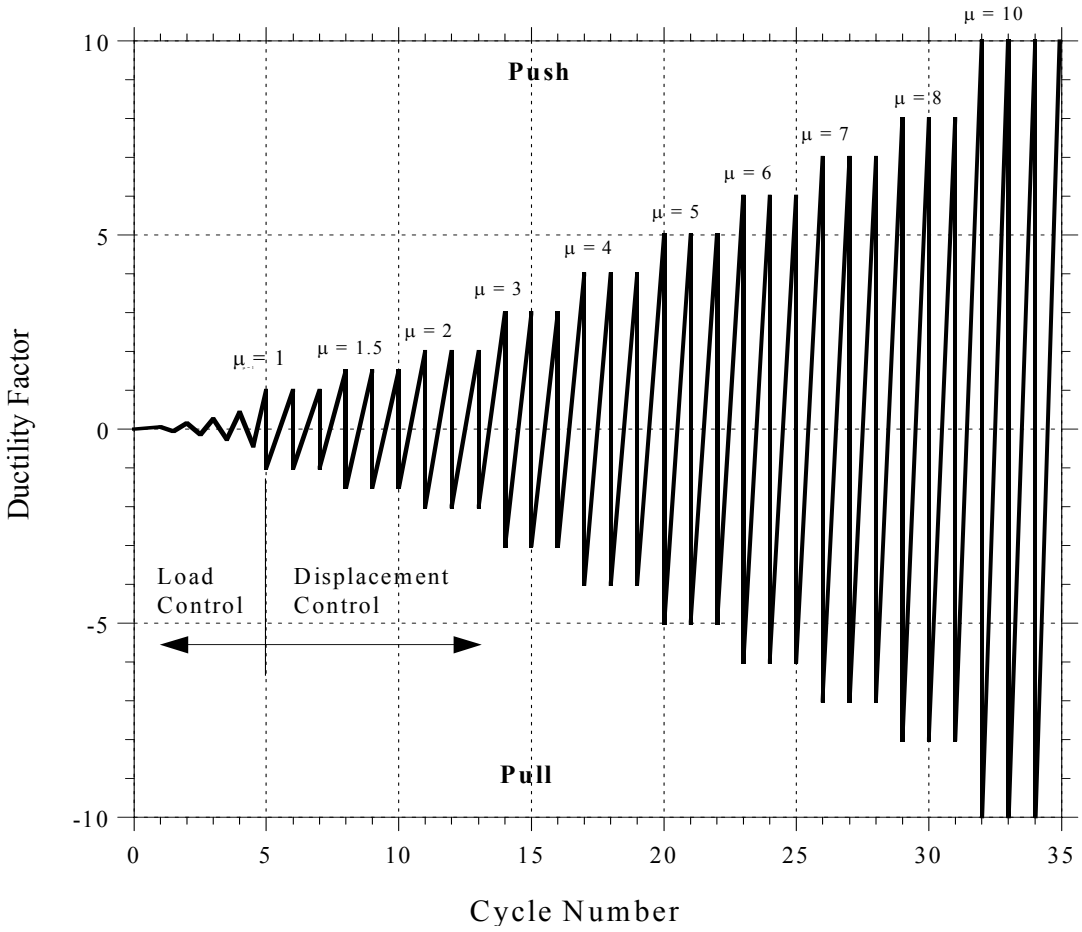

Figure 2-4: Recommended Loading Sequence

Table 2-5: Specimen Max/Min Parameters [11]

Parameter	Minimum	Maximum
Circular Column Diameter	30 cm (12 in)	183 cm (72 in)
Rectangular Column Aspect Ratio	1:1	2:1
Flexure Span (H/D)	> 4	-
Shear Span (H/D)	-	< 3
Vertical Reinforcement Ratio, ρ	1 %	3%
Horizontal Reinforcement Ratio, ρ	-	< 1%
Lap Splice Length	20 d_{bl}	40 d_{bl}
Axial Load Ratio, P/ (f'c * Ag)	10%	30%

ρ = As/ bd
d_{bl} = diameter of reinforcement
P = axial load applied to column
Ag = cross sectional area of specimen
f'c = concrete compressive strength
H/D = column height / column diamter

The criteria of Table 2-5 set the design capacity for the as-built specimens reflective of field columns with sub par seismic resistant ability. This is necessary since the performance of the strengthening system for additional shear capacity, lap splice clamping, and plastic hinge confinement cannot be evaluated unless the forces required for an as-built failure have been exceeded.

For the purpose of the current investigation, the laboratory specimens were fabricated and tested pursuant to the HITEC protocol outlined in Section 2.2.3.

2.3 Implemented Test Procedure

2.3.1 Specimen Design

Following the HITEC criteria, a minimum of six (6) 50% scale concrete test columns were constructed. 60 cm (2 ft.) diameter circular columns and 44 cm (17 in.) square columns were chosen for the experimental testing portion of this research on the novel composite jacketing system. The 60 cm column diameter corresponds to the prototype column diameter of 1.2 meters at 50 % scale. 44 cm square columns were chosen such that its diagonal is 62 cm and will therefore provide for a direct comparison with the circular columns in the appropriate set.

With the column geometries chosen for the laboratory testing, the design of the column reinforcement was determined based on the column parameters in Table 2-4. Since the reinforcement ratio is limited to less than 3 % for the test procedure, 19 mm diameter (#6 rebar) reinforcement was used for the column cages. The column hoop reinforcement was designed to scale according to the same transverse reinforcement design (M13 hoops @ 30 cm on center) present in most pre-1970 superstructure elements. This was achieved with M6 (#2) hoops at 12 cm (5 in.) on center throughout the column.

Table 2-6 summarizes the parameters used for the laboratory testing and Figure 2-5

through Figure 2-10 depict the resulting construction details of these test columns, presenting the elevation and cross-sectional layouts of the reinforcement as well as overall dimensions.

Table 2-6: Specimen Design Parameters [11]

Parameter		Shear	Flexural (Continuous)	Flexural (Lap Splice)
Circular Column Diameter		61 cm	61 cm	61 cm
Rectangular Column Aspect Ratio		1:1	1:1	1:1
Shear/Flexure Span (H/D)		4	6	6
Vertical Reinforcement Ratio	**Circular**	2.1%	2.1%	2.1%
	Square	2.7 %	2.7%	2.7%
Horizontal Reinforcement Ratio	**Circular**	0.02%	0.02%	0.02%
	Square	0.05%	0.05%	0.05%
Axial Load Ratio P/ (f'c * Ag)	**Circular**	11%	29%	29%
	Square	12%	29%	29%

It should be noted that an axial load is applied to simulate the load on an in-use field column due to deck and traffic loading. The axial load is important, as noted in Section 2.1 and illustrated in Figure 2-3 with the relationship of the column's axial load to the column's moment capacity. Over-loading or under-loading a test column will affect the ductility of the test column due to the interaction of a column's moment capacity with its axial load, where higher loads decreases the column's bending capacity which in turn decreases the column's ductility. The HITEC protocol placed limits on the appropriate level of axial loading as noted in Table 2-5 [11]. This parameter appropriately models as-built column loads without underrating the possible as-built column's ductility.

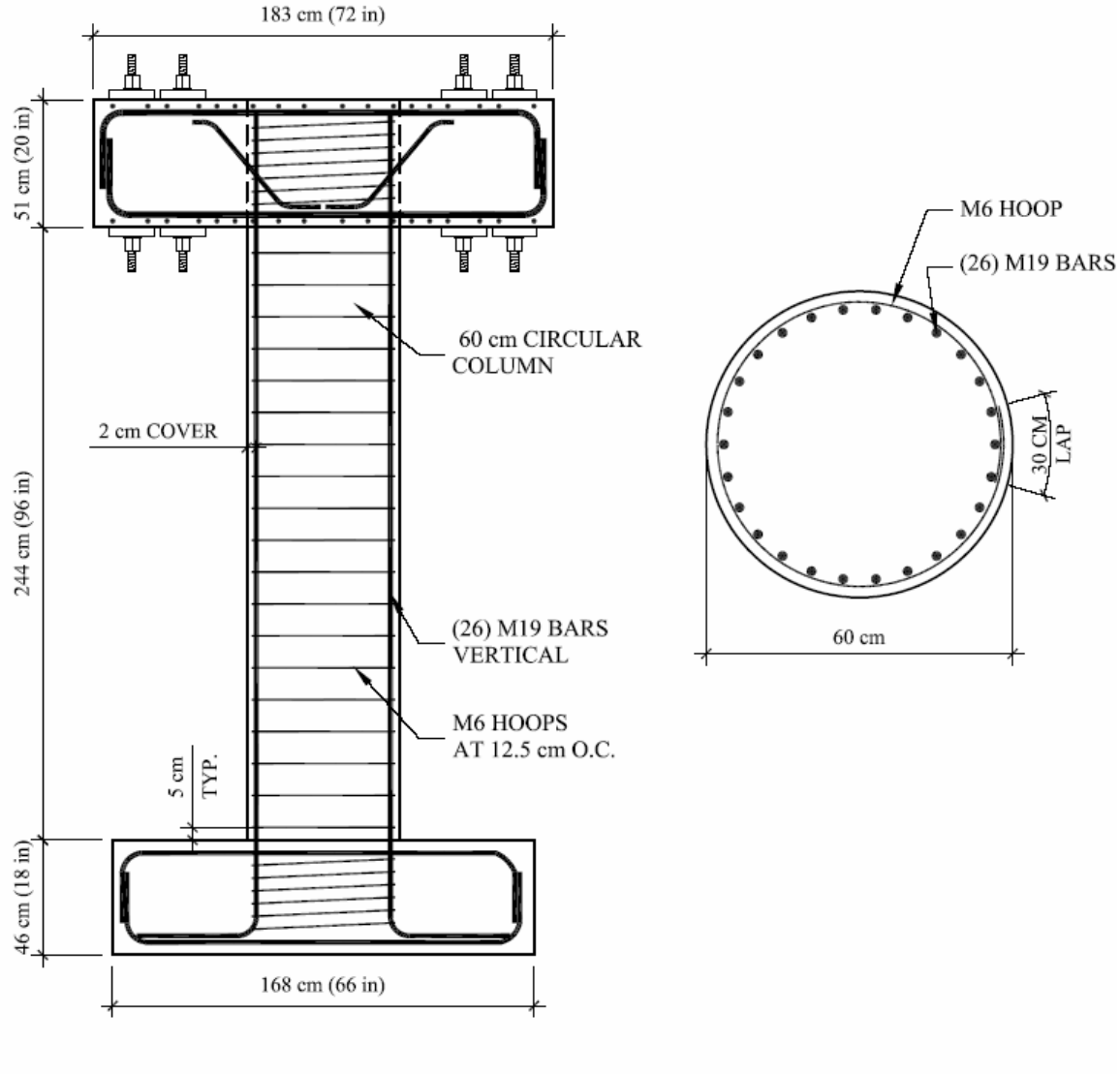

Figure 2-5: Details of the Circular Shear Column Test Specimen

The circular shear column shown schematically in Figure 2-5 had an applied axial load during testing of 650 KN (145 kips). This is based on an 11% axial load ratio.

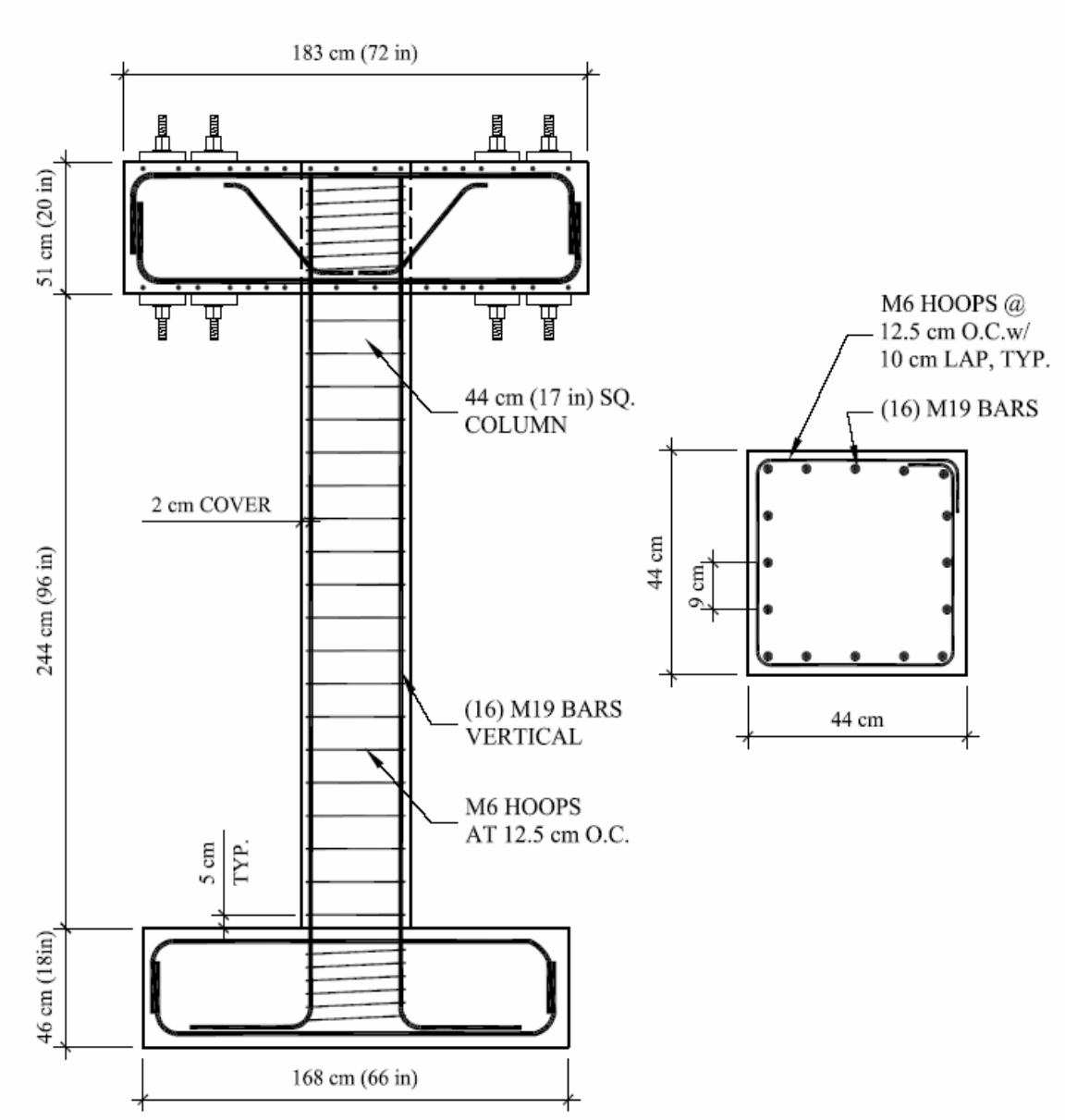

Figure 2-6: Details of the Square Shear Column Test Specimen

The square shear column shown schematically in Figure 2-6 had an applied axial load during testing of 460 KN (105 kips). This is based on a 12% axial load ratio.

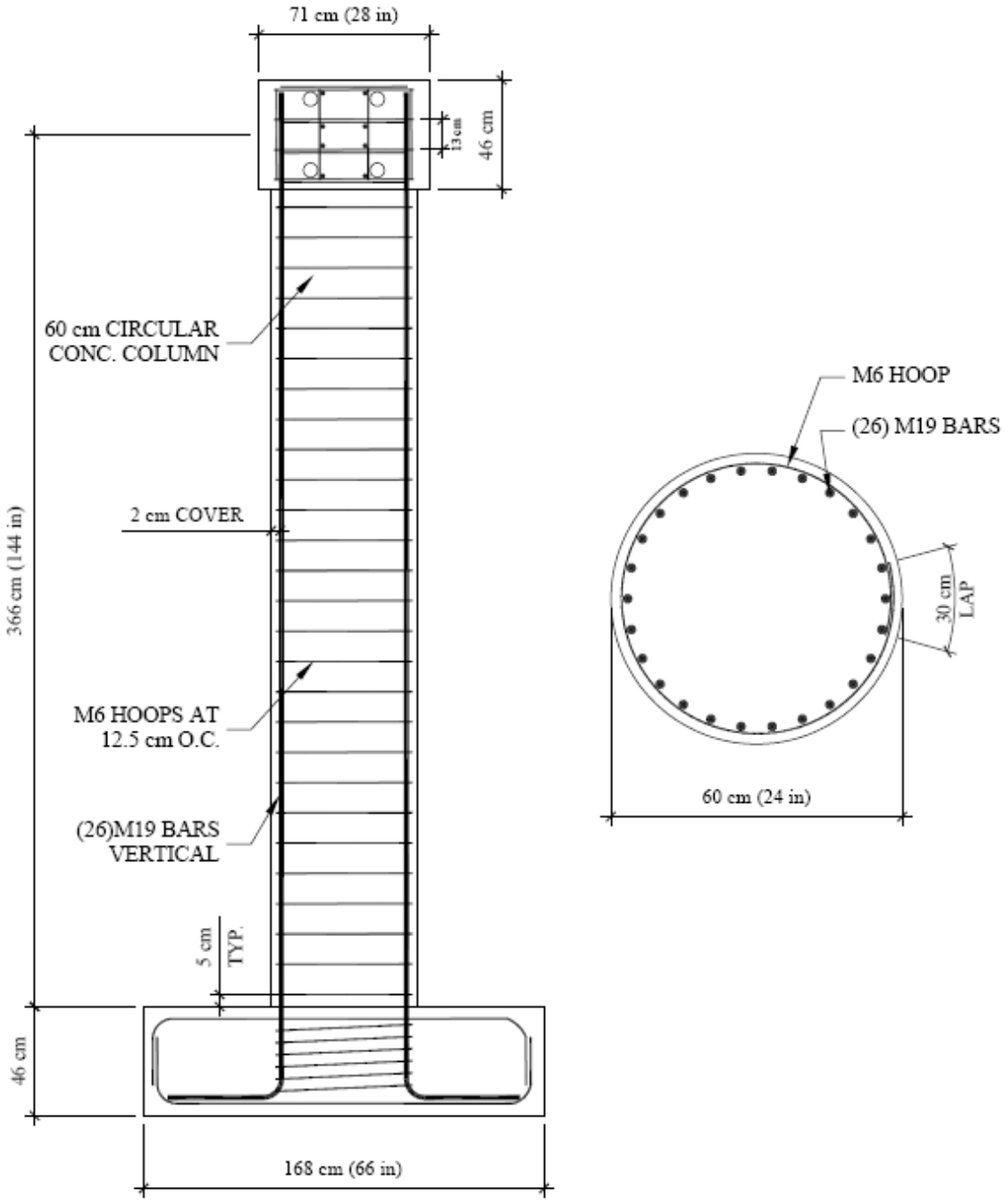

Figure 2-7: Details of the Circular Continuously Reinforced Flexure Column Test Specimen

The circular flexure column shown schematically in Figure 2-7 had an applied axial load during testing of 1780 KN (400 kips). This is based on a 29% axial load ratio.

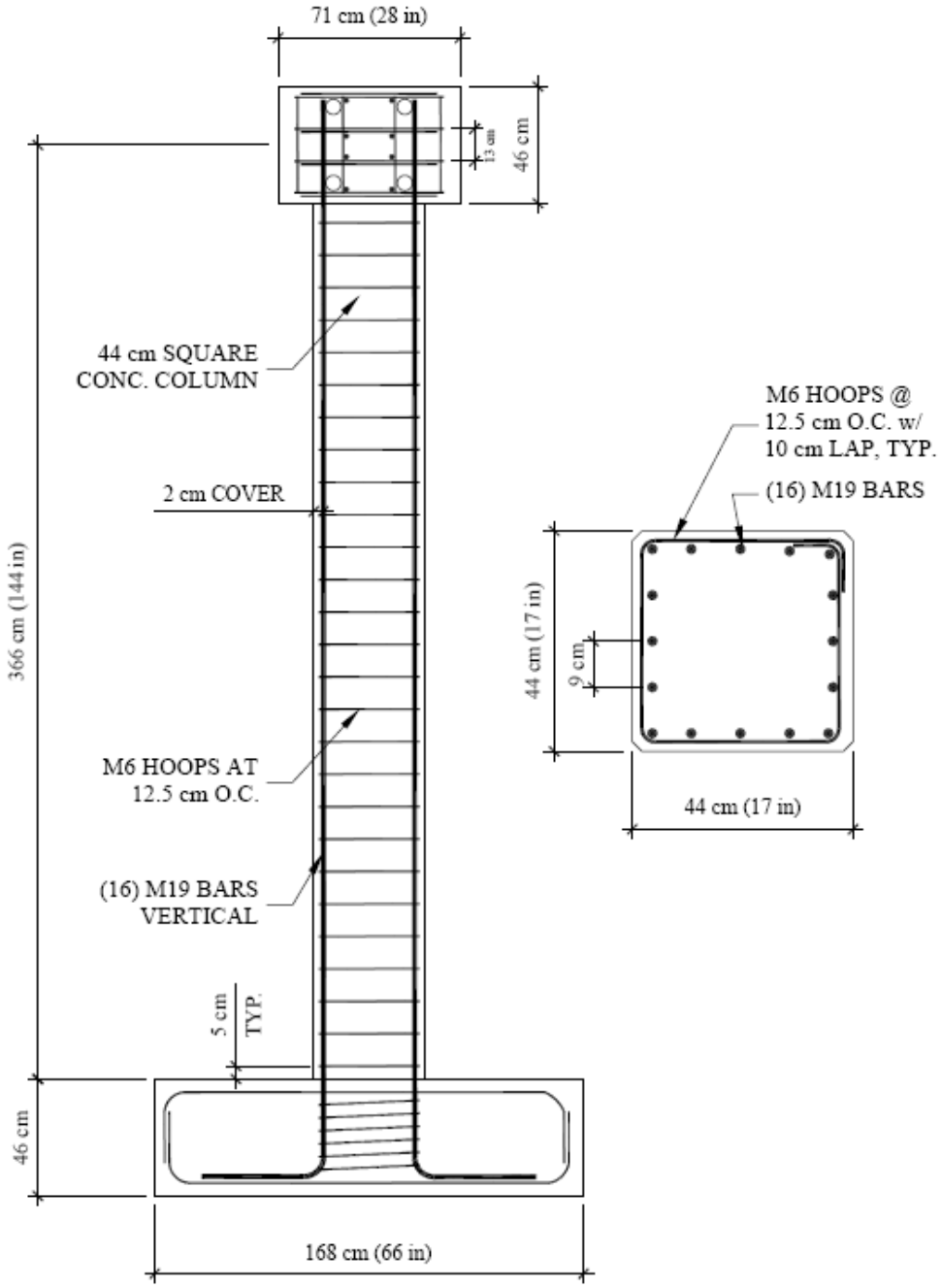

Figure 2-8: Details of the Square Continuously Reinforced Flexure Column Test Specimen

The square flexure column shown schematically in Figure 2-8 had an applied axial load during testing of 1155 KN (260 kips). This is based on a 29% axial load ratio.

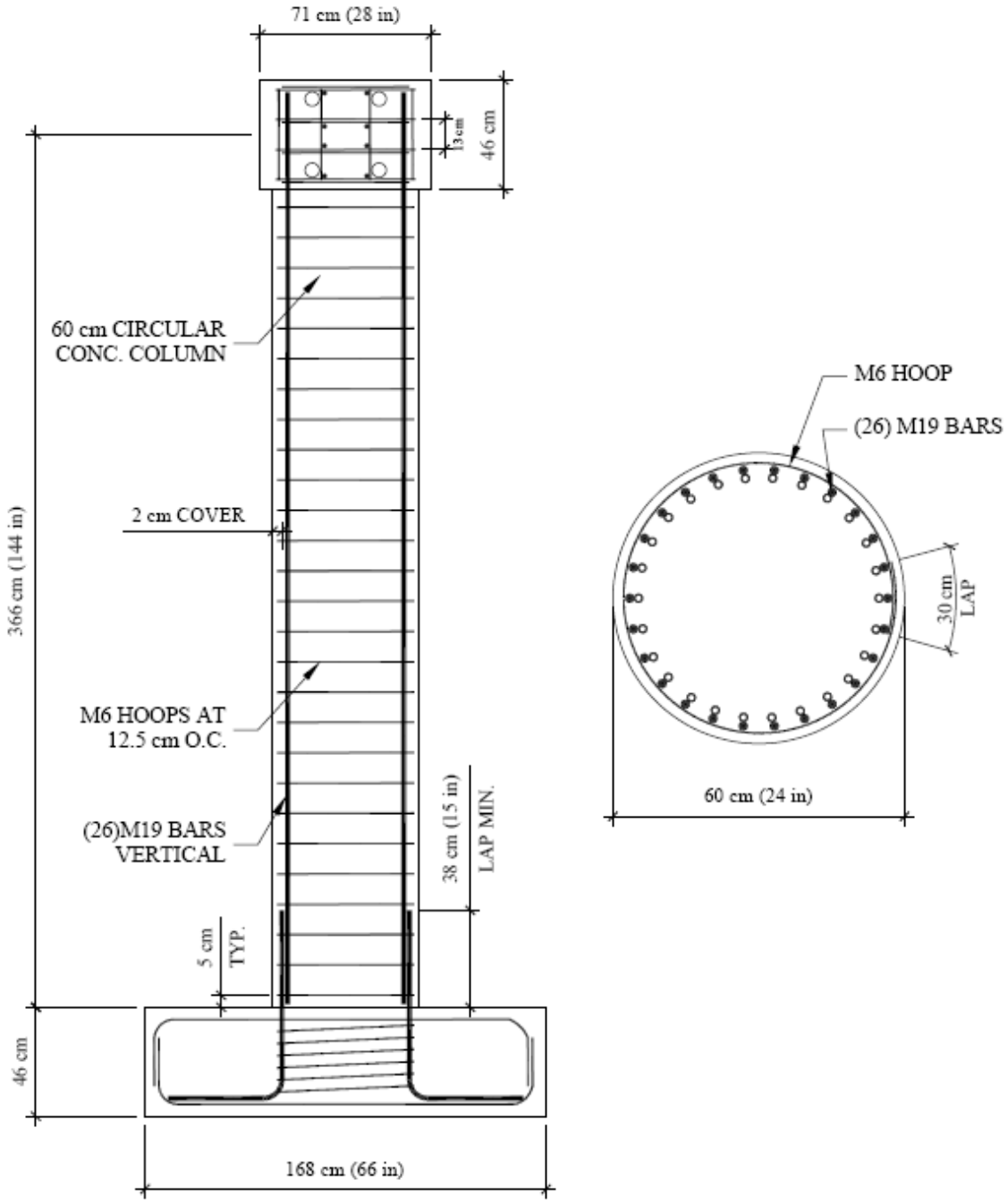

Figure 2-9: Details of the Circular Lap Reinforced Flexure Column Test Specimen

The circular flexure column shown schematically in Figure 2-9 had an applied axial load during testing of 1780 KN (400 kips). This is based on a 29% axial load ratio.

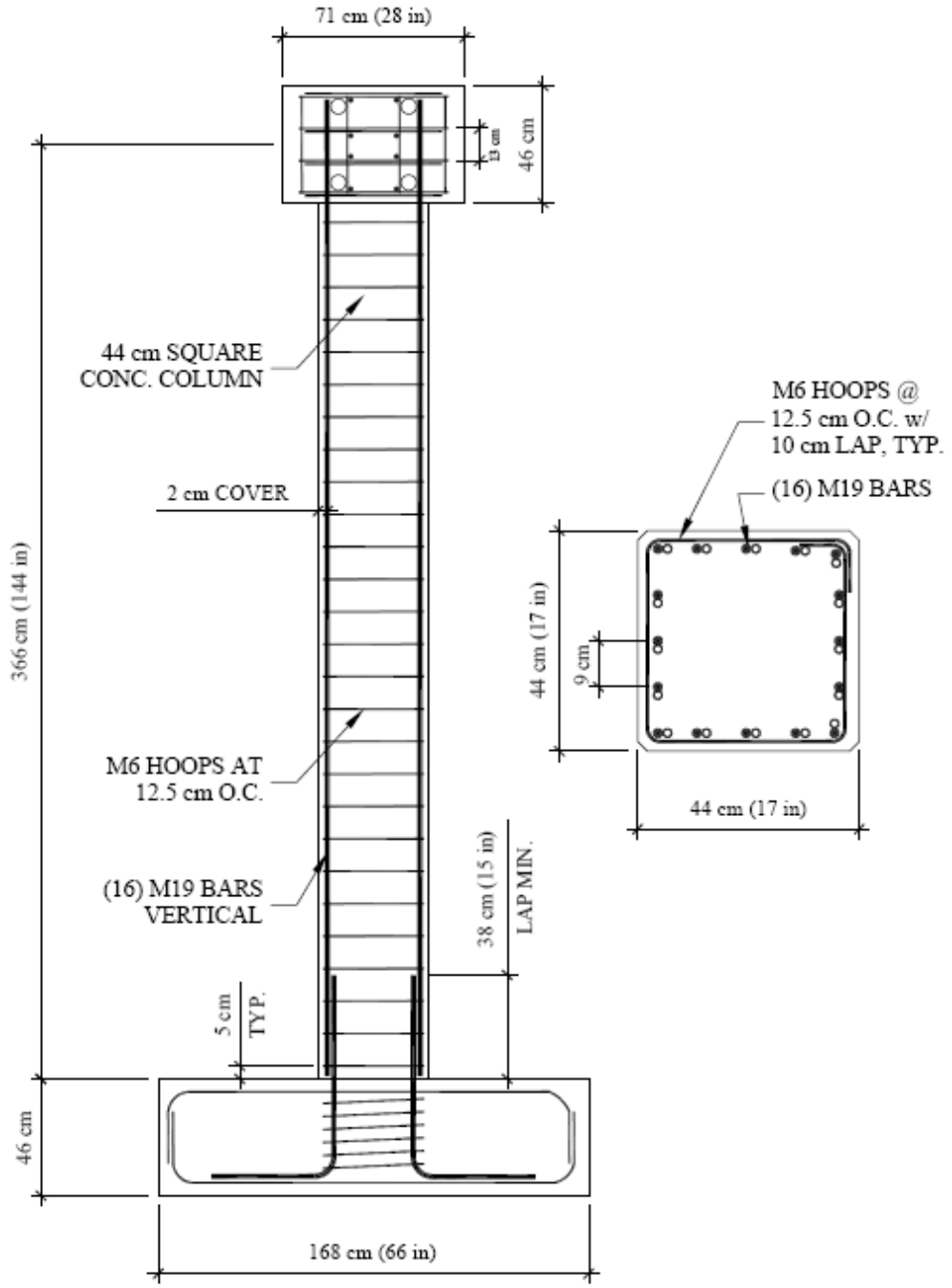

Figure 2-10: Details of the Square Lap Reinforced Flexure Column Test Specimen

The square flexure column shown schematically in Figure 2-10 had an applied axial load during testing of 1155 KN (260 kips). This is based on a 29% axial load ratio.

The experimental shear columns, circular and square as shown in Figure 2-5 and Figure 2-6 respectively, were each designed at 2.44 meters (8 ft) high from top of base to bottom of load stub. The base and load stub were then designed for these columns to provide the proper restraint. The construction layout for the load stub is shown in Figure 2-11 and Figure 2-12.

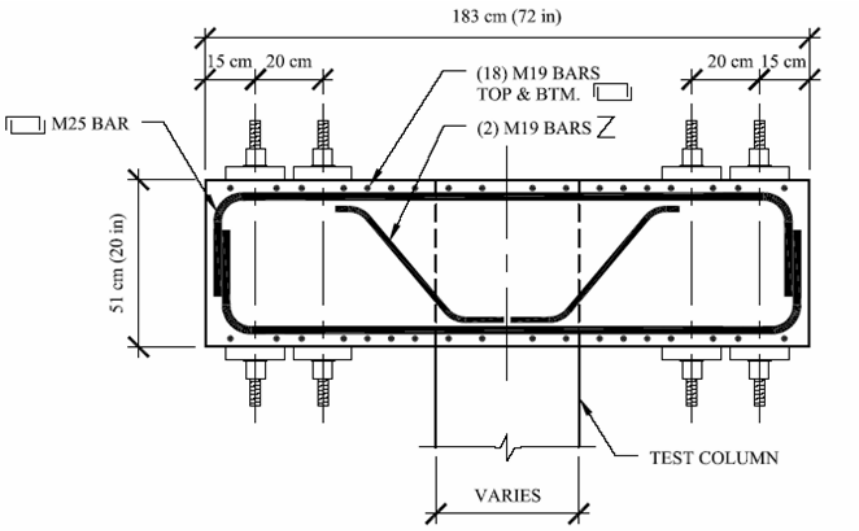

Figure 2-11: Schematic of Longitudinal Section of Shear Column Load Stub

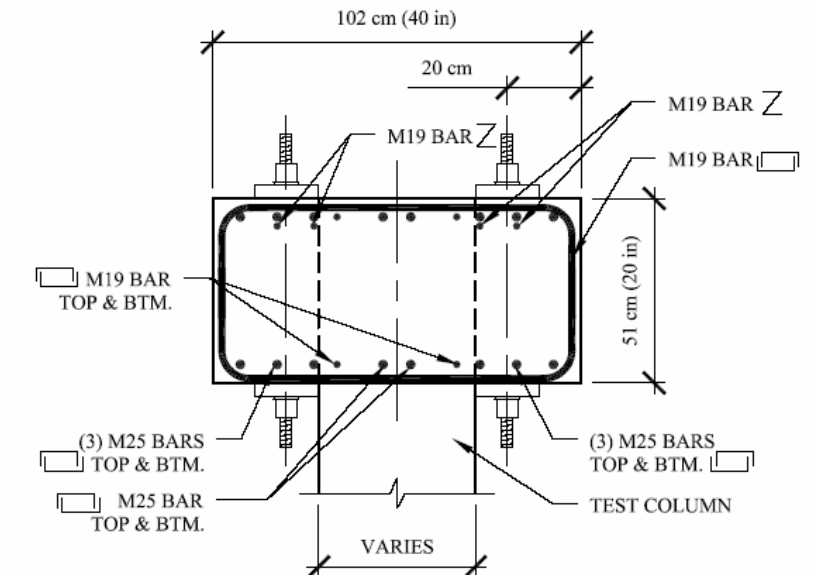

Figure 2-12: Schematic of Transverse Section of Shear Column Load Stub

Since these shear columns are being tested as having a fixed base and fixed cap (fixed = no rotation, only deflection), the base and load stub design required the necessary strength and capacity to transfer high deflections with no rotation to the column specimen without inducing failure. This "fixed-fixed" scheme was used in order to produce the required load in the column necessary to replicate the introduction of a shear failure mechanism in an "as-built" column.

For the column base, the construction details were the same for all six (6) test columns and are shown in Figures 2-13 to 2-15. This is due to the fact that all the column analysis is based on a fixed restraint at the base. The flexure columns detailed with continuous reinforcement shown in Figure 2-7 and Figure 2-8 and lap reinforced illustrated in Figure 2-9 and Figure 2-10 required a different construction configuration. Their heights are specified at 3.66 meter (12 ft) from top of base to center of load stub. The load stub configuration for the flexure columns is different and rather simple in comparison with the shear columns, since its main use is to provide a way to connect the test column to the loading mechanism. The flexural columns' load stub construction schematics are shown in Figure 2-16 and Figure 2-17.

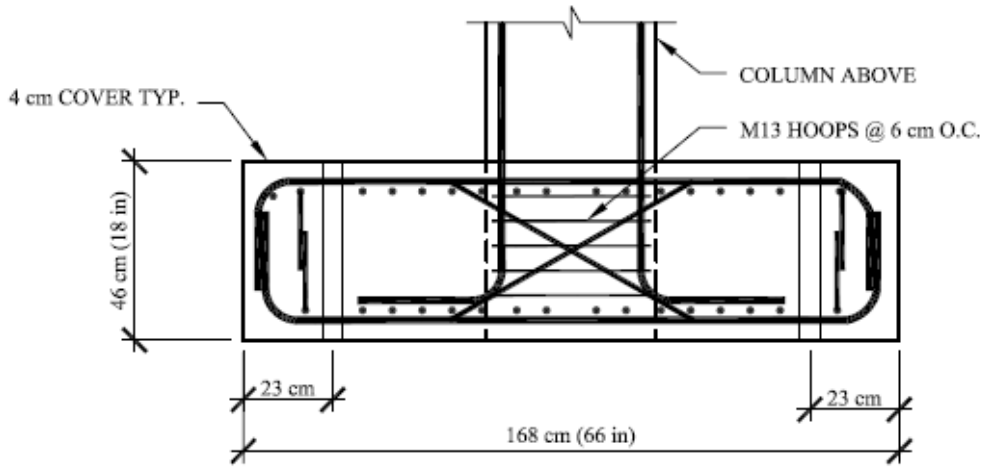

Figure 2-13: Sectional Schematic of Column Base

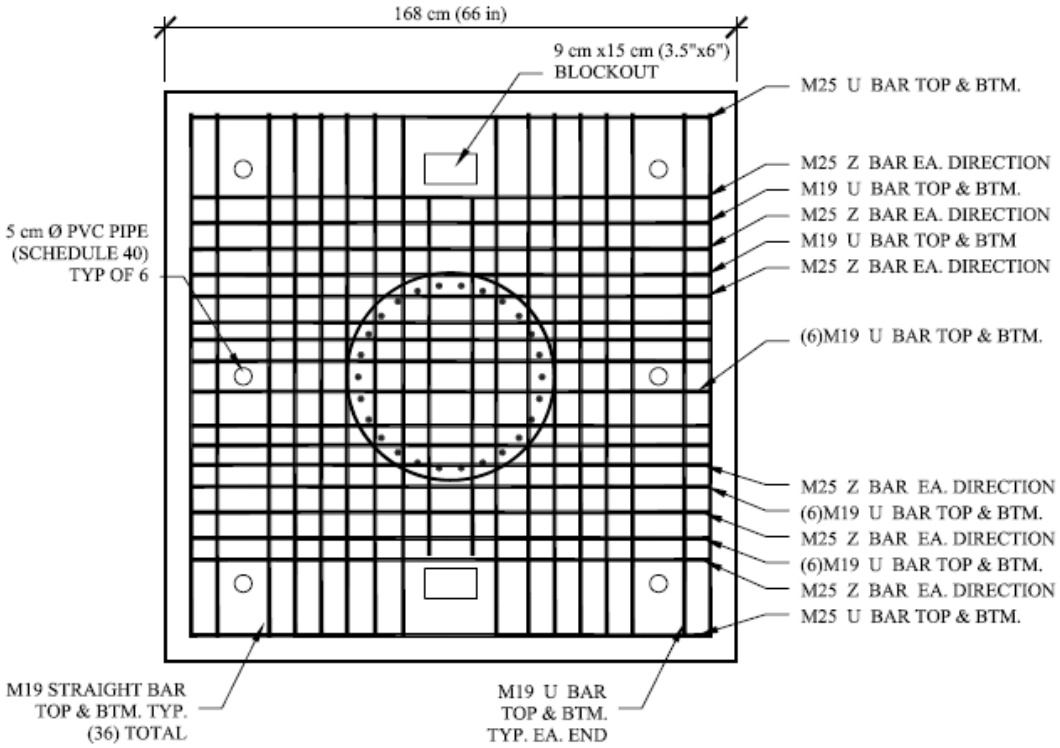

Figure 2-14: Plan View Schematic of Circular Column Base

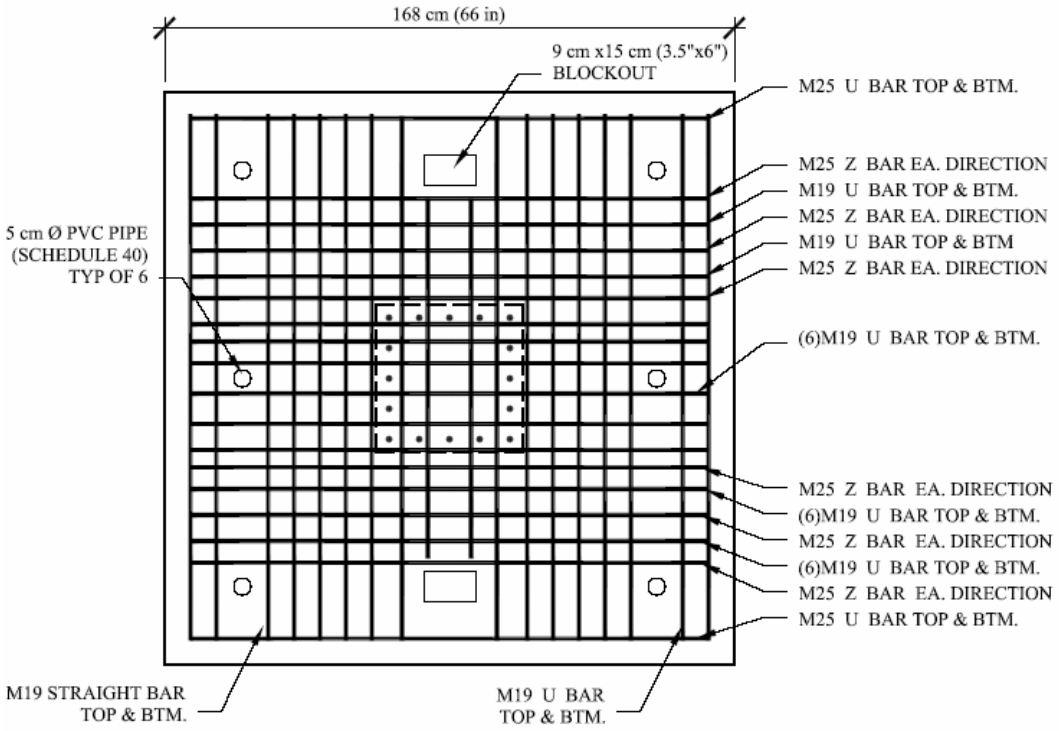

Figure 2-15: Plan View Schematic of Square Column Base

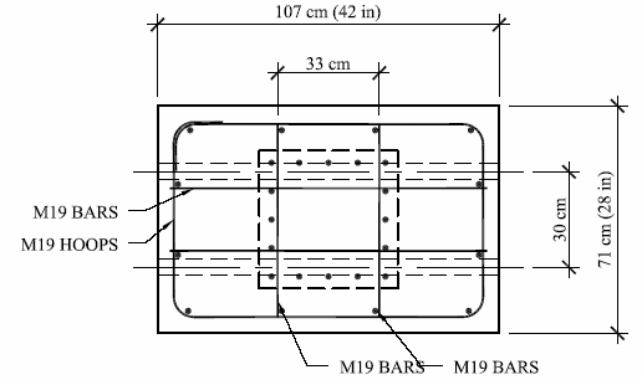

Figure 2-16: Flexure Load Stub Plan View Schematic

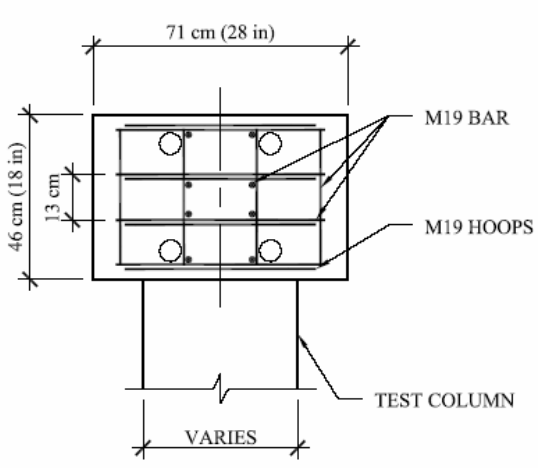

Figure 2-17: Flexure Load Stub Section Schematic

With the testing protocol chosen and the column elements designed, each of the tests specimens can then be constructed. This progression is presented in the following chapters based on the column type, since each had their own construction processes due to geometry and reinforcement layout. The retrofit of each of the test columns was not dependant on the column types and is therefore presented below as a standard fabrication procedure.

2.3.2 Retrofit Application

The novel carbon/epoxy/expansive foam sandwich panel retrofit jackets used as part of

this study are produced by Merkel Composites. The number of carbon layers and the thickness of the foam core were designed based on requirements of performance set by the HITEC protocol [11] for retrofitted specimens. A typical cross section of the applied retrofit jacket is given by a schematic in Figure 2-18.

The process of application involves a wet-layup process and the need for a jacket mold. The photographs in Figure 2-19 to Figure 2-29 show the jacket application process. A steel mold was used for the retrofit of the experimental test columns. The mold was first cleaned, polished and then a release agent was applied to the interior face of the mold before the fabric was placed as shown in Figures 2-18.

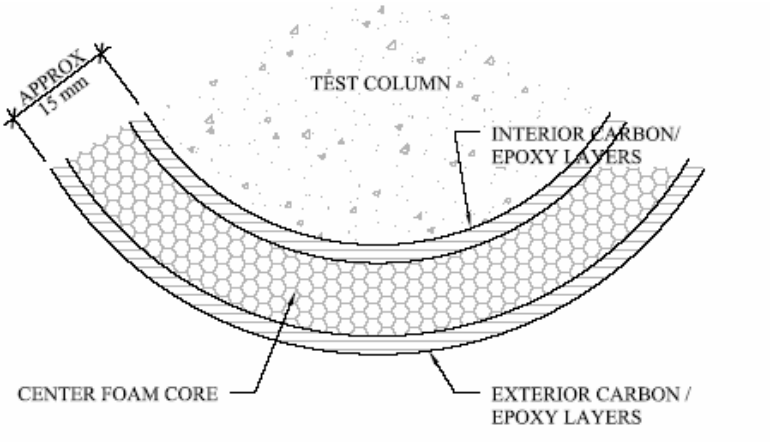

Figure 2-18: Cross Section of Typical Retrofit Jacket

The composite layers were constructed with a two-part epoxy resin that was weighed and mixed at a 2:1 ratio of resin to hardener. This system was used to wet out the unidirectional carbon sheets. The first fabric layer was draped in the mold and then pressed to remove any entrapped air before the next layer was added to the exterior shell construction in the jacket mold. This process is shown in Figure 2-20 and Figure 2-21. The process was then repeated as required to obtain the necessary composite thickness of approximately 1.5 mm for each column.

Figure 2-19: Application of Mold Release

Figure 2-20: Placement of Carbon Fabric

In order to prepare the concrete substrate for application of the inner layer of the composite, the surface was lightly sanded by hand and then the epoxy mixture was rolled onto the surface as illustrated in Figure 2-22. A unidirectional carbon fabric was then horizontally placed around the column circumference processed following the same procedures as used for the exterior skin.

With the carbon composite skins formed, the prepared steel mold was then lifted into place. Before the mold was placed, a half inch steel plate was placed at the base of the column to provide for the necessary jacket gap between the column and its base. The seal between the mold and steel plate was provided by simple modeling clay. This progression of lifting and placing the steel mold around the column is shown in Figure 2-24 and Figure 2-25.

Figure 2-21: Jacket Construction

Figure 2-22: Column Preparation

Figure 2-23: Shell Construction

Figure 2-24: Placement of Steel Mold

Figure 2-25: Placement of Steel Mold

With the steel mold in place and prior to bolting the mold halves together, the exterior composite shell halves were lapped at the seams. This was accomplished by tucking one edge under the other as seen in Figure 2-26. The lap length varied in the column wrapping on the 6-columns due to the construction process from 10 cm to 20 cm. Once this lapping was complete the mold was bolted together at the seams.

Figure 2-26: Lapping of the Jacket Seams

Figure 2-27: Pouring of Expandable Foam Core

With the carbon jacket shells constructed within the steel mold, the mold in place and bolted together, an expanding resin to foam system was prepared for installation as the retrofit jacket foam core center. The core material was comprised of a two-part urethane type resin system with each component weighed to ensure the proper 2:1 ratio. Once the mixture was combined and mixed, it was immediately poured into the void between the two carbon shells. The core component had a quick set time of 90 seconds requiring the immediacy of placement. A demonstration of this placement is presented in Figure 2-27.

Once the foam mixture was in place, a 4-hour cure was used before the removal of the steel mold shown in Figure 2-28. During this cure time, the foam component expands and also

undergoes an exothermic reaction. This reaction has the added benefit of forcing resin into the fabric skins, post curing the carbon shells, and increasing the compaction of the fabric layers, thereby increasing the mechanical properties of the composite. Once the jacket has cured, the removal of the mold may take place. This is shown in Figure 2-29. At this time, the column strengthening system is complete.

Figure 2-28: Curing of Jacket

Figure 2-29: Removal of Steel Mold

Each square and circular column jacket was formed with the same process as described above and with the same circular steel mold. This provided the same retrofit procedure for all six-test columns with only the addition of extra core material in the square jackets as illustrated in Figure 2-30.

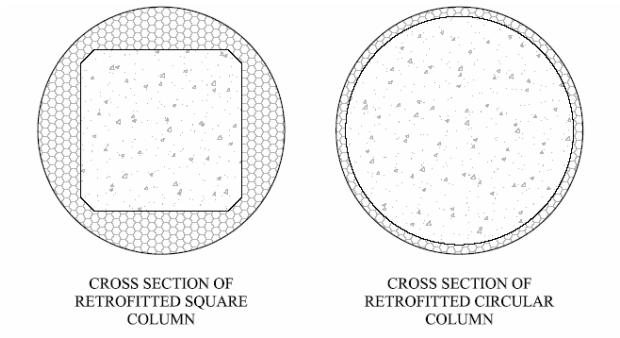

Figure 2-30: Retrofitted Column Cross Section Schematics

2.3.3 Testing Procedure

The testing procedure requires different loading values for the laboratory experiments because each column varies in its reinforcement layout. For each column a need for determining the specimen's non-strengthened ductility will be required. To establish a test specimen's theoretical curvature and displacement ductility per the testing protocol, moment curvature analysis was used based on the specific reinforcement and cross sectional properties used for the test. An example of the moment curvature and ductility calculations performed for each column is shown in Figure 2-31.

The details in the example are denoted by numerical annotation, as listed below:

1. This table identifies the column properties.
    a. Height is the column height defined as the clear height dimension (top of base to bottom of load stub),
    b. f'c is the concrete compressive strength determined by cylinder compression tests,
    c. f_y is the yield strength of the internal steel reinforcement,
    d. d_b is the diameter of the column reinforcement bars, and
    e. A_s is the area of tension reinforcement of a given cross section.

Column Ductility *Square Shear Column*

Height (cm):	244	c (cm):	15.62		I_g (cm^4):	219561
f'c (MPa):	43.0	d (cm):	38.42		I_e (cm^4):	153693
fy (MPa):	467.44	d' (cm):	4.76		E (MPa):	31241
d_b (cm):	1.91	b (cm):	43.18		P (kN):	458
As (cm^2):	45.42	a (cm):	13.28		M (cm-kN):	39046

1 2 3

Column Ductility Design:

At Theoretical First Yield

4

$\phi_y = M / E I_e =$	0.00008	
$\Delta_y = \phi_y L^2 / 3 =$	1.612	cm
$V_y = M_y /$ Height =	160	kN

At Probable Postyield:

5

Plastic Hinge = $0.2 L^1 =$	48.77	cm
$\phi_u = .005 / c =$	0.00032	
$\Delta_p = (\phi_u - \phi_y) L_p (L - L_p/2) =$	2.556	cm
$\Delta_u = \Delta_y + \Delta_p =$	4.168	cm

Theoretical Column Ductilities:

6

$\mu = \phi_u / \phi_y =$	**3.94**
$\mu = \Delta_u / \Delta_y =$	**2.59**

Loading Sequence:

Load Control:

$V_y =$ **160 kN**

$V_{yi} =$ **256 kN**

7

% V_y	V (kN)
0.25	40
0.50	80
0.75	120
1.00	160

Displacement Control:

8

μ	Δ (cm)
1.00	1.612
1.50	2.418
2.00	3.223
3.00	4.835
4.00	6.447
5.00	8.058
6.00	9.670
8.00	12.893
10.00	16.117

Figure 2-31: Example of Column Testing Sequence Calculation for As-Built Test Specimens

All of these items were determined based on the HITEC parameters in Table 2-5 and Table 2-6 as part of the specimen configurational parameters.

2. This table lists the calculated cross sectional section properties determined according to accepted reinforced concrete column design procedures [39].
    a. c is the depth of the compression area of the column when axially loaded,
    b. d is the distance from the extreme compression fiber to the centroid of the tension reinforcement,
    c. d' is the distance from the extreme compression fiber to the centroid of the compression reinforcement,
    d. b is the cross-sectional width, and
    e. a is the design variable for the depth of the equivalent rectangular stress block distributed over a compression zone bounded by edges of the cross section and a straight line located parallel to the neutral axis at a distance $\beta_1 c$ from the maximum compressive strain.
3. This table lists the calculated strength properties of the test column wherein
    a. Ig is the gross moment of inertia,
    b. Ic is the cracked moment of inertia based on a 70% standard reduction of the gross moment of inertia,
    c. E is the Young's modulus for concrete ($E = 57000 \sqrt{f'c}$ for normal weight concrete),
    d. P is the applied axial load based on the HITEC protocol axial load ratio, and
    e. M is the available moment capacity within the column with the noted axial loading (determined using accepted concrete column design [39] with an interaction

diagram as shown in Figure 2-3).

4. These equations calculate the first yield of the column under the loading listed in the values of annotation 3 [38].
5. These equations calculate the probable post yield deflection and curvature responses of the column under the loading listed in the values of annotation 3 [38].
6. These values represent the calculated column ductilities based on deflection and curvature [38]. These become the base line for the retrofitted column ductility performance reviewed at the end of testing to determine if strengthening procedure meets the standards set by the testing protocol.
7. This table presents the values used in the laboratory testing as part of the cyclic loading sequence described in Figure 2-4 while under load control.
8. This table presents the values used in the laboratory testing as part of the cyclic loading sequence described in Figure 2-4 while under displacement control loading levels.

The values of annotation 7 and 8 are based off the moment-curvature analysis and ductility measurement, respectively. Figures 2-32 through Figure 2-37 present the load testing sequence calculations for each of the test columns.

With the testing protocol set, the test elements designed, the strengthening process in place and the procedure of the experimental testing assigned each column was then tested. The subsequent chapters present the testing results.

Column Ductility

Circular Shear Column

Height (cm):	244	c (cm):	25.12	I_g (cm^4):	677872
f'c (MPa):	43.00	d (cm):	56.20	I_e (cm^4):	474511
fy (MPa):	467.44	d' (cm):	4.76	E (MPa):	31241
d_b (cm):	1.91	b (cm):	60.96	P (kN):	649
As (cm^2):	74.20	a (cm):	21.35	M (cm-kN):	77806

Column Ductility Design:

At Theoretical First Yield

$\phi_y = M / E I_e =$	0.00005	
$\Delta_y = \phi_y L^2 / 3 =$	1.040	cm
$V_y = M_y /$ Height =	319	kN

At Probable Postyield:

Plastic Hinge = $0.2 L^1 =$	48.77	cm
$\phi_u = .005 / c =$	0.00020	
$\Delta_p = (\phi_u - \phi_y) L_p (L - L_p/2) =$	1.569	cm
$\Delta_u = \Delta_y + \Delta_p =$	2.609	cm

Theoretical Column Ductilities:

$\mu = \phi_u / \phi_y =$	**3.79**
$\mu = \Delta_u / \Delta_y =$	**2.51**

Loading Sequence:

Load Control:

V_y = 319 kN

V_{yi} = 511 kN

% V_y	V (kN)
0.25	80
0.50	160
0.75	239
1.00	319

Displacement Control:

μ	Δ (cm)
1.00	1.040
1.50	1.560
2.00	2.080
3.00	3.121
4.00	4.161
5.00	5.201
6.00	6.241
8.00	8.322
10.00	10.402

Figure 2-32: Circular Shear Column Testing Sequence Calculations

Column Ductility *Square Shear Column*

Height (cm):	244	c (cm):	15.62	I_g (cm^4):	219561
f'c (MPa):	43.0	d (cm):	38.42	I_e (cm^4):	153693
fy (MPa):	467.44	d' (cm):	4.76	E (MPa):	31241
d_b (cm):	1.91	b (cm):	43.18	P (kN):	458
As (cm^2):	45.42	a (cm):	13.28	M (cm-kN):	39046

Column Ductility Design:

At Theoretical First Yield

$\phi_y = M / E I_e =$	0.00008	
$\Delta_y = \phi_y L^2 / 3 =$	1.612	cm
$V_y = M_y$ / Height =	160	kN

At Probable Postyield:

Plastic Hinge = $0.2 L^1 =$	48.77	cm
$\phi_u = .005 / c =$	0.00032	
$\Delta_p = (\phi_u - \phi_y) L_p (L - L_p/2) =$	2.556	cm
$\Delta_u = \Delta_y + \Delta_p =$	4.168	cm

Theoretical Column Ductilities:

$\mu = \phi_u / \phi_y =$	**3.94**
$\mu = \Delta_u / \Delta_y =$	**2.59**

Loading Sequence:

Load Control:

$V_y =$ **160 kN**

$V_{yi} =$ **256 kN**

% V_y	V (kN)
0.25	40
0.50	80
0.75	120
1.00	160

Displacement Control:

μ	Δ (cm)
1.00	1.612
1.50	2.418
2.00	3.223
3.00	4.835
4.00	6.447
5.00	8.058
6.00	9.670
8.00	12.893
10.00	16.117

Figure 2-33: Square Shear Column Testing Sequence Calculations

Column Ductility *Circular Continuous Flexural*

Height (cm):	366	c (cm):	26.80	I_g (cm^4):	677872
f'c (MPa):	39.50	d (cm):	56.20	I_e (cm^4):	474511
fy (MPa):	467.44	d' (cm):	4.76	E (MPa):	29721
d_b (cm):	1.91	b (cm):	60.96	P (kN):	1779
As (cm^2):	74.20	a (cm):	22.78	M (cm-kN):	70174

Column Ductility Design:

At Theoretical First Yield

$\phi_y = M / E I_e =$	0.00005	
$\Delta_y = \phi_y L^2 / 3 =$	2.219	cm
$V_y = M_y /$ Height =	192	kN

At Probable Postyield:

Plastic Hinge = 0.2 L^{1} =	73.15	cm
$\phi_u = .005 / c =$	0.00019	
$\Delta_p = (\phi_u - \phi_y) L_p (L - L_p/2) =$	3.294	cm
$\Delta_u = \Delta_y + \Delta_p =$	5.513	cm

Theoretical Column Ductilities:

$\mu = \phi_u / \phi_y =$	**3.75**
$\mu = \Delta_u / \Delta_y =$	**2.48**

Loading Sequence:

Load Control:

V_y = 192 kN

V_{yi} = 307 kN

% V_y	V (kN)
0.25	48
0.50	96
0.75	144
1.00	192

Displacement Control:

μ	Δ (cm)
1.00	2.219
1.50	3.328
2.00	4.438
3.00	6.657
4.00	8.875
5.00	11.094
6.00	13.313
8.00	17.751
10.00	22.189

Figure 2-34: Circular Continuously Reinforced Flexural Column Testing Sequence Calculations

Column Ductility *Square Continuous Flexural*

Height (cm):	366	c (cm):	17.23	I_g (cm^4):	219561
f'c (MPa):	39.50	d (cm):	38.42	I_e (cm^4):	153693
fy (MPa):	467.44	d' (cm):	4.76	E (MPa):	29747
d_b (cm):	1.91	b (cm):	43.18	P (kN):	1156
As (cm^2):	45.42	a (cm):	14.64	M (cm-kN):	40795

Column Ductility Design:

At Theoretical First Yield

$\phi_y = M / E I_e =$	0.00009	
$\Delta_y = \phi_y L^2 / 3 =$	3.979	cm
$V_y = M_y /$ Height =	112	kN

At Probable Postyield:

Plastic Hinge = 0.2 L [1] =	73.15	cm
$\phi_u = .005 / c =$	0.00029	
$\Delta_p = (\phi_u - \phi_y) L_p (L - L_p/2) =$	4.841	cm
$\Delta_u = \Delta_y + \Delta_p =$	8.820	cm

Theoretical Column Ductilities:

$\mu = \phi_u / \phi_y =$	**3.25**
$\mu = \Delta_u / \Delta_y =$	**2.22**

Loading Sequence:

Load Control:

V_y = 112 kN

V_{yi} = 178 kN

% V_y	V (kN)
0.25	28
0.50	56
0.75	84
1.00	112

Displacement Control:

μ	Δ (cm)
1.00	3.979
1.50	5.968
2.00	7.958
3.00	11.937
4.00	15.916
5.00	19.895
6.00	23.874
8.00	31.832
10.00	39.790

Figure 2-35: Square Continuously Reinforced Flexural Column Testing Sequence Calculations

Column Ductility *Circular Lap Splice Flexural*

Height (cm):	366	c (cm):	24.89	I_g (cm^4):	677872
f'c (MPa):	49.30	d (cm):	56.20	I_e (cm^4):	474511
fy (MPa):	467.44	d' (cm):	4.76	E (MPa):	33230
d_b (cm):	1.91	b (cm):	60.96	P (kN):	1779
As (cm^2):	74.20	a (cm):	21.16	M (cm-kN):	79271

Column Ductility Design:

At Theoretical First Yield

$\phi_y = M / E I_e =$	0.00005	
$\Delta_y = \phi_y L^2 / 3 =$	2.242	cm
$V_y = M_y /$ Height =	217	kN

At Probable Postyield:

Plastic Hinge = 0.2 L^1 =	73.15	cm
$\phi_u = .005 / c =$	0.00020	
$\Delta_p = (\phi_u - \phi_y) L_p (L - L_p/2) =$	3.627	cm
$\Delta_u = \Delta_y + \Delta_p =$	5.869	cm

Theoretical Column Ductilities:

$\mu = \phi_u / \phi_y =$	**4.00**
$\mu = \Delta_u / \Delta_y =$	**2.62**

Loading Sequence:

Load Control:

$V_y =$ **217 kN**

$V_{yi} =$ **347 kN**

% V_y	V (kN)
0.25	54
0.50	108
0.75	163
1.00	217

Displacement Control:

μ	Δ (cm)
1.00	2.242
1.50	3.363
2.00	4.484
3.00	6.726
4.00	8.968
5.00	11.209
6.00	13.451
8.00	17.935
10.00	22.419

Figure 2-36: Circular Lap Reinforced Flexural Column Testing Sequence Calculations

Column Ductility *Square Lap Splice Flexural*

Height (cm):	366	c (cm):	14.60	I_g (cm^4):	219561
f'c (MPa):	49.30	d (cm):	38.42	I_e (cm^4):	153693
fy (MPa):	467.44	d' (cm):	4.76	E (MPa):	32311
d_b (cm):	1.91	b (cm):	43.18	P (kN):	1156
As (cm^2):	45.42	a (cm):	12.41	M (cm-kN):	43777

Column Ductility Design:

At Theoretical First Yield

$\phi_y = M / E I_e =$	0.00009	
$\Delta_y = \phi_y L^2 / 3 =$	3.931	cm
$V_y = M_y /$ Height =	128	kN

At Probable Postyield:

Plastic Hinge = $0.2 L^1 =$	73.15	cm
$\phi_u = .005 / c =$	0.00034	
$\Delta_p = (\phi_u - \phi_y) L_p (L - L_p/2) =$	6.123	cm
$\Delta_u = \Delta_y + \Delta_p =$	10.054	cm

Theoretical Column Ductilities:

$\mu = \phi_u / \phi_y =$	**3.88**
$\mu = \Delta_u / \Delta_y =$	**2.56**

Loading Sequence:

Load Control:

V_y = 128 kN

V_{yi} = 205 kN

% V_y	V (kN)
0.25	32
0.50	64
0.75	96
1.00	128

Displacement Control:

μ	Δ (cm)
1.00	3.931
1.50	5.897
2.00	7.862
3.00	11.793
4.00	15.725
5.00	19.656
6.00	23.587
8.00	31.449
10.00	39.312

Figure 2-37: Square Lap Reinforced Flexural Column Testing Sequence Calculations

3. Experimental Tests and Results for Shear Columns

3.1 Introduction

The objective of the test program was to evaluate a new composite jacketing system for its suitability as a retrofit alternative. The evaluation was conducted pursuant to the published HITEC procedure [11] to enable assessment of whether the new system could meet standardized requirements.

In this chapter, the testing and evaluation of the carbon fabric - expansive foam core sandwich panel jacket applied to the two (2) reinforced concrete shear test columns with circular and square cross sections is outlined. Each of these columns was tested under increasing cyclic quasi-static lateral loads to ascertain if the retrofit jacket allowed each column to:

1. Attain or exceed the HITEC protocol specifications for improved ductility;
2. Ensure stability under repetitive cycling at a pre-specified displacement, and
3. Provide adequate energy absorption during cycling as evident by the area within the hysteresis loops.

3.2 Test Specimens Construction

Laboratory experiments for the expansive foam sandwich panel jacketed systems were conducted under the guidelines of Report No. 2001/10 "FRP Composite Column Wrap Durability Evaluation" submitted to HITEC and outlined in Chapter 2 [11]. Since the objective of the testing is to evaluate the composite retrofit system, such that the appropriate retrofit standards are met, the concrete columns were constructed to model a general field superstructure column that would require retrofitting. The test columns were therefore built to the required HITEC protocol specifications in order to ensure that the system could be comprehensively assessed.

With the retrofitted columns being the focus of the testing, both the load stub and base were designed to carry the applied test loads without failure. This was to ensure that the failure mechanism of each test was within the column retrofit area or in the connection region between the column and base/load stub. Because the interior steel reinforcement in the column is expected to yield, only the column longitudinal reinforcement bars were strain-gauged. A total of thirty-six gages were applied to the shear column reinforcement bars, as illustrated in Figure 3-1 and Figure 3-2.

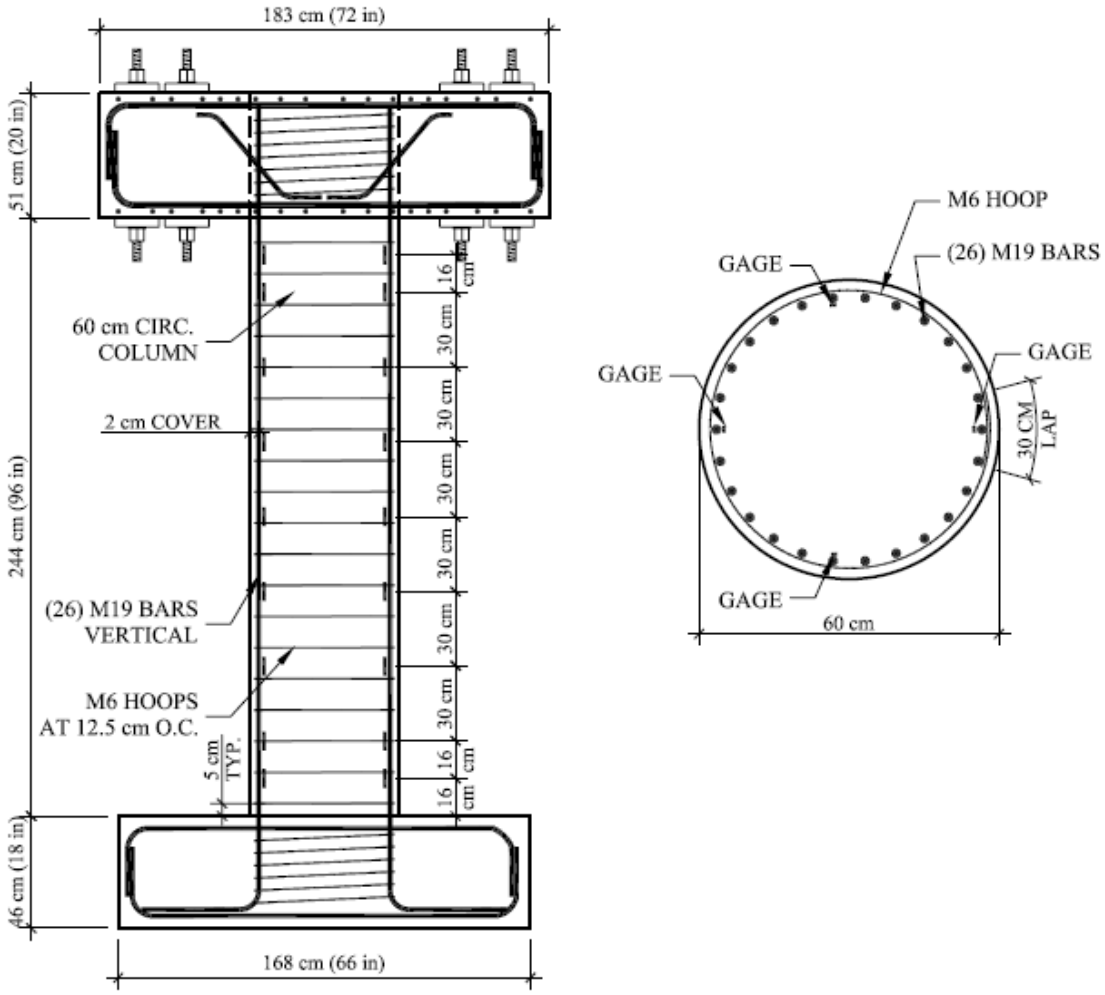

Figure 3-1: Schematic Showing Strain Gage Location on Circular Shear Column Reinforcing Cage

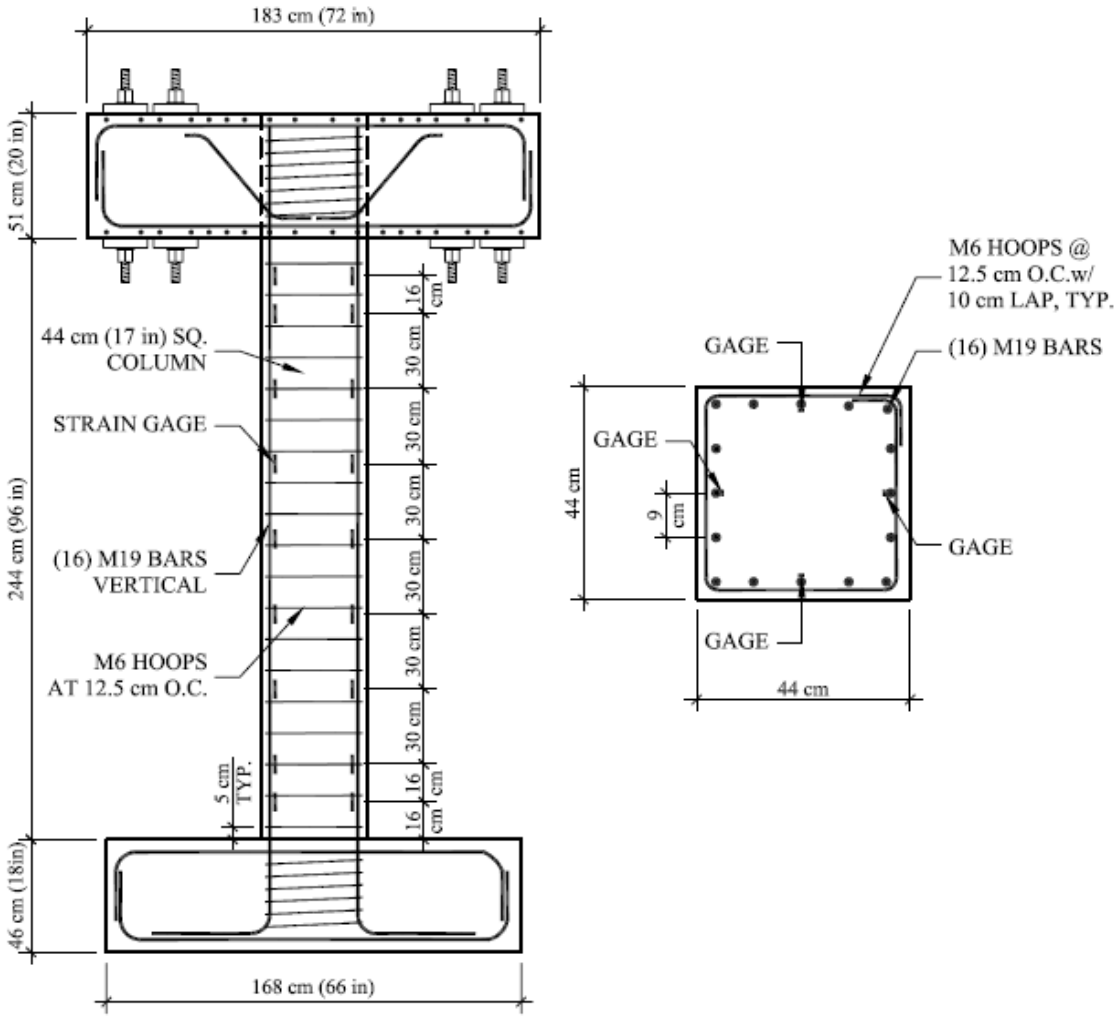

Figure 3-2: Schematic Showing Strain Gage Location on Square Shear Column Reinforcing Cage

With formwork built, concrete mix on-site and reinforcement prepared (strain-gauged) for testing, each of the shear columns was then constructed at the testing site. Stages of construction were photographed and included:

1. Completed reinforcement cages
2. Completed column concrete placement
3. Jacket application (as shown in Chapter 2)

The first construction stage involved the production of a square and circular column reinforcing cage. These column cages were formed with straight vertical bars and transverse hoops tied together. These column cages were constructed in tandem with the column bases. The reinforcement strength was tested at this time with reinforcement bars taken from the same batch as those used in the construction of the column cages. These results are listed in Table 3-1. Yield strength was measured at the stress level where the material strain changes from elastic deformation to plastic deformation, causing it to deform permanently (0.2%) and the ultimate strength is taken as the level of maximum stress that the reinforcement bar could withstand.

Figure 3-3: Shear Column Cages

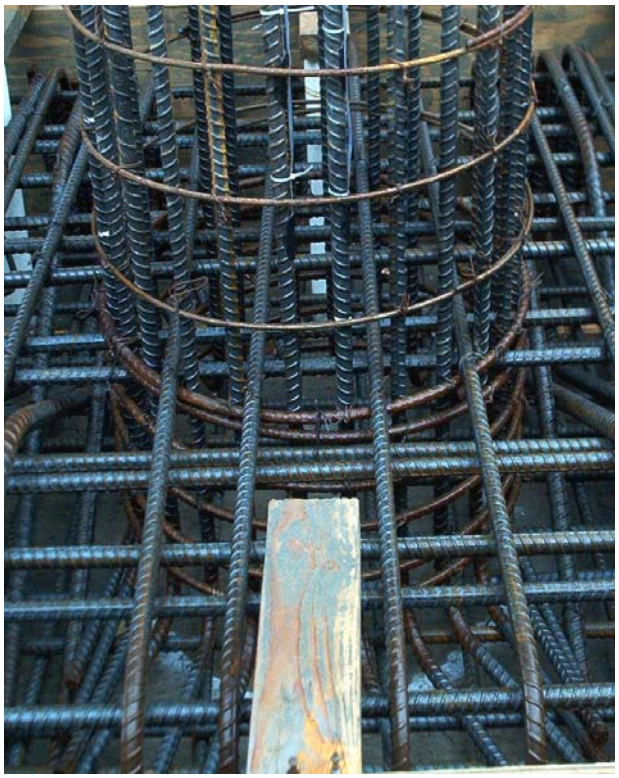

Figure 3-4: Shear Column Base

Table 3-1: Reinforcement Tension Test Data

Sample	*1*	*2*	*3*	***Average***
6 mm Diameter Horizontal Bar				
Yield Strength (MPa)	387.7	400.3	404.5	**397.5**
Ultimate Strength (MPa)	456.5	466.3	462.1	**461.6**
19 mm Diameter Vertical Bar				
Yield Strength (MPa)	476.2	477.2	473.0	**475.5**
Ultimate Strength (MPa)	764.2	766.8	762.9	**764.7**

Once the column base cages were encased within the column's casting formwork, concrete was poured as shown in Figure 3-5. The concrete poured was specified to have minimum 28 day compression strength of 20.7 MPa (3000 psi). Nine test cylinders were cast at this time as well to enable determination of the progression in the concrete compression strength until the day of testing. Figure 3-6 shows a finished base and Table 3-2 lists the resulting concrete compression strength taken from the test cylinders.

Figure 3-5: Column Base Concrete Pour

Figure 3-6: Finished Column Base Concrete

Table 3-2: Shear Column Base Concrete Compression Strength

	1	*2*	*3*	***Average***
7-Day Strength (MPa)	24.3	25.2	23.6	**24.4**
28-Day Strength (MPa)	37.7	37.4	37.6	**37.6**
D.O.T. Strength (MPa)	43.0	43.7	42.7	**43.2**

Once the column bases were poured, the formwork for the column was added around the reinforcement cages. Once in place the concrete was poured. This is illustrated in Figure 3-7 and Figure 3-8. Figure 3-7 shows the large hopper that was used to lift the concrete over the formed square column to allow for the placement of concrete from the top of the formwork. Figure 3-7 shows the use of a concrete vibrator which was dropped into the concrete filled column to ensure proper consolidation (removal of voids and air bubbles).

Figure 3-7: Shear Column Concrete Placement

Figure 3-8: Vibrating Shear Column Concrete for proper consolidation

The resulting concrete column was specified to have minimum 28 day compression strength of 20.7 MPa. Table 3-3 lists the compression values of the concrete cast in cylinders for the concrete shear columns. The day of testing (D.O.T.) strength is less than the 28-Day strength due to the fact that the columns were tested less than 28 days after beginning cast. Even though the concrete compression strength exceeded the minimum of 20.7 MPa, this does not necessarily invalidate the testing. A minimum concrete strength was given for test specimen protocol, but not a maximum. As these values are more than double the specified 28 day compression strength, this will affect the required axial pre-load on the columns. This pre-load is a function of compression strength and cross sectional area of the column. For the circular shear column the pre-load was 650 kN creating an axial load ratio of 5.4%. This is below the minimum requirement of 10% due to the fact that the pre-load value was based on 7-day concrete strength. The square column was pre-load 460 kN producing an axial load ratio of 5.5% which is also below the minimum 10% axial load ratio.

Table 3-3: Shear Column Concrete Compression Strength

	1	*2*	*3*	***Average***
7-Day Strength (MPa)	26.7	27.2	26.5	**26.8**
28-Day Strength (MPa)	43.5	47.5	45.3	**45.4**
D.O.T. Strength (MPa)	41.9	44.0	43.2	**43.0**

Due to the load stub complexity required on the shear columns, additional concrete was required to be placed prior to the conclusion of the test column construction. The load stubs were constructed such that the size and reinforcement due would support the testing procedure and test set-up required to induce a shear failure within the column. Figure 3-9 and Figure 3-10 show the amount of reinforcement steel present in the shear load stubs. The already cast circular column body can be seen in the center of Figure 3-10. After the load stubs were constructed and form

work added, concrete was placed to complete the two shear test columns. Table 3-4 below summarizes the concrete compressive strength from cylinders cast for the shear load stubs.

Figure 3-9: Shear Specimen Load Stub Cage

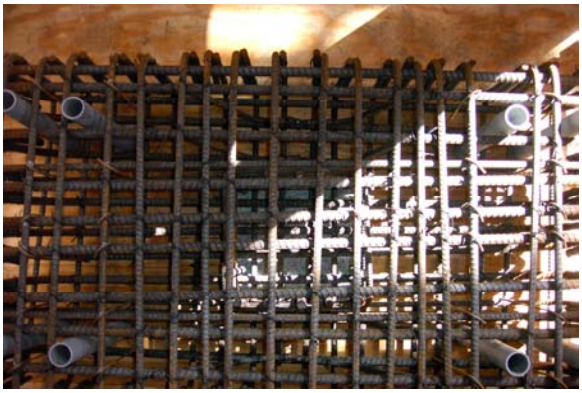

Figure 3-10: Shear Specimen Load Stub Cage

Table 3-4: Shear Column Load Stub Concrete Compression Strength

	1	*2*	*3*	***Average***
7-Day Strength (MPa)	28.3	26.8	27.0	**27.3**
28-Day Strength (MPa)	32.1	31.9	30.4	**31.5**
D.O.T. Strength (MPa)	41.8	38.9	43.9	**41.5**

With the construction of the shear test columns completed, the columns were scheduled to be wrapped with the experimental strengthening jackets 19 days after column concrete had been poured. This process is outlined in Chapter 2 since the process is common in all six of the test columns. With the retrofit jackets construction complete, thirty-two, 50 mm long strain gauges were applied to the jacket. These gauges were placed horizontally in the hoop direction on each face of the column in the same dimensional pattern as the reinforcement gauges in Figure 3-1 and Figure 3-2. These strain gauges were applied with a self-leveling adhesive to ensure a good bond to the carbon/epoxy jacket. Figure 3-11 and Figure 3-12 show the completed application of the jacket strain gages.

Figure 3-11: Jacket Gages at Located at North Load Face of Shear Column

Figure 3-12: Jacket Strain Gages at North and West Faces of Shear Column

3.2.1 Test Program

Each experimental shear test column was tied down to the laboratory's strong floor via six (6) high strength bars. Each of the bars was stressed to 445 kN (100 kips) to ensure stability of the base during testing. A schematic for the shear test set-up is given in Figure 3-13.

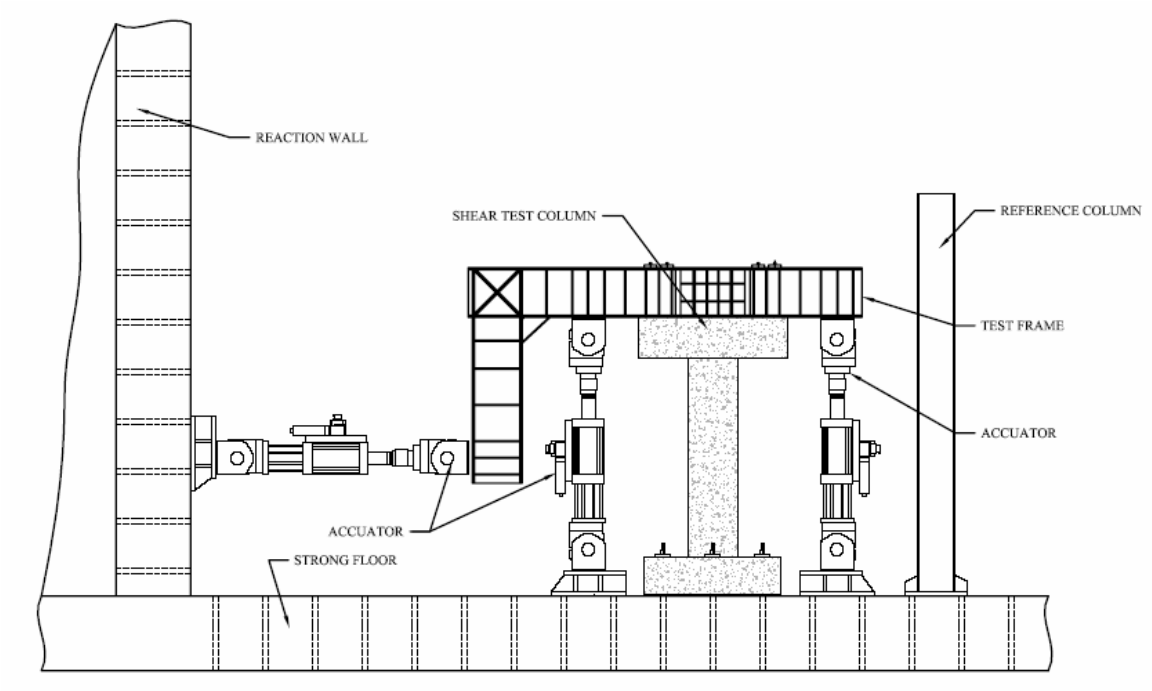

Figure 3-13: Typical Test Set-Up for Shear Columns

For the two experimental shear columns, the test set-up comprised of a shear test frame which was attached to the top of a column's load stub by means of eight (8) high strength bars pre-stressed to 445 kN (100 kips) each. This frame restrained the rotation at the top of the column, modeling a fixed support condition. A rotation-restricted condition is necessary to induce forces on the test column required for a structural shear failure. The load setup applied to the frame to restrict the column motion to strictly linear displacement was also used to simulate bridge superstructure self-weight. This compression load is given in Chapter 2 below Figure 2-5 and Figure 2-6 and was maintained through the (2) vertical actuators in conjunction with the testing program software. A 978 kN (220 kip) capacity actuator with a 22 cm (9-inch) stroke, reacting against the strong wall was attached to the leg of the frame providing the cyclic seismic horizontal load simulation. Figure 3-14 and Figure 3-15 are given to show this test set-up for the shear test columns.

Figure 3-14: Overview of Shear Test Set-Up

Figure 3-15: Overview of Shear Test Set-Up

With the test column connected to the load frame, the testing of the shear column began. In the following section, the testing and general observations for the circular and square shear column are reviewed.

3.3 Circular Shear Column

3.3.1 Observations

The retrofit circular shear column with continuous column reinforcement was constructed and was wrapped with the experimental retrofit jacket and then tested approximately 24 days after the specimen had been cast.

Based on the listed material properties in Table 3-1 and Table 3-3, which were determined from earlier material testing, the theoretical yield force V_y = 319 kN (72 kips) and ideal flexural capacity V_{yi} = 511 kN (115 kips) were calculated using the procedure presented in Chapter 3 for each of the shear columns. The pseudo-superstructure load applied to the column was 592 kN (133 kips) in addition to the 58 kN (13 kip) weight of the testing frame acting as the columns axial load. Assuming an elasto-plastic response approximation, the experimental first yield displacement Δ_y = 1.006 cm (0.396 in) was expected based on the above values.

The theoretical ductilities corresponding to curvature and deflection for the constructed, non-retrofitted column was then determined from the above calculated column design values. (See Chapter 2 Figure 2-32 for calculations). The resulting "as-built" column ductilities based on deflection ($\mu_\Delta = \Delta_u/\Delta_y$) and column curvature ($\mu_\phi = \phi_u/\phi_y$) are listed in Table 3-5. According to the HITEC protocol, the retrofitted column must exceed these calculated values by the specified amounts of: μ_ϕ = 2.0 x "as-built" and μ_Δ = 1.5 x "as-built".

Table 3-5: Resulting "As-Built" Ductilities

ϕ_y =	0.00005	μ_ϕ =	3.79
ϕ_u =	0.00020		
Δ_y =	1.040 cm	μ_Δ =	2.51
Δ_u =	2.609 cm		

With the "as-built" theoretical column ductilities calculated, the loading sequence for the test was established. The circular shear column testing was begun under load control. The column was stiffer than anticipated at the end of the load control cycles. Neither the experimental deflection nor column reinforcement strains came close to the theoretical values under its Vy loading (a load of 319 kN should yield a deflection of 1.01 cm). Once reinforcement gauge readings reached 2000 με (strain when reinforcement stress has reached its yield point: $\varepsilon = f_y/E$) it was determined that the steel reinforcement had yielded. At the Vy loading the rebar strains were slightly less than 50% of the yield strain (900 με) as seen in Figure 3-15. The strain gauges on North Face were damaged during construction with only one gauge functioning at testing; therefore the South Face readings measurements were available to determine reinforcement yielding.

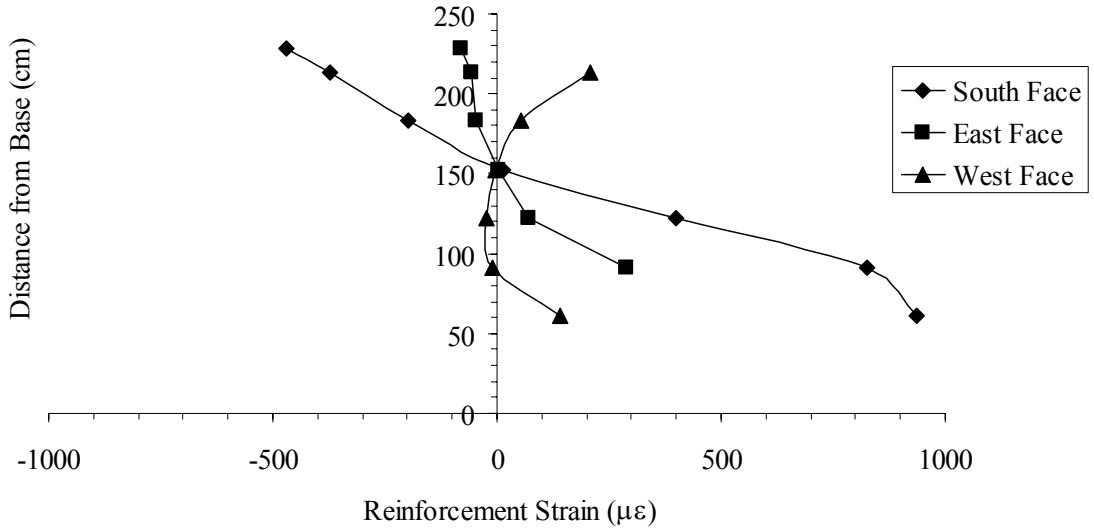

Figure 3-16: Reinforcement Test Strains at Vy Loading

Figures 3-17 through Figure 3-19 show how the rebar strain changed under load control cycles at different locations along the column.

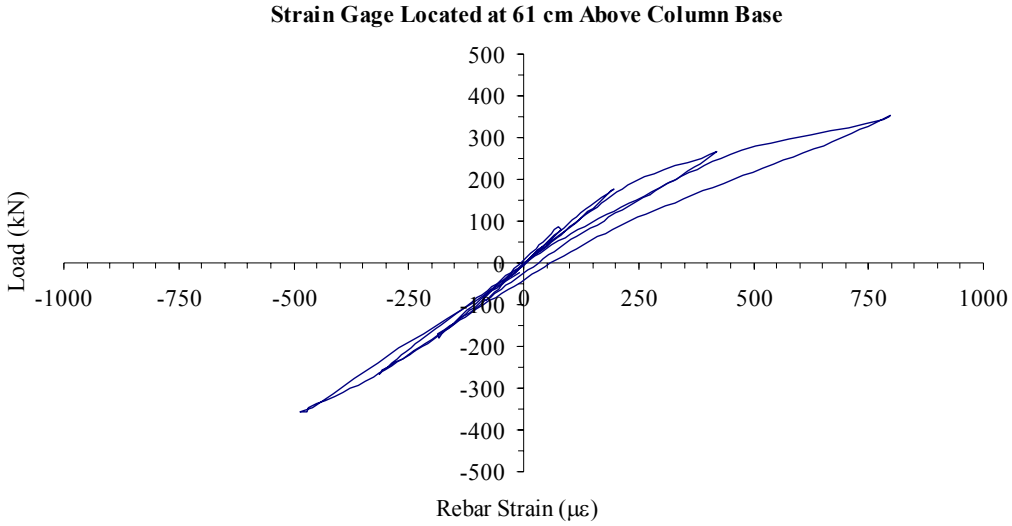

Figure 3-17: South Face Reinforcement Test Strains under Force Loading

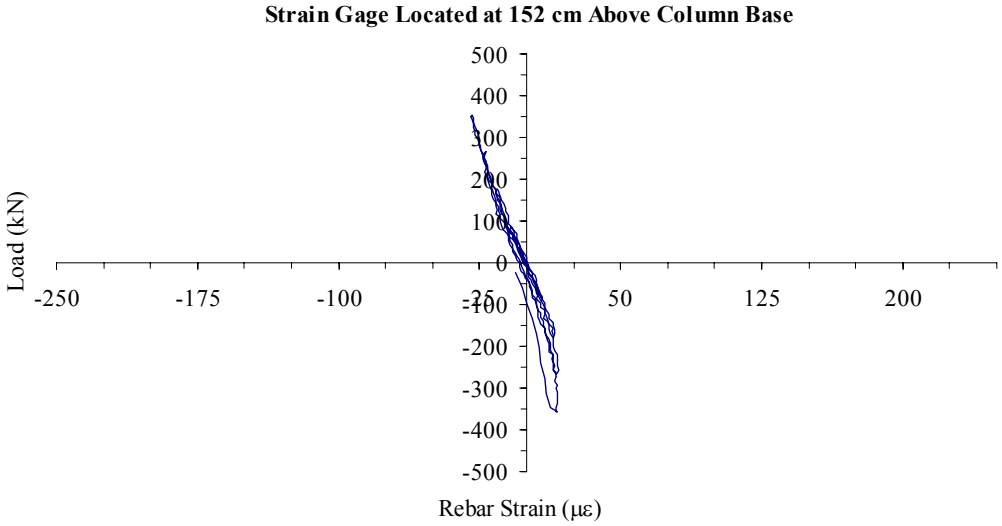

Figure 3-18: South Face Reinforcement Test Strains under Force Loading

Mid-column reinforcement strains in Figure 3-18 are minimal and show that a reverse in positive to negative strains under positive direction loading. This confirms that column is behaving in the expected fixed-fixed column representation. This is seen in the column's curvature and bending stresses moving toward zero at the column's midpoint and then reversing in direction along the top half of the column to become a mirror image of the bottom half.

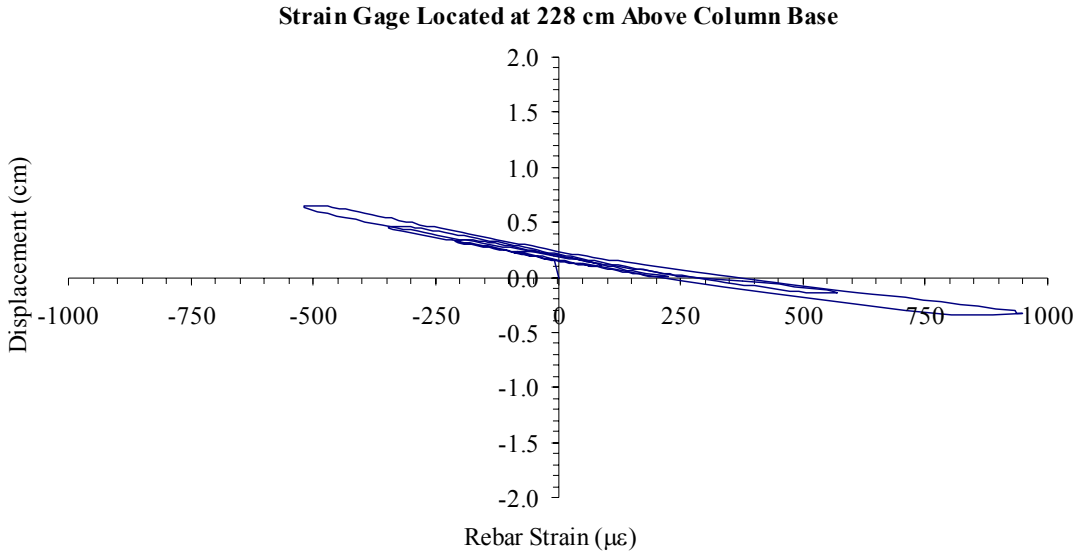

Figure 3-19: South Face Reinforcement Test Strains under Force Loading

Once the testing was cycled at Vy loading, it was then switched to deflection control. At this time reinforcement yielding was expected at the first ductility level ($\mu = 1.0$). This did occur as shown in Figure 3-20, which verifies that the calculated column values are within the appropriate range for further analysis of the test column's retrofitted behavior.

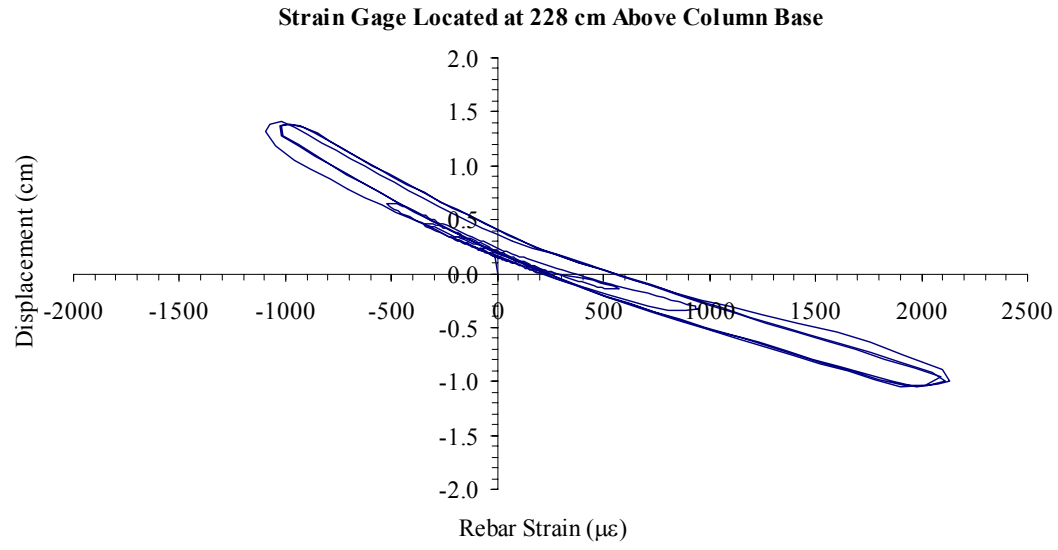

Figure 3-20: South Face Reinforcement Test Strains at $\mu = 1$

Under deflection load control the reinforcement strains continued to increase. Figure 3-21 through Figure 3-26 show the strain at ductility level 6 displacements at different locations of the column.

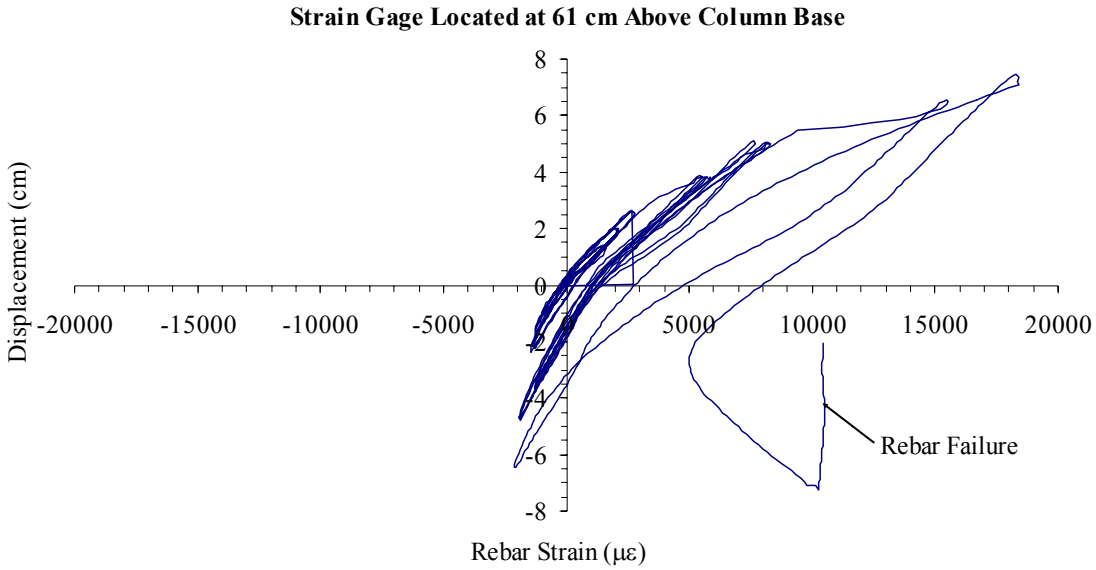

Figure 3-21: South Face Reinforcement Test Strains at μ = 6.0

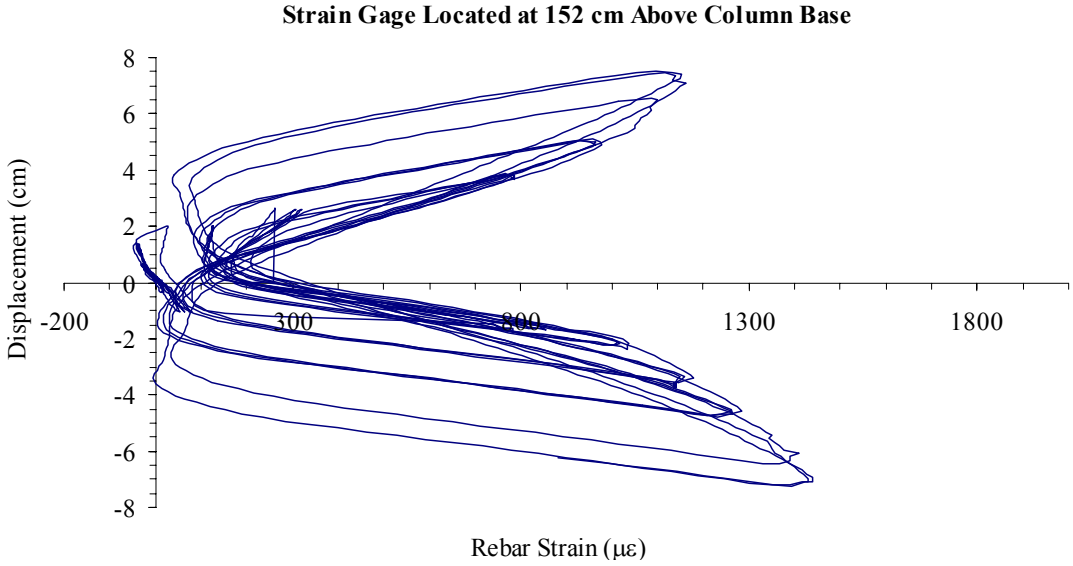

Figure 3-22: South Face Reinforcement Test Strains at μ = 6.0

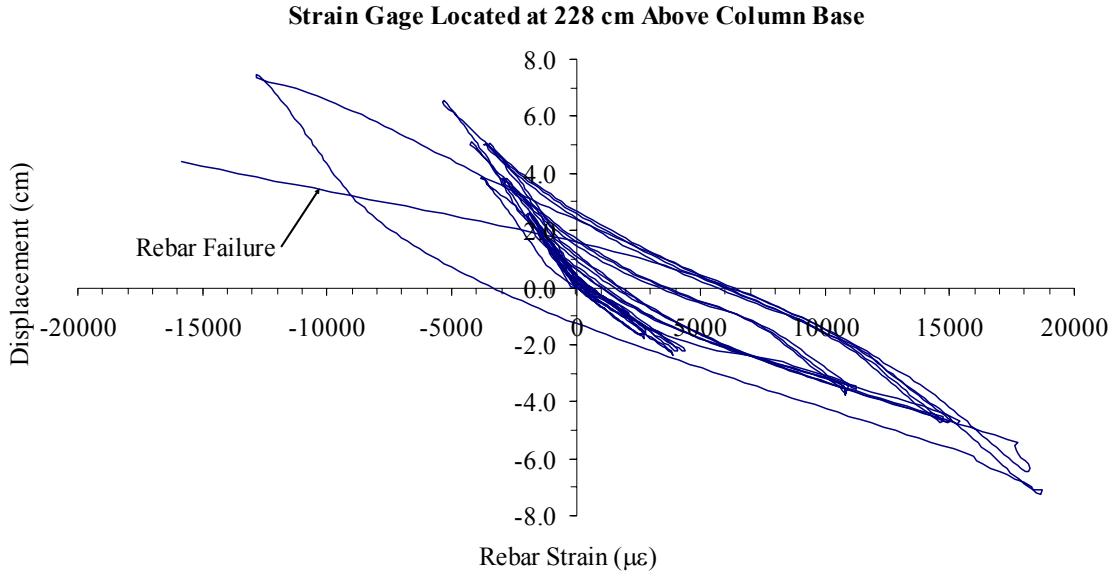

Figure 3-23: South Face Reinforcement Test Strains at μ = 6.0

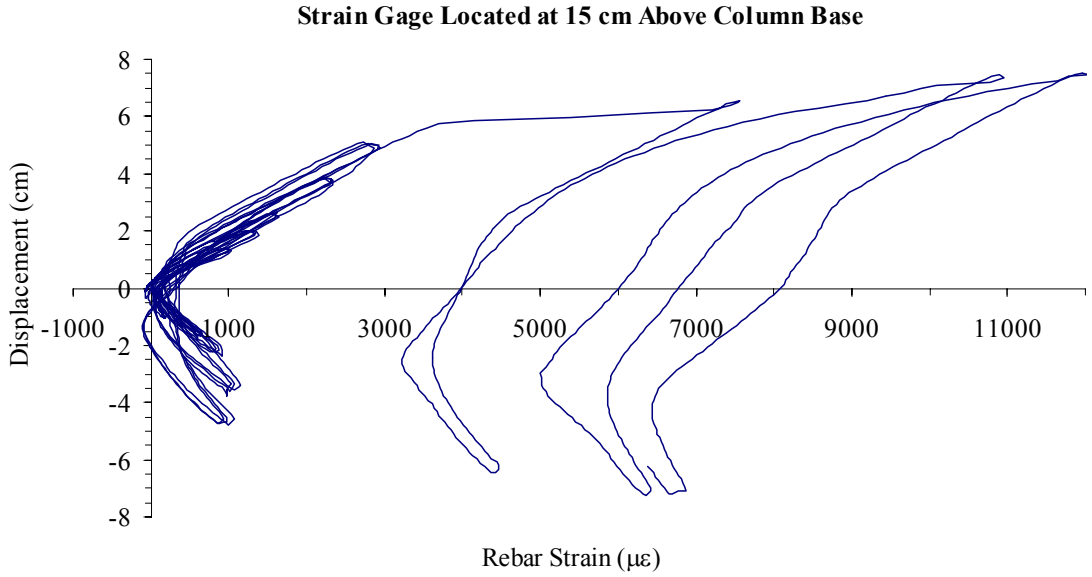

Figure 3-24: East Face Reinforcement Test Strains at μ = 6.0

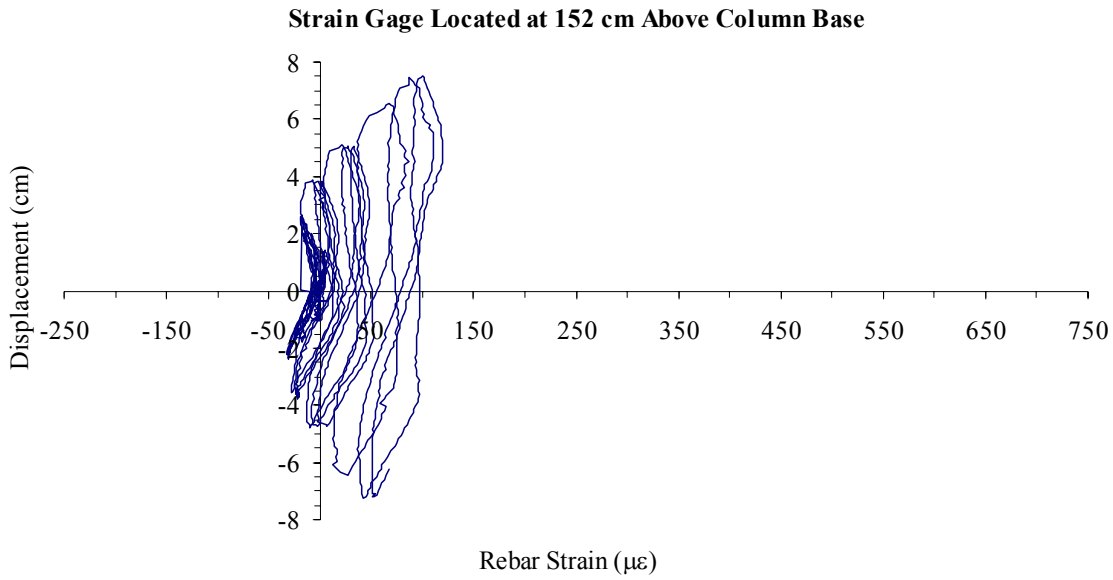

Figure 3-25: West Face Reinforcement Test Strains at μ = 6.0

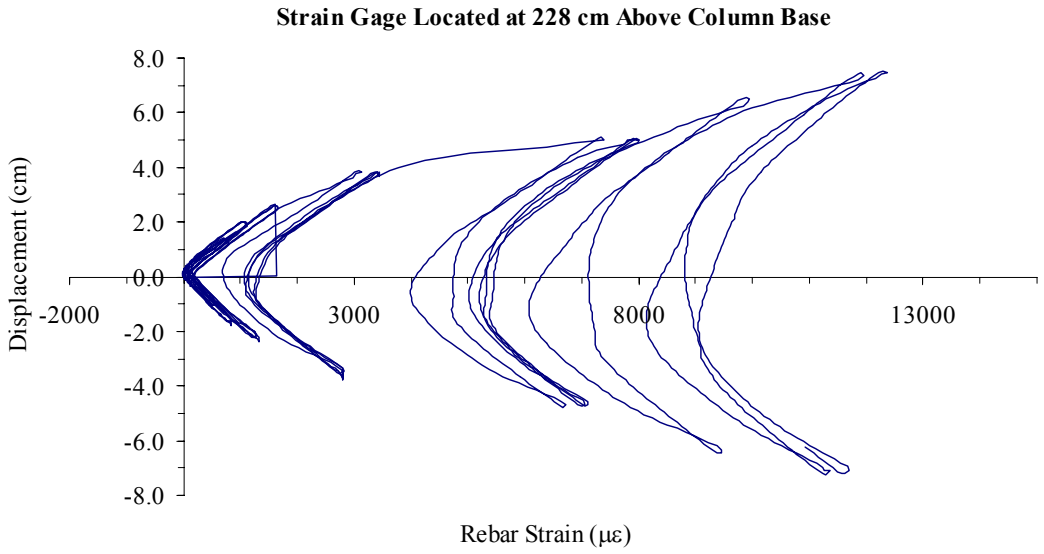

Figure 3-26: West Face Reinforcement Test Strains at μ = 6.0

Figure 3-27 and Figure 3-28 show the column during load controlled and deflection controlled testing.

Figure 3-27: Shear Column during Load Controlled Cycling

Figure 3-28: Column under 4.8 cm Deflection Cycling

Under load controlled cycling the strengthening jacket exhibited minor flexure cracking in the plastic hinge regions (first 45 cm from the top and bottom of the column). The jacket also began to emit noticeable noise under the deflection controlled cycles as the jacket fibers fractured and as the carbon fabric began to separate at the column hinge region. Under a level of 4.8 cm applied deflection, equivalent to ductility Level 4, the retrofit jacket began to experience obvious fractures and separation of the construction seam at the top of the column as illustrated in Figure

3-29. Within the next few cycles, visible crushing at the bottom of the jacket was also seen as shown in Figure 3-30.

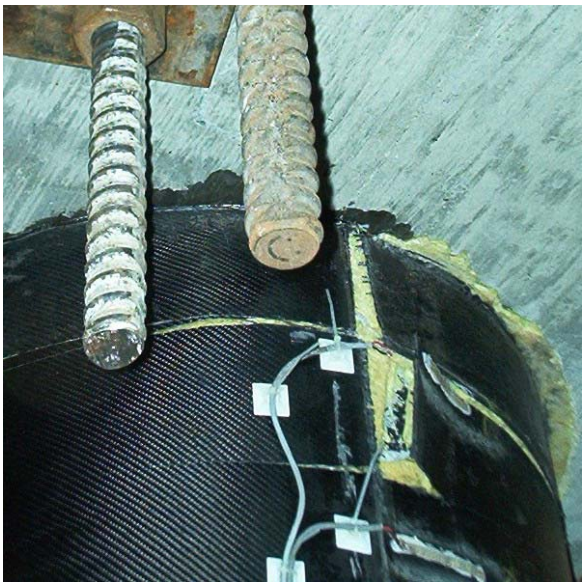

Figure 3-29: Jacket Splitting at Seam

Figure 3-30: Jacket Splitting at Seam

At the first cycle at ductility Level 6 loading, the allowable push of 979 kN (220 kips) for the test actuator was attained before the set test deflection of 7.4 cm (2.9 inches). The second and third cycles did reach the desired displacement of 7.4 cm due to deterioration of the column's load carrying capacity. A sign of impeding failure is the column inability to maintain the load required during repetitive cycling through a specified ductility level (i.e. a noticeable drop in the load needed to induce the same displacement measurement). Figure 3-31 through Figure 3-33 show the deflection to strain relationship of the jacket at different locations for ductility level 6.

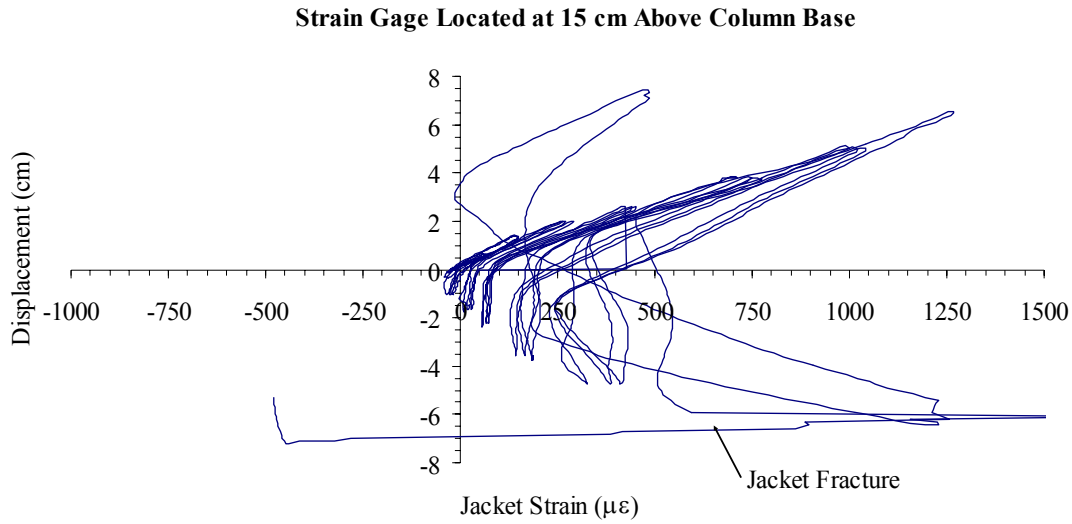

Figure 3-31: North Face Jacket Test Strains at μ = 6.0

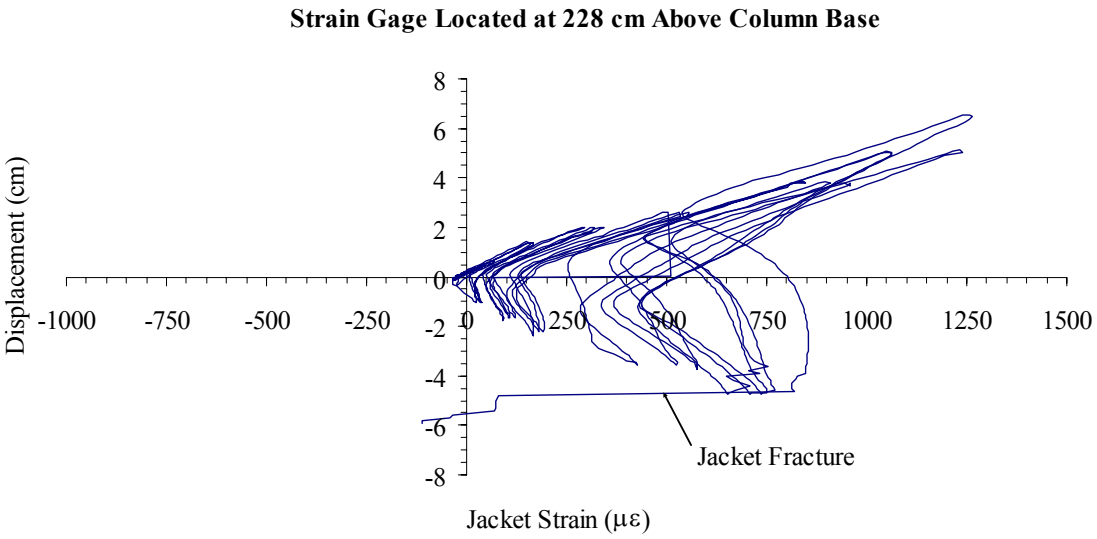

Figure 3-32: South Face Jacket Test Strains at μ = 6.0

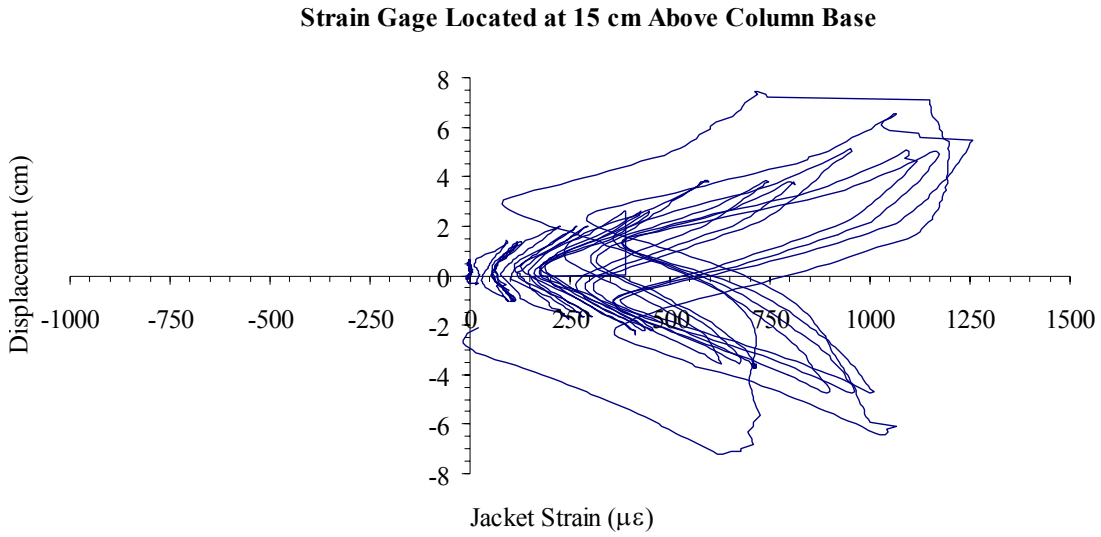

Figure 3-33: East Face Jacket Test Strains at μ = 6.0

During the first cycle of ductility Level 8 loading, a brittle shear failure occurred. The failure produced a loud sound as the jacket ruptured. This rupture is shown in Figure 3-34. Large pieces of the interior foam core came loose from the fractured carbon shell as the jacket ruptured. A missing section of the jacket's interior foam layer is pictured in Figure 3-35.

Figure 3-34: Jacket Failure

Figure 3-35: Jacket Failure

3.3.2 Test Results

Stability under cyclic loading during the circular shear testing was measured to the displacement length of 7.28 cm (2.87 inches) with the column failure occurring at a deflection of 7.68 cm (3.02 inches). A hysteresis plot of the circular shear columns applied load to the resulting column displacement is seen in Figure 3-36. This graph shows a stable push-pull response with the positive push data mirroring the negative pull data about the zero load and zero displacement axes. The area outlined within the data point of graph is smooth elliptical shape with no abrupt jumps or drops in data to indicate instability.

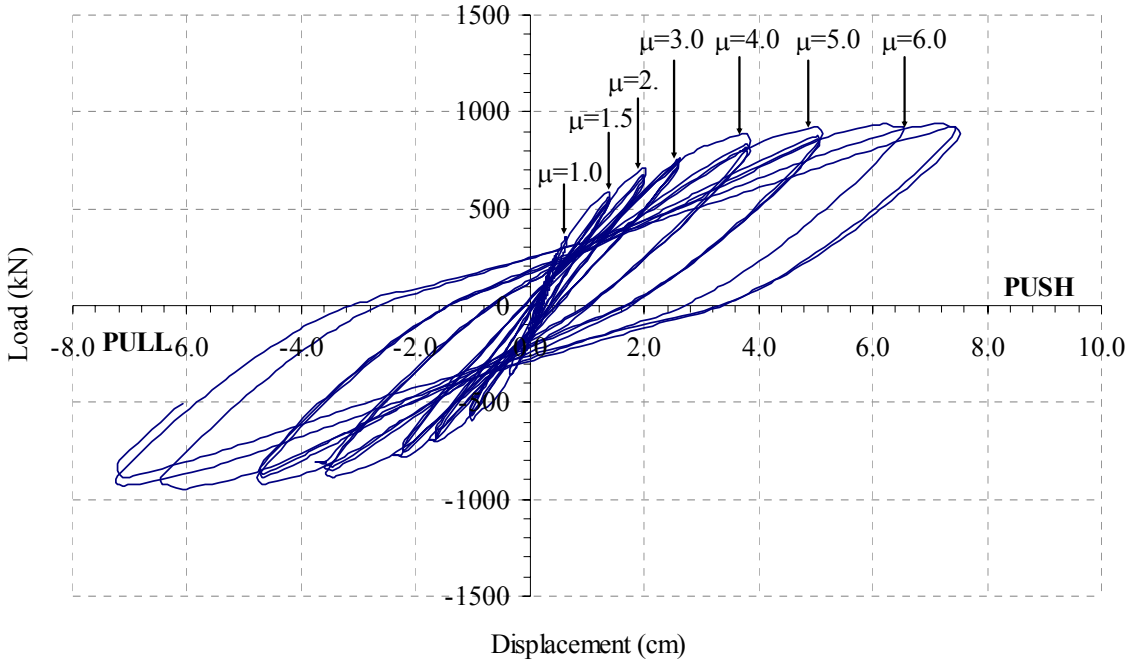

Figure 3-36: Circular Shear Column Load vs. Displacement Test Results

The test column's final retrofitted ductility calculation utilized the 7.28 cm measurement given that this was the displacement length the test specimen achieved during the last stable loading cycle. Table 3-6 lists the final results collected from the circular shear column experiment used in the retrofit system analysis.

Table 3-6: Circular Shear Column Final Test Results

Maximum Test Load	979 kN
Failure Initiation Load	832 kN
Maximum Displacement	7.28 cm

The results from the experiment for the circular shear column were compiled to establish the column's retrofitted ductilities in terms of displacement and curvature. These values were then evaluated against the "as-built" ductilities in Table 3-7 to determine if the retrofitted column surpassed the baseline set by the HITEC guidelines. The retrofitted shear column failed at a forced displacement of 7.28 cm, as noted in Table 3-6, which results in a deflection ductility of $\mu_\Delta = 7.24$ and a curvature ductility of $\mu_\phi = 12.56$. These results listed in Table 3-7, show that the retrofitted ductilities exceeded the criteria set by the HITEC protocol.

Table 3-7: Circular Shear Column Ductility Comparison

Ductility	"As-Built"	Retrofit	*Ductility Increase*
μ_Δ	2.51	7.24	*2.88*
μ_ϕ	3.79	12.56	*3.31*

With the additional ductility provided by the retrofit jacket, the shear column exceeded the required specifications set by the HITEC protocol to qualify as an acceptable retrofit procedure. The tested column deformed elastically to the set failure load and exceeded the increased ductility requirements.

Improved performance and increased ductility would be expected from this system if the production of the jacket were adjusted to increase the half-inch gap between the base/load stub and jacket to 2.5 cm or 3.8 cm (1 or 1-1/2 inches). The increase of this gap can improve performance given that the jacket failure began at the base of the column where an inadequate base to jacket gap was provided. Increasing the jacket to base/load stub gap would also ensure

that the load stub and base are not integrated into the ductility/stiffness of the column thus allowing the column to perform independently of the supporting elements.

Strengthening the jacket seam would also increase the performance of the retrofit system. Viewing the jacket strains at ductility level 6.0 in Figure 3-37, it is apparent that the material had not reached its maximum strain capacity since the measurements are well below failure strains associated with a typical carbon fiber. Table 3-8 provides a summary of the all the peak strains at ductility levels associated with the testing.

Table 3-8: Peak Test Strains (με)

	Level Vy	Level 1.0	Level 1.5	Level 2.0	Level 3.0	Level 4.0	Level 6.0
Rebar	935	2093	2692	4292	10531	14508	FAIL
Jacket	81	185	672	1145	1646	1940	2838

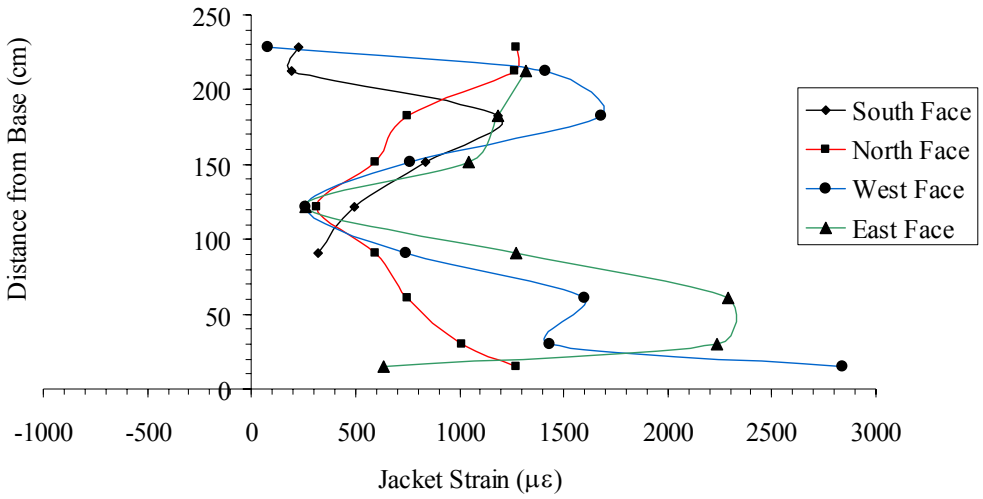

Figure 3-37: Jacket Strains at Level 6 Load Cycle

The column's internal reinforcement underwent considerable strain while the jacket strains remained relatively low. With the jacket failure not due to material failure, the construction seam appeared to be the failure mechanism becoming visible with the splitting of the

jacket seam prior to column failure. Finding a better means of constructing the jacketing system to improve the performance of the seams would enhance the retrofit abilities of the system. If the early failure of the jacket due to poor seam construction was prevented, the system performance would likely be maximized.

3.4 Square Shear Column

3.4.1 Observations

The retrofit test of a square shear column with continuous column reinforcement was constructed and was wrapped with the experimental retrofit jacket approximately 21 days after the specimen had been cast.

Based on the listed material properties in the above Table 3-1 and Table 3-3, which were determined from earlier material testing, the theoretical yield force V_y = 160 kN (36 kips) and ideal flexural capacity V_{yi} = 258 kN (58 kips) were calculated using the procedure presented in Chapter 2 for the square shear columns. The pseudo-superstructure load applied to the column was 400 kN (90 kips) in addition to the 58 kN (13 kip) weight of the testing frame acting as the columns axial load. Assuming an elasto-plastic response approximation, the experimental first yield displacement Δ_y = 1.61 cm was expected based on the above values.

The theoretical ductilities corresponding to curvature and deflection for the constructed, non-retrofitted column was then determined from the above calculated column design values. (See Chapter 2 Figure 2-33 for calculations). The resulting "as-built" column ductilities are based on the deflection ($\mu_\Delta = \Delta_u/\Delta_y$) and column curvature ($\mu_\phi = \phi_u/\phi_y$) are listed in Table 3-9. According to HITEC protocol, the retrofitted column must exceed these calculated values by the specified amounts of μ_ϕ = 2.0 x "as-built" and μ_Δ = 1.5 x "as-built".

Table 3-9: Resulting "As-Built" Ductilities

ϕ_y =	0.00008	μ_ϕ =	3.94
ϕ_u =	0.00032		
Δ_y =	1.612 cm	μ_Δ =	2.59
Δ_u =	4.168 cm		

With the "as-built" theoretical column ductilities calculated, the loading sequence for the test was established. The square shear column testing was begun under load control. The column displayed additional stiffness than anticipated at the end of the load control cycles. Neither the experimental deflection nor column reinforcement strains came close to the theoretical values under its Vy loading (a load of 160 kN should yield a deflection of 1.61 cm). At the Vy loading the rebar strains were slightly less than 50% of the yield strain (750 με) as seen in Figure 3-38.

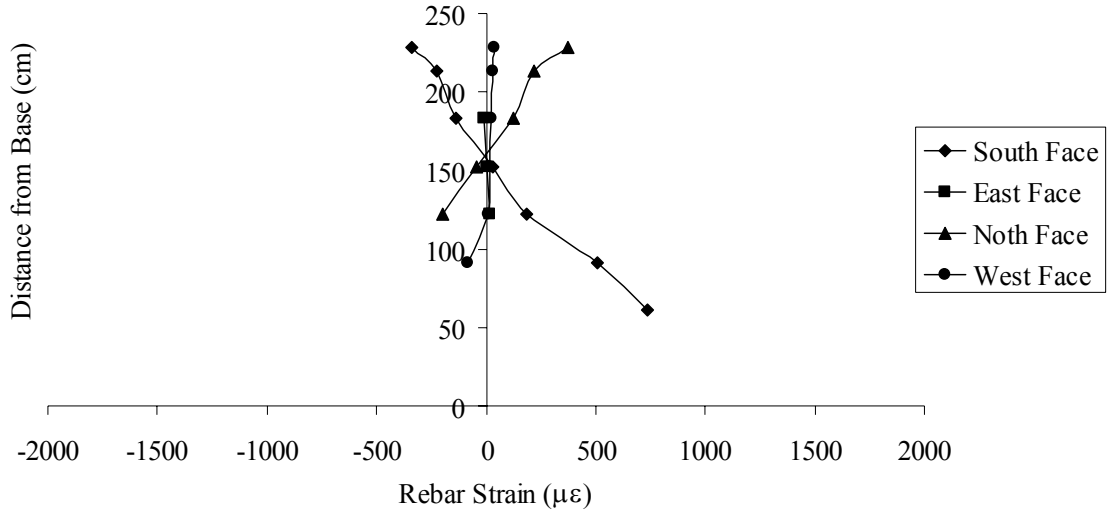

Figure 3-38: Reinforcement Test Strains at Vy Loading

Figure 3-39 through Figure 3-44 show how the rebar strain changed under load control cycles at different locations along the column.

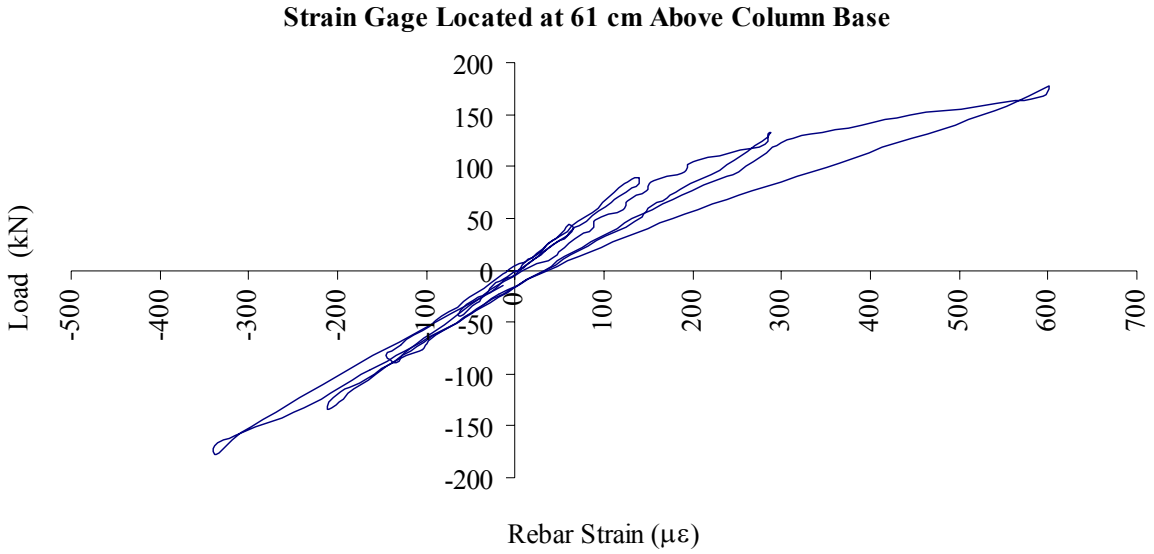

Figure 3-39: South Face Reinforcement Strains under Force Loading

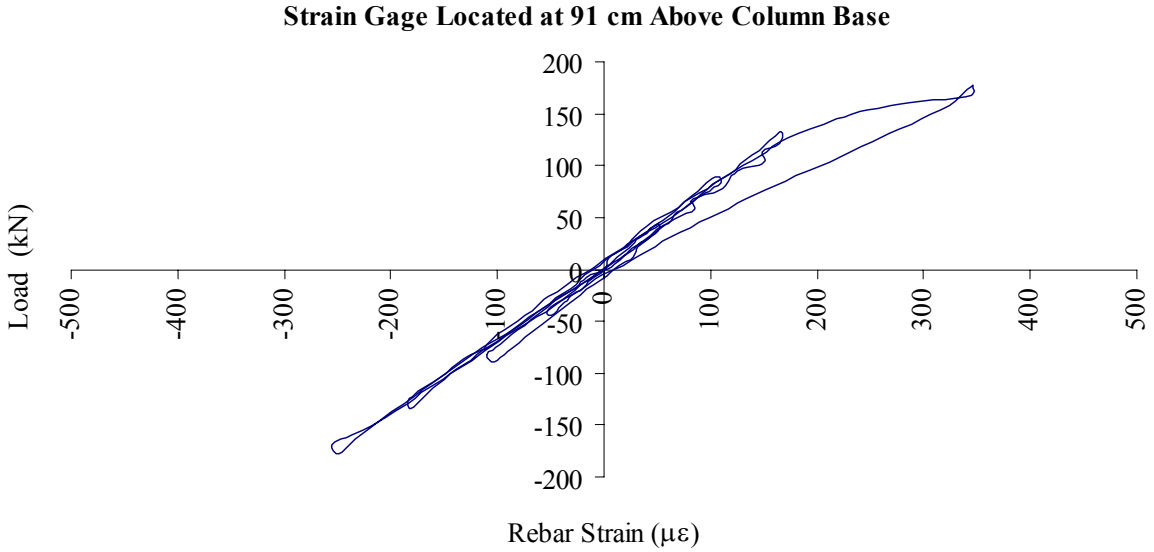

Figure 3-40: South Face Reinforcement Strains under Force Loading

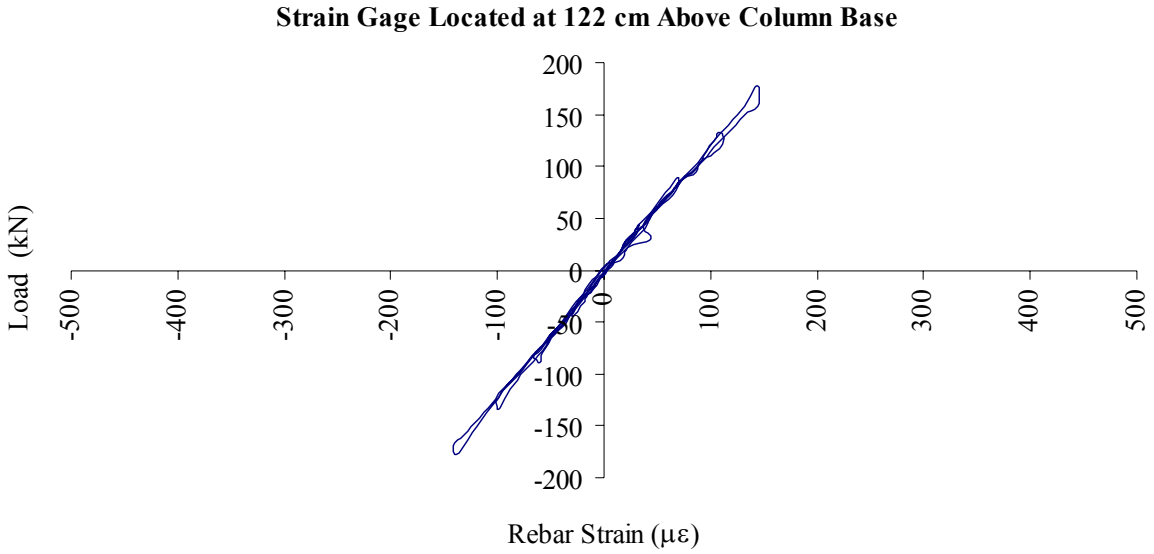

Figure 3-41: South Face Reinforcement Strains under Force Loading

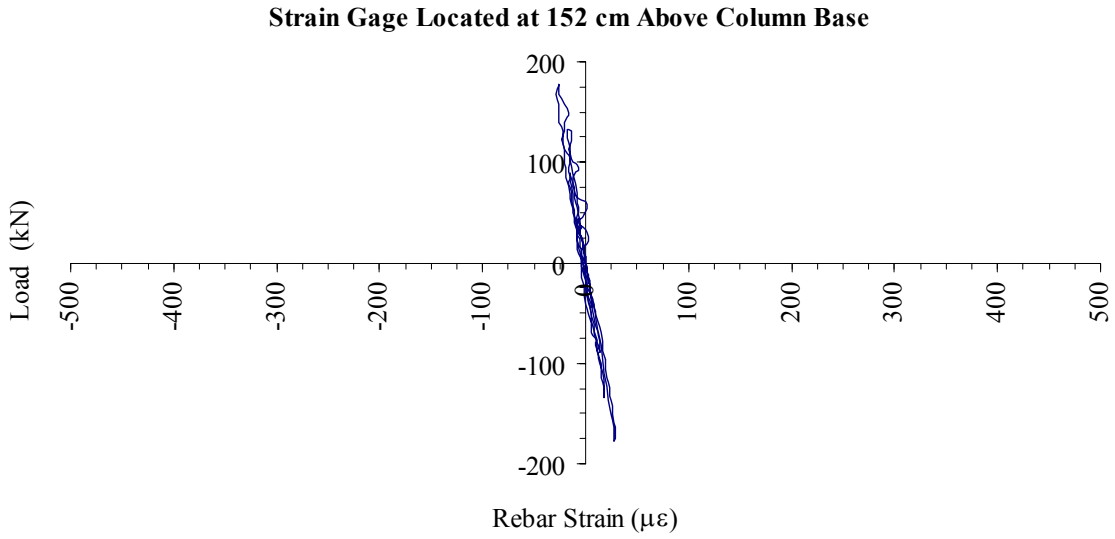

Figure 3-42: South Face Reinforcement Strains under Force Loading

Mid-column reinforcement strains in Figure 3-42 are minimal and show a reverse in positive to negative strains under positive direction loading. This confirms that column is behaving in the expected fixed-fixed column representation. This is seen by the column's

curvature and bending stresses moving toward zero at the column's midpoint and then reversing in direction or sign along the top half of the column to become a mirror image of the bottom half.

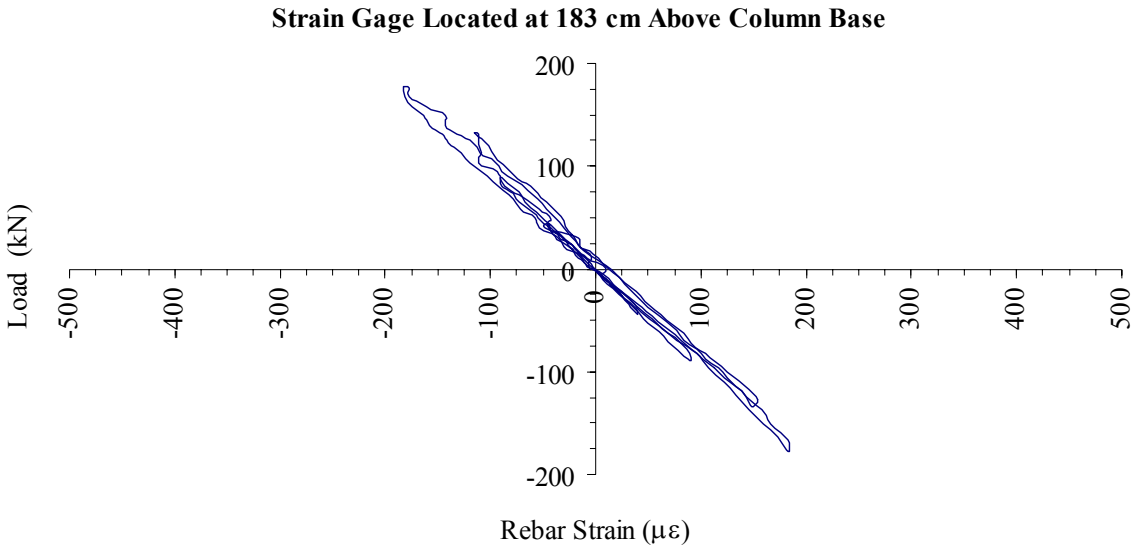

Figure 3-43: South Face Reinforcement Strains under Force Loading

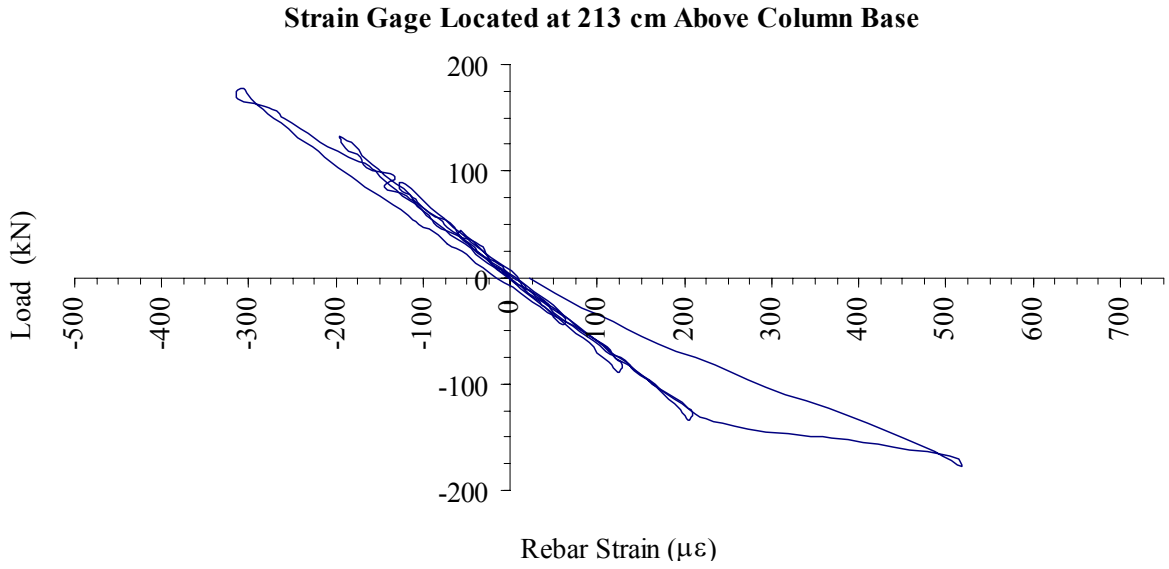

Figure 3-44: South Face Reinforcement Strains under Force Loading

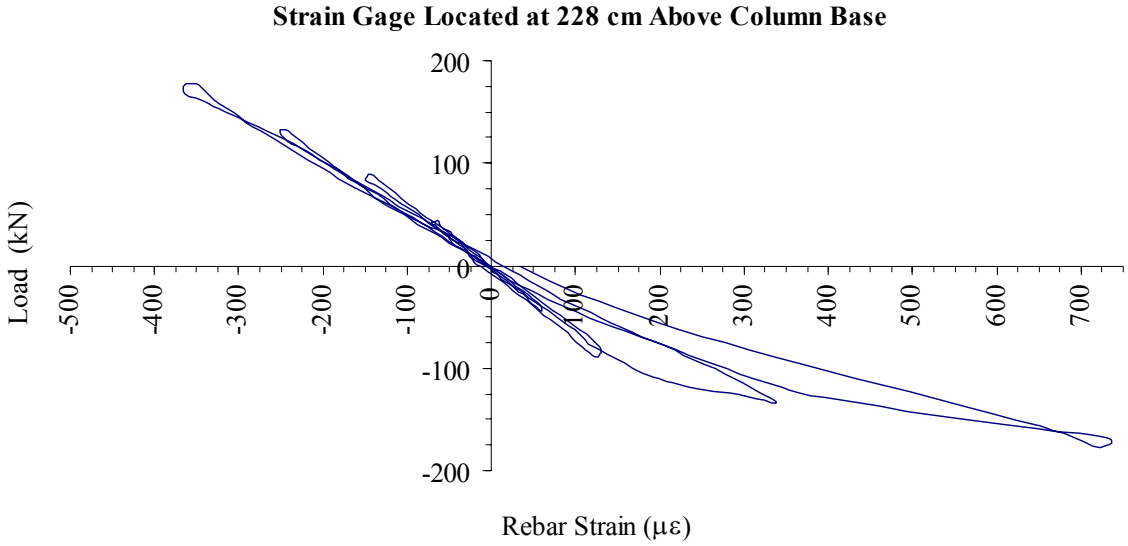

Figure 3-45: South Face Reinforcement Strains under Force Loading

Once the testing was cycled at Vy loading, it was changed to deflection control. At this time, reinforcement yielding was expected at the first ductility level (μ = 1.0). Figure 3-46 shows this occurred, which verifies that the calculated column values are within the appropriate range for further analysis of the test column's retrofitted behavior.

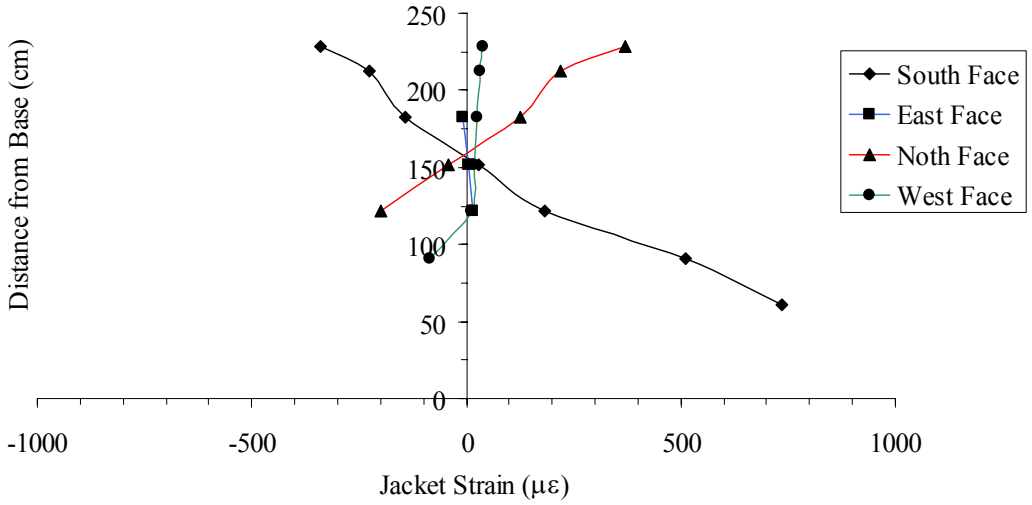

Figure 3-46: Reinforcement Test Strains at μ=1.0

South Face reinforcement strain measurements taken from the bottom of the column (61 cm from base) continue to increase at each increasing ductility level cycle. Figure 3-47 to Figure 3-51 show the strain in the reinforcement at ductility level 8 at different locations of the column.

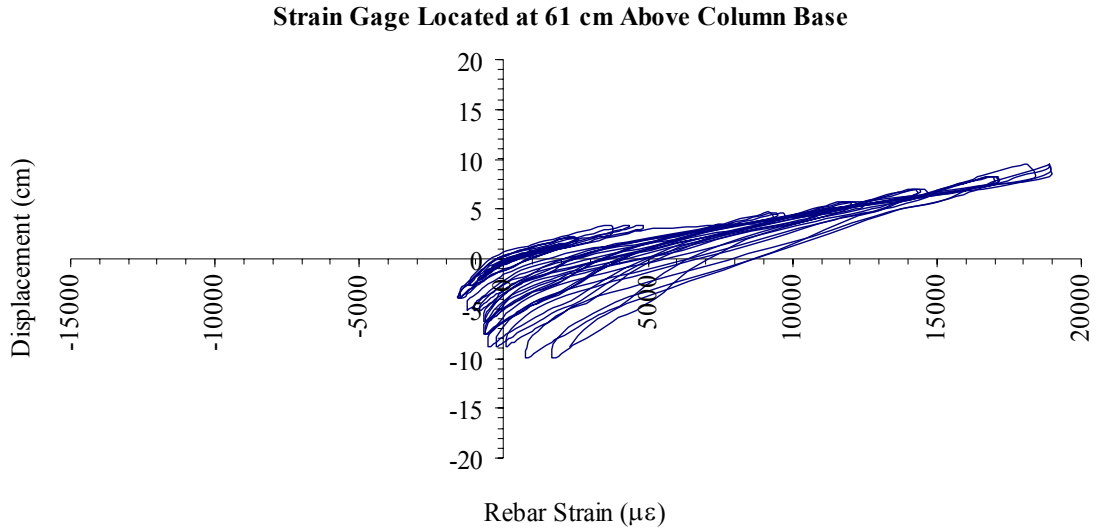

Figure 3-47: South Face Reinforcement Test Strains at μ=8.0

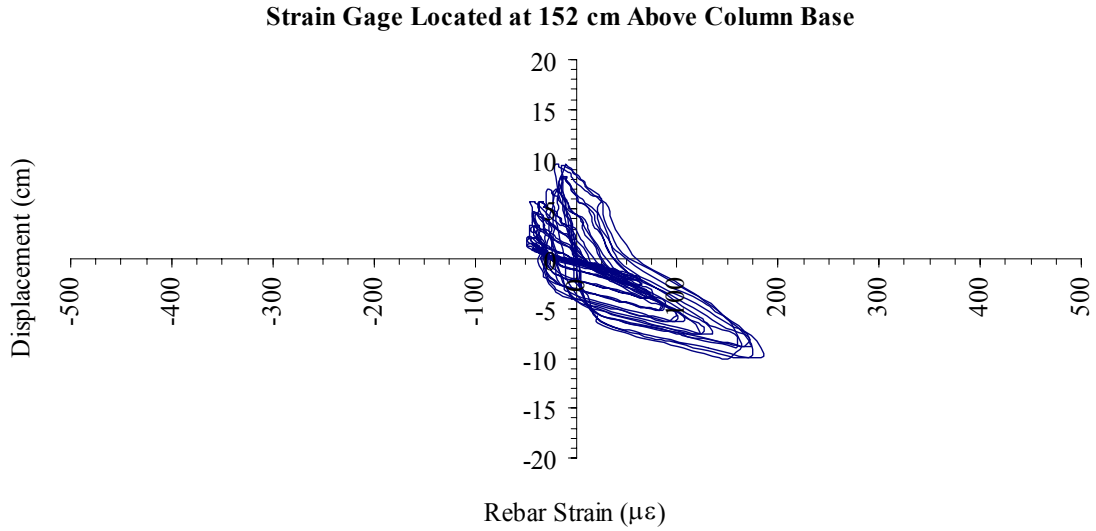

Figure 3-48: South Face Reinforcement Test Strains at μ=8.0

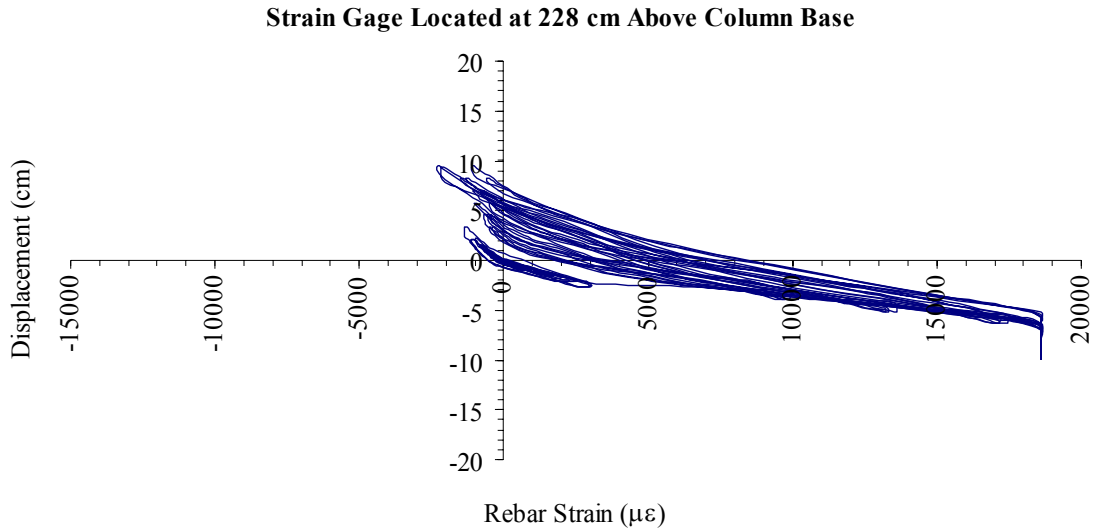

Figure 3-49: South Face Reinforcement Test Strains at μ=8.0

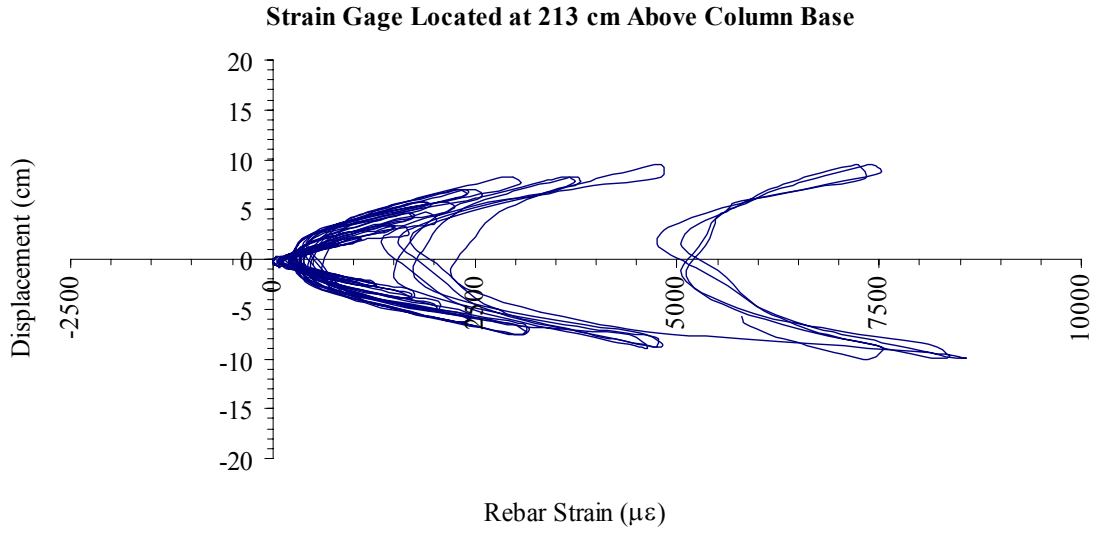

Figure 3-50: West Face Reinforcement Test Strains at μ=8.0

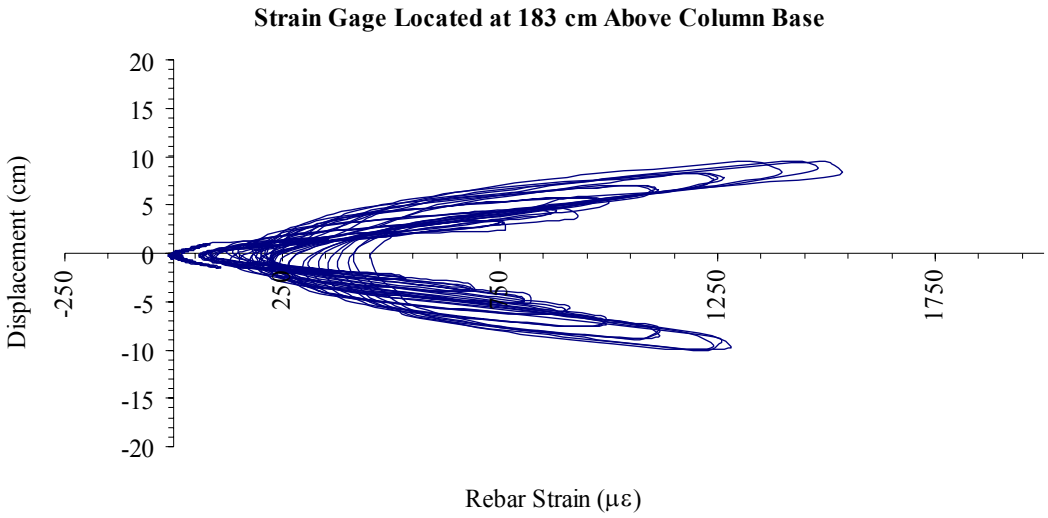

Figure 3-51: East Face Reinforcement Test Strains at μ=8.0

Figure 3-52 and Figure 3-53 are pictures of the column during deflection load control testing.

Figure 3-52: Shear Column during testing

Figure 3-53: Column under 9.7 cm Deflection

Under deflection load control the jacket exhibited minor flexure cracking in the plastic hinge regions (first 45 cm from top and bottom of column). Under a 7.28 cm applied deflection at ductility Level 6, the retrofit jacket began to experience noticeable fractures and a separation of the construction seam as illustrated in Figure 3-54 with visible crushing at the bottom of the jacket. Also seen in Figure 3-55 is splitting at the top of the jacket at the location of a patch applied during the jacket construction.

Figure 3-54: Jacket Splitting at Seam

Figure 3-55: Jacket Splitting at Seam

During the cycling of ductility Level 8 loading, a noticeable drop in the load required to reach the designated level of displacement was experienced. This is considered to be a failure mode according to the HITEC procedure. When the displacement loading has decreased to 85% of the maximum capacity load, the retrofit column is considered to have failed. Figure 3-56 to Figure 3-59 show the jacket strains versus displacement at ductility 8 at various locations on column.

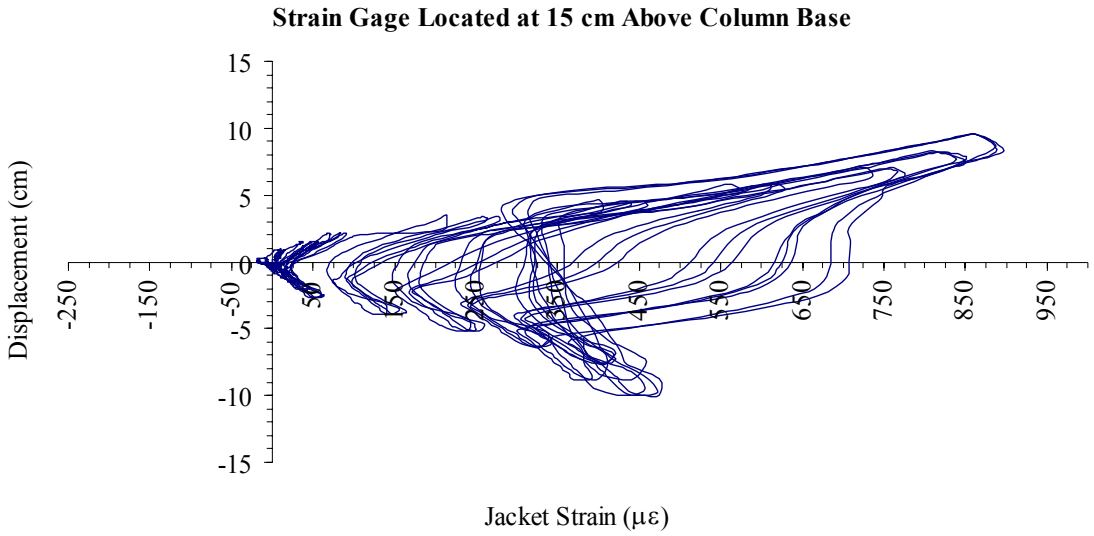

Figure 3-56: South Face Jacket Test Strains at μ=8.0

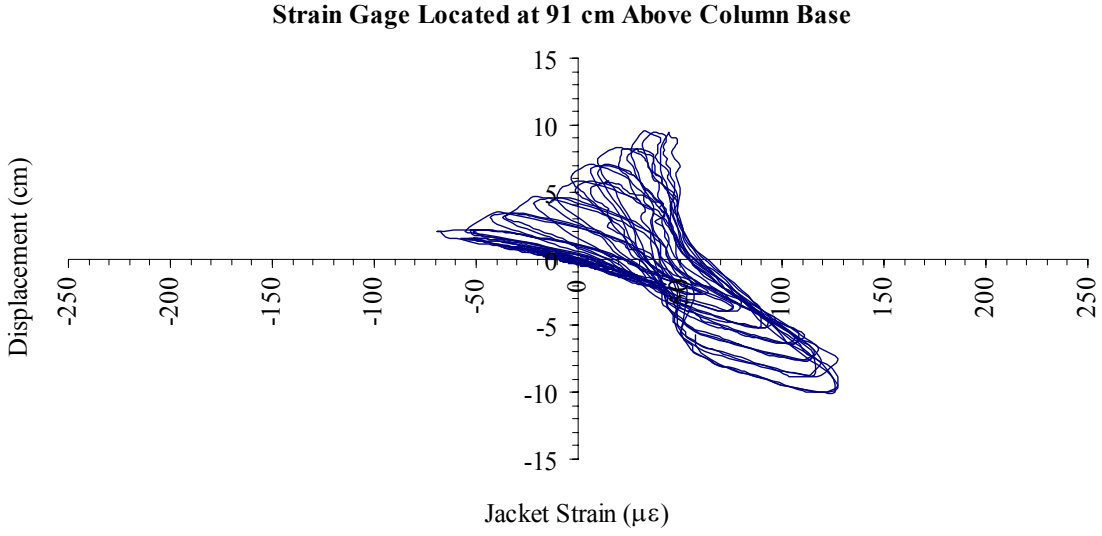

Figure 3-57: South Face Jacket Test Strains at μ=8.0

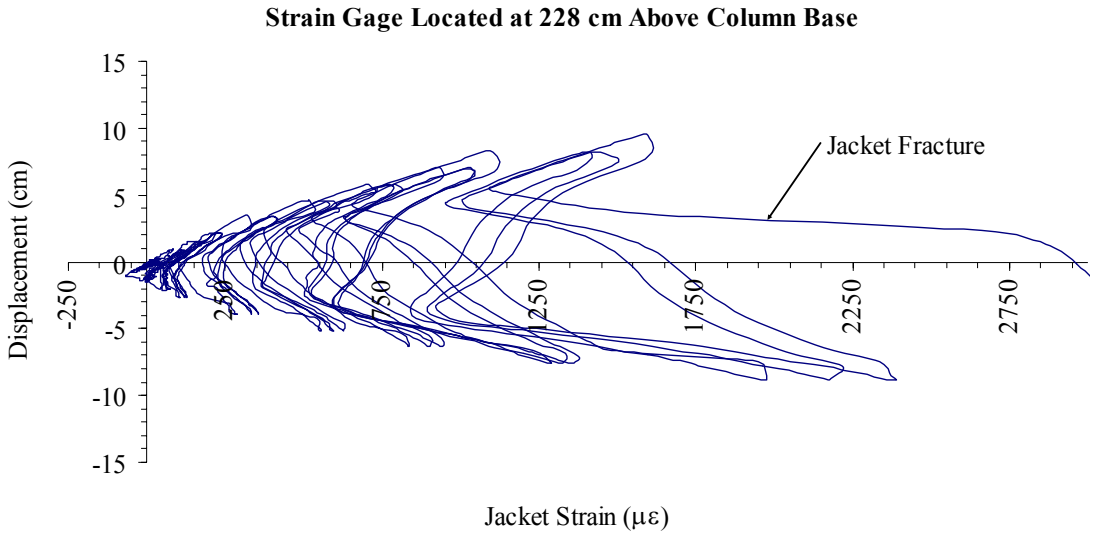

Figure 3-58: South Face Jacket Test Strains at μ=8.0

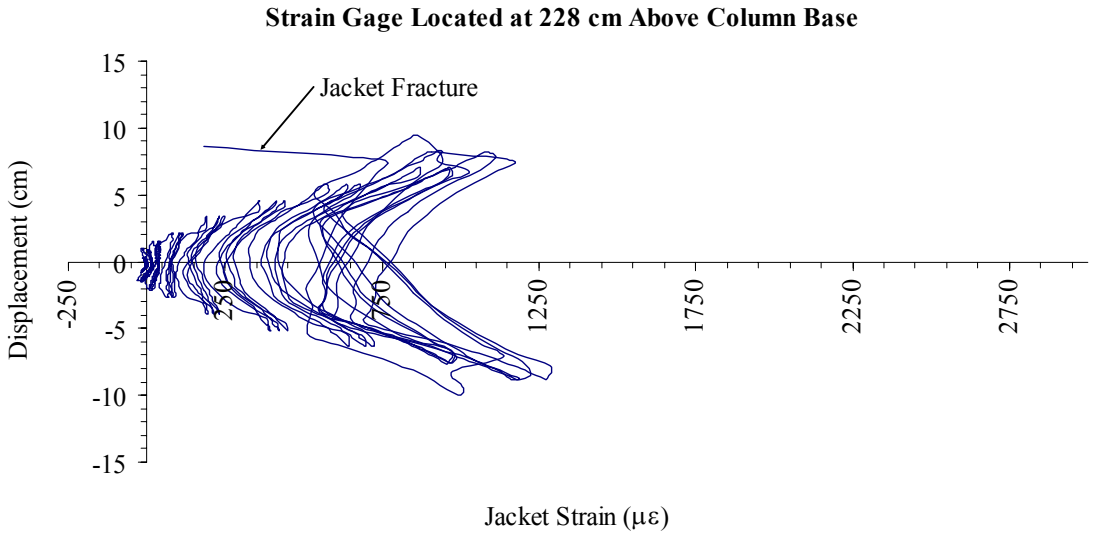

Figure 3-59: West Face Jacket Test Strains at μ=8.0

3.4.2 Test Results

The tested square shear column deformed elastically to the failure displacement level of 9.710 cm (3.823 inches). The failure was seen in the drop of loading required to displace the column during its cyclic loading. A hysteresis plot of the square shear column's applied load to the resulting column displacement is seen in Figure 3-60. This graph shows a stable push-pull response with the positive push data mirroring the negative pull data about the zero load and zero displacement axes. The area outlined within the data point of graph is smooth elliptical shape with no abrupt jumps or drops in data to indicate instability.

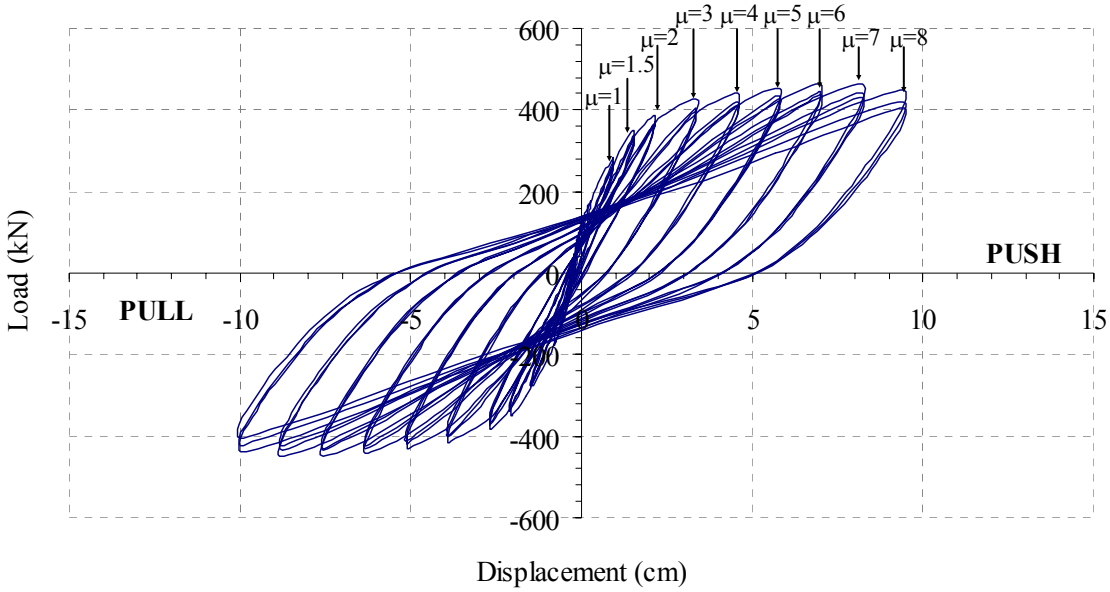

Figure 3-60: Shear Column Load vs. Displacement Test Results

Table 3-10: Square Shear Column Final Test Results

Maximum Test Load	467 kN
Failure Initiation Load	396 kN
Maximum Displacement	9.71 cm

Table 3-10 lists the final results collected from the square shear column experiment used in the retrofit system analysis. The results from the square shear column were compiled to

establish the column's retrofitted ductilities in terms of displacement and curvature. These values were then evaluated against the "as-built" ductilities in Table 3-11 to determine if the retrofitted column surpassed the baseline set by the HITEC guidelines. The retrofitted shear column failed at a forced displacement of 9.71 cm, noted in Table 3-10, which results in a deflection ductility of $\mu_\Delta = 6.05$ and a curvature ductility of $\mu_\phi = 10.35$. These results listed in Table 3-11, show that the retrofitted ductilities exceeded the criteria set by the HITEC protocol.

Table 3-11: Square Shear Column Ductility Comparison

Ductility	"As-Built"	Retrofit	*Ductility Increase*
μ_Δ	2.59	6.05	*2.34*
μ_ϕ	3.94	10.35	*2.63*

With the additional ductility provided by the retrofit jacket, the shear column exceeded the required specifications set by the HITEC protocol to qualify as an acceptable retrofit procedure. The tested column deformed elastically to the set failure load and exceeded the increased ductility requirements.

Improved performance and increased ductility would be anticipated from this system if the jacket seam of the retrofit system could be further strengthened. Viewing the jacket strains at ductility level 8.0 in Figure 3-61, it is apparent that the material did not reach its maximum strain capacity since the measurements are well below failure strains associated with a typical carbon fiber/epoxy system.

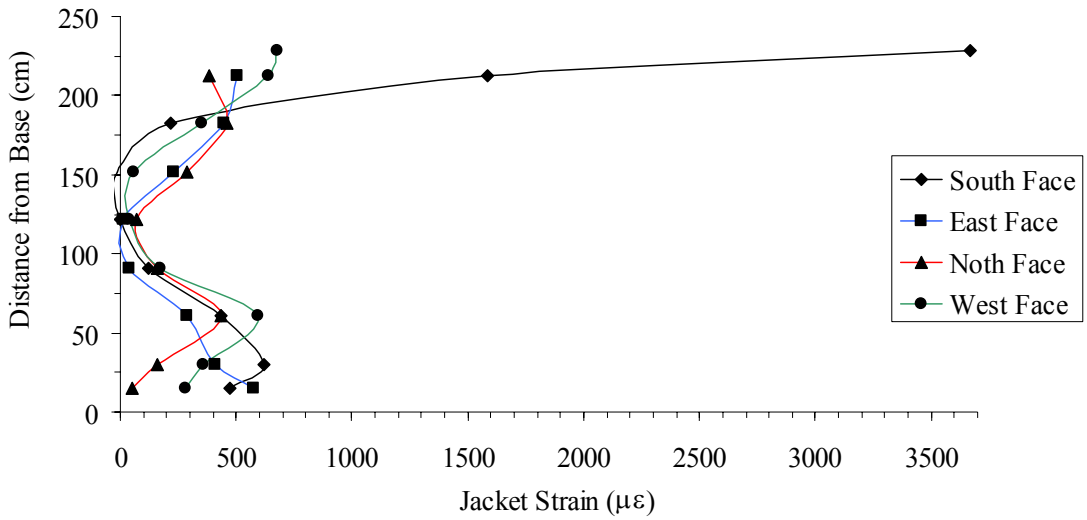

Figure 3-61: Jacket Strains at Level 8 Load Cycle

Table 3-12 provides a summary of the all the peak strains at ductility levels associated with the testing.

Table 3-12: Peak Test Strains (με)

	Level Vy	Level 1.0	Level 1.5	Level 2.0	Level 3.0	Level 4.0	Level 6.0	Level 8.0
Rebar	734	2432	3060	9734	13178	17115	FAIL	FAIL
Jacket	77	174	259	349	629	949	1379	3670

The column's steel reinforcement experienced considerable strain while the jacket strains remained relatively low, just as with the circular shear column. With the jacket failure not due to material failure, the construction seam appeared once again to be the failure mechanism as observed in Figure 3-54. Finding a better means of constructing the jacketing system to improve the performance of the seams would enhance the retrofit abilities of the system. If the early failure of the jacket due to poor seam construction was prevented, the system performance would likely be maximized.

4. Experimental Tests and Results for Continuously Reinforced Flexure Columns

4.1 Introduction

The objective of the test program was to evaluate a new composite jacketing system for its suitability as a retrofit alternative. The evaluation was conducted pursuant to the published HITEC procedure [11] to enable assessment of whether the new system could meet standardized requirements.

In this chapter, the testing and evaluation of the carbon fabric - expansive foam core sandwich panel jacket applied to each of the continuously reinforced flexure concrete test columns with circular and square cross sections is outlined. Each of these columns was tested under increasing cyclic quasi-static lateral loads to ascertain if the retrofit jacket allowed each column to:

1. Attain or exceed the HITEC protocol specifications for improved ductility;
2. Ensure stability under repetitive cycling at a pre-specified displacement, and
3. Provide adequate energy absorption during cycling as evident by the area within the hysteresis loops.

4.2 Test Specimens Construction

Laboratory experiments for the expansive foam sandwich panel jacketed system were conducted under the guidelines of Report No. 2001/10 "FRP Composite Column Wrap Durability Evaluation" submitted to HITEC and outlined in Chapter 2 [11]. The test columns were therefore built to the specified HITEC protocol requirements in order to ensure the strengthening of the columns will met the retrofit standards.

With the retrofitted columns being the focus of the testing, both the load stub and base were designed to carry the applied test loads without failure. This was to ensure that the failure

mechanism of each test was within the column retrofit area or at the connection area between the column and base/load stub. Because the interior tension reinforcement in the column was expected to yield, only the column longitudinal reinforcement bars were strain-gauged. A total of twenty (20) gages were applied in the load direction of the flexure column reinforcement bars, as illustrated in Figure 4-1 and Figure 4-2.

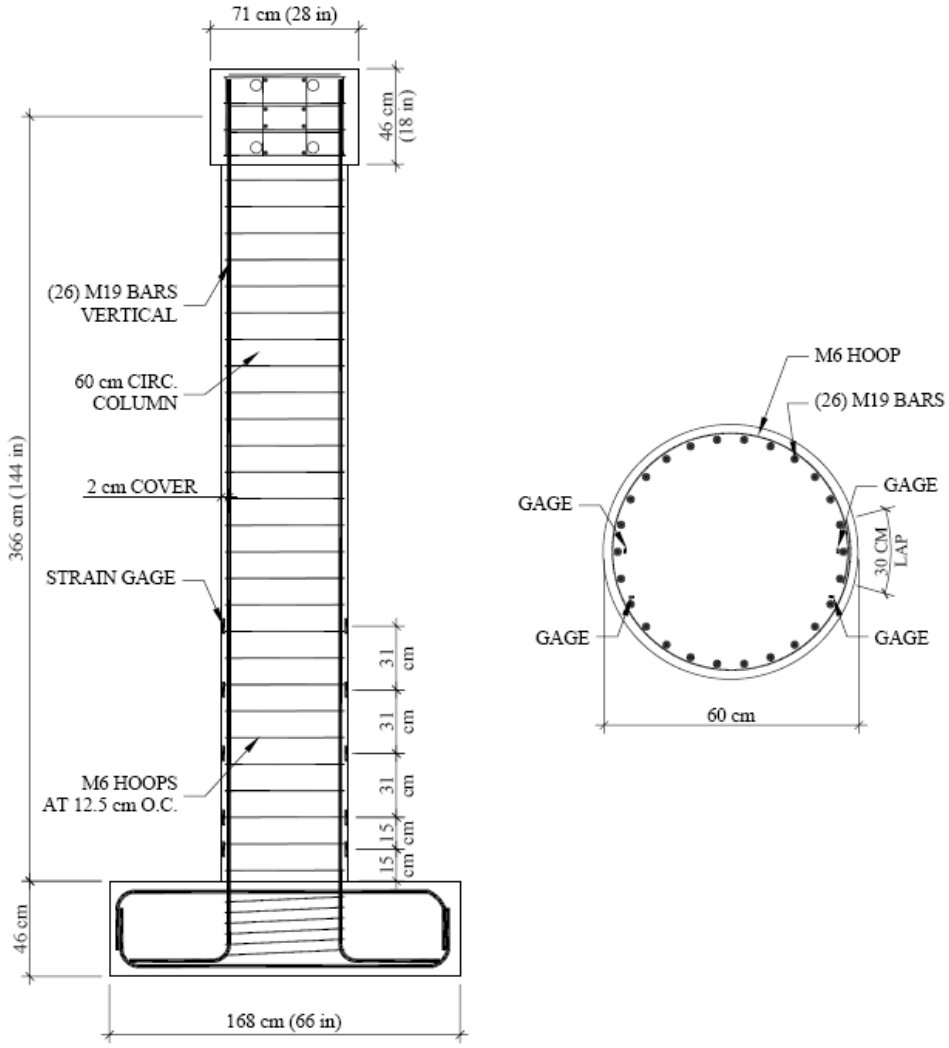

Figure 4-1: Schematic Showing Strain Gage Location on Circular Shear Column Reinforcing Cage

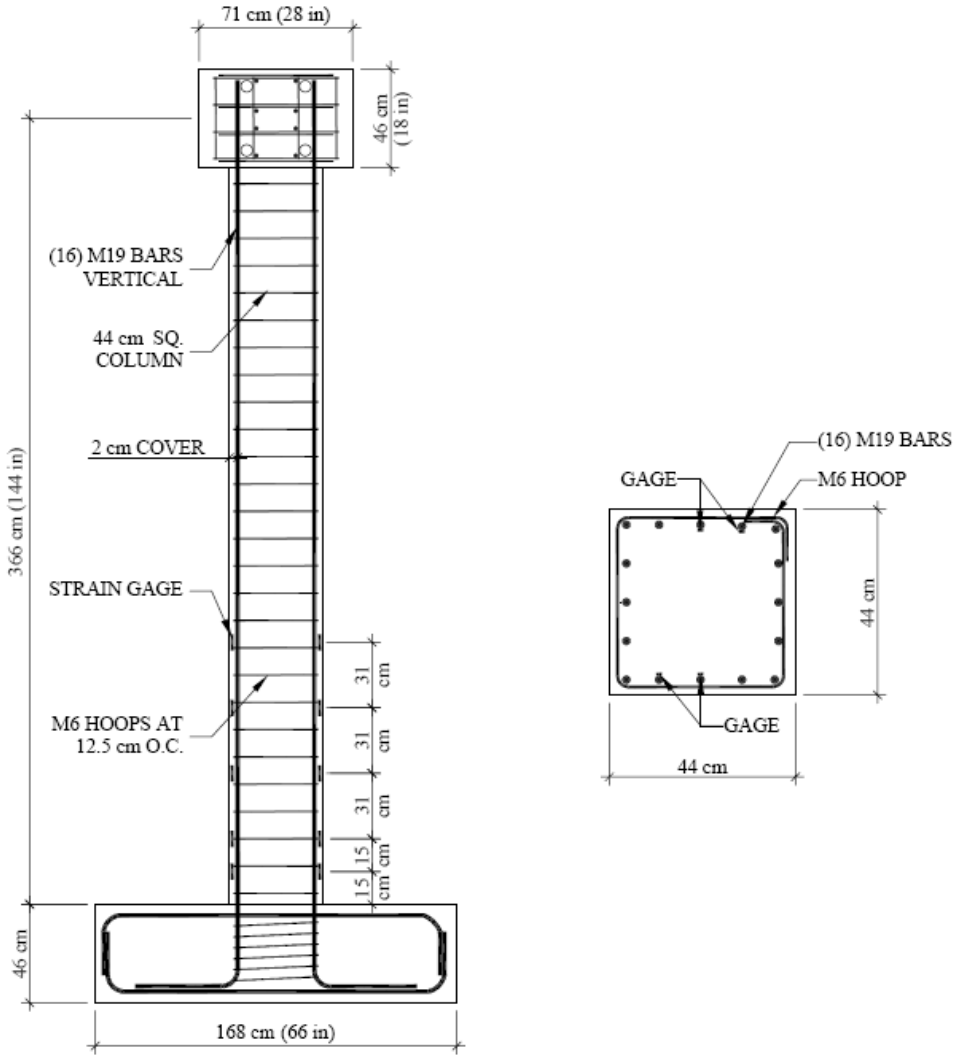

Figure 4-2: Schematic Showing Strain Gage Location on Square Flexure Column Reinforcing Cage

With formwork built, concrete mix on-site and reinforcement prepared (strain-gauged) for testing, each of the flexure columns was then constructed at the testing site. Construction of the columns was photographed at various stages of construction, including:

1. Completed reinforcement cages (as shown in Chapter 3)
2. Completed column concrete placement (as shown in Chapter 3)
3. Jacket application (as shown in Chapter 2)

The first construction stage involved the production of a square and circular column reinforcing cage. These column cages were formed with straight vertical bars and transverse hoops tied together. These column cages were constructed in tandem with the column bases.

The reinforcement strength was tested at this time using reinforcing bars taken from the same batch as those used in the construction of the column cages. These results are listed in Table 4-1. Yield strength was measured at the load level which the material strain changes from elastic deformation to plastic deformation, causing it to deform permanently (0.2%) and the ultimate strength is taken as the maximum stress that the reinforcement bar could withstand.

Table 4-1: Reinforcement Tension Test Data

Sample	*1*	*2*	*3*	***Average***
6 mm Diameter Horizontal Bar				
Yield Strength (MPa)	387.7	400.3	404.5	**397.5**
Ultimate Strength (MPa)	456.5	466.3	462.1	**461.6**
19 mm Diameter Vertical Bar				
Yield Strength (MPa)	476.2	477.2	473.0	**475.5**
Ultimate Strength (MPa)	764.2	766.8	762.9	**764.7**

Once the column base cages were encased within the column's casting formwork, concrete was poured. The concrete poured was specified to have minimum 28 day compression strength of 20.7 MPa (3000 psi). Nine test cylinders were cast at this time as well to enable determination of the progression in the concrete compression strength until the day of testing. Table 4-2 lists the resulting concrete compression strength taken from the test cylinders.

Table 4-2: Continuous Reinforced Flexure Column Base Concrete Compression Strength

	1	*2*	*3*	***Average***
7-Day Strength (MPa)	24.3	25.2	23.6	**24.4**
28-Day Strength (MPa)	33.2	32.7	34.5	**33.5**
D.O.T. Strength (MPa)	43.2	41.8	41.3	**42.1**

Once the column bases were poured, the formwork for the column was added around the reinforcement cages. Once in place the concrete was placed by means of a large hopper used to lift the concrete over the formed column. This allowed for the placement of concrete from the top of the formwork. After placement of the concrete a vibrator was dropped into the now filled column to ensure proper consolidation (removal of voids and air bubbles).

The resulting concrete column was specified to have a minimum 28 day compression strength of 20.7 MPa. Table 4-3 lists the compression values of the continuously reinforced concrete columns. Even though the concrete compression strength exceeded the minimum of 20.7 MPa, this does not necessarily invalidate the testing. A minimum concrete strength was given for test specimen protocol, but not a maximum. As these values are approximately double the specified 28 day compression strength, this will affect the required axial pre-load on the columns. This pre-load is a function of compression strength and cross sectional area of the column. For the circular flexure column the pre-load was 1780 kN creating an axial load ratio of 17.5% which is within the HITEC requirement limits. The square column was pre-load 1155 kN producing an axial load ratio of 16.6% which is also within the HITEC requirement limits [11].

Table 4-3: Continuous Reinforced Flexure Column Concrete Compression Strength

	1	*2*	*3*	***Average***
7-Day Strength (MPa)	28.3	28.9	28.4	**28.5**
28-Day Strength (MPa)	35.8	36.6	35.6	**36.0**
D.O.T. Strength (MPa)	39.8	40.8	37.9	**39.5**

With the construction of the continuously reinforced flexure test columns completed, the columns were scheduled to be wrapped with the experimental strengthening jackets 17 days after column concrete had been poured. (This process is outlined in Chapter 2 since the process is common in all six of the test columns.) With the retrofit jackets construction complete, twenty, 50 mm long strain gauges were applied to the jacket. These gauges were placed horizontally in the hoop direction on each face of the column in the same dimensional pattern as the reinforcement gauges in Figure 4-1 and Figure 4-2. These strain gauges were applied with a self-leveling adhesive to ensure a good bond to the carbon jacket. Figure 4-3 and Figure 4-4 show the completed application of the jacket strain gages.

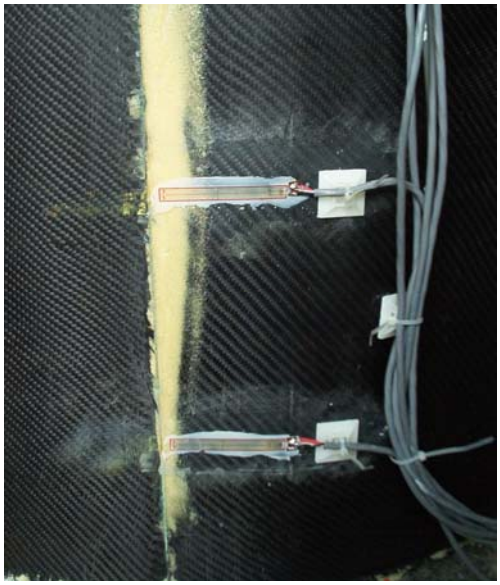

Figure 4-3: Jacket Gages Located at Seam

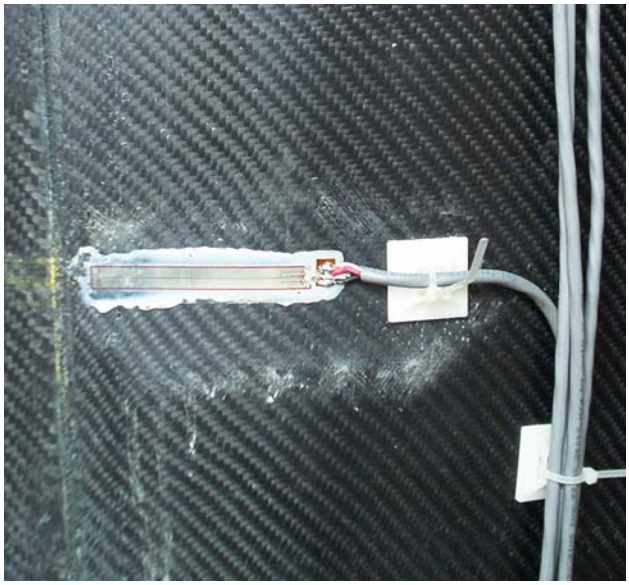

Figure 4-4: Close Up of Jacket Strain Gage Area

4.2.1 Test Program

Each experimental continuously reinforced flexure test column was tied-down to the laboratory's strong floor via six (6) high strength bars. Each of the bars was stressed to 445 kN

(100 kips) to ensure stability of the base during testing. A schematic for the flexure test set-up is given in Figure 4-5.

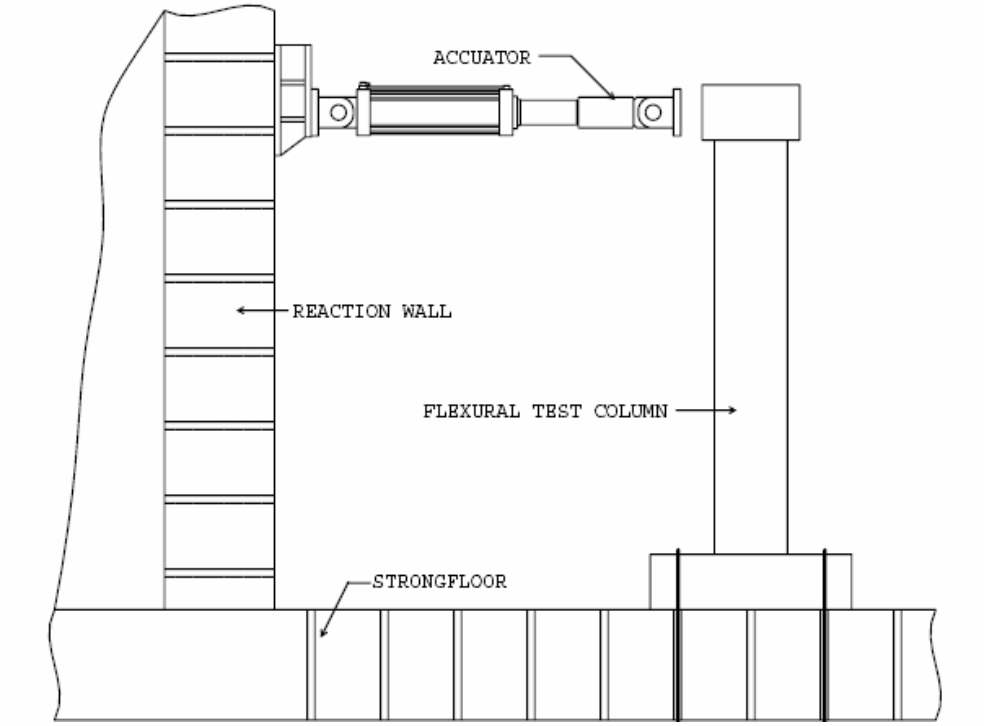

Figure 4-5: Typical Test Set-Up for Flexural Columns

For the two experimental continuously reinforced flexure columns, the test set-up was comprised of a 978 kN (220 kip) capacity actuator with a 22 cm (9-inch) stroke, reacting against the strong wall which was attached to the top of a column's load stub by means of four (4) high strength bars. Atop the load stub was a frame supporting two (2) load cells used to apply a compression load to simulate bridge superstructure self-weight. This pre-described compression load is given in Chapter 2 below Figure 2-7 and Figure 2-8. Figure 4-6 and Figure 4-7 show this test set-up for the continuously reinforced flexural test columns.

Figure 4-6: Overview of Flexure Test Set-Up

Figure 4-7: Overview of Flexure Test Set-Up

With the test column connected to the load frame, the testing of the flexure columns began. In the following section, the testing and general observation for each of the continuously reinforced flexural columns: circular and square are reviewed.

4.3 Circular Continuously Reinforced Flexural Column

4.3.1 Observations

The circular column with continuous column reinforcement was constructed, wrapped with the experimental retrofit jacket and then tested approximately 68 days after the specimen had been cast.

Based on the listed material properties in Table 4-1 and Table 4-3, which were determined from earlier material testing, the theoretical yield force V_y = 192 kN (43 kips) and ideal flexural capacity V_{yi} = 307 kN (69 kips) were calculated using the procedure presented in

Figure 2-31 for circular continuously reinforced flexural column. The pseudo-superstructure load applied to the column was 1780 kN (400 kips) acting as the columns axial load. Assuming an elasto-plastic response an experimental first yield displacement of Δ_y = 2.323 cm (0.914 in) was expected based on the above values.

The theoretical ductilities corresponding to curvature and deflection for the constructed, non-retrofitted column were then determined from the calculated column design values. (See Chapter 2 Figure 2-34 for calculations). The resulting "as-built" column ductilities based on deflection ($\mu_\Delta = \Delta_u/\Delta_y$) and column curvature ($\mu_\phi = \phi_u/\phi_y$) are listed in Table 4-4. According to HITEC protocol, the retrofitted column must exceed these calculated values by the specified amounts of μ_ϕ = 2.0 x "as-built" and μ_Δ = 1.5 x "as-built".

Table 4-4: Resulting "As-Built" Ductilities

ϕ_y =	0.00005	μ_ϕ =	3.58
ϕ_u =	0.00019		
Δ_y =	2.323 cm	μ_Δ =	2.39
Δ_u =	5.560 cm		

With the "as-built" theoretical column ductilities calculated, the loading sequence for the test was established. The circular continuously reinforced flexural column testing was begun under load control. The strains on column's south face reinforcement approached the theoretical values under its Vy loading (a load of 192 kN should yield a deflection of 2.323 cm). Once reinforcement gauge readings reached 2000 με (strain when reinforcement stress has reached its yield point: $\varepsilon = f_y/E$) it was determined that the column reinforcement had yielded. At the Vy loading the rebar strains were slightly less than the yield strain (1843 με) as seen in Figure 4-8.

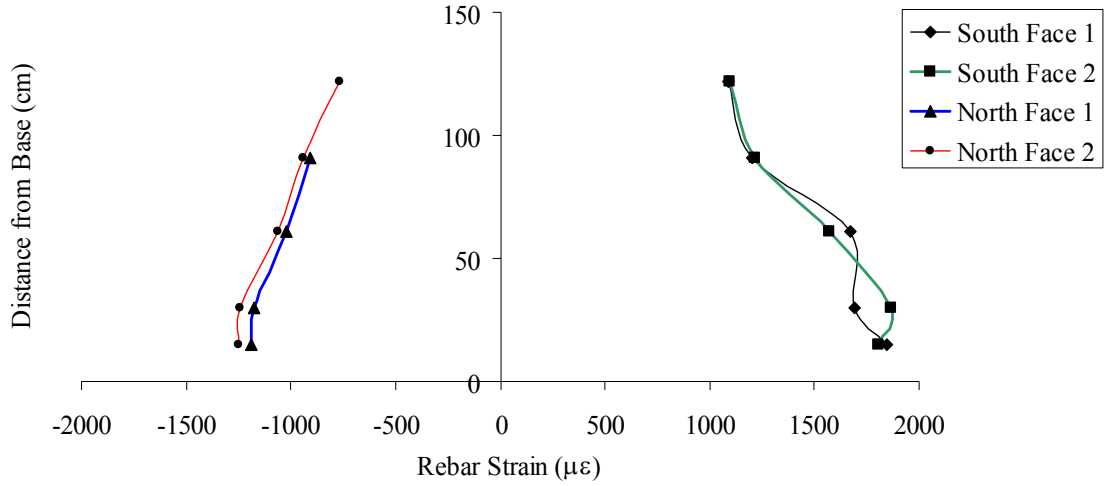

Figure 4-8: Reinforcement Test Strains at Vy Loading

Figures 4-9 through Figure 4-13 show changes in the rebar strain as a function of load control cycles at different locations along the column.

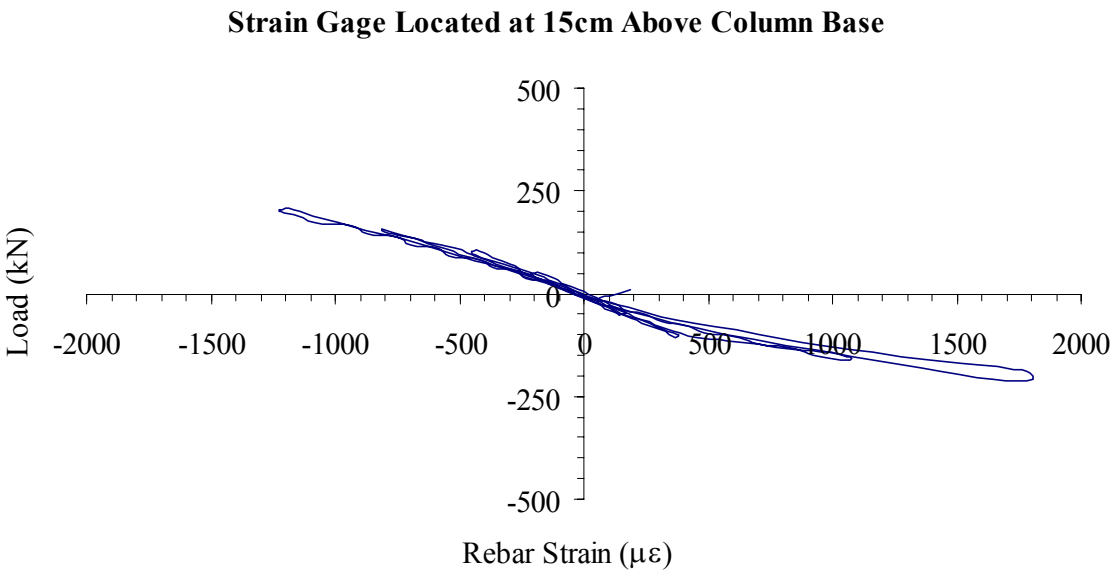

Figure 4-9: South Face 1 Reinforcement Test Strains under Force Loading

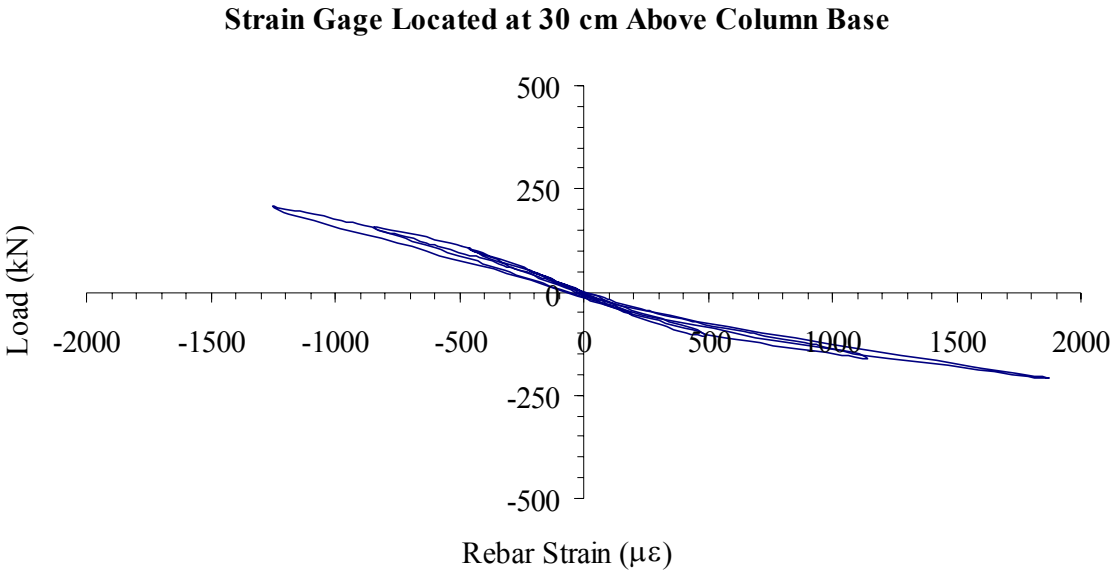

Figure 4-10: South Face 1 Reinforcement Test Strains under Force Loading

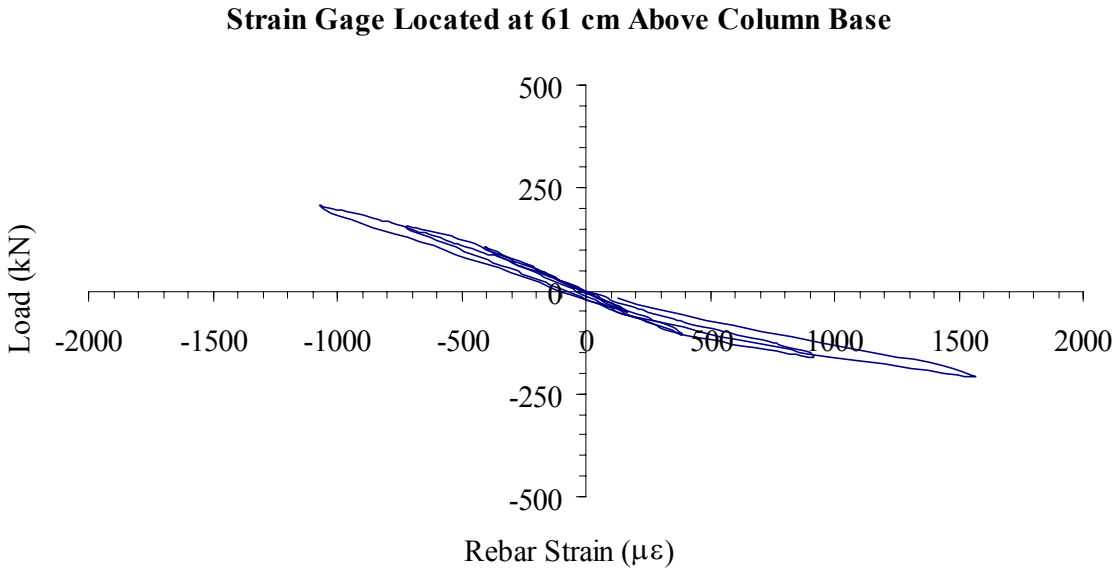

Figure 4-11: South Face 1 Reinforcement Test Strains under Force Loading

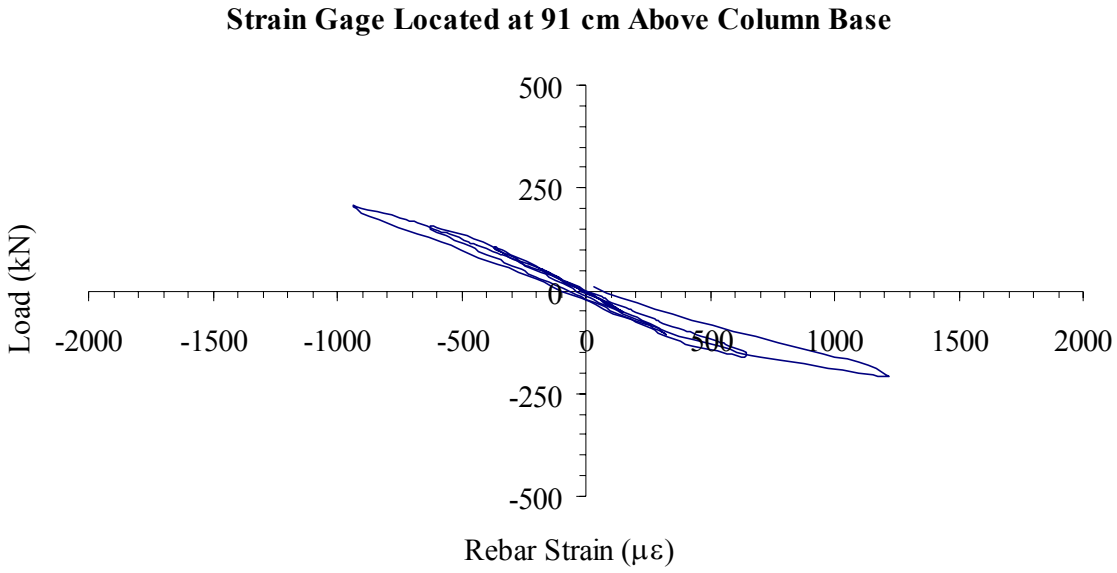

Figure 4-12: South Face 1 Reinforcement Test Strains under Force Loading

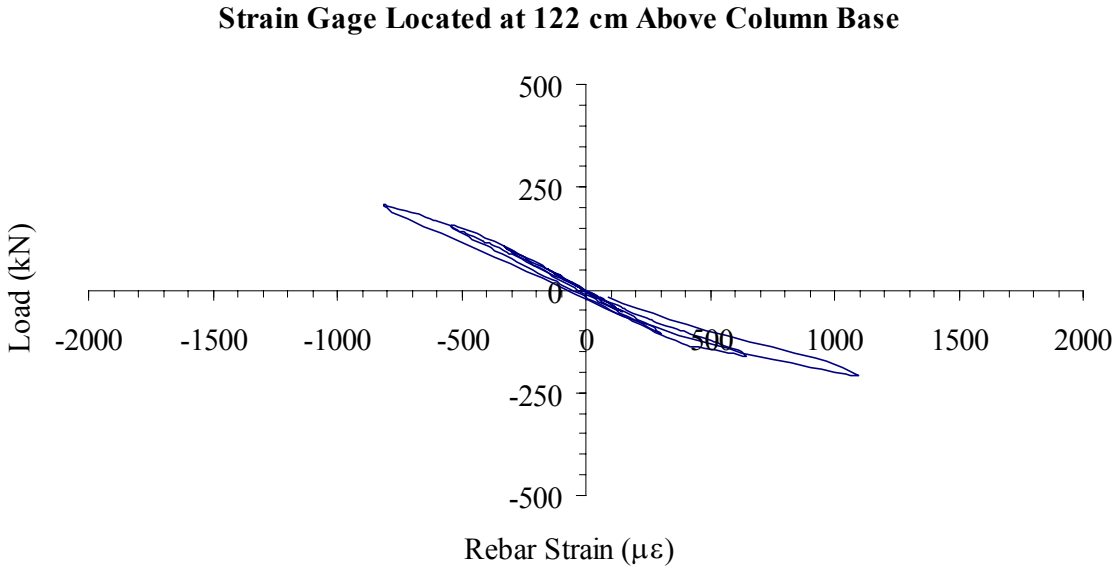

Figure 4-13: South Face 1 Reinforcement Test Strains under Force Loading

After the end of the load control cycles, it was determined that ductility level 1.0 had been reached. This is shown in Figure 4-14 which illustrates that the predicted displacement of 2.323 cm (0.914 in) was reached under a 192 kN loading. A 100% of Vy loading a displacement of 2.832 cm was recorded. This larger displacement indicts that the un-retrofitted column's ductility may be slightly less than calculated.

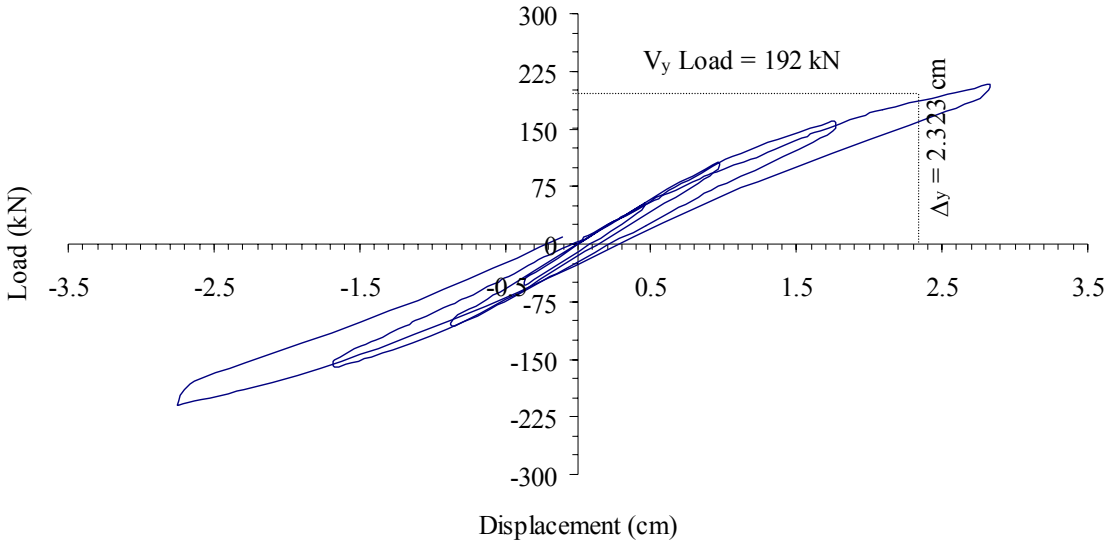

Figure 4-14: Profile at Force Loading Reached at μ = 1

Under deflection load control the reinforcement strains continued to increase. Figure 4-15 through Figure 4-19 show the strain at ductility level 6 displacement at different locations of the column.

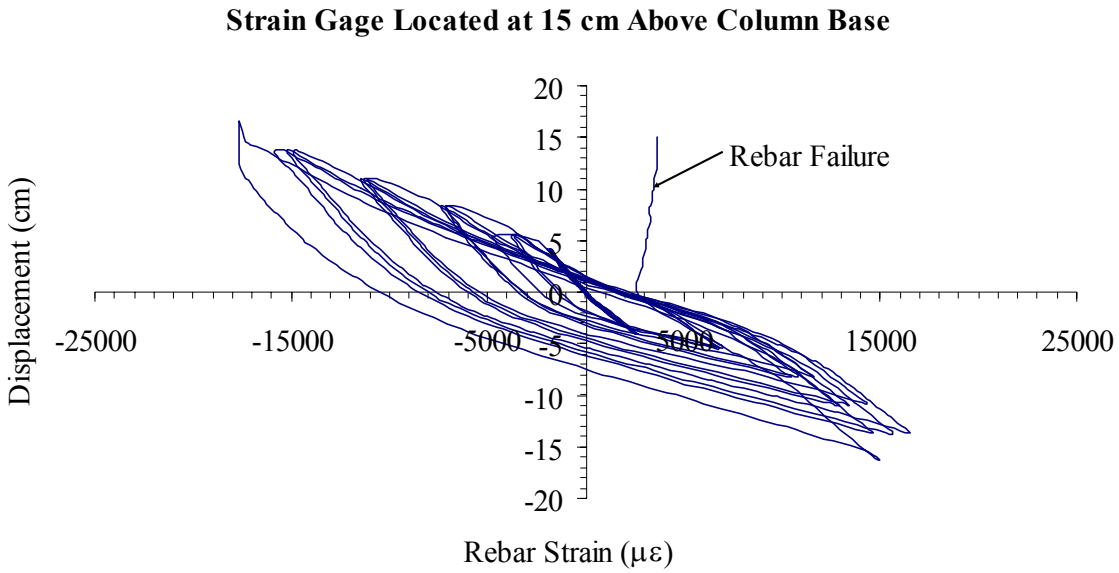

Figure 4-15: South Face 2 Reinforcement Test Strains at μ = 6.0

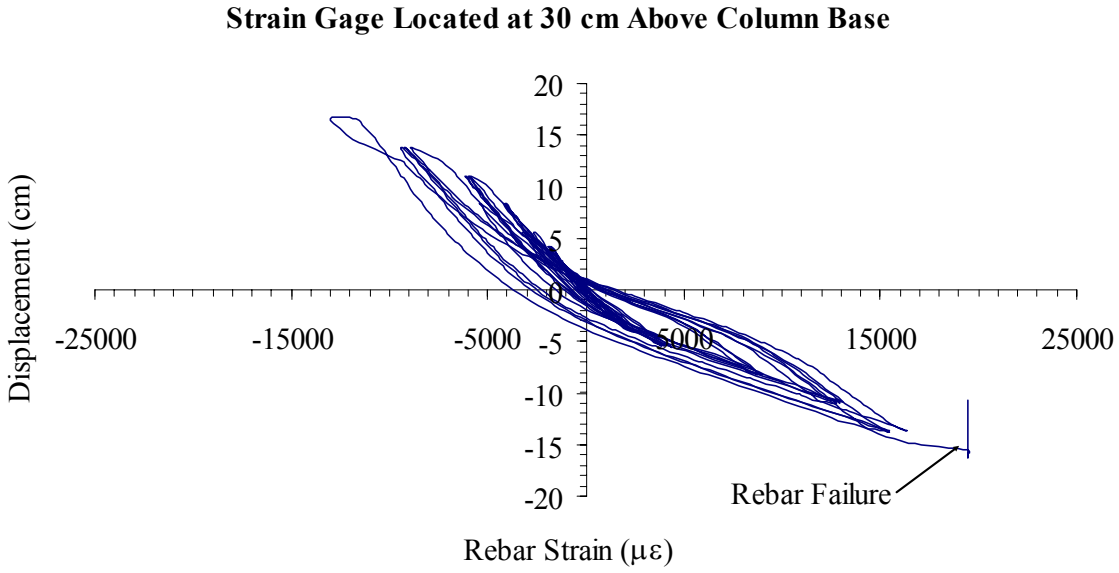

Figure 4-16: South Face 2 Reinforcement Test Strains at μ = 6.0

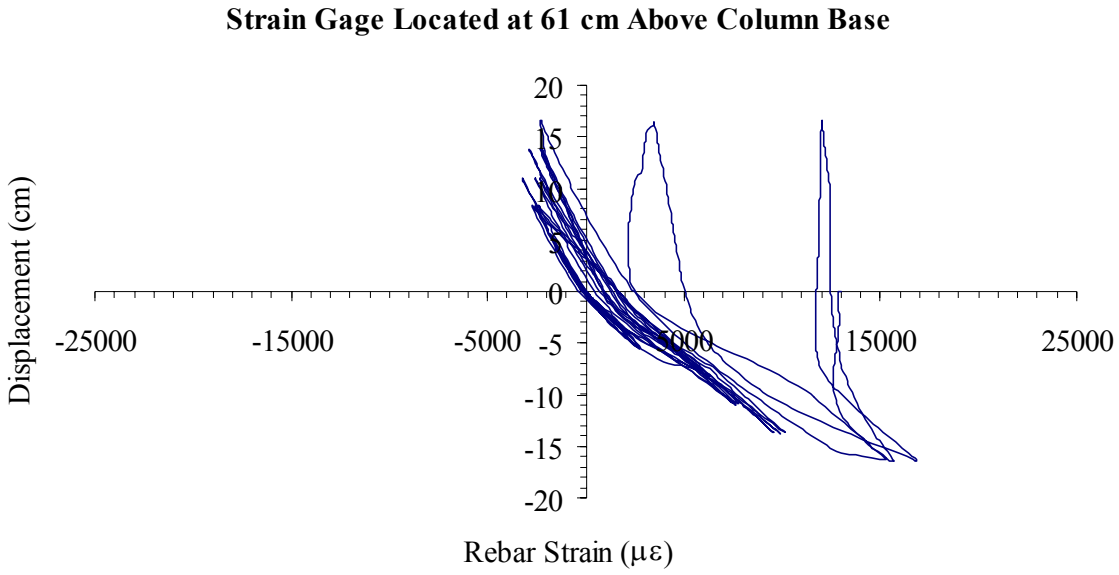

Figure 4-17: South Face 2 Reinforcement Test Strains at μ = 6.0

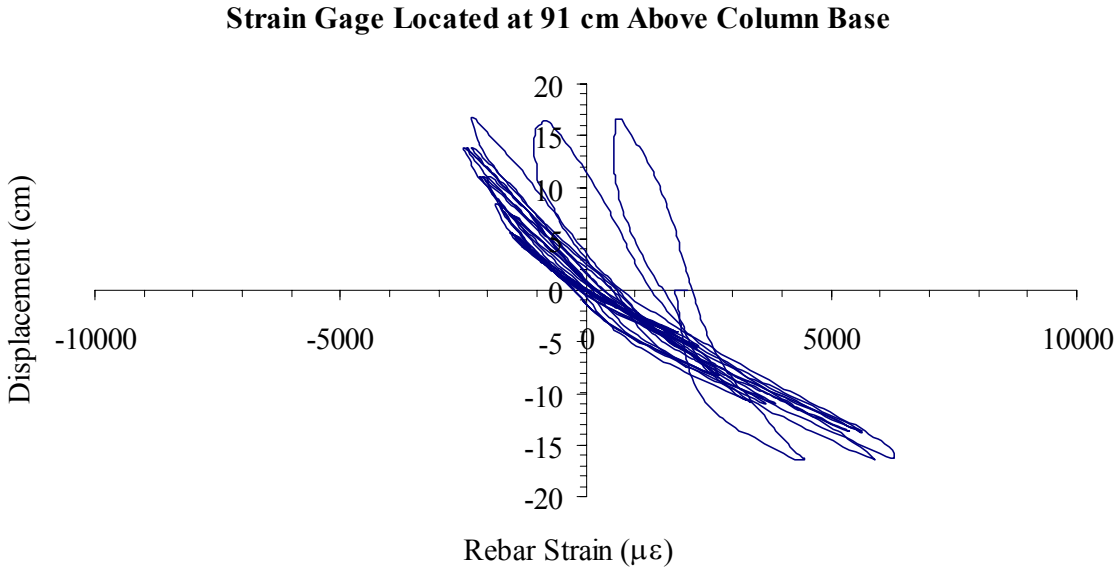

Figure 4-18: South Face 2 Reinforcement Test Strains at μ = 6.0

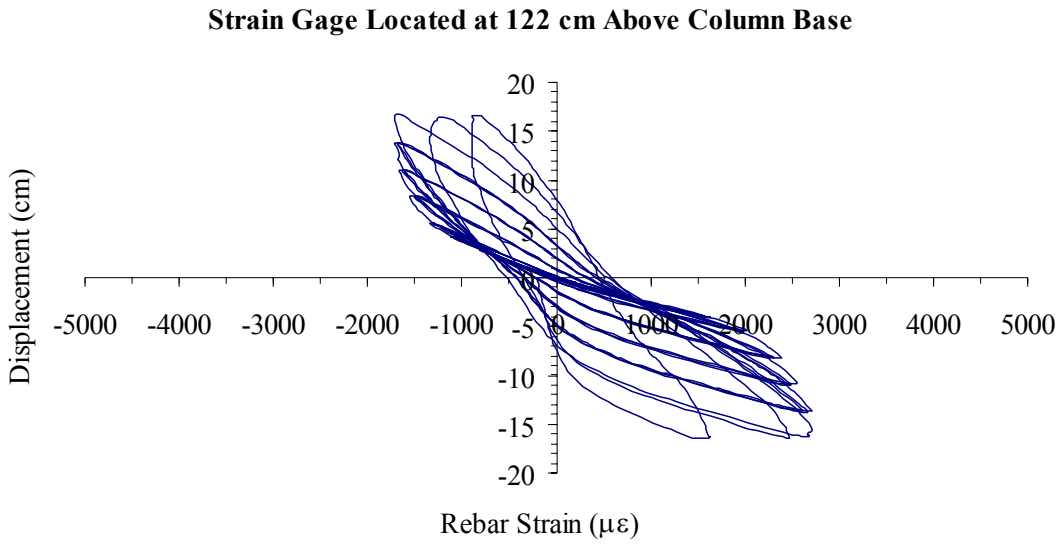

Figure 4-19: South Face 2 Reinforcement Test Strains at μ = 6.0

Figure 4-20 and Figure 4-21 show the column during deflection induced control testing.

Figure 4-20: Continuously Reinforced Circular Flexural Column during testing

Figure 4-21: Continuously Reinforced Circular Flexural Column during testing

Under displacement control cycling, the jacket exhibited minor flexural cracking in the plastic hinge regions (extending to a height of 73 cm from the bottom of the column) most noticeably along the jacket seam as shown in Figure 4-22. Under a 9.291 cm applied deflection equivalent to ductility Level 4, the retrofit jacket began to experience an obvious separation of the construction seam illustrated in Figure 4-23.

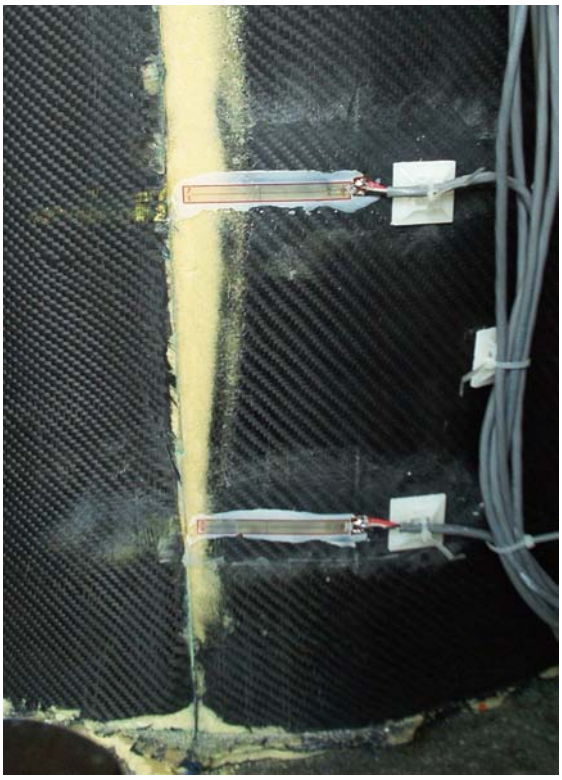

Figure 4-22: Jacket Splitting at Seam

Figure 4-23: Jacket Splitting at Seam

After the first cycle at ductility Level 6 loading, a noticeable decrease in structural integrity was witnessed with decrease in load. The strain along the column jacket was reviewed to determine if softening of the column's load capacity was due to the failure of the column behind the strengthening jacket. Figure 4-15 and Figure 4-16 showed that the longitudinal reinforcement in the column's plastic hinge region had failed by this point in testing. Figure 4-24

through Figure 4-27 show the deflection to strain relationship of the jacket at 30 cm from base of column under ductility 6.

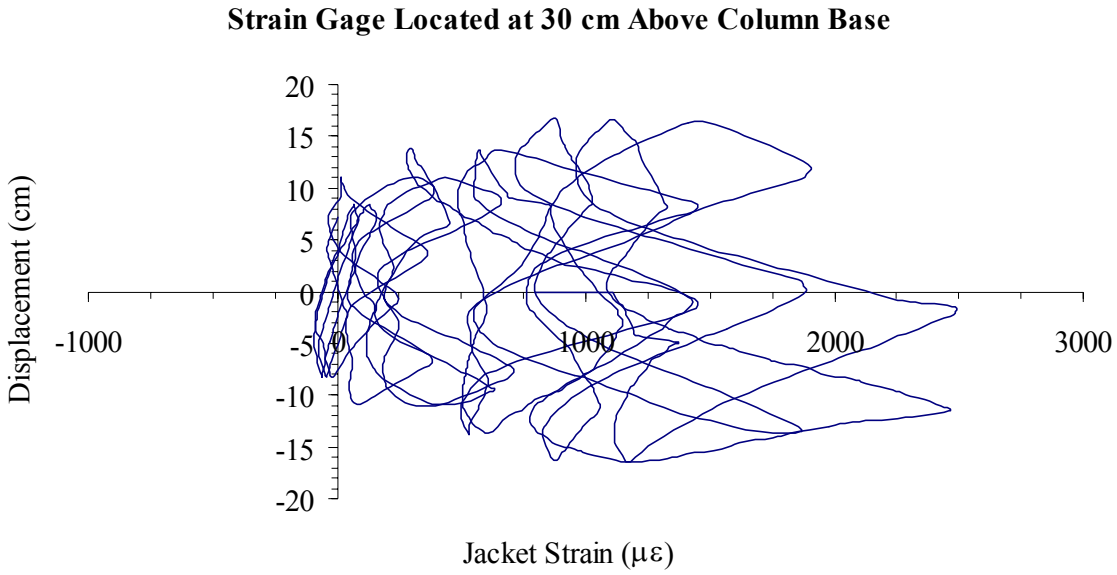

Figure 4-24: South Face Jacket Test Strains at μ = 6.0

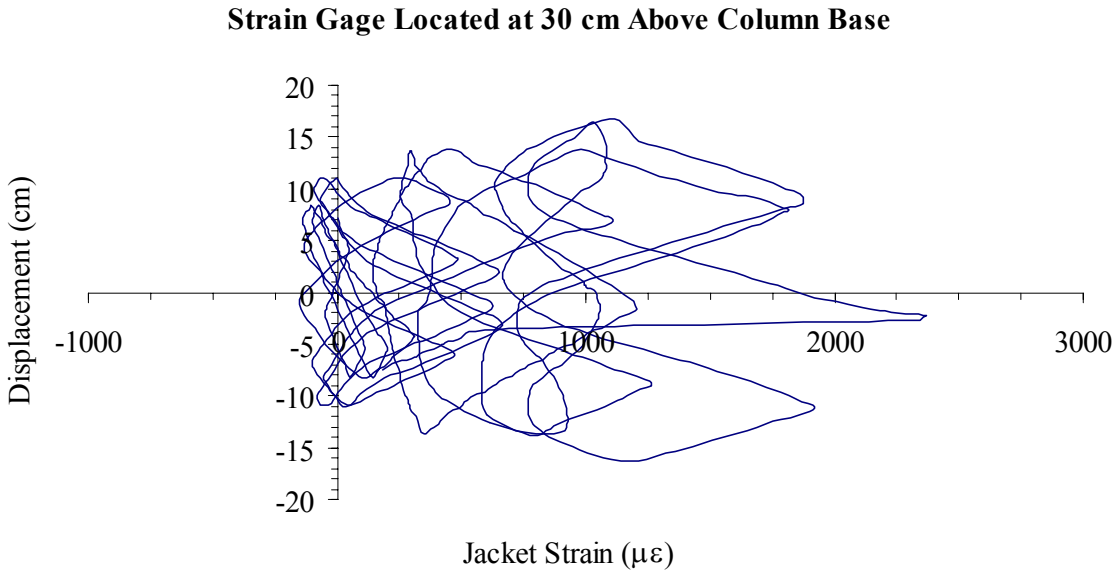

Figure 4-25: North Face Jacket Test Strains at μ = 6.0

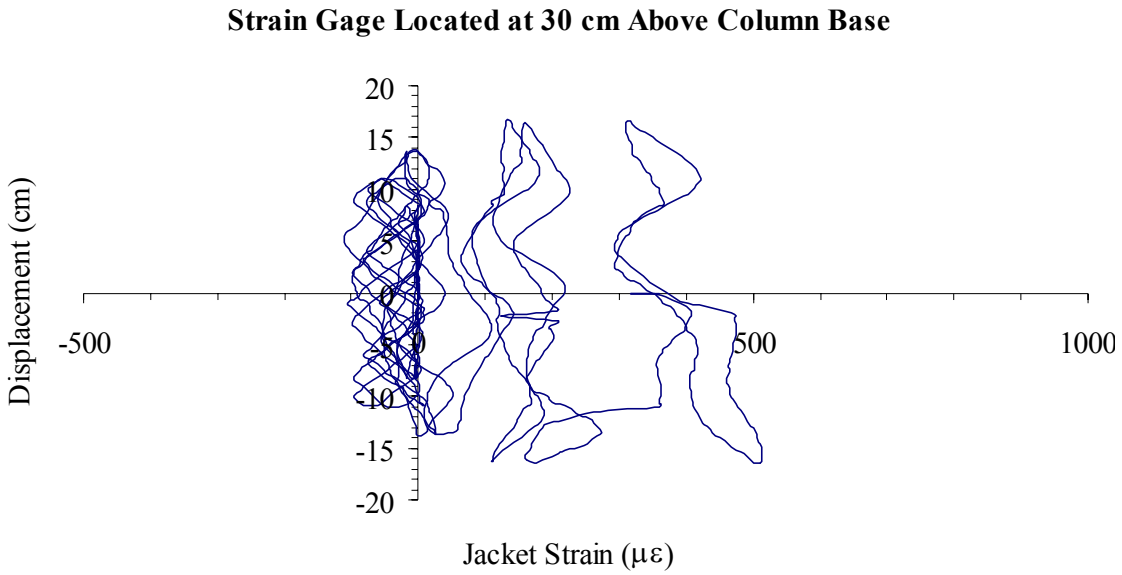

Figure 4-26: East Face Jacket Test Strains at μ = 6.0

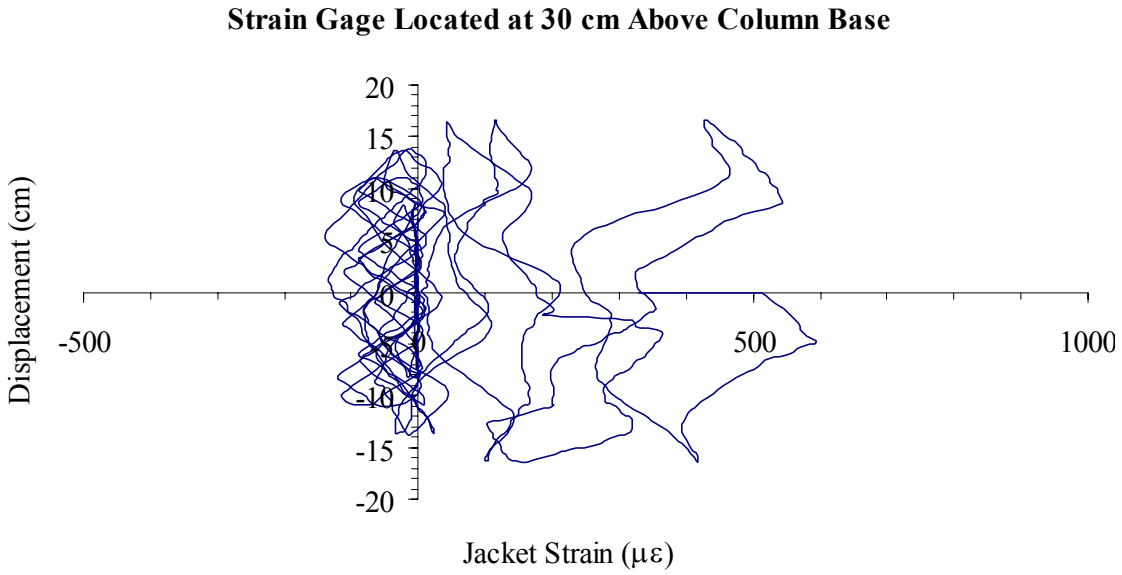

Figure 4-27: West Face Jacket Test Strains at μ = 6.0

During the first cycle at ductility Level 8 loading jacket/confinement failure occurred through splitting as shown in Figure 4-28. A close-up of the crushing of concrete column with

exposed internal reinforcement is shown in Figure 4-29 and it is clear that premature failure of the seam caused failure of the column. The effect of the seam on the failure can be clearly seen through the vertical crack in the concrete which coincides with the vertical end of the inner carbon fabric layer. This would have been avoided had the overlap region in the composite been longer, thereby avoiding an abrupt end of column testing resulting from the seam failure.

Figure 4-28: Jacket Failure

Figure 4-29: Close up of Jacket Failure

4.3.2 Test Results

Stability under cyclic loading during the continuously reinforced circular flexural column testing was measured to the displacement length of 16.55 cm (6.517 inches) with the column failure occurring with a 15% drop in load during the level 6 ductility cycle. A hysteresis plot of the circular flexure is seen in Figure 4-30. This graph shows a stable push-pull response with the

positive push data mirroring the negative pull data about the zero load and zero displacement axes. The area outlined within the data point of graph is smooth elliptical shape with no major jumps or drops during an induced cycle to indicate instability. A slight dip in the load under the first cycle of ductility level 5 is observed as the jacket seam began to fail. There was also a considerable loss of load carrying capacity noticed during the ductility level 6 cycles.

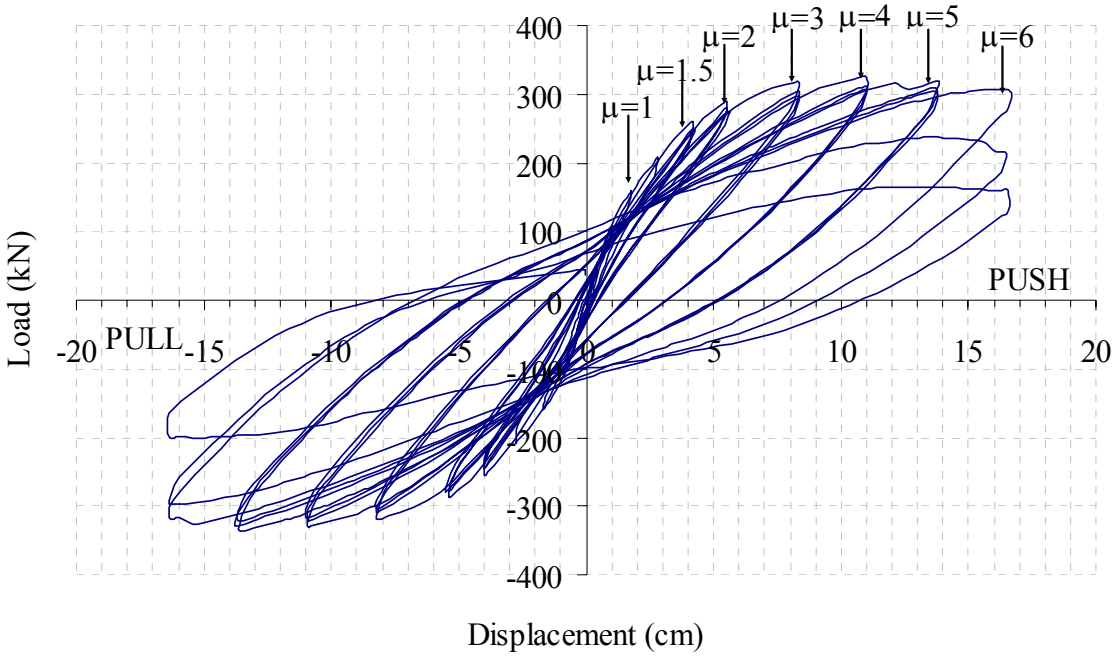

Figure 4-30: Flexure Column Load vs. Displacement Test Results

The test column's final retrofitted ductility calculation utilized the 16.55 cm measurement given that this was the displacement length the test specimen achieved during the last loading cycle. Table 4-5 lists the final results collected from the continuously reinforced circular flexural column experiment used in the retrofit system analysis.

Table 4-5: Continuously Reinforced Circular Flexural Column Final Test Results

Maximum Test Load	323 kN
Failure Initiation Load	275 kN
Maximum Displacement	16.55 cm

The results from the experiment for the circular flexure column were compiled to establish the column's retrofitted ductilities in terms of displacement and curvature. These values were then evaluated against the "as-built" ductilities in Table 4-4 to determine if the retrofitted column surpassed the baseline set by the HITEC guidelines. The retrofitted column failed at forced displacement of 16.55 cm, as noted in Table 4-5, which results in a deflection ductility of $\mu_\Delta = 7.13$ and a curvature ductility of $\mu_\phi = 12.35$. These results listed in Table 4-6, show that the retrofitted ductilities exceeded the criteria set by the HITEC protocol.

Table 4-6: Continuously Reinforced Circular Flexural Column Ductility Comparison

Ductility	"As-Built"	Retrofit	*Ductility Increase*
μ_Δ	2.39	7.13	*2.98*
μ_ϕ	3.58	12.35	*3.45*

With the additional ductility provided by the retrofit jacket, the continuously reinforced circular column exceeded the required specifications set by the HITEC protocol to qualify as an acceptable retrofit procedure. The tested column deformed elastically to the set failure load and exceeded the increased ductility requirements.

Improved performance and increased ductility would be expected from this system if the production of the jacket were adjusted to strengthen the jacket's seam. Viewing the jacket strains at ductility level 6.0 in Figure 4-24 to Figure 4-27, it is apparent that the material had not reached its maximum strain capacity since the measurements are well below failure strains associated with a typical carbon fiber.

Table 4-7 is a summary of the all the peak strains at ductility levels associated with the testing.

Table 4-7: Peak Test Strains (με)

	Level 1.0	Level 1.5	Level 2.0	Level 3.0	Level 4.0	Level 5.0	Level 6.0
Rebar	1863	2675	6694	10236	18582	FAIL	FAIL
Jacket	269	408	698	1446	1893	2248	2276

The column's internal reinforcement was stressed to failure while the jacket strains remained relatively low in comparison to the expected minimum strain level of the carbon/epoxy material of 10000 με. Jacket failure was due to a split along the seam which was un-reinforced. Improvements in the seam would enhance overall performance and maximize system level performance.

4.4 Square Continuously Reinforced Flexural Column

4.4.1 Observations

The square column with continuous column reinforcement was constructed, wrapped with the experimental retrofit jacket and then tested approximately 72 days after the specimen had been cast.

Based on the listed material properties in Table 4-1 and Table 4-3, which were determined from earlier material testing, the theoretical yield force V_y = 112 kN (25 kips) and ideal flexural capacity V_{yi} = 178 kN (40 kips) were calculated using the procedure presented in Figure 2-31 for square continuously reinforced flexural column. The pseudo-superstructure load applied to the column was 1155 kN (260 kips) acting as the columns axial load. Assuming an

elasto-plastic response, an experimental first yield displacement of Δ_y = 3.979 cm (1.567 in) was expected based on the above values.

The theoretical ductilities corresponding to curvature and deflection for the constructed, non-retrofitted column was then determined from the calculated column design values. (See Chapter 2 Figure 2-35 for calculations). The resulting "as-built" column ductilities based on deflection ($\mu_\Delta = \Delta_u/\Delta_y$) and column curvature ($\mu_\phi = \phi_u/\phi_y$) are listed in Table 5-8. According to HITEC protocol, the retrofitted column must exceed these calculated values by the specified amounts of μ_ϕ = 2.0 x "as-built" and μ_Δ = 1.5 x "as-built".

Table 4-8: Resulting "As-Built" Ductilities

ϕ_y =	0.00009	μ_ϕ =	3.25
ϕ_u =	0.00029		
Δ_y =	3.979 cm	μ_Δ =	2.22
Δ_u =	8.820 cm		

With the "as-built" theoretical column ductilities calculated, the loading sequence for the test was established. The square continuously reinforced flexural column testing was begun under load control. The strains along the column's south face reinforcement approached the theoretical values under its Vy loading (a load of 112 kN should yield a deflection of 3.979 cm). Once reinforcement gauge readings reached 2000 με (strain when reinforcement stress has reached its yield point: $\varepsilon = f_y/E$) it was determined that the column reinforcement had yielded. At the Vy loading the rebar strains were slightly less than the yield strain (1691 με) as seen in Figure 4-31. Figure 4-32 through Figure 4-36 show how the rebar strain changed under load control cycles at different locations along the column.

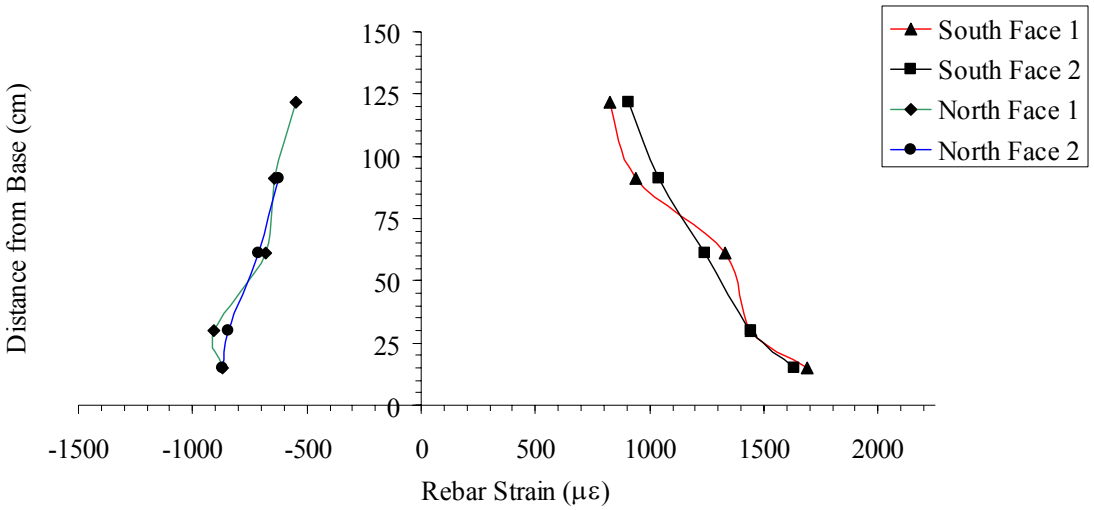

Figure 4-31: Reinforcement Test Strains at Vy Loading

Strain Gage Located at 15 cm Above Column Base

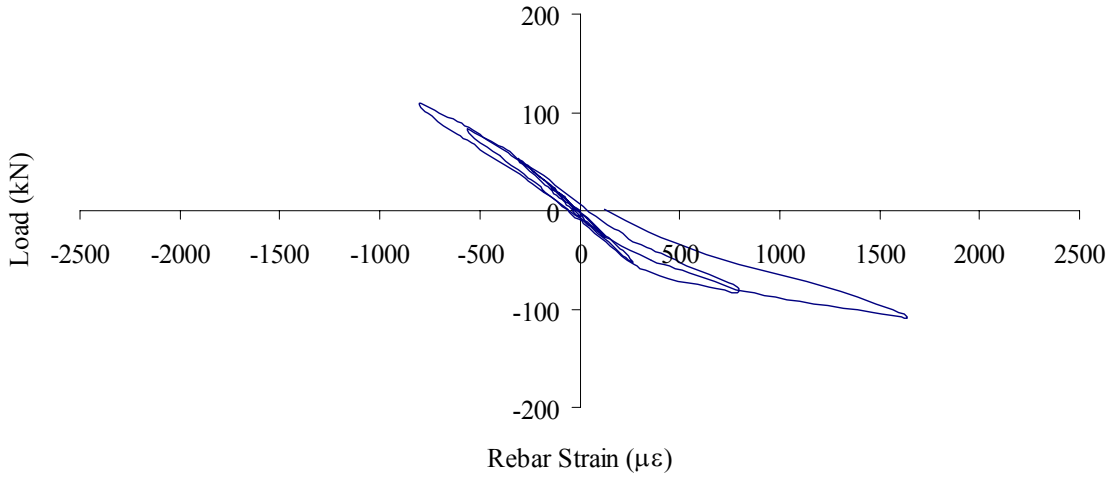

Figure 4-32: South Face 1 Reinforcement Test Strains under Force Loading

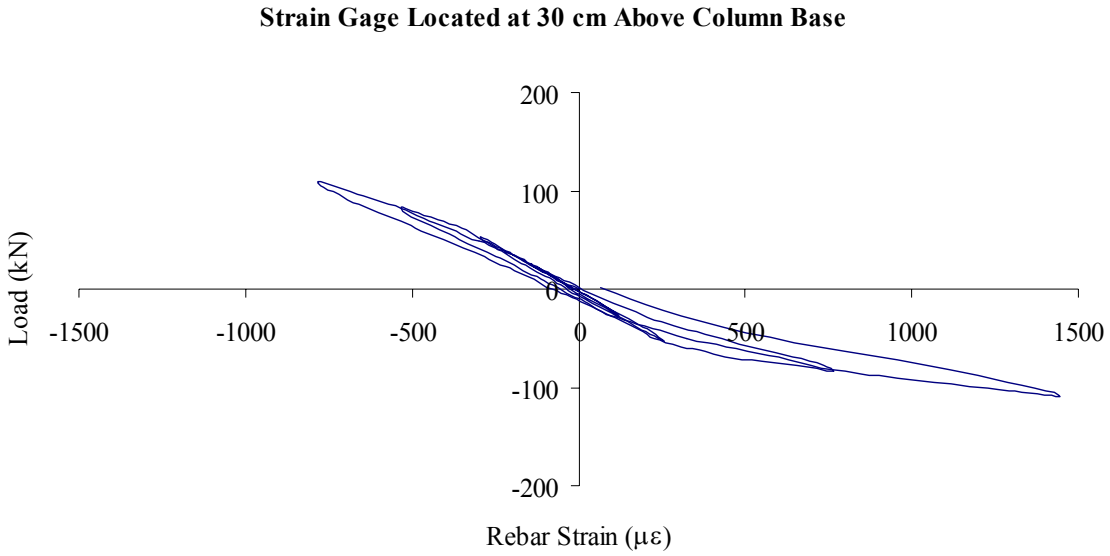

Figure 4-33: South Face 1 Reinforcement Test Strains under Force Loading

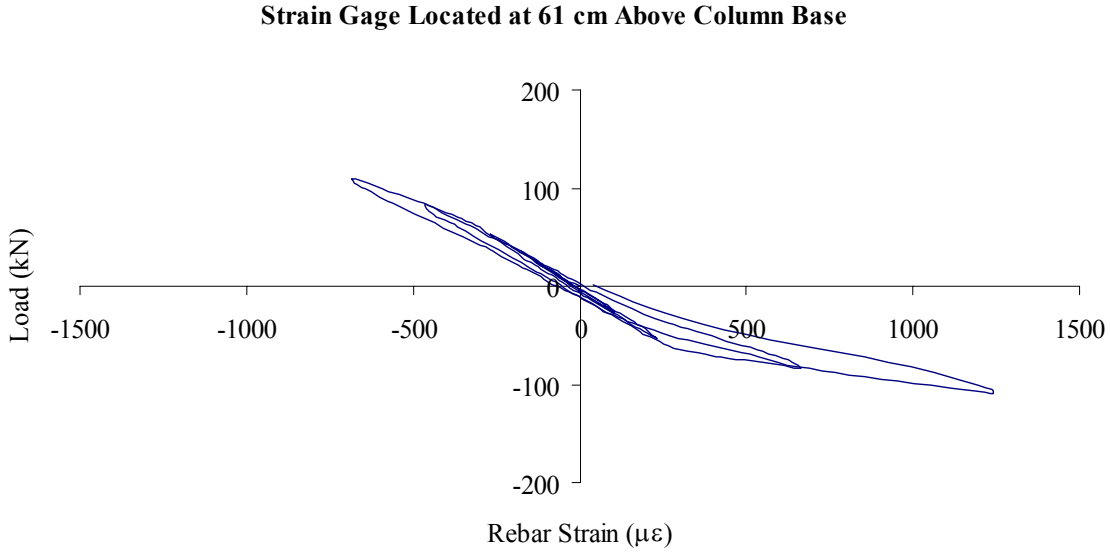

Figure 4-34: South Face 1 Reinforcement Test Strains under Force Loading

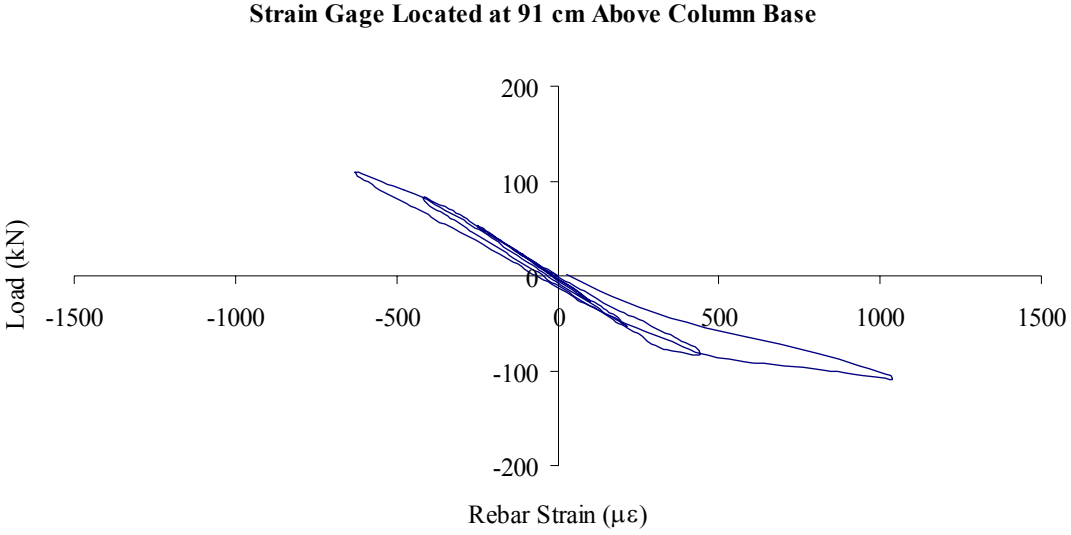

Figure 4-35: South Face 1 Reinforcement Test Strains under Force Loading

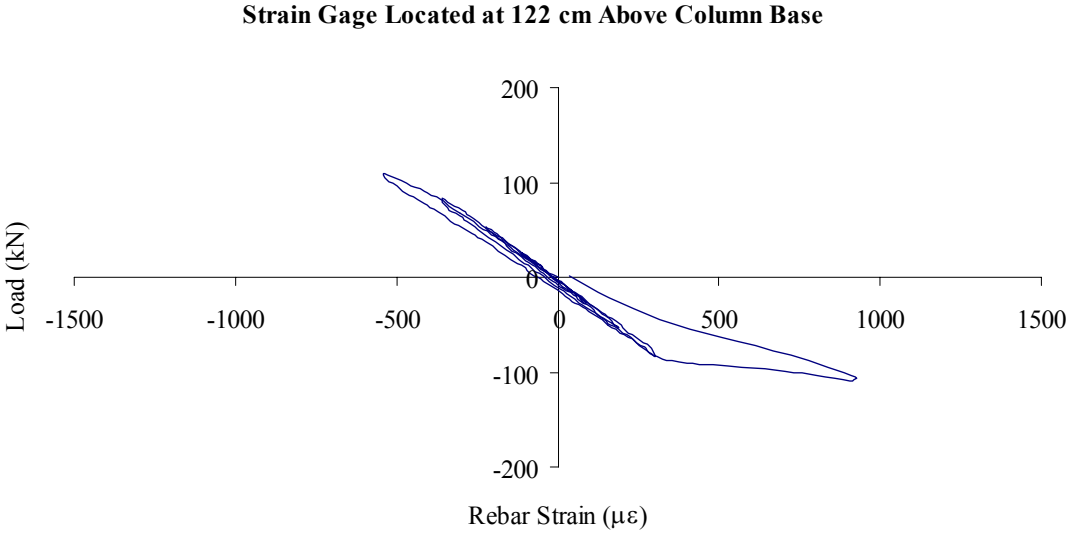

Figure 4-36: South Face 1 Reinforcement Test Strains under Force Loading

After the end of the load control cycles, it was determined that ductility level 1.0 had not been reached. Figure 4-37 shows the strain in South Face 1 reinforcement at different location as the column was put through each cycle. From this graph, it is noted that readings show that the gage 15 cm from base shows yield in the reinforcement by the end of the ductility level 1 cycle.

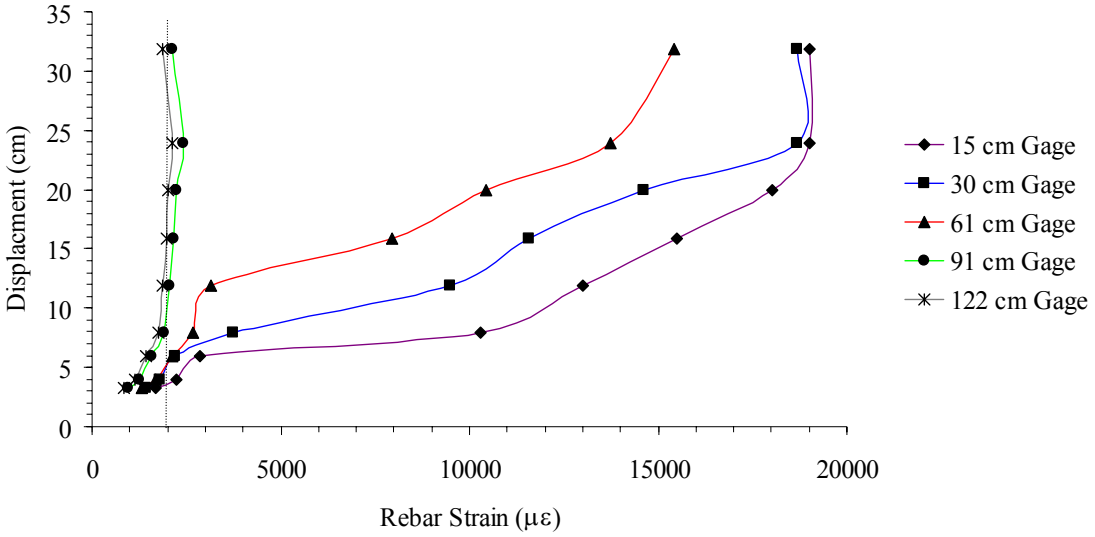

Figure 4-37: Load vs. Displacement showing Force Loading reached μ = 1

Under deflection load control the reinforcement strains continued to increase. Figure 4-38 through Figure 4-42 show the strain at ductility level 6 displacements at different locations of the column.

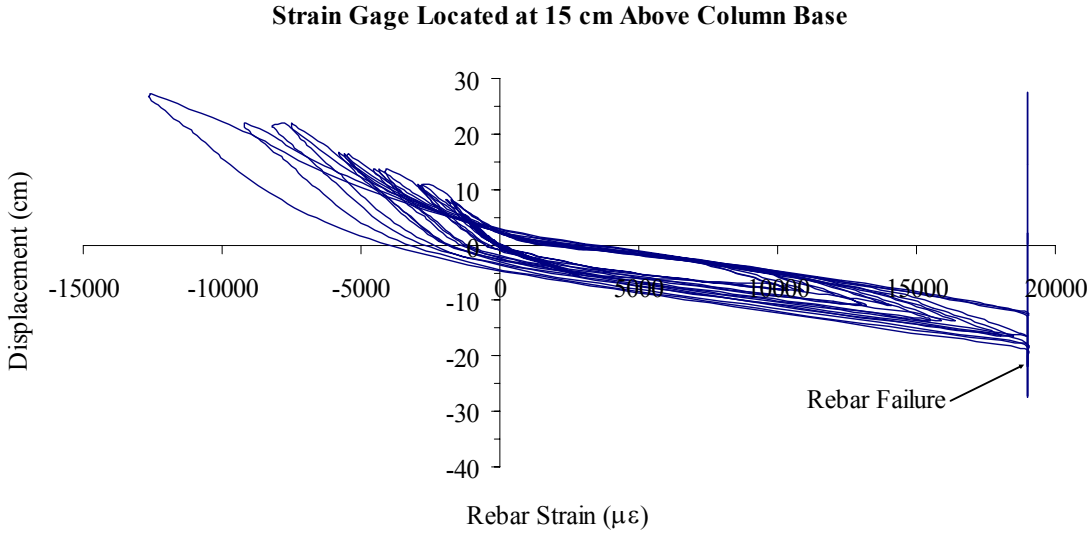

Figure 4-38: South Face 2 Reinforcement Test Strains at μ = 8.0

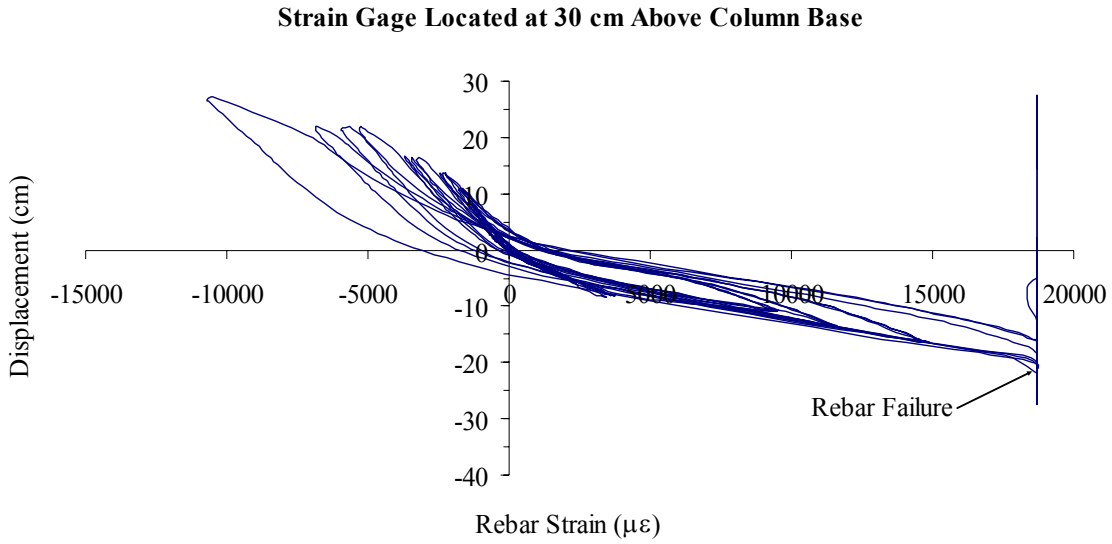

Figure 4-39: South Face 2 Reinforcement Test Strains at μ = 8.0

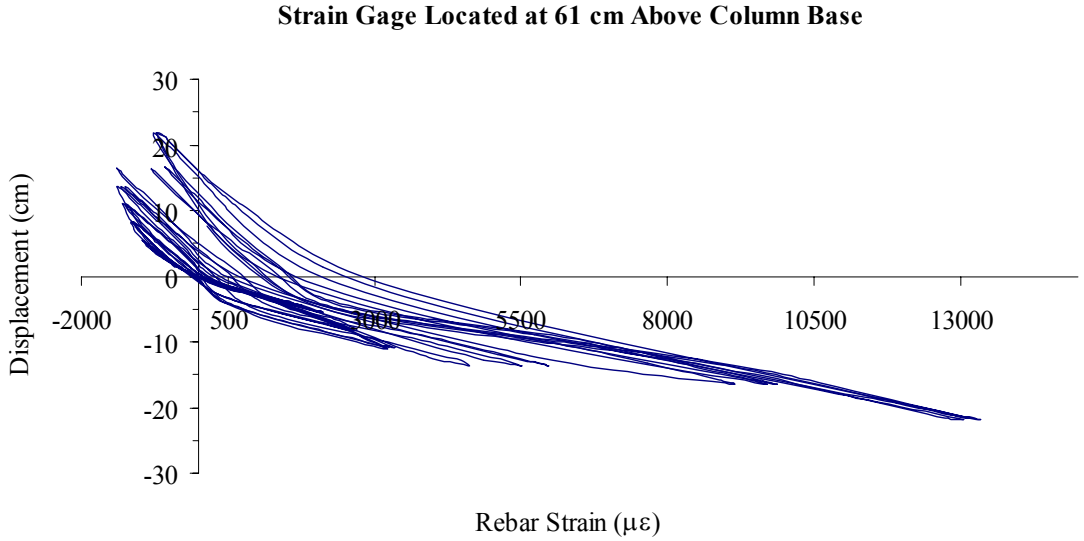

Figure 4-40: South Face 2 Reinforcement Test Strains at μ = 8.0

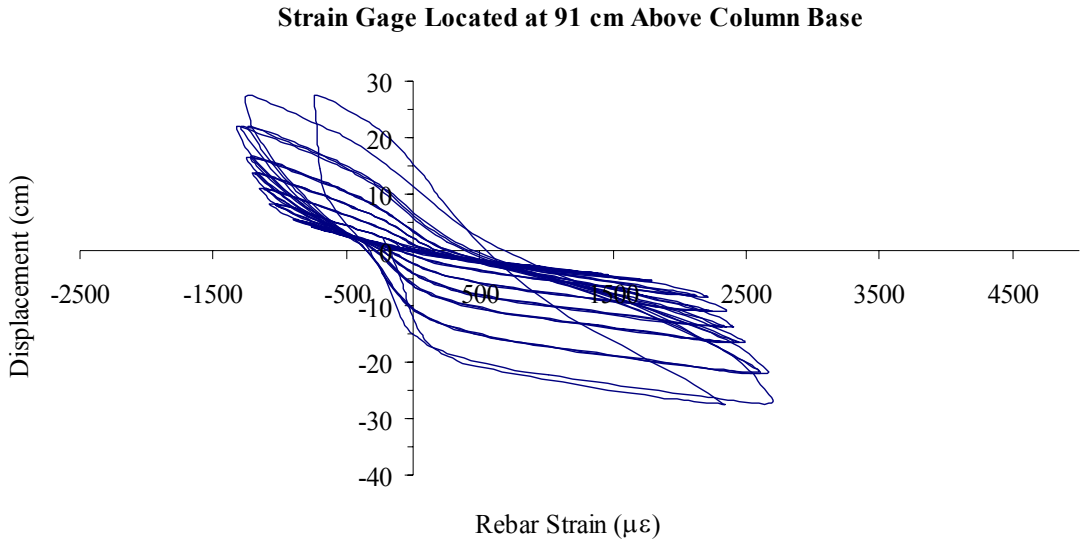

Figure 4-41: South Face 2 Reinforcement Test Strains at μ = 8.0

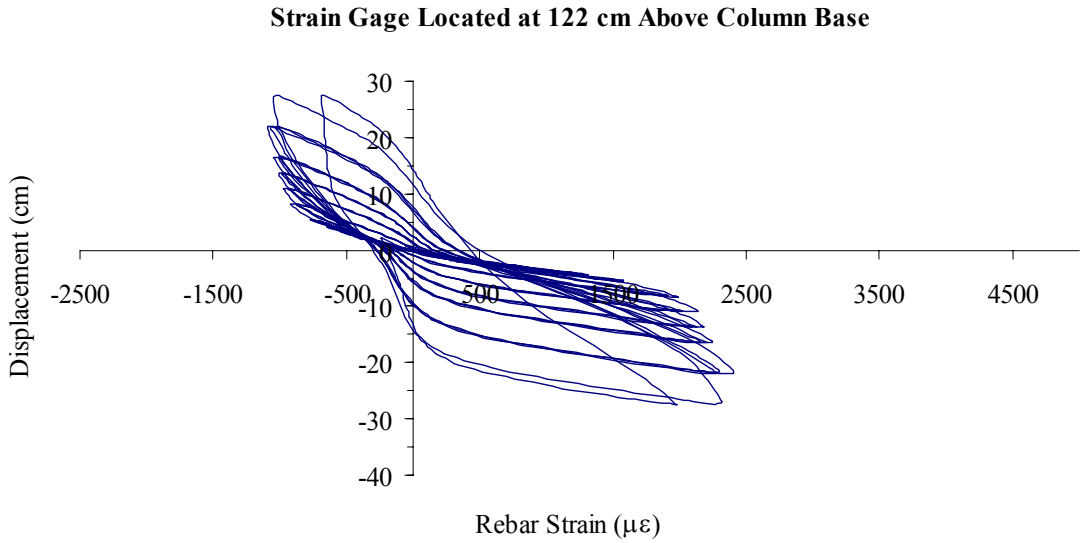

Figure 4-42: South Face 2 Reinforcement Test Strains at μ = 8.0

Figure 4-43 and Figure 4-44 show the column during the pre-specified deflection induced control testing in a pull then a push cycle position.

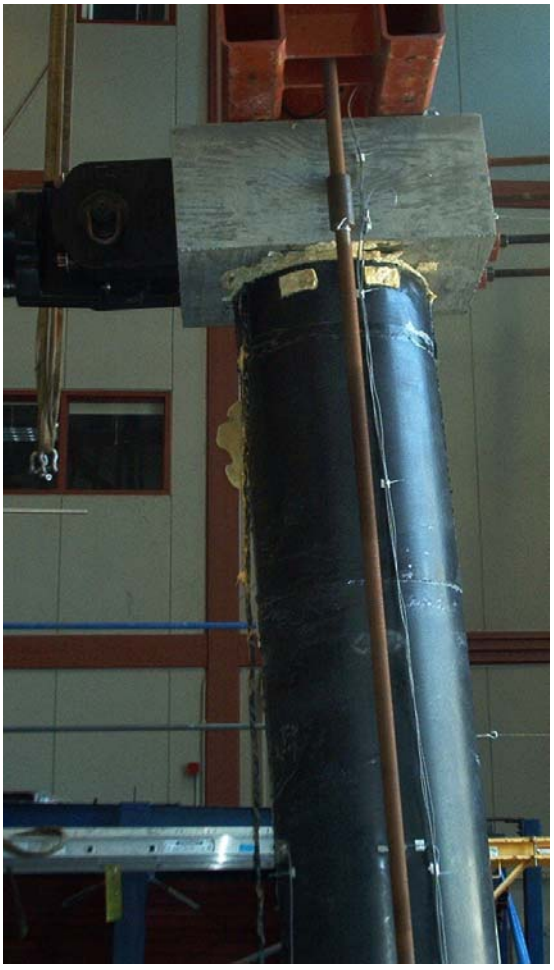

Figure 4-43: Continuously Reinforced Square Flexural Column during testing

Figure 4-44: Continuously Reinforced Square Flexural Column during testing

Under displacement control cycling, the jacket exhibited minor flexure cracking in the plastic hinge regions (first 73 cm from the bottom of the column) most noticeably along the top of the plastic hinge in the hoop direction during the level 3 ductility cycle as shown in Figure 4-45. Under a 19.89 cm applied deflection at ductility Level 5, the retrofit jacket showed an obvious separation of the construction seam along the overlap region as illustrated in Figure 4-46.

Figure 4-45: Horizontal Jacket Splitting

Figure 4-46: Jacket Splitting at Seam

After the second cycle of ductility at level 8 loading, the jacket failed and separated from column. The strain along the column jacket was reviewed to determine if the rupture of the strengthening jacket was due to material failure. Figure 4-38 to Figure 4-39 showed that the longitudinal reinforcement in the column's plastic hinge region had failed by this point in testing. Figure 4-47 through Figure 4-50 show the response of the jacket strains at a height of 15 cm from base of column under ductility 8.

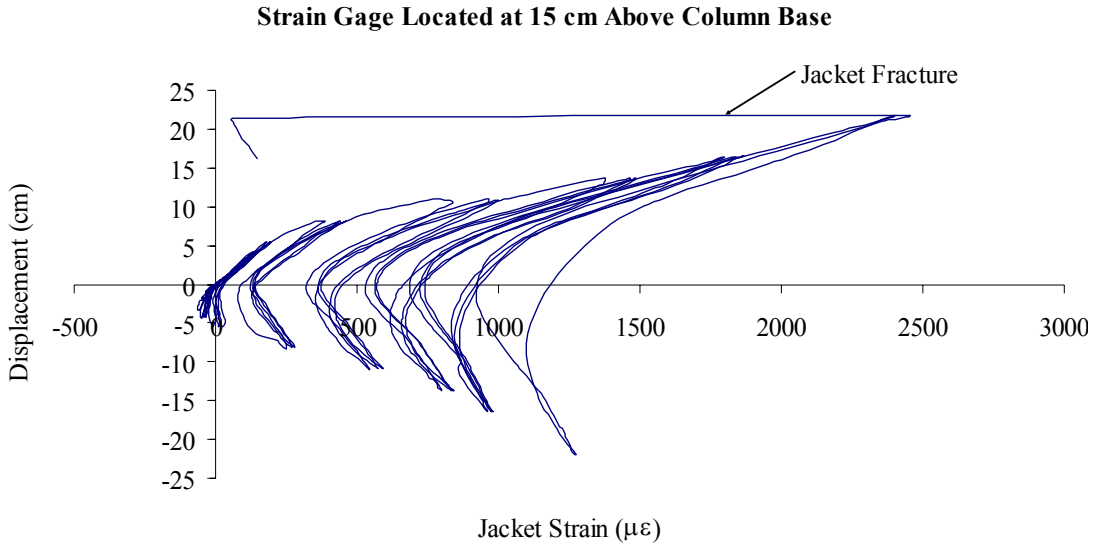

Figure 4-47: South Face Jacket Test Strains at μ = 8.0

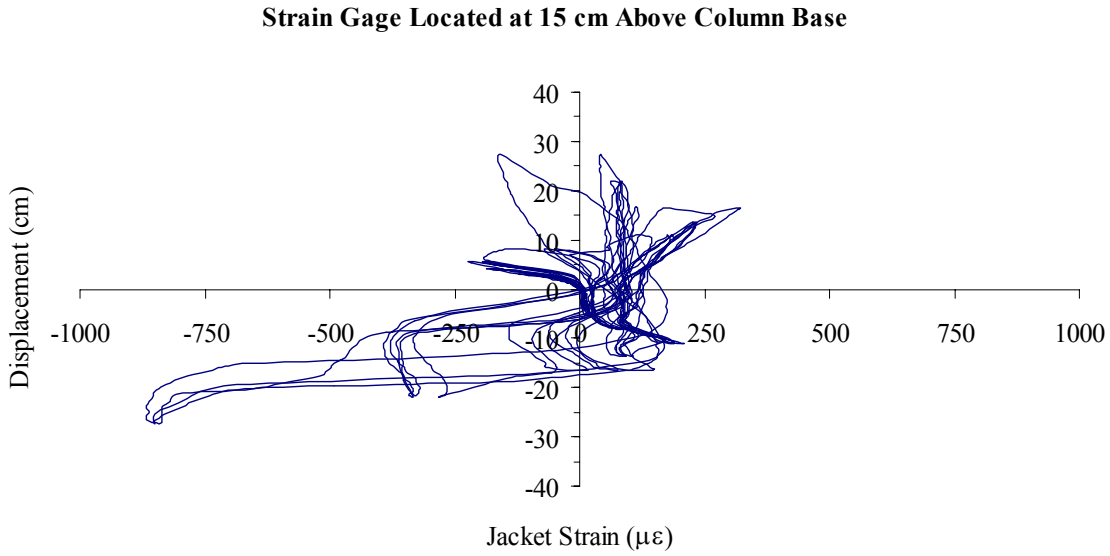

Figure 4-48: North Face Jacket Test Strains at μ = 8.0

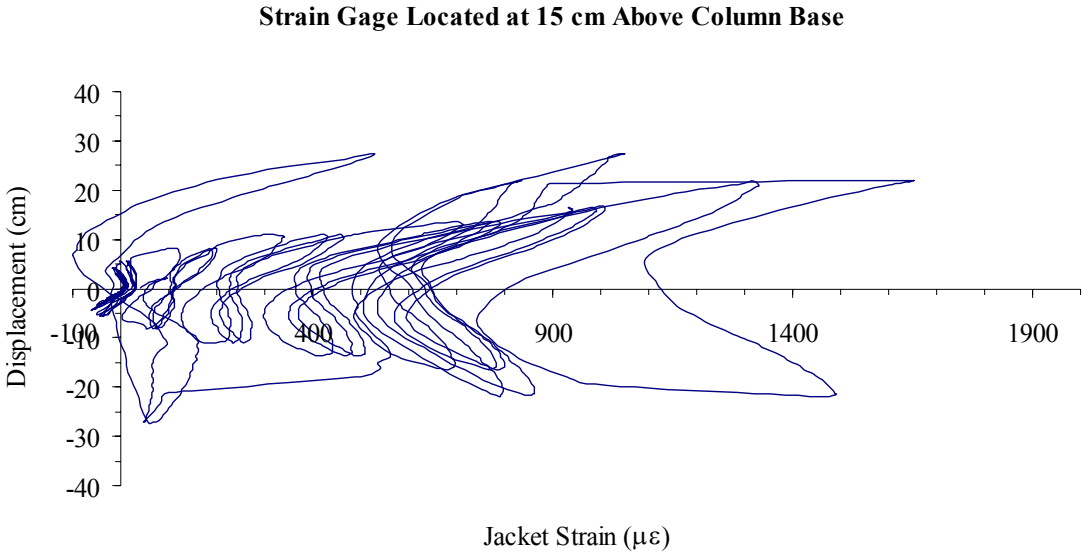

Figure 4-49: East Face Jacket Test Strains at μ = 8.0

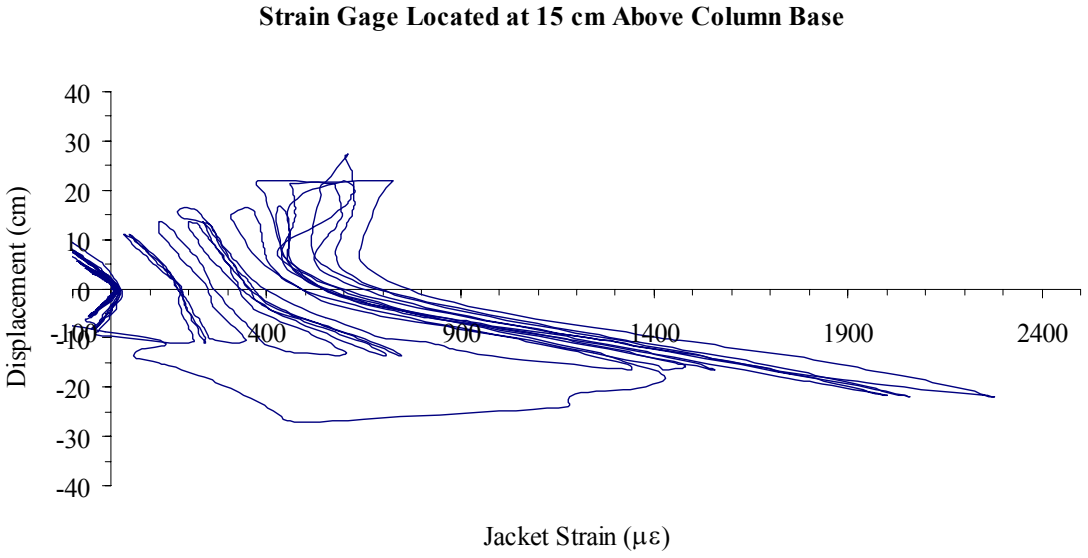

Figure 4-50: West Face Jacket Test Strains at μ = 8.0

As previously noted, during the second cycle at ductility Level 8 loading, a jacket/confinement failure occurred. This jacket split is shown in Figure 4-51 and a close-up of the jacket with the exposed internal carbon jacket layer is shown in Figure 4-52. Unlike in the previous circular column case, failure was caused by the failure at the composite splice region with some fracture in the carbon/epoxy itself.

Figure 4-51: Square Column Jacket Failure

Figure 4-52: Close up of Jacket Failure

4.4.2 Test Results

Stability under cyclic loading during the continuously reinforced square flexural column testing was measured at the displacement length of 23.874 cm (9.399 inches) with the column

failure occurring with the failure of the strengthening jacket causing a significant drop in load capacity. A hysteresis plot of the square flexure column is seen in Figure 4-53. This graph shows a stable push-pull response with the positive push data mirroring the negative pull data about the zero load and zero displacement axes up until ductility level 6. The area outlined within the data point of graph is smooth elliptical shape with no major jumps or drops during an induced cycle to indicate instability. There was a considerable loss of load carrying capacity noticed during the ductility level 8 cycles which indicates column instability. Testing was terminated after second cycle due to this hysteresis response.

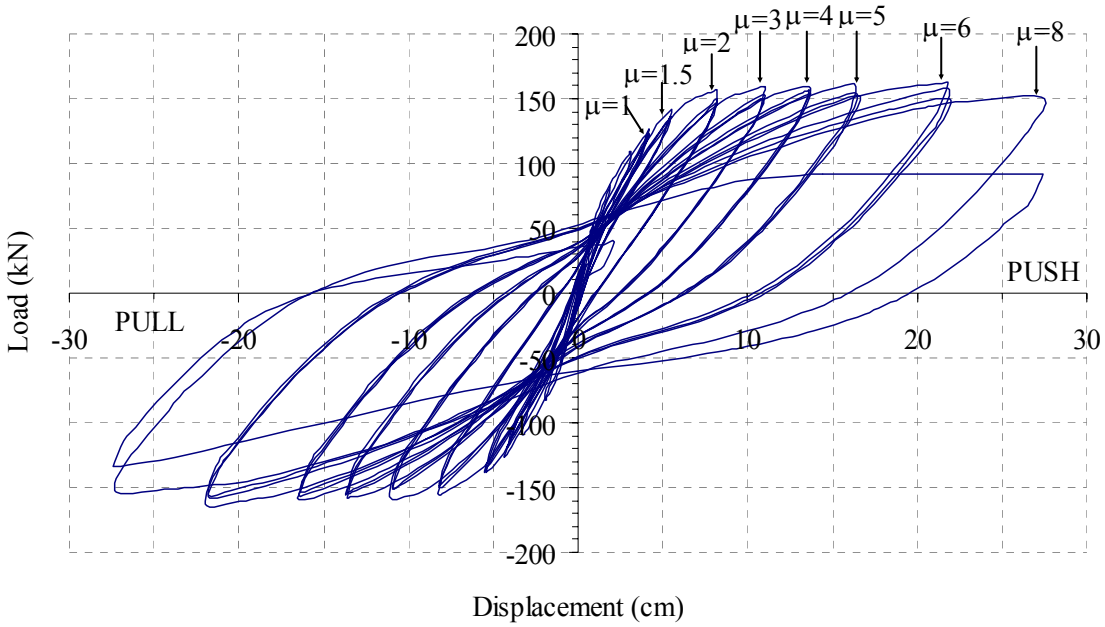

Figure 4-53: Flexure Column Load vs. Displacement Test Results

The test column's final retrofitted ductility calculation utilized the 21.929 cm measurement given that this was the displacement length achieved during the last completed loading cycle. The column did not finish all three (3) cycles of ductility level 8 and hysteretic

stability could not be maintained. Table 4-9 lists the final results collected from the continuously reinforced circular flexural column experiment used in the retrofit system analysis.

Table 4-9: Continuously Reinforced Square Flexural Column Final Test Results

Maximum Test Load	162 kN
Failure Initiation Load	138 kN
Maximum Displacement	21.929 cm

The results from the experiment for the circular flexure column were compiled to establish the column's retrofitted ductilities of displacement and curvature. These values were then evaluated against the "as-built" ductilities in Table 4-8 to determine if the retrofitted column surpassed the baseline set by the HITEC guidelines. The retrofitted column failed at a forced displacement of 21.929 cm, as noted in Table 4-9, which results in a deflection ductility of μ_Δ = 5.51 and a curvature ductility of μ_ϕ= 9.35. These results listed in Table 4-10, show that the retrofitted ductilities exceeded the criteria set by the HITEC protocol.

Table 4-10: Continuously Reinforced Circular Flexural Column Ductility Comparison

Ductility	"As-Built"	Retrofit	*Ductility Increase*
μ_Δ	2.22	5.51	*2.48*
μ_ϕ	3.25	9.35	*2.88*

With the additional ductility provided by the retrofit jacket, the continuously reinforced square column exceeded the required specifications set by the HITEC protocol to qualify as an acceptable retrofit procedure. The tested column deformed elastically to the set failure load and exceeded the increased ductility requirements.

Improved performance and increased ductility would be expected from this system if the production of the jacket were adjusted to strengthen the jacket's seam. Viewing the jacket strains

at ductility level 8.0 in Figure 4-47 to Figure 4-50, it is apparent that the material had not reached its maximum strain capacity since the measurements are well below failure strains associated with a typical carbon/epoxy material.

Table 4-11 provides a summary of the all the peak strains at ductility levels associated with the testing.

Table 4-11: Peak Test Strains (με)

	Level 1.0	**Level 1.5**	**Level 2.0**	**Level 3.0**	**Level 4.0**	**Level 5.0**	**Level 6.0**
Rebar	2239	3145	10575	13003	15594	FAIL	FAIL
Jacket	411	556	279	591	842	1555	2026

The column's internal reinforcement was stressed to failure while the jacket strains remained relatively low. With the jacket failure not due to material failure, the construction seam is the failure mechanism of concern. Visibly, the splitting of the seam was witnessed during testing and was the starting point for the jacket failure. While the joint held better in this case, this is still the weak link and further study is indicated to ensure that the jacket segments do not separate under cyclic load.

5. Experimental Tests and Results for Lapped Reinforced Flexure Columns

5.1 Introduction

The objective of the test program was to evaluate a new composite jacketing system for its suitability as a retrofit alternative. The evaluation was conducted pursuant to the published HITEC procedure [11] to enable assessment of whether the new system could meet standardized requirements.

In this chapter, the testing and evaluation of the carbon fabric - expansive foam core sandwich panel jacket applied to each of the lapped reinforced flexure concrete test columns with circular and square cross sections is outlined. Each of these columns was tested under increasing cyclic quasi-static lateral loads to ascertain if the retrofit jacket allowed each column to:

1. Attain or exceed the HITEC protocol specifications for improved ductility;
2. Ensure stability under repetitive cycling at a pre-specified displacement, and
3. Provide adequate energy absorption during cycling as evident by the area within the hysteresis loops.

5.2 Test Specimens Construction

The construction was completed as described in previous chapters with the only difference being the existence of a lap splice. The test columns were built to the required HITEC protocol specifications in order to ensure that a clear comparison of the response for the retrofitted column could be made with the requirements.

With the retrofitted columns being the focus of the testing, both the load stub and base were designed to carry the applied test loads without failure. This was to ensure that the failure mechanism of each test was within the column retrofit area or within the connection region between the column and base/load stub. Because the interior steel reinforcement in the column is

expected to yield, only the column longitudinal reinforcement bars were strain-gauged. A total of twenty (20) gages were applied in the load direction of the column reinforcement, as illustrated in Figure 5-1 and Figure 5-2.

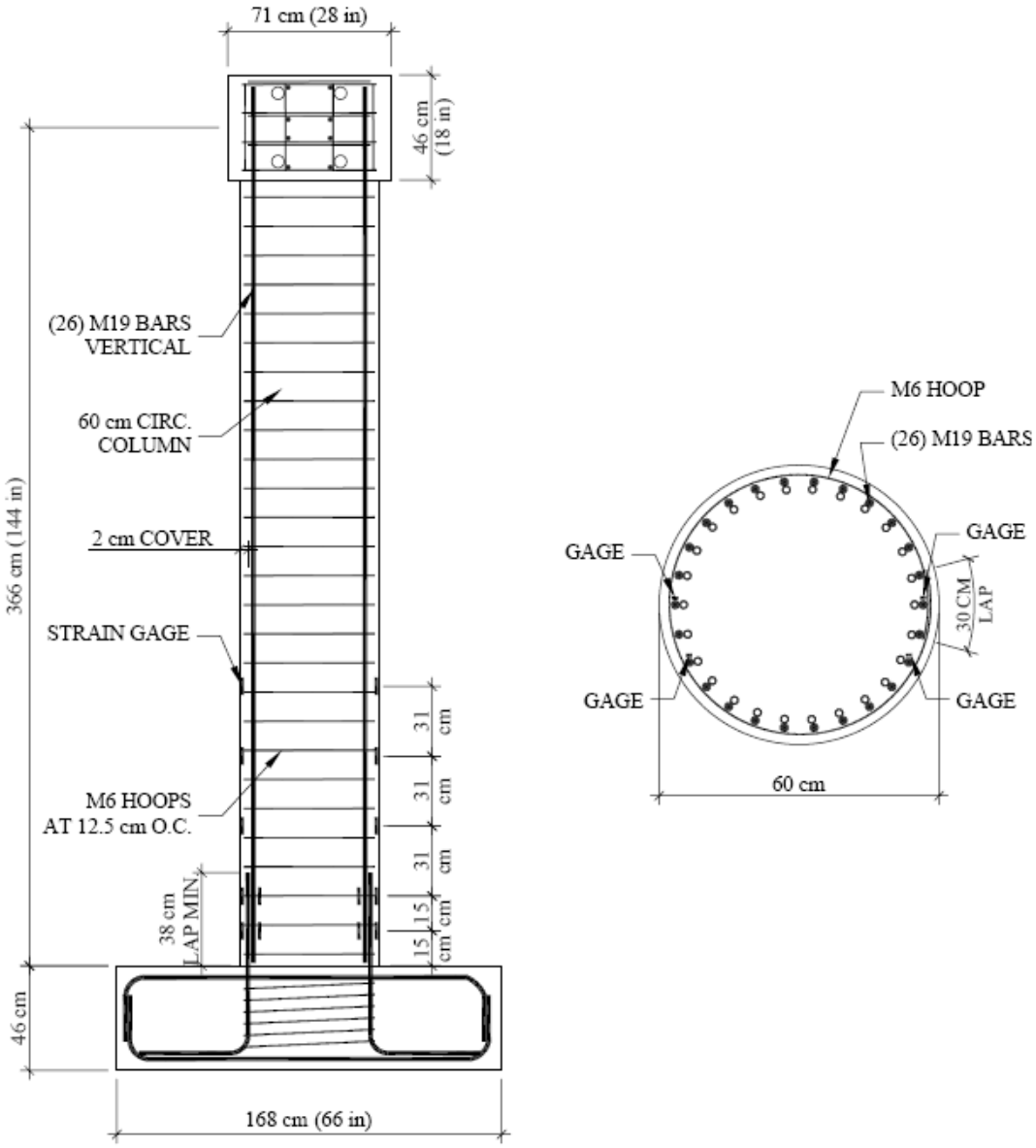

Figure 5-1: Schematic Showing Strain Gage Location on Lapped Reinforced Flexural Circular Column Reinforcing Cage

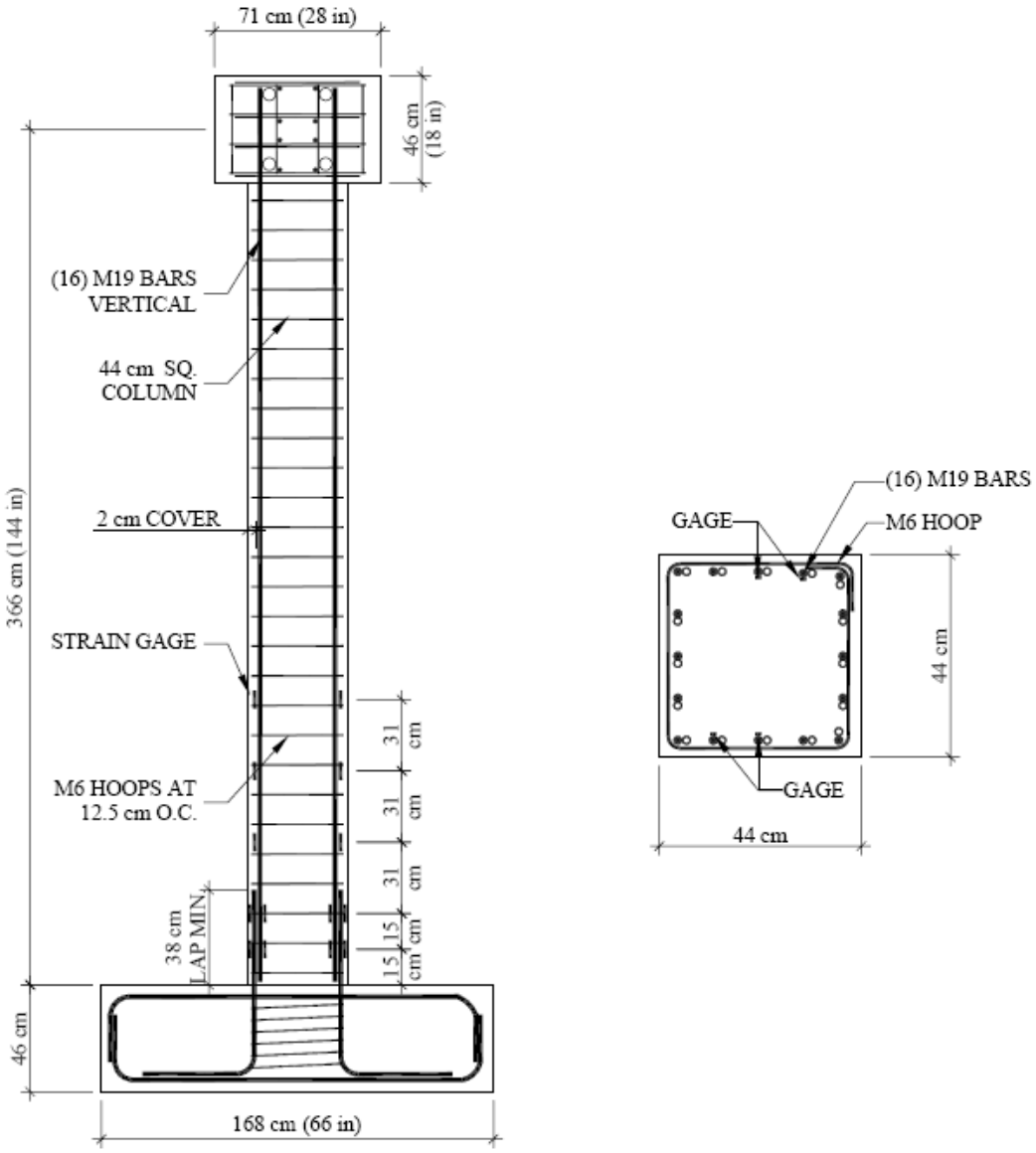

Figure 5-2: Schematic Showing Strain Gage Location on Lapped Reinforced Square Flexure Column Reinforcing Cage

The first construction stage involved the production of a square and circular column reinforcing cage. These column cages were formed with straight vertical bars and transverse hoops tied together. These column cages were constructed in tandem with the column bases. Reinforcing bar strength was given previously in Table 4-1.

Once the column base cages were encased within the column's casting formwork, concrete was poured. The concrete poured was specified to have minimum 28 day compression strength of 20.7 MPa (3000 psi). Nine test cylinders were cast at this time as well to enable determination of the progression in the concrete compression strength until the day of testing. Table 5-2 lists the resulting concrete compression strength taken from the test cylinders. Placement of the forming and pouring of the concrete followed previously documented procedures (Chapter 3 and Chapter 4).

Table 5-1: Lapped Reinforced Flexure Column Base Concrete Compression Strength

	1	*2*	*3*	***Average***
7-Day Strength (MPa)	24.3	25.2	23.6	**24.4**
28-Day Strength (MPa)	37.7	37.4	37.6	**37.6**
D.O.T. Strength (MPa)	51.8	50.2	51.9	**51.3**

The resulting concrete column was specified to have a minimum 28 day compression strength of 20.7 MPa. Table 5-2 lists the compression values of the concrete in the lapped reinforced concrete columns. Even though the concrete compression strength exceeded the minimum of 20.7 MPa, this does not necessarily invalidate the testing. A minimum concrete strength was given for test specimen protocol, but not a maximum. As these values are approximately double the specified 28 day compression strength, this will affect the required axial pre-load on the columns since this pre-load is a function of compression strength and cross sectional area of the column. For the circular flexure column the pre-load was 1780 kN creating an axial load ratio of 13.5% which is within the HITEC requirement limits. The square column was pre-load 1155 kN producing an axial load ratio of 12.8% which is also within the HITEC requirement limits [11].

Table 5-2: Lapped Reinforced Flexure Column Concrete Compression Strength

	1	*2*	*3*	***Average***
7-Day Strength (MPa)	29.4	29.5	29.9	**29.6**
28-Day Strength (MPa)	47.1	45.1	47.6	**46.6**
D.O.T. Strength (MPa)	50.7	48.5	48.5	**49.3**

With the construction of the lapped reinforced flexure test columns completed, the columns were scheduled to be wrapped with the experimental strengthening jackets 62 days after column concrete had been poured. (This process is outlined in Chapter 2 since the process is common in all six of the test columns.) Unlike other retrofitted columns, the lap spliced reinforced column jackets did not continue to the top of the column, but were stopped 45 cm from the column load stub.

With the retrofit jackets construction complete, twenty, 50 mm long strain gauges were applied to the jacket. These gauges were placed horizontally in the hoop direction on each face of the column in the same dimensional pattern as the reinforcement gauges in Figure 5-1 and Figure 5-2. These strain gauges were applied with a self-leveling adhesive to ensure a good bond to the carbon jacket.

5.2.1 Test Program

As with the other experimental retrofitted concrete test columns, each lapped reinforced flexure test column was tied-down to the laboratory's strong floor via six (6) high strength bars. The details of the test setup are the same as described previously in Chapter 4 for the continuously reinforced flexure columns.

In the following sections, the testing and general observation for each of the lapped reinforced flexural columns: circular and square are reviewed.

5.3 Circular Lapped Reinforced Flexural Column

5.3.1 Observations

The circular column with lapped column reinforcement was constructed, wrapped with the experimental retrofit jacket and then tested approximately 62 days after the specimen had been cast.

Based on the material properties listed in Table 4-1 and Table 5-2, which were determined from earlier material testing, the theoretical yield force V_y = 217 kN (49 kips) and ideal flexural capacity V_{yi} = 347 kN (78 kips) were calculated using the procedure presented in Figure 2-31 for the circular lapped reinforced flexural column. The pseudo-superstructure load applied to the column was 1780 kN (400 kips) acting as the columns axial load. Assuming an elasto-plastic response approximation, the experimental first yield displacement Δ_y = 2.242 cm (0.883 in) was expected based on the above values.

The theoretical ductilities corresponding to curvature and deflection for the constructed, non-retrofitted column was then determined from the above calculated column design values. (See Chapter 2 Figure 2-36 for calculations). The resulting "as-built" column ductilities based on deflection ($\mu_\Delta = \Delta_u/\Delta_y$) and column curvature ($\mu_\phi = \phi_u/\phi_y$) are listed in Table 5-3. According to the HITEC protocol, the retrofitted column must exceed these calculated values by the specified amounts of μ_ϕ = 2.0 x "as-built" and μ_Δ = 1.5 x "as-built".

Table 5-3: Resulting "As-Built" Ductilities

ϕ_y =	0.00005	μ_ϕ =	4.00
ϕ_u =	0.00020		
Δ_y =	2.242 cm	μ_Δ =	2.62
Δ_u =	5.869 cm		

With the "as-built" theoretical column ductilities calculated, the loading sequence for the test was established. The circular lapped reinforced flexural column testing was begun under load control. The column's south face reinforcement strains were not close to the theoretical values under its Vy loading (a load of 192 kN should yield a deflection of 2.242 cm). The reinforcement gauge readings should have reached 2000 με (strain when reinforcement stress has reached its yield point: $\varepsilon = f_y/E$) to determined if the column reinforcement had yielded. At the Vy loading the rebar strains was less than the yield strain (1421 με) as seen in Figure 5-3.

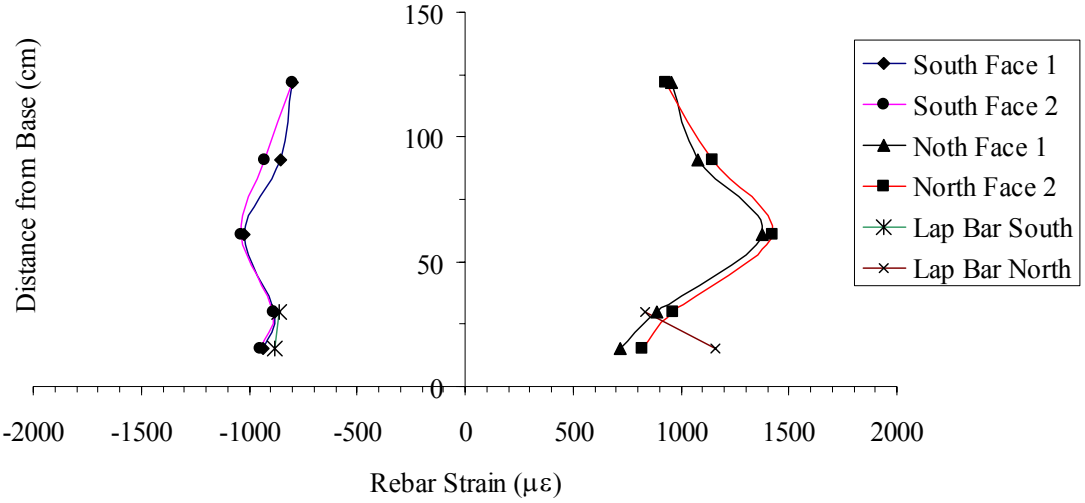

Figure 5-3: Reinforcement Test Strains at Vy Loading

Figure 5-4 through Figure 5-10 show how the rebar strain change under load control cycles at different locations along the column. The splice bars are the footing dowels lapped over a height of 38 cm next to the vertical reinforcement bars of the column. Only the portion on the splice bars lapped spliced with the column reinforcement were strain gauged.

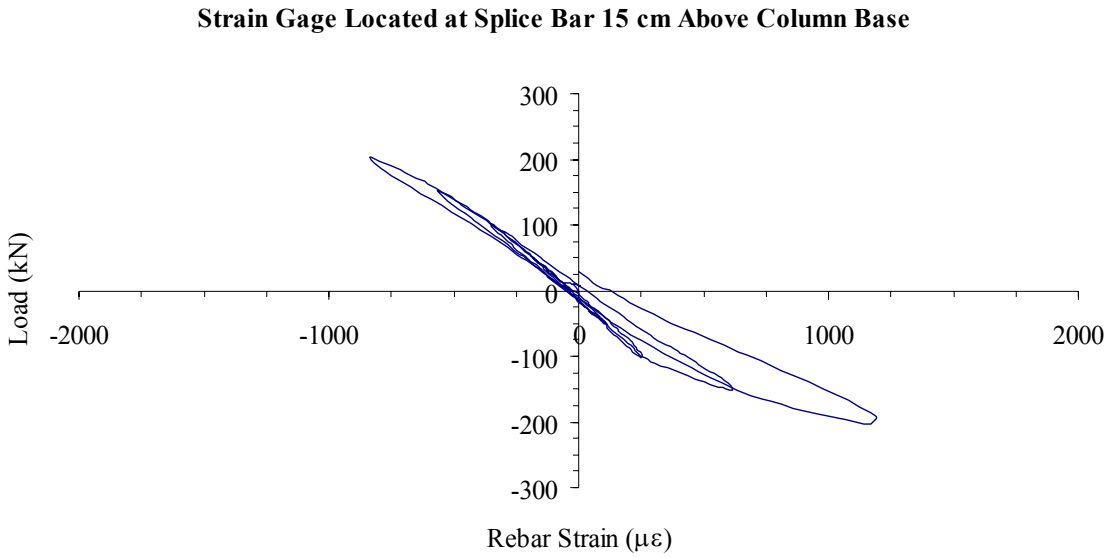

Figure 5-4: North Face 1 Reinforcement Test Strains under Force Loading

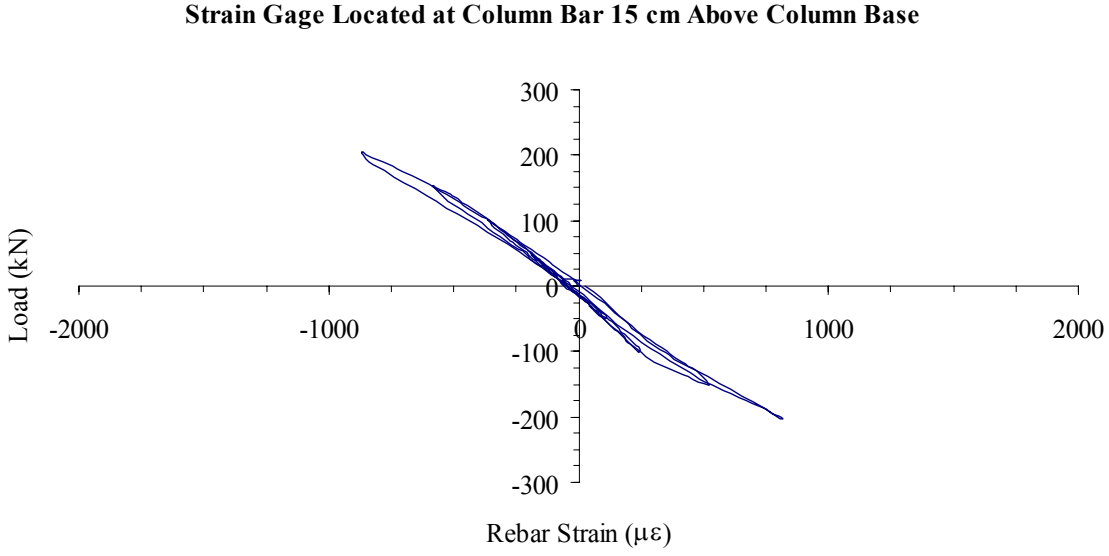

Figure 5-5: North Face 1 Reinforcement Test Strains under Force Loading

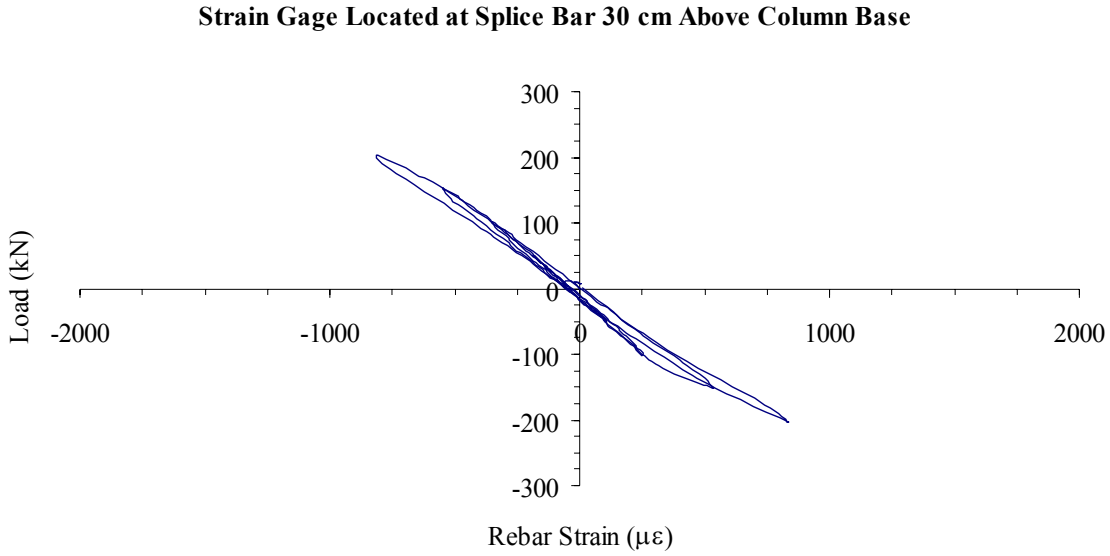

Figure 5-6: North Face 1 Reinforcement Test Strains under Force Loading

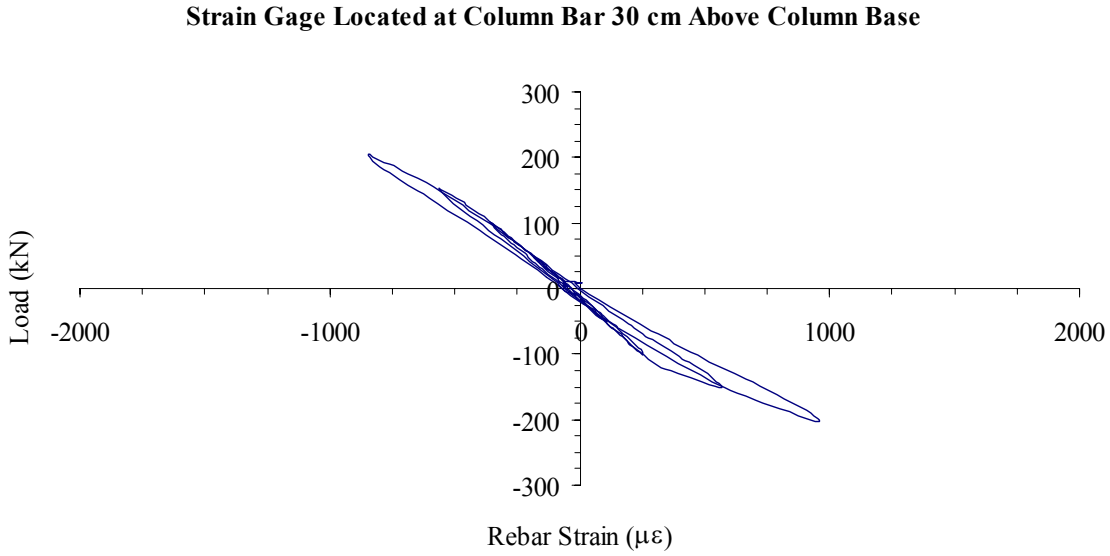

Figure 5-7: North Face 1 Reinforcement Test Strains under Force Loading

Strain Gage Located at Column Bar 61 cm Above Column Base

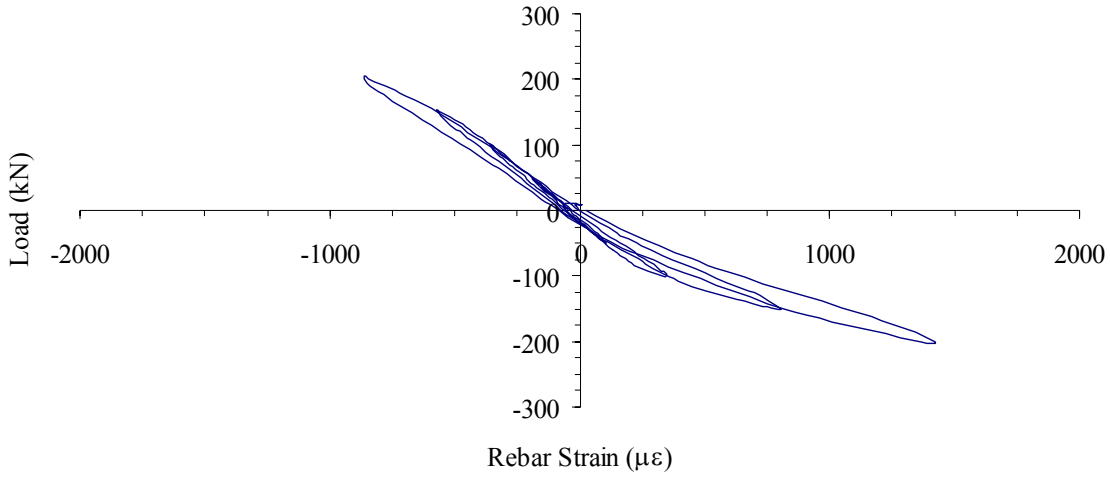

Figure 5-8: North Face 1 Reinforcement Test Strains under Force Loading

Strain Gage Located at Column Bar 91 cm Above Column Base

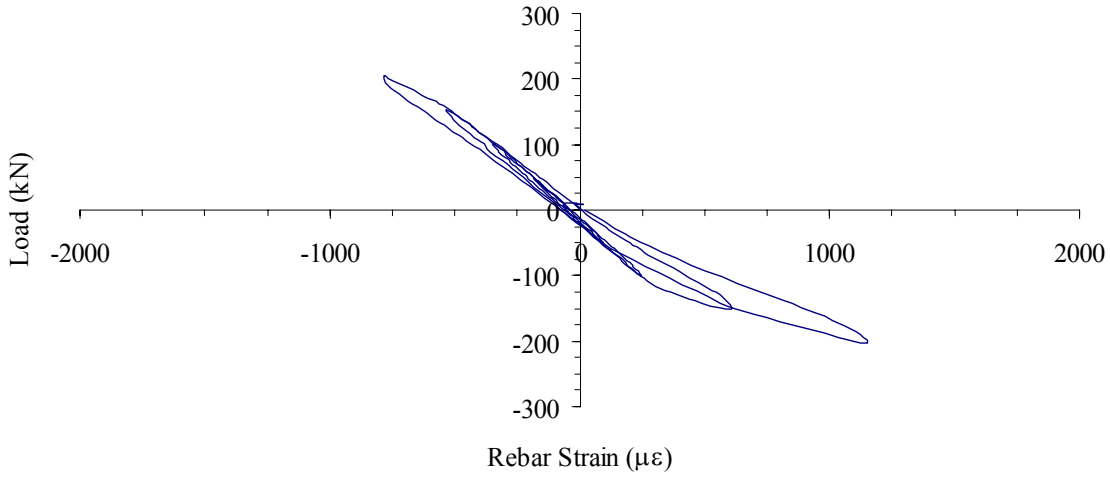

Figure 5-9: North Face 1 Reinforcement Test Strains under Force Loading

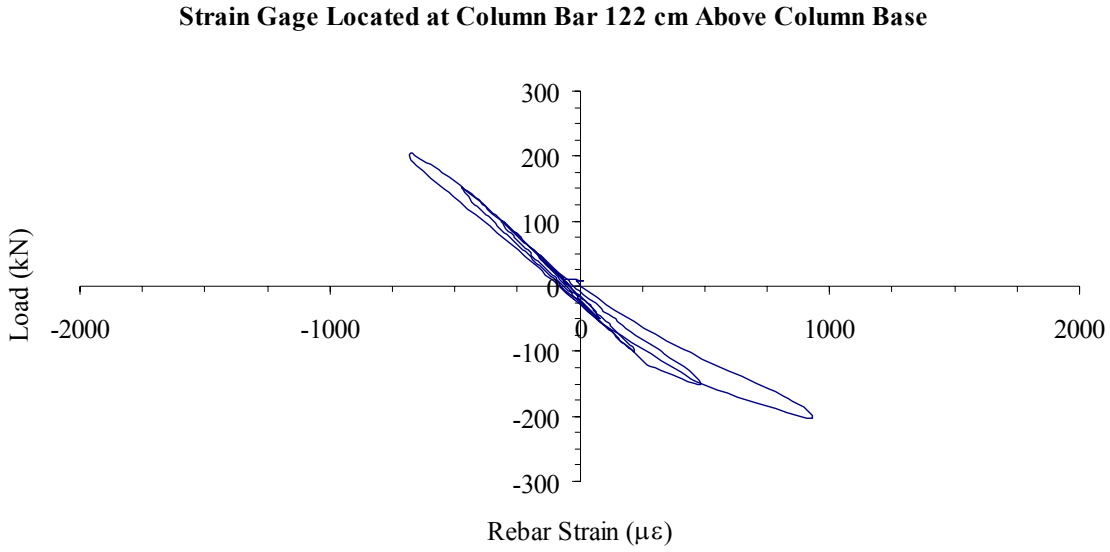

Figure 5-10: North Face 1 Reinforcement Test Strains under Force Loading

After the end of the load control cycles, it was determined that ductility level 1.0 had not been reached as the predicted displacement of 2.242 cm (0.883 in) was not reached under a 217 kN loading. It was noted that the maximum rebar strain was not taken from the strain gage closest to the column base, but just above the end of the lapped splice reinforcement. Under deflection load control the reinforcement strains continued to increase. Figure 5-11 through Figure 5-17 show the strain at ductility level 8 displacements at different locations of the column.

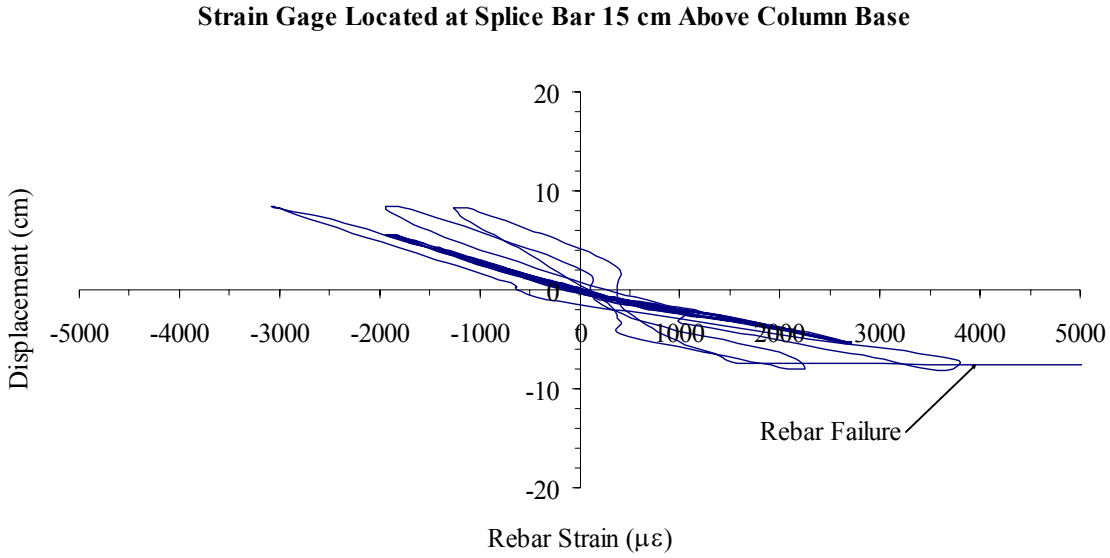

Figure 5-11: North Face 1 Reinforcement Test Strains at μ = 8.0

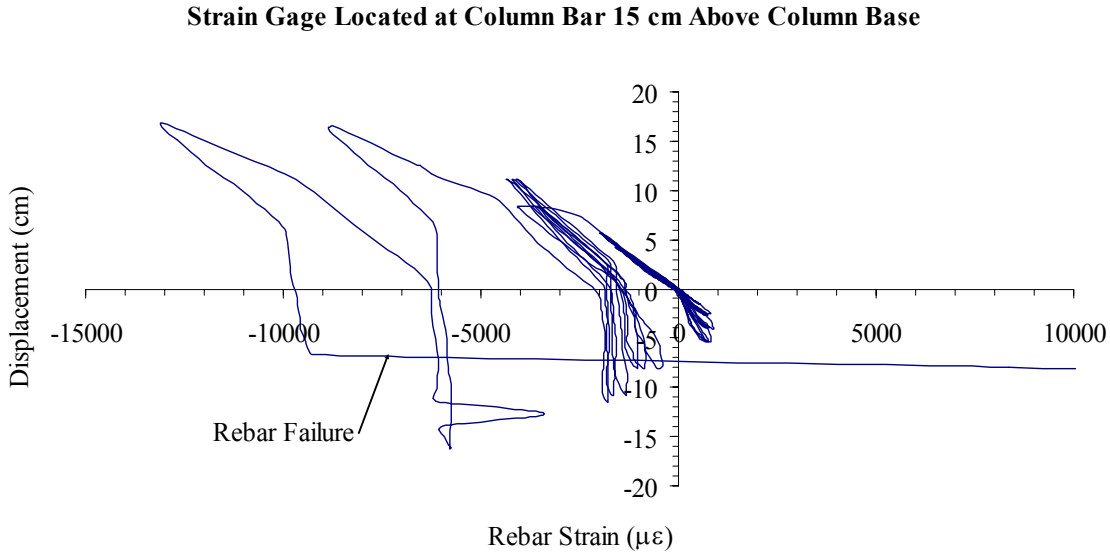

Figure 5-12: North Face 1 Reinforcement Test Strains at μ = 8.0

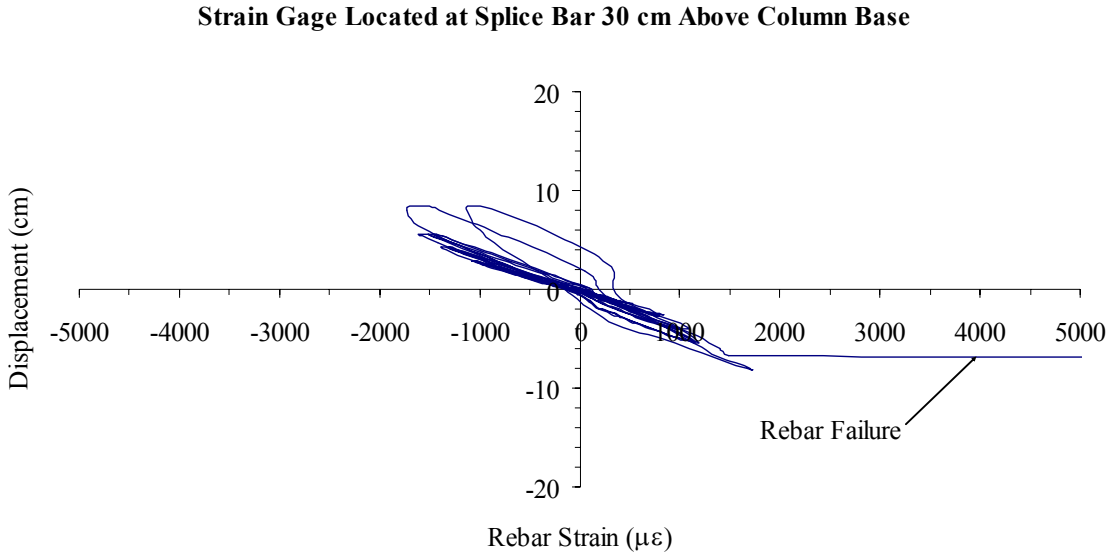

Figure 5-13: North Face 1 Reinforcement Test Strains at μ = 8.0

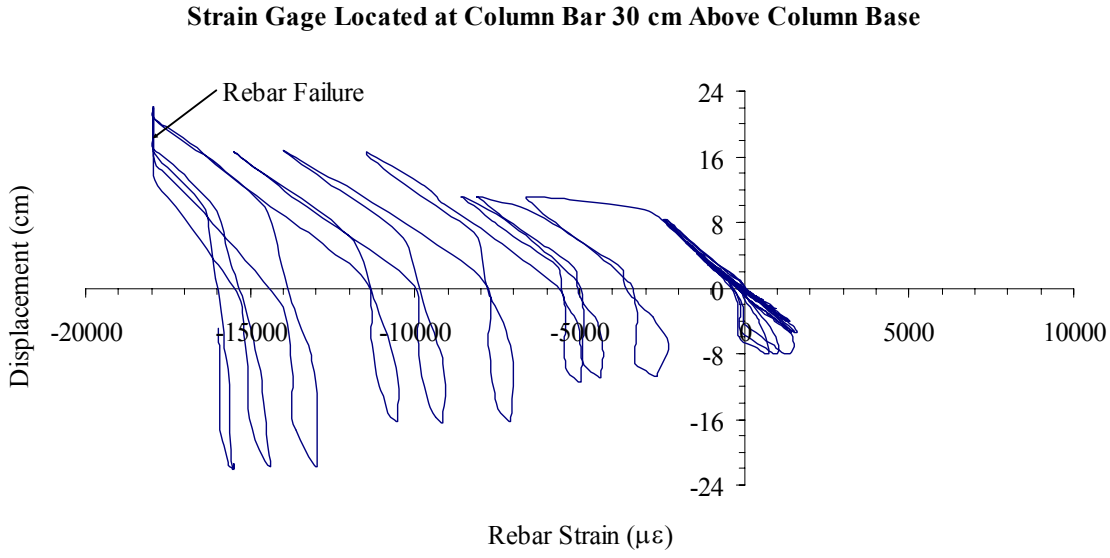

Figure 5-14: North Face 1 Reinforcement Test Strains at μ = 8.0

Strain Gage Located at Column Bar 61 cm Above Column Base

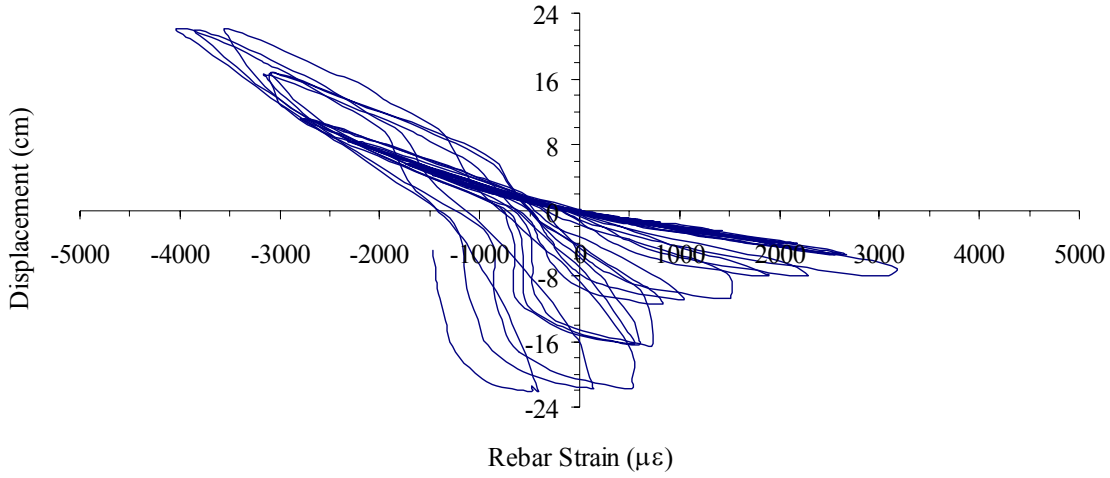

Figure 5-15: North Face 1 Reinforcement Test Strains at μ = 8.0

Strain Gage Located at Column Bar 91 cm Above Column Base

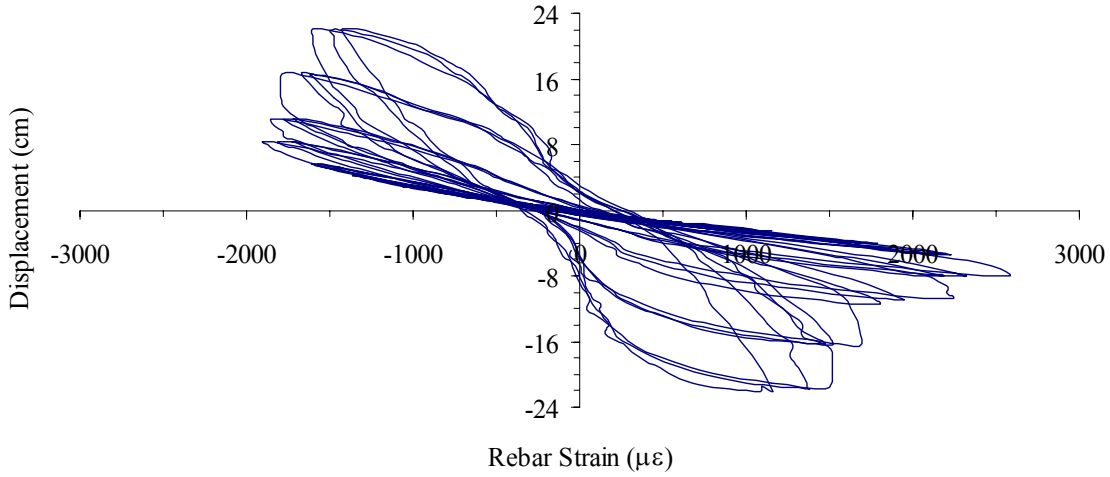

Figure 5-16: North Face 1 Reinforcement Test Strains at μ = 8.0

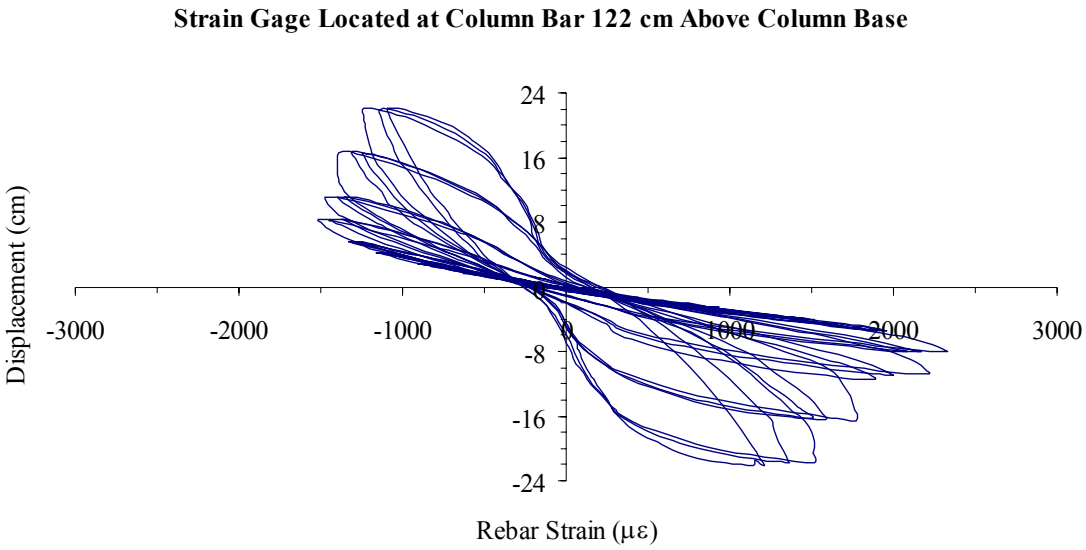

Figure 5-17: North Face 1 Reinforcement Test Strains at μ = 8.0

Figure 5-18: Lapped Reinforced Circular Flexural Column during testing

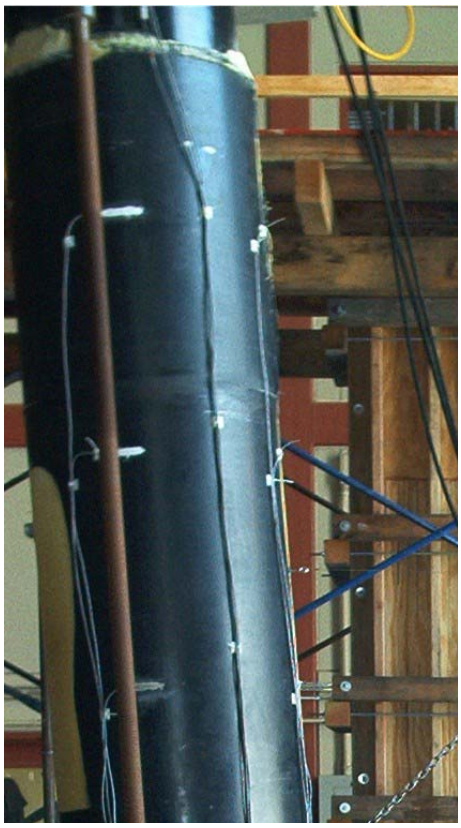

Figure 5-19: Lapped Reinforced Circular Flexural Column during testing

As the testing was continued under cycles of increased enforced displacements (see Figure 5-18 and Figure 5-19), the column began to separate from the footing base and cracks began to appear in the footing as well. Under an 8.968 cm applied deflection at ductility Level 4, the column began to separate from the footing base as shown in Figure 5-20.

Figure 5-20: Lifting of the Column from the Footing during Testing

The exterior of the composite jacket also exhibited minor flexure cracking most noticeably at the top of the plastic hinge region of the composite jacket (extending to a height of 73 cm from the bottom of the column) in the hoop direction, as shown in Figure 5-21 and Figure 5-22 marked with a white marker. These noticeable hoop cracks first began to appear at displacement ductility level 3 cycling.

Figure 5-21: Composite Jacket Breaking in Hoop Direction of Column

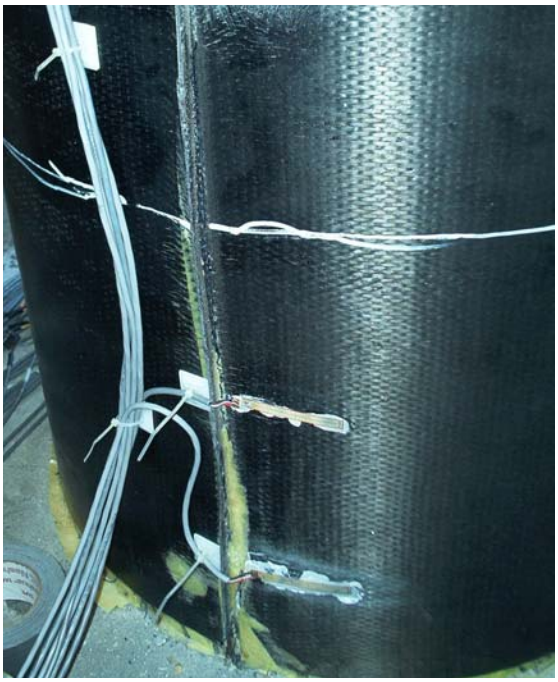

Figure 5-22: Composite Jacket Breaking in Hoop Direction of Column

After the first cycle at ductility Level 8 loading, a noticeable decrease in structural integrity was witnessed with decrease in load. The strains along the column jacket was reviewed to determine if softening of the column's load capacity was due to the failure of the column behind the retrofit composite jacket. After reviewing rebar strains it was noted that both the splice bars and the 15 cm located column bars had failed during ductility level 4 cycling and were no longer taking additional strain increases. Figure 5-23 through Figure 5-26 show the deflection to strain relationship of the composite jacket at different locations along the column under ductility 8.

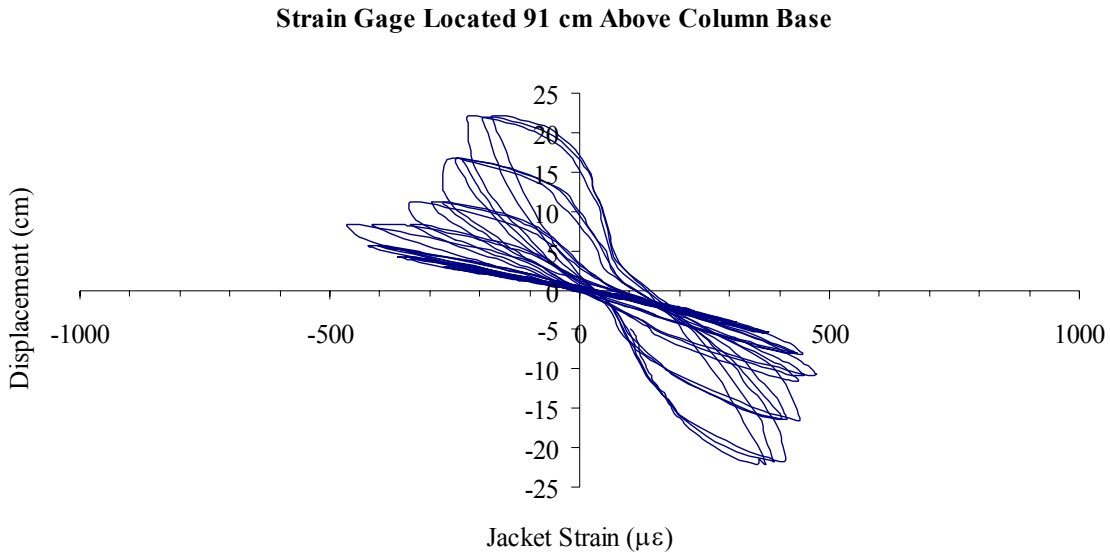

Figure 5-23: South Face Jacket Test Strains at μ = 8.0

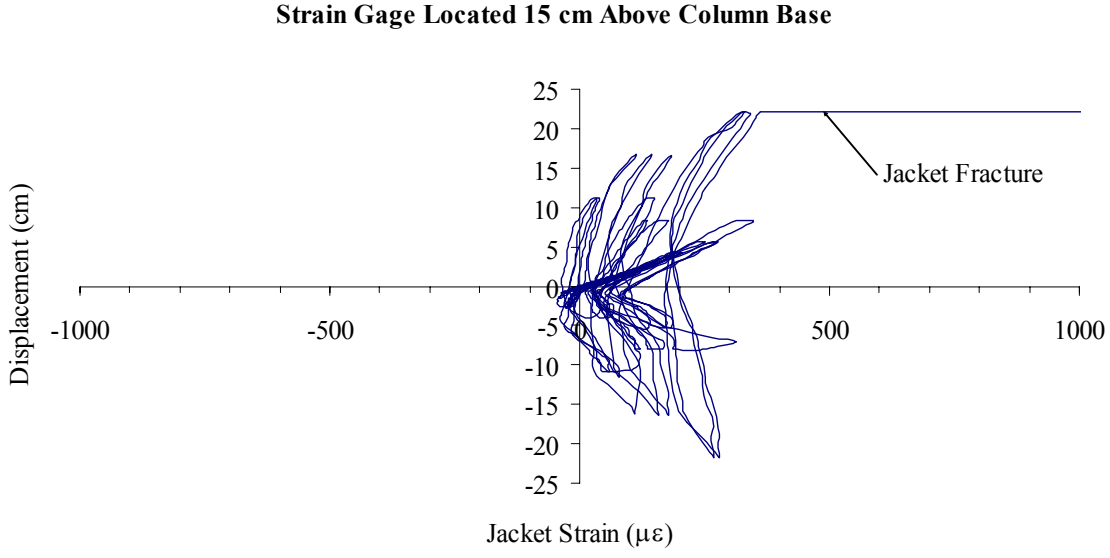

Figure 5-24: North Face Jacket Test Strains at μ = 8.0

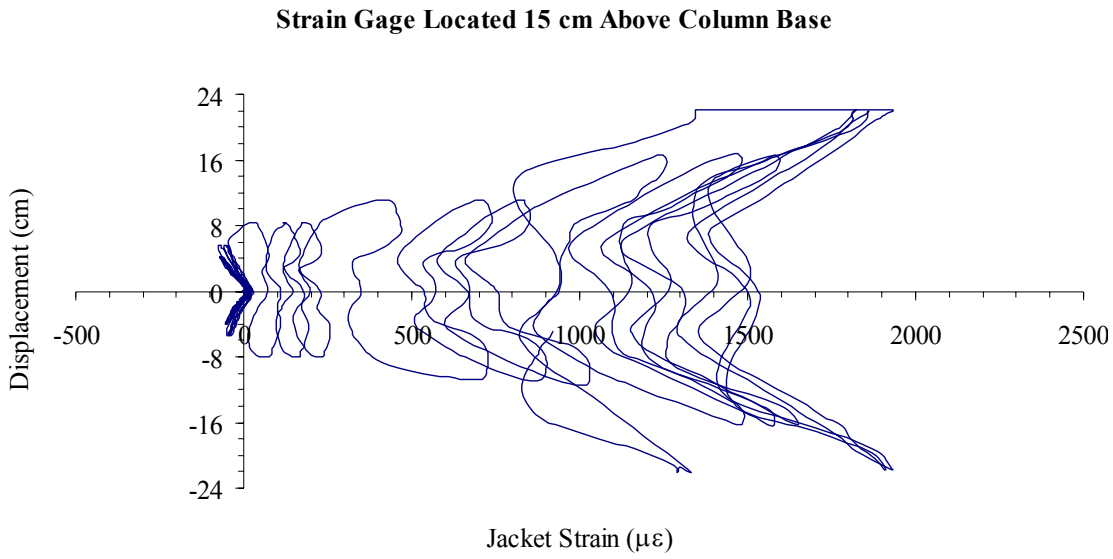

Figure 5-25: East Face Jacket Test Strains at μ = 8.0

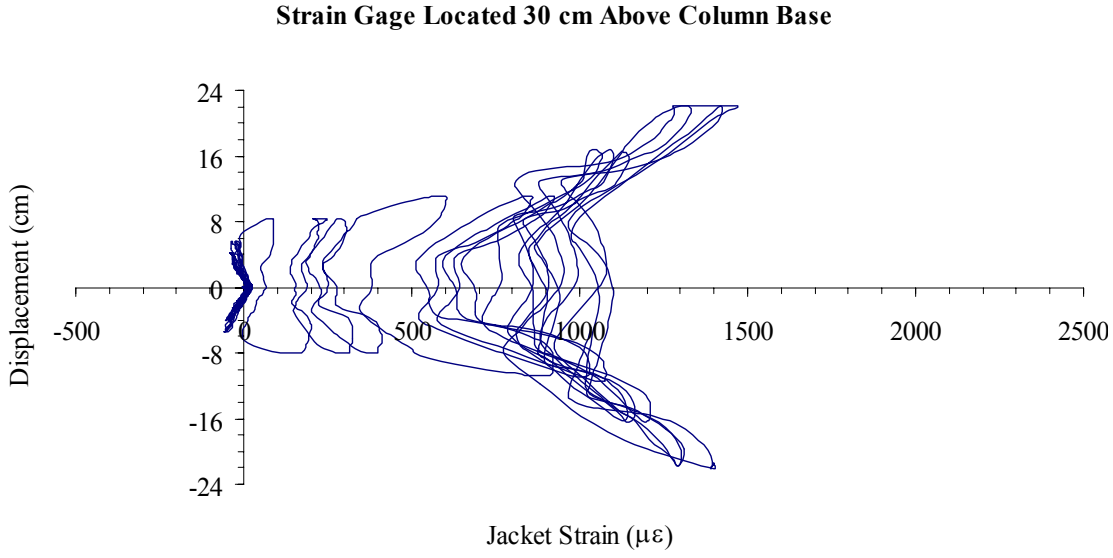

Figure 5-26: West Face Jacket Test Strains at μ = 8.0

During the third cycle at ductility Level 8 loading, column failure was deemed to have occurred due to 15% drop in load required to displacement the column 17.935 cm. This load decrease may have been due to the lap splice clamping failure of the column's footing splice bars

and column's vertical reinforcement. As seen in Figure 5-27, the column had begun to pull away from the base causing the base concrete to crack and spall.

Figure 5-27: Concrete Base Cracking and Spalling

5.3.2 Test Results

Stability under cyclic loading during the lapped reinforced circular flexural column testing was measured to the displacement length of 22.075 cm (8.691 inches) with the column failure occurring due to the 15% drop in load at the level 8 ductility cycle. A hysteresis plot of the lapped reinforced circular flexure column's applied load to the resulting column displacement is seen in Figure 5-28. This graph shows a stable push-pull response with the positive push data mirroring the negative pull data about the zero load and zero displacement axes. The area outlined within the data point of graph is smooth elliptical shape with no major jumps or drops during an induced cycle to indicate instability. The decrease in load carrying capacity from the

maximum load achieved in level 4 was noticed during the ductility level 6 cycles and continued to further decrease with each additional ductility level.

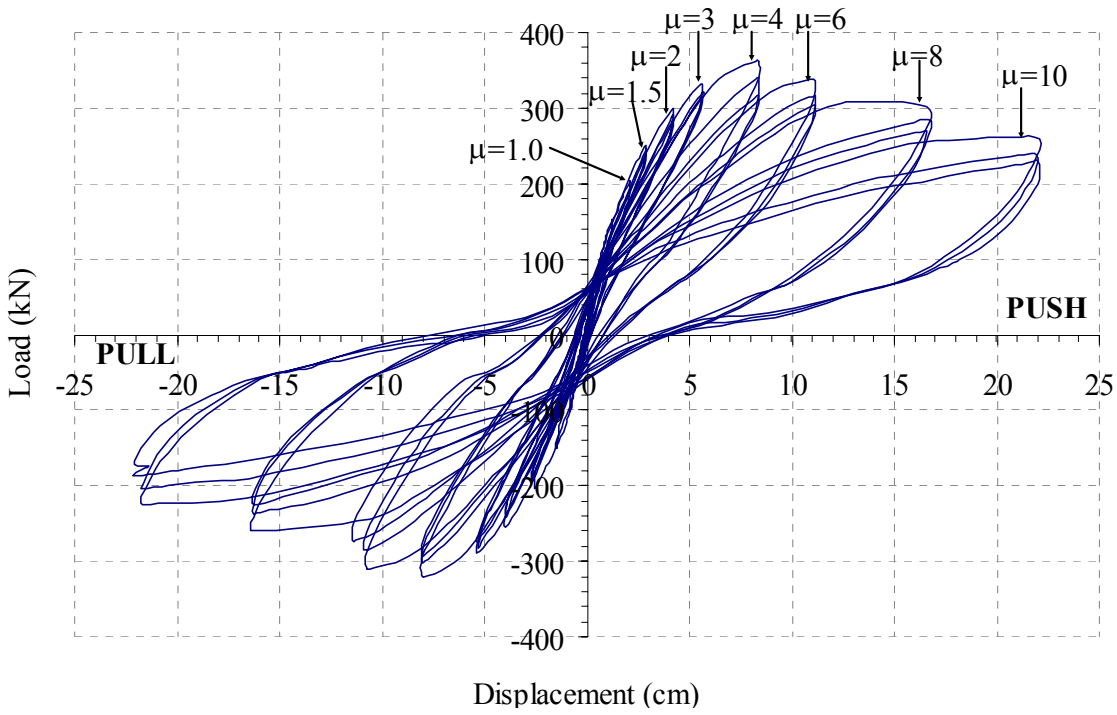

Figure 5-28: Flexure Column Load vs. Displacement Test Results

The test column's final retrofitted ductility calculation utilized the 16.82 cm measurement given that this was the displacement length the test specimen achieved during the ductility level 8 loading cycle. Table 5-4 lists the final results collected from the continuously reinforced circular flexural column experiment used in the retrofit system analysis.

Table 5-4: Lapped Reinforced Circular Flexural Column Final Test Results

Maximum Load	362 kN
Failure Initiation Load	307 kN
Maximum Displacement	16.82 cm

The results from the experiment for the circular flexure column were compiled to establish the column's retrofitted ductilities in terms of displacement and curvature. These values were then evaluated against the "as-built" ductilities in Table 5-3 to determine if the retrofitted column surpassed the baseline set by the HITEC guidelines. The retrofitted column failed at a forced displacement of 16.827 cm, as noted in Table 5-4, which results in a deflection ductility of $\mu_\Delta = 6.42$ and a curvature ductility of $\mu_\phi = 11.04$. These results listed in Table 5-5, show that the retrofitted ductilities exceeded the criteria set by the HITEC protocol.

Table 5-5: Lapped Reinforced Circular Flexural Column Ductility Comparison

Ductility	"As-Built"	Retrofit	*Ductility Increase*
μ_Δ	2.62	6.42	*2.45*
μ_ϕ	4.00	11.04	*2.76*

With the additional ductility provided by the retrofit jacket, the lapped reinforced circular column exceeded the required specifications set by the HITEC protocol to qualify as an acceptable retrofit procedure. The tested column deformed elastically to the set failure load and exceeded the increased ductility requirements.

Viewing the jacket strains at ductility level 8.0 in Figure 5-23 to Figure 5-26, it is apparent that the material did not reach its maximum strain capacity since the measurements are well below failure strains associated with a typical carbon/epoxy systems. Table 5-6 provides a summary of the all the peak strains at ductility levels associated with the testing.

Table 5-6: Peak Test Strains ($\mu\varepsilon$)

	Level 1.0	**Level 1.5**	**Level 2.0**	**Level 3.0**	**Level 4.0**	**Level 6.0**	**Level 8.0**
Rebar	1335	2068	2666	FAIL	FAIL	FAIL	FAIL
Jacket	261	301	368	430	1047	1646	1401

The column's steel reinforcement was stressed to failure while the jacket strains remained relatively low. With the jacket failure not due to material failure, the jacket's ability to provide additional lap splice clamping pressure appears to be in question. Unlike the previous retrofitted columns, no construction seam failure was observed, therefore no visible failure of the jacketing system were witnessed.

5.4 Square Lapped Reinforced Flexural Column

5.4.1 Observations

The square column with lapped column reinforcement was constructed, wrapped with the experimental retrofit jacket and then tested approximately 64 days after the specimen had been cast.

Based on the material properties listed in Table 4-1 and Table 5-3, which were determined from earlier material testing, the theoretical yield force V_y = 128 kN (28.8 kips) and ideal flexural capacity V_{yi} = 205 kN (46 kips) were calculated using the procedure presented in Figure 2-31 for a square lapped reinforced flexural column. The pseudo-superstructure load applied to the column was 1155 kN (260 kips) acting as the columns axial load. Assuming an elasto-plastic response approximation, the experimental first yield displacement Δ_y = 3.931 cm (1.548 in) was expected based on the values listed above.

The theoretical ductilities corresponding to curvature and deflection for the constructed, non-retrofitted column were then determined from the above calculated column design values. (See Chapter 3 Figure 2-35 for calculations). The resulting "as-built" column ductilities based on deflection ($\mu_\Delta = \Delta_u/\Delta_y$) and column curvature ($\mu_\phi = \phi_u/\phi_y$) are listed in Table 5-7. According to the HITEC protocol, the retrofitted column must exceed these calculated values by the specified amounts of μ_ϕ = 2.0 x "as-built" and μ_Δ = 1.5 x "as-built".

Table 5-7: Resulting "As-Built" Ductilities

ϕ_y =	0.00009	μ_ϕ =	3.88
ϕ_u =	0.00034		
Δ_y =	3.931 cm	μ_Δ =	2.56
Δ_u =	10.054 cm		

With the "as-built" theoretical column ductilities calculated, the loading sequence for the test was established. The square lapped reinforced flexural column testing was begun under load control. The testing values for theoretical column yielding were surpassed under the Vy level loading (a load of 128 kN should yield a deflection of 3.931 cm). It was determined that ductility level 1.0 and level 1.5 ductility had been reached. This is shown in Figure 5-29 which illustrates that predicted displacement of 5.897 cm (2.322 in) was reached under a 128 kN loading. A 100% at Vy loading a displacement of 5.949 cm was recorded. This larger displacement indicts that the un-retrofitted column's ductility may be slightly less than calculated.

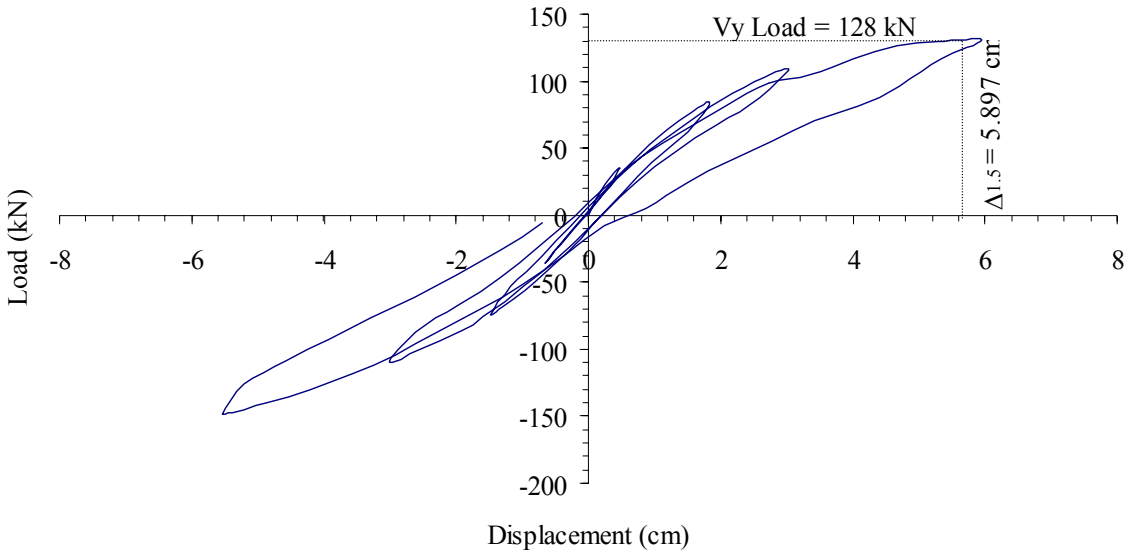

Figure 5-29: Load vs. Displacement showing Force Loading reached μ = 1.5

The column's south face steel reinforcement strain readings also surpassed that for theoretical yielding. Once the reinforcement gage reading read 2000 με (strain when reinforcement stress has reached its yield point: $\varepsilon = f_y/E$) it was determined that the column reinforcement had yielded. At the Vy loading the rebar reached a strain of 2456 με as seen in Figure 5-30.

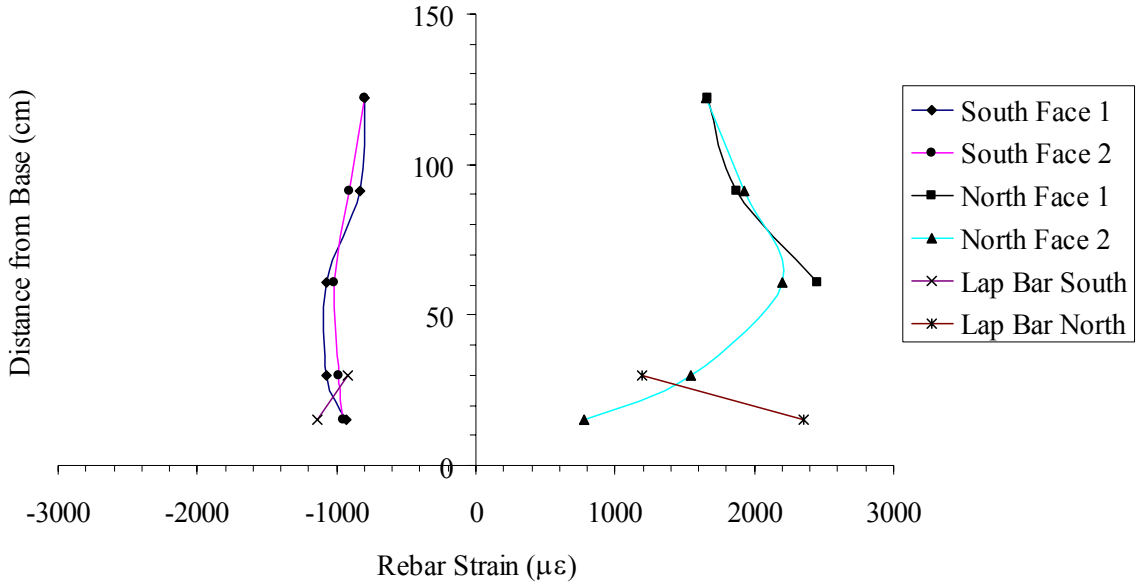

Figure 5-30: Reinforcement Test Strains at Vy Loading

Figures 5-31 through Figure 5-37 show how the rebar strain changed under load control cycles at different locations along the column. Reinforcement along the north face was used for comparison as this side of the test column's reinforcement was the first to reach yield level strain readings. The splice bars are the footing dowels lapped over a height of 38 cm next to the vertical reinforcement bars of the column. Only the portion on the splice bars lapped spliced with the column reinforcement were strain gauged.

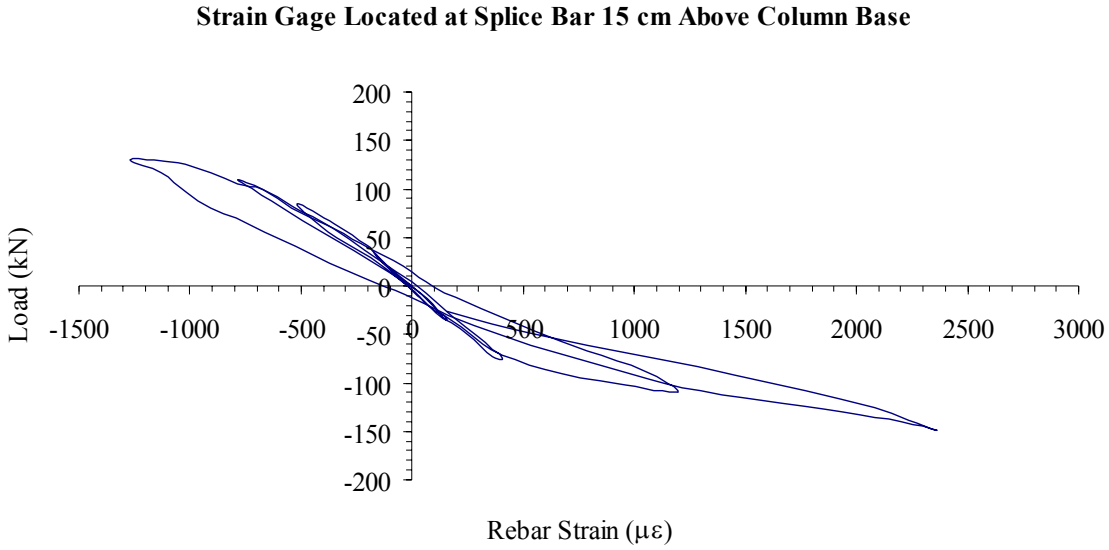

Figure 5-31: North Face 2 Reinforcement Test Strains under Force Loading

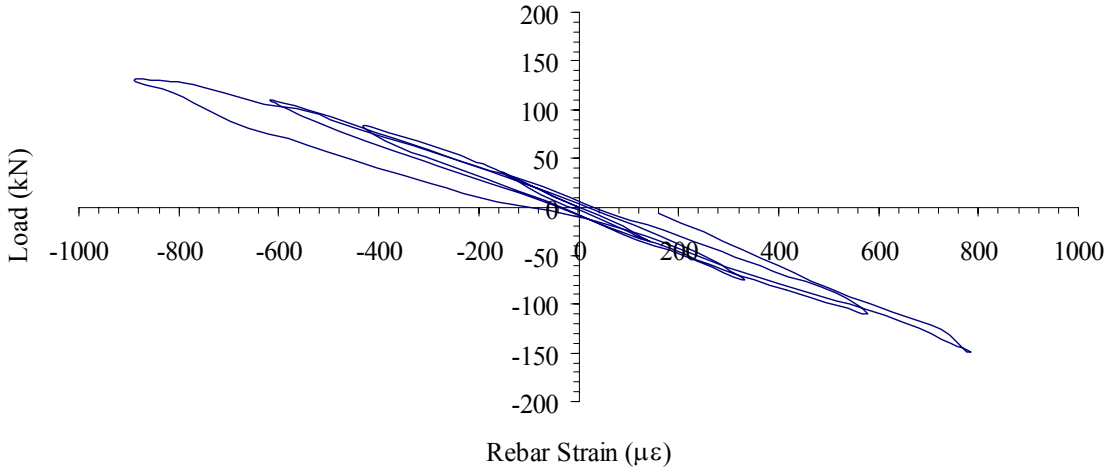

Figure 5-32: North Face 2 Reinforcement Test Strains under Force Loading

Strain Gage Located at Splice Bar 30 cm Above Column Base

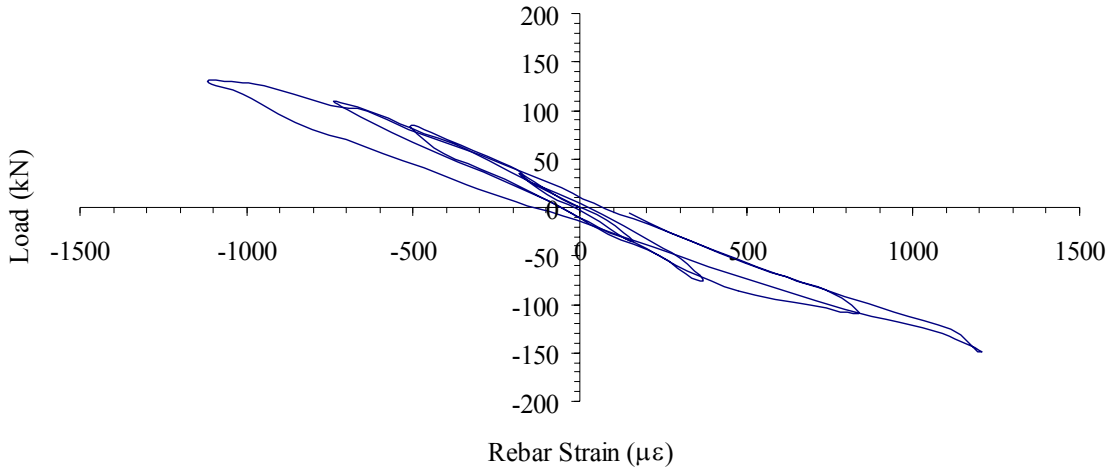

Figure 5-33: North Face 2 Reinforcement Test Strains under Force Loading

Strain Gage Located at Column Bar 30 cm Above Column Base

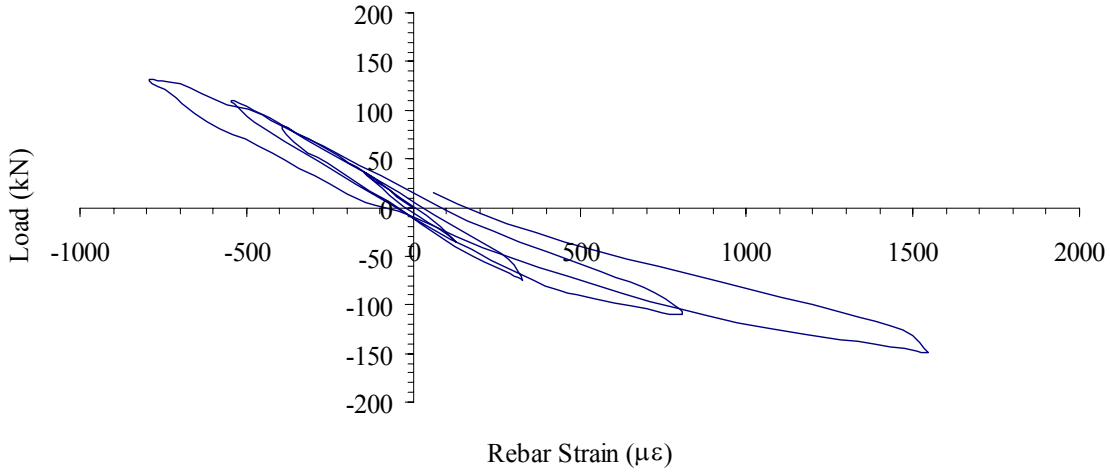

Figure 5-34: North Face 2 Reinforcement Test Strains under Force Loading

Strain Gage Located at Column Bar 61 cm Above Column Base

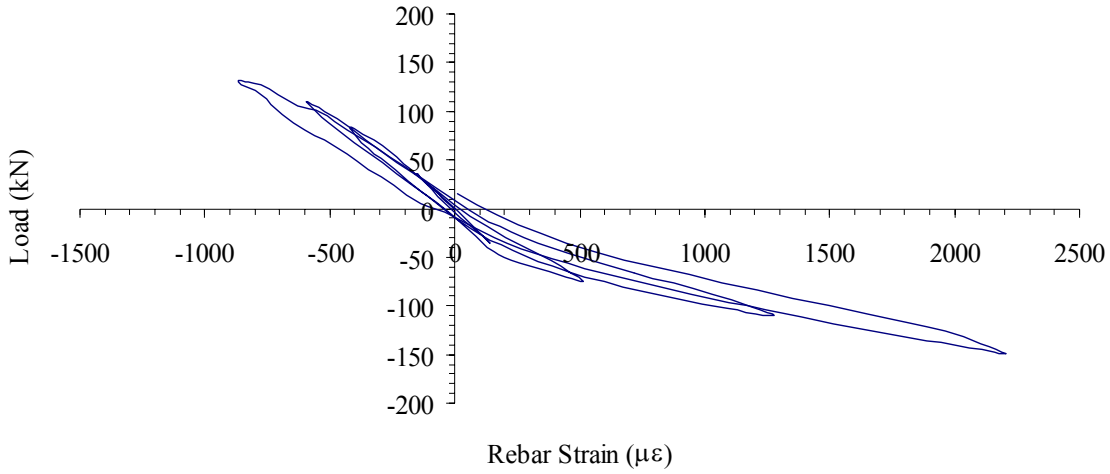

Figure 5-35: North Face 2 Reinforcement Test Strains under Force Loading

Strain Gage Located at Column Bar 91 cm Above Column Base

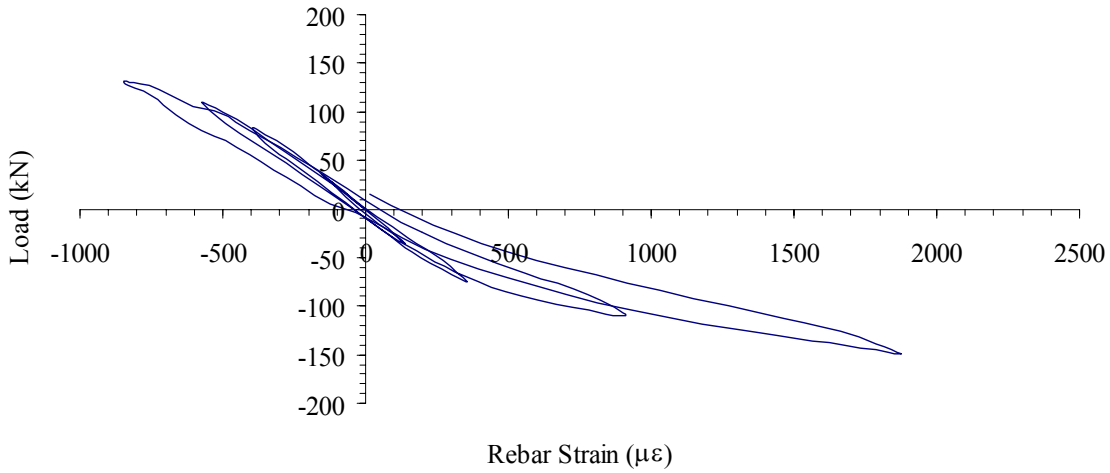

Figure 5-36: North Face 1 Reinforcement Test Strains under Force Loading

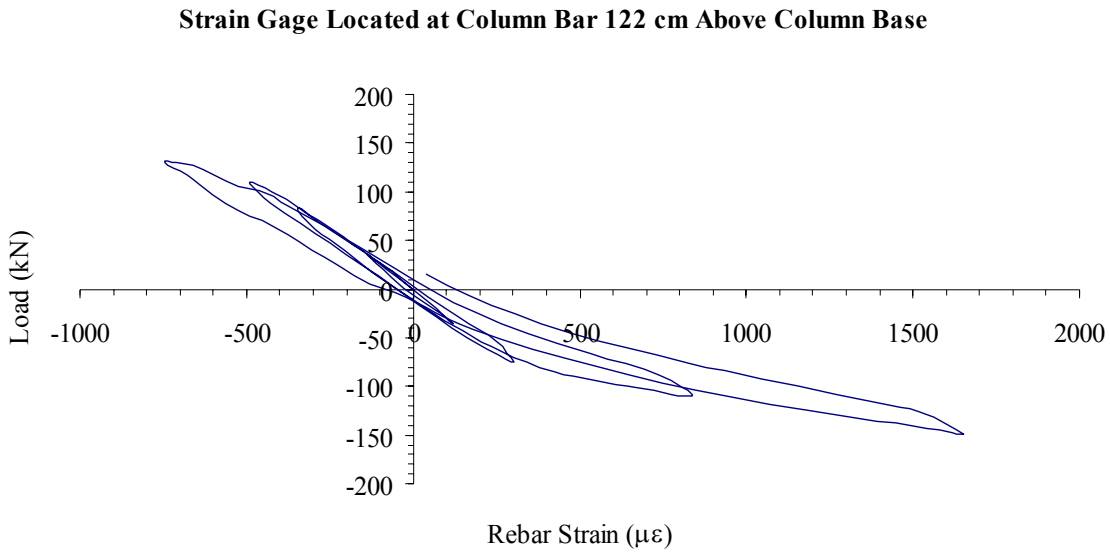

Figure 5-37: North Face 2 Reinforcement Test Strains under Force Loading

It was noted that the maximum rebar strain was not taken from the strain gage closest to the column base, but just above the lapped splice end of the reinforcement. Under deflection load control the reinforcement strains continued to increase. Figure 5-38 through Figure 5-44 show the strain at ductility level 6 displacements at different locations of the column.

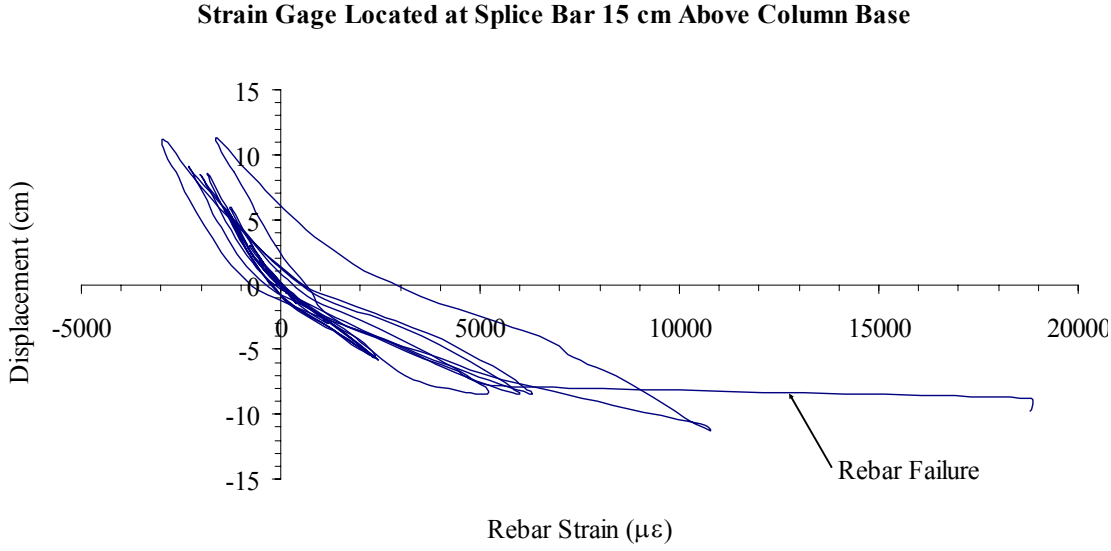

Figure 5-38: North Face 2 Reinforcement Test Strains at μ = 6.0

Strain Gage Located at Column Bar 15 cm Above Column Base

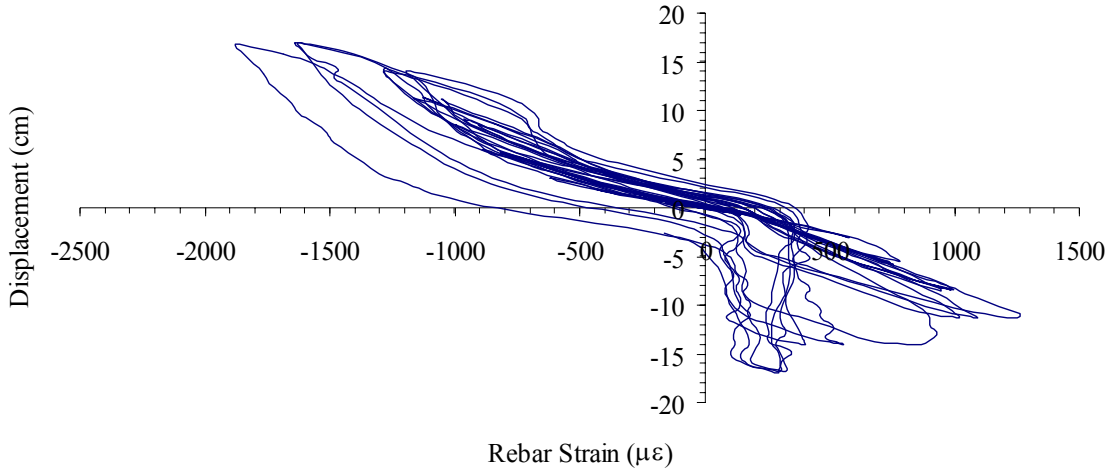

Figure 5-39: North Face 2 Reinforcement Test Strains at μ = 6.0

Strain Gage Located at Splice Bar 30 cm Above Column Base

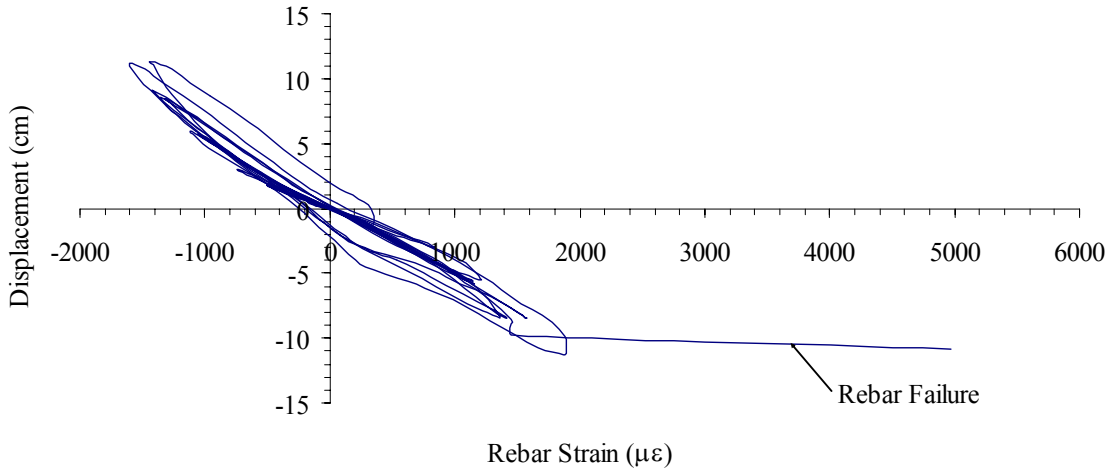

Figure 5-40: North Face 2 Reinforcement Test Strains at μ = 6.0

Strain Gage Located at Column Bar 30 cm Above Column Base

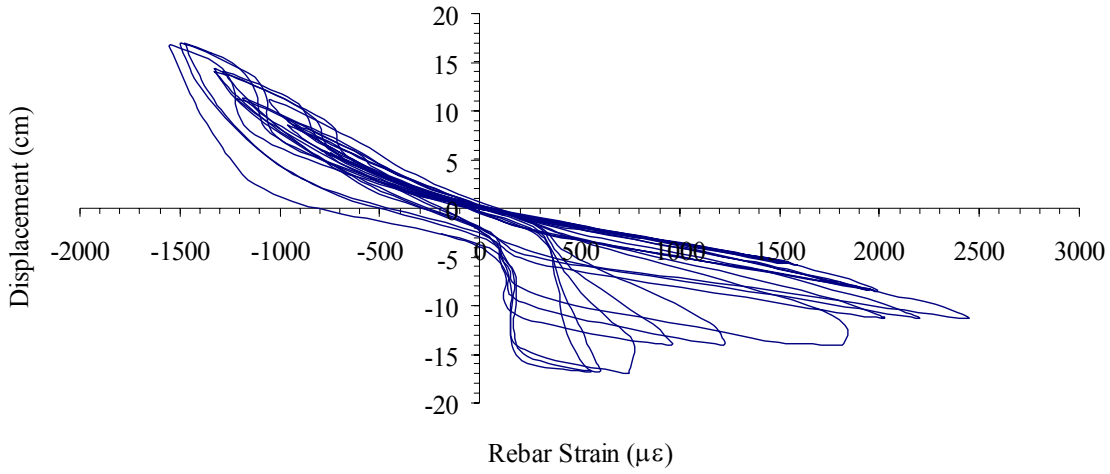

Figure 5-41: North Face 2 Reinforcement Test Strains at μ = 6.0

Strain Gage Located at Column Bar 61 cm Above Column Base

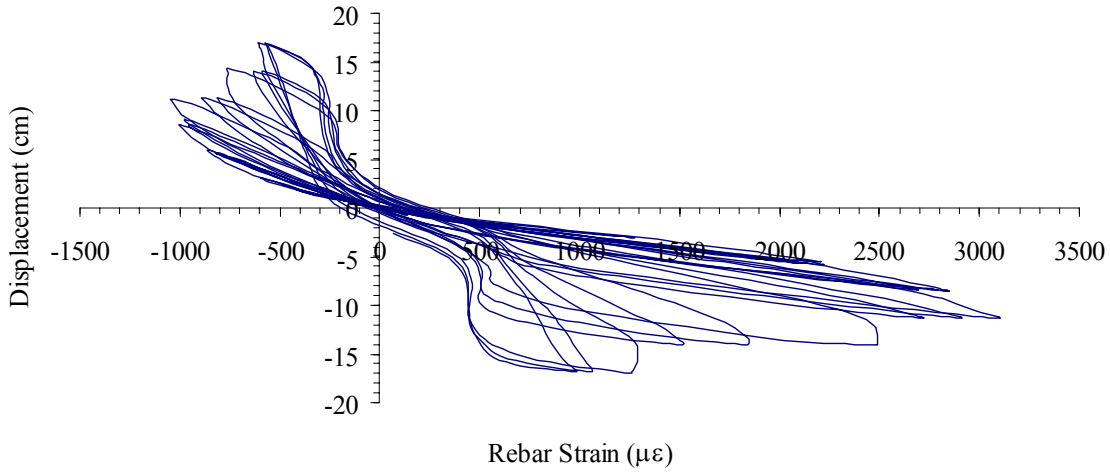

Figure 5-42: North Face 2 Reinforcement Test Strains at μ = 6.0

Strain Gage Located at Column Bar 91 cm Above Column Base

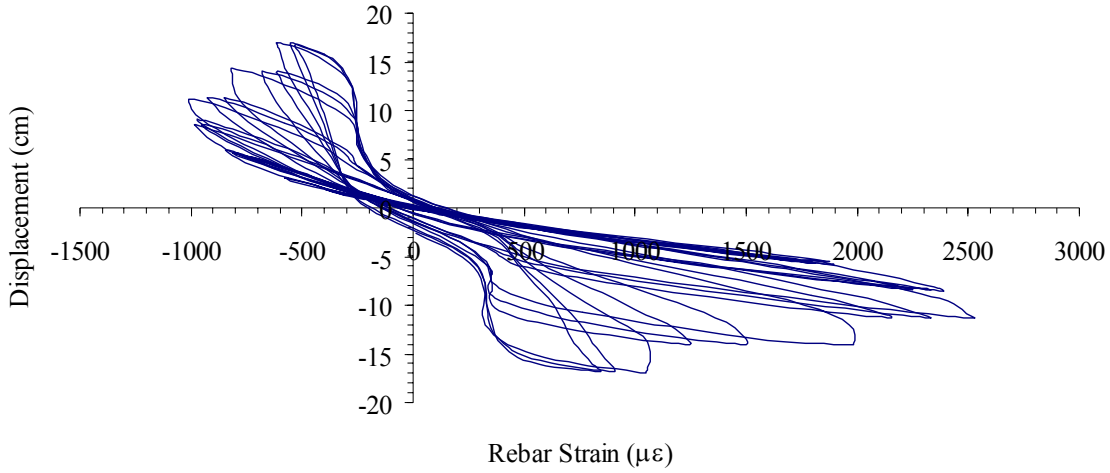

Figure 5-43: North Face 2 Reinforcement Test Strains at μ = 6.0

Strain Gage Located at Column Bar 122 cm Above Column Base

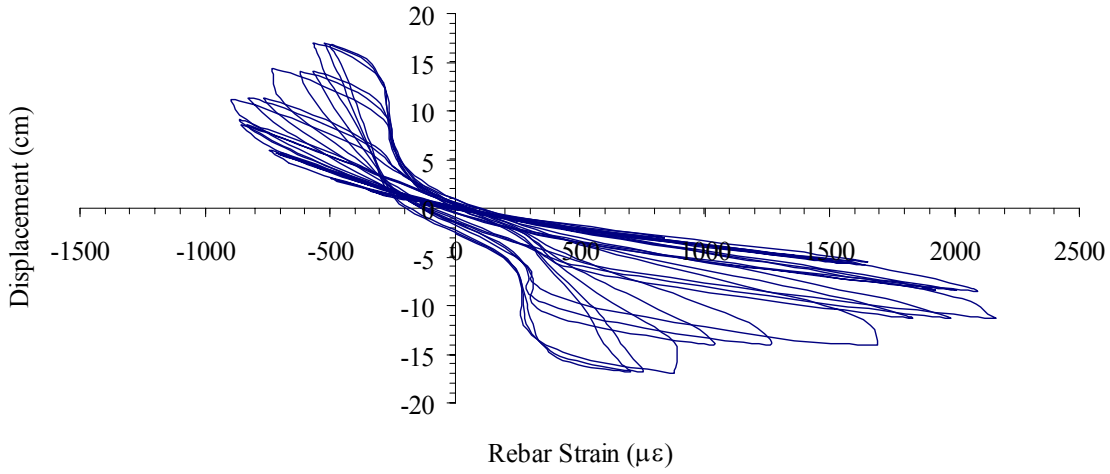

Figure 5-44: North Face 2 Reinforcement Test Strains at μ = 6.0

Under deflection load control the strengthening jacket exhibited minor flexure cracking in the plastic hinge regions (extending to a height of 73 cm from the bottom of the column) most

noticeably along the jacket seam at the base of the column, shown in Figure 5-45. This strengthening jacket fracturing was amplified by crushing of the jacket against the base as the column's reinforcement splice began failing causing the column to rise up off the concrete footing base. Under an 11.794 cm applied deflection at ductility Level 3, the column and base gap became more visibly pronounced as the column continued to further rise up off the footing base, illustrated in Figure 5-46.

Figure 5-45: Jacket Splitting at Seam

Figure 5-46: Jacketed Column Rising Up Creating Gap with Concrete Base

Column testing continued with increased displacement controlled loading to a 23.587 cm (9.287 in) calculated ductility level 6. Figure 5-47 shows the column during this deflection load control testing.

Figure 5-47: Lapped Reinforced Square Flexural Column during testing

After the first cycle at ductility Level 6 loading, a noticeable decrease in structural integrity was witnessed as the required load to displace the column the required 23.587 cm began to decline. The strain along the column jacket was reviewed to determine if softening of the column's load capacity was due to the failure of the column behind the strengthening jacket. Figure 5-38 and Figure 5-40 showed that the footing splice reinforcement bars in the column's lapped with the column reinforcement had failed by this point in testing. Figure 5-48 through Figure 5-51 show the deflection to strain relationship of the jacket at 15 cm from base of column under ductility 6.

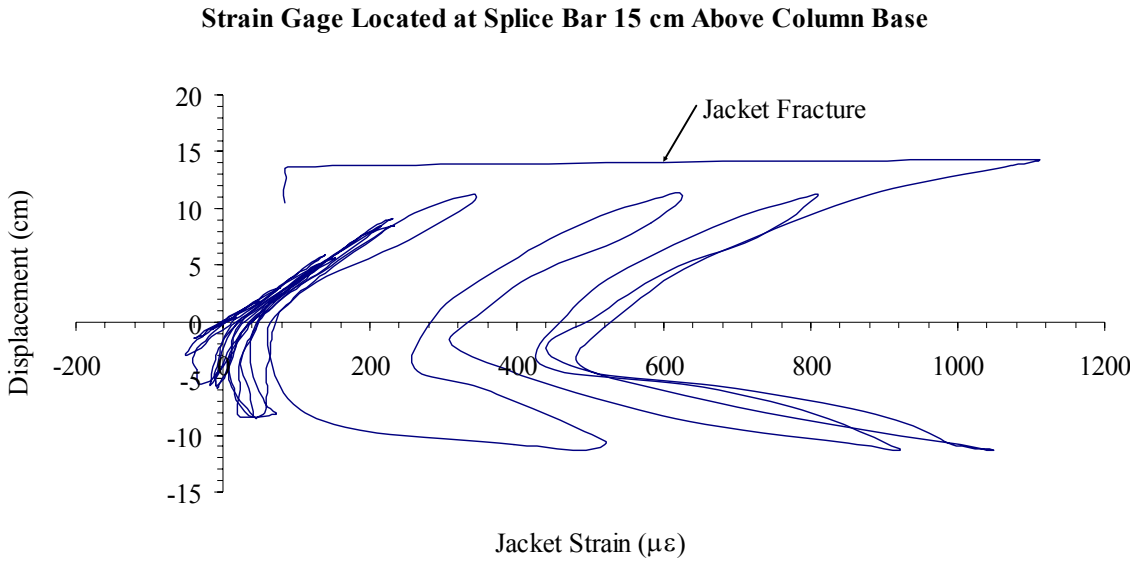

Figure 5-48: South Face Jacket Test Strains at μ = 6.0

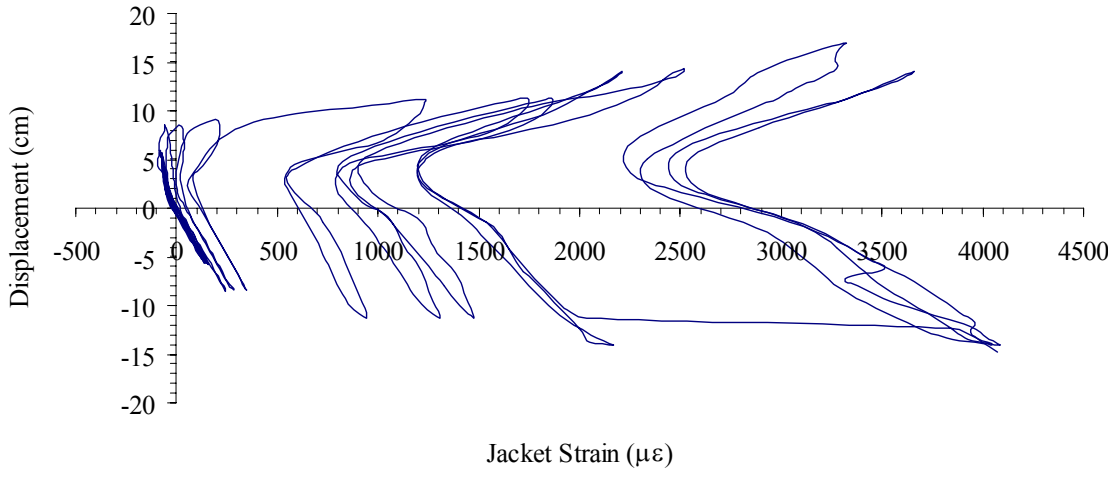

Figure 5-49: North Face Jacket Test Strains at μ = 6.0

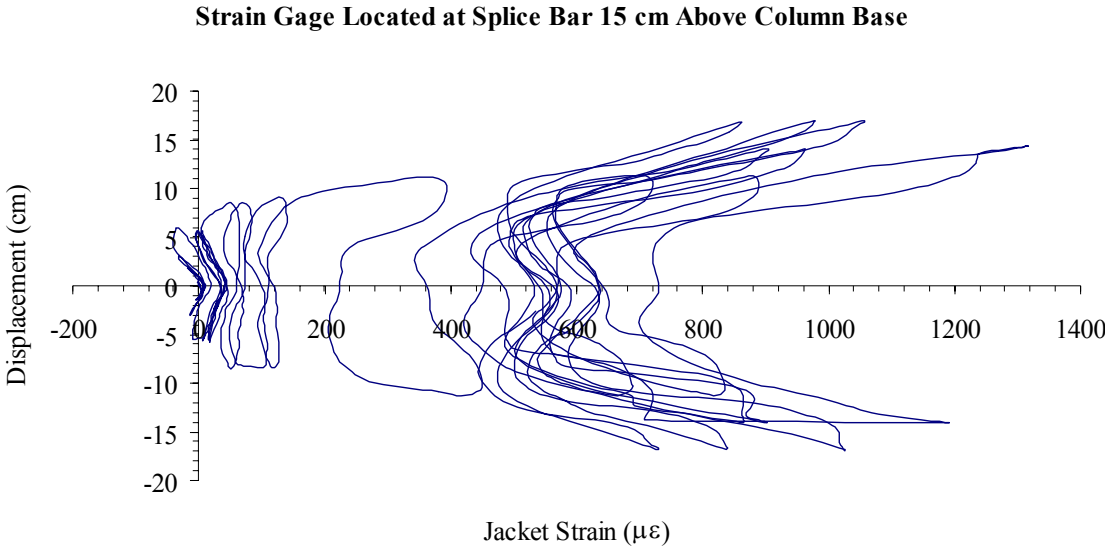

Figure 5-50: East Face Jacket Test Strains at μ = 6.0

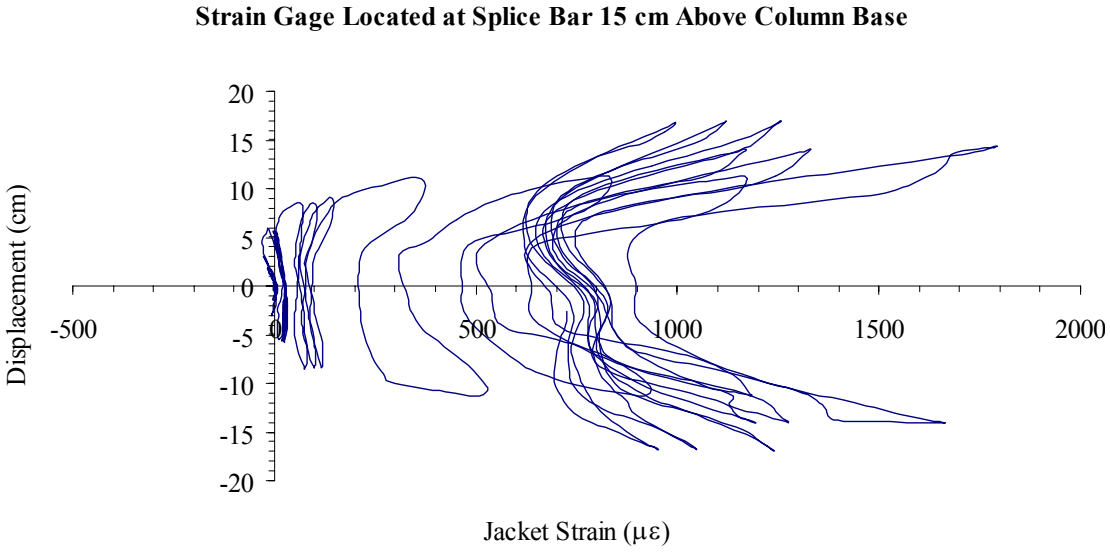

Figure 5-51: West Face Jacket Test Strains at μ = 6.0

5.4.2 Test Results

Stability under cyclic loading during the testing of the lapped reinforced square flexural column was measured to the displacement length of 16.94 cm (6.659 inches) with the column failure occurring with the 15% drop in load during the level 6 ductility cycle. A hysteresis plot of the square flexure column's applied load to the resulting column displacement is shown in Figure 5-52. This graph shows a stable push-pull response with the positive push data mirroring the negative pull data about the zero load and zero displacement axes. The area outlined within the data point of graph is smooth elliptical shape with no major jumps or drops during an induced cycle to indicate instability. The decrease in load carrying capacity from the maximum load achieved in level 5 was noticed during the ductility level 6 cycles and continued to further decrease with each additional ductility level.

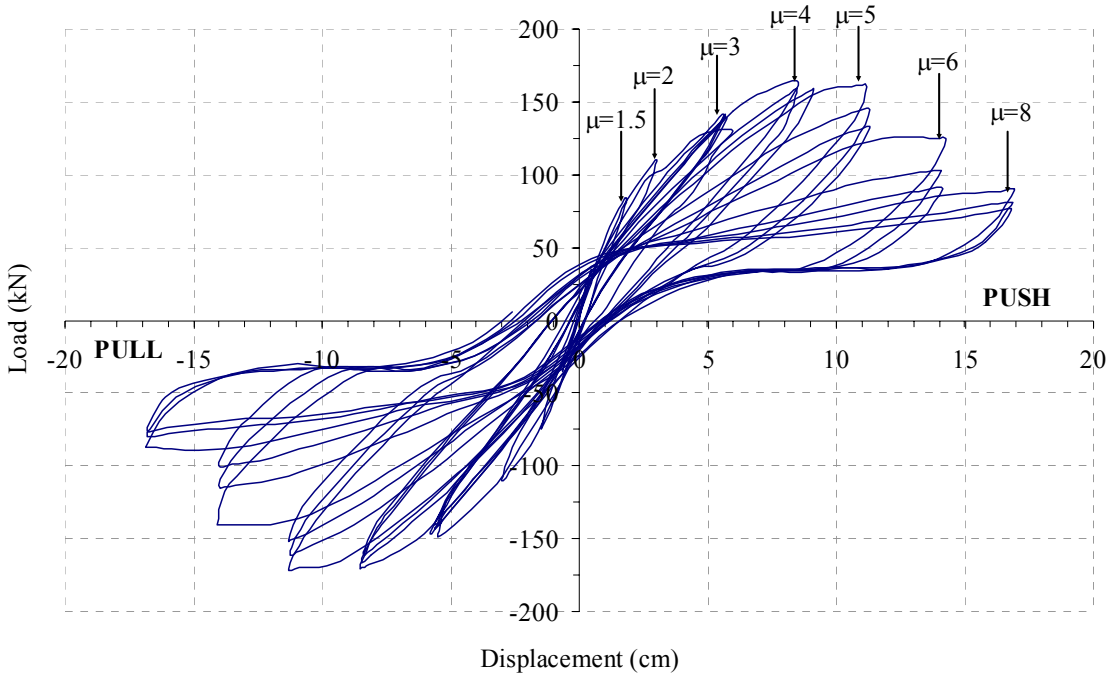

Figure 5-52: Flexure Column Load vs. Displacement Test Results

The test column's final retrofitted ductility calculation utilized the 16.94 cm measurement given that this was the displacement length the test specimen achieved during the last stable loading cycle. The following Table 5-8 lists the final results collected from the lapped reinforced square flexural column experiment used in the retrofit system analysis.

Table 5-8: Lapped Reinforced Square Flexural Column Final Test Results

Maximum Load	163.7 kN
Failure Initiation Load	139.1 kN
Maximum Displacement	16.94 cm

The results from the experiment for the square flexure column were compiled to establish the column's retrofitted ductilities: displacement and curvature. These values were then evaluated against the "as-built" ductilities in Table 5-7 to determine if the retrofitted column surpassed the baseline set by the HITEC guidelines. The retrofitted column failed at a forced displacement of 16.94 cm, as noted in Table 5-8, which results in a deflection ductility of μ_Δ = 4.31 and a curvature ductility of μ_ϕ= 7.13. These results listed in Table 5-9, show that the retrofitted ductility in displacement exceeded the criteria set by the HITEC protocol, but the curvature ductility did not meet or exceed the 2.0 fold increase.

Table 5-9: Lapped Reinforced Square Flexural Column Ductility Comparison

Ductility	"As-Built"	Retrofit	*Ductility Increase*
μ_Δ	2.56	4.31	*1.68*
μ_ϕ	3.88	7.13	*1.84*

With the minimal additional ductility provided by the retrofit jacket, the lapped reinforced square column in not pass the required specifications set by the HITEC protocol to qualify as an acceptable retrofit procedure. The tested column did deform elastically to the set

failure load but did not exceed the increased ductility requirements.

Improved performance and increased ductility would be expected from this system if the production of the jacket were adjusted to increase the gap from the footing base to the start of the jacket. Viewing the jacket strains at ductility level 6.0 in Figure 6-59 to Figure 6-62, it is apparent that the material did not reach its maximum strain capacity since the measurements are well below failure strains associated with a typical carbon/epoxy system.

Table 6-11 provides a summary of the all the peak strains at ductility levels associated with the testing.

Table 5-10: Peak Test Strains (με)

	Level 1.5	**Level 2.0**	**Level 3.0**	**Level 4.0**	**Level 5.0**	**Level 6.0**
Rebar	2456	2470	6310	FAIL	FAIL	FAIL
Jacket	591	580	704	1478	4081	1097

The column's steel reinforcement was stressed to failure while the jacket strains remained relatively minimal. With the jacket failure not due to material failure, the construction of the jacket is the failure mechanism of concern. Visibly, the splitting of the seam exacerbated by crushing against the concrete base was witnessed during testing and was the starting point for the jacket failure. Finding a better means of constructing the jacketing system to improve the performance would enhance the retrofit abilities of the system. If the early failure of the jacket was prevented, it is held that the system performance would be maximized.

6. Summary and Conclusion

Due to the life safety issues associated with aging, deficient or under-performing structures in need of retrofitting, the use of rehabilitation systems has become more common within the civil engineering practice. The use of fiber reinforced polymer (FRP) jackets for the purpose of seismic retrofit of columns has been shown to be an efficient option for rehabilitation in addition to numerous other strengthening options, such as base isolation procedures, steel jacketing systems, and the addition of an additional reinforcement cage through an encapsulating concrete jacket.

A proposed retrofitting method needs to be analyzed to determine if it will perform properly when utilized on a deficient structure. Performance is critical, since a strengthening system's main objective is to prevent catastrophic failures. The performance of any strengthening system is based on how it responds to the main aspects of retrofit design. Being aware of the existing column's structural weaknesses from studying past failures, the following issues become the main design concerns for a seismic retrofit: inadequate concrete confinement and lap splice length, insufficient shear strength, as well as lack of structural ductility.

As each of the column design requirements can be addressed within a strengthening system, an approach of addressing each of them using a composite jacket was also presented in Chapter 1. Due to the fact that a number of reviews have recently been published in literature, the information is not repeated herein.

Given design requirements, and information on the material available for constructing a strengthening system, a manner of testing a new system is required. Standardized testing procedures require that limits to be set on how the testing is conducted and a protocol was presented in Chapter 2 which included the requirements for the specimens that were tested, limits for performance as well as how these limits are defined and measured. Three testing protocol

were presented with the HITEC protocol procedure chosen for the experimental testing presented within this report.

Each of the (6) six tests columns were designed within the HITEC test protocol guidelines. Figure 2-5 through Figure 2-10 show the schematic for each of the test columns constructed, retrofitted and tested. The construction requirements, the column retrofit procedure and the theoretical column strengths and ductility calculation for the all test columns were also presented within the chapter. As each of the test columns were constructed, retrofitted and then tested, much data was collected and presented for each of the tests. This data was divided into three chapters with the circular and square shear columns testing and data presented in Chapter 3, the continuously reinforced circular and square columns provided in Chapter 4 and the lapped splice reinforced circular and shear column presented in Chapter 5.

The test results presented in Chapter 3 through Chapter 5 included observations made at the time of fabrication and testing and include results pertinent to ductility levels, hysteretic stability, strain levels and failure modes. The following discussion provides a comparison between the tests themselves, with existing data from similar tests with other composite jacketing systems and with steel jacketing systems.

6.1 Comparison of Experimental Test Results with HITEC Protocol Requirements

Each of the experimental shear tests for the circular and square columns showed increased ductility above theoretical as-built column as well as the pre-specified HITEC specification as presented in Chapter 3. Figure 6-1 shows the lateral load-displacement curves for both of these shear test columns and their as-built responses.

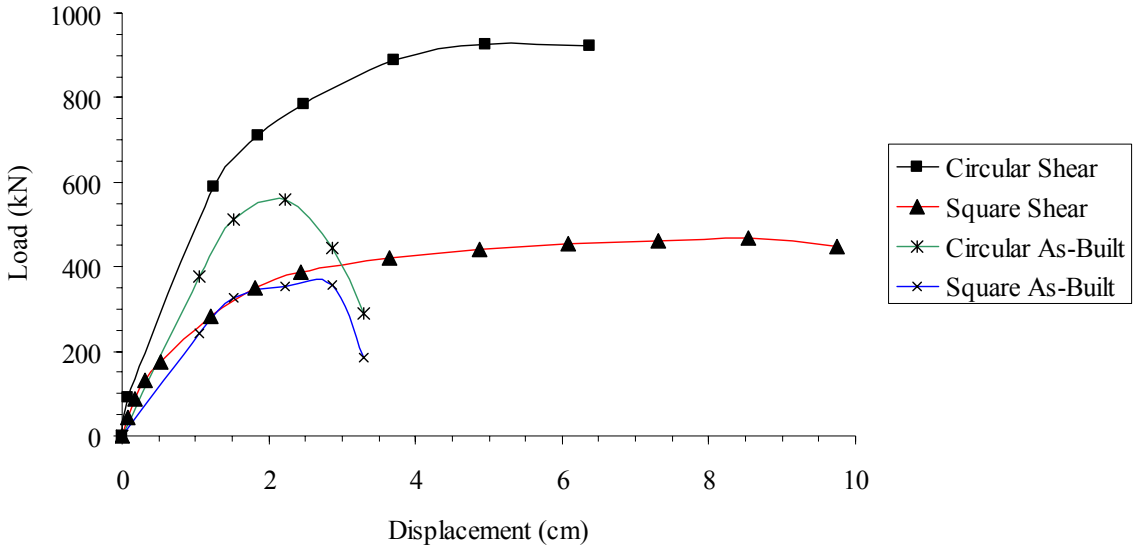

Figure 6-1: Comparison of Tested Shear Column Lateral Load-Displacement Curves

Each of the retrofitted shear columns performed beyond the requirements set under the HITEC testing protocol and Table 6-1 shows a comparison of test results with those of the theoretical values for the as-built column. This table shows a 191% increase in the circular column's ability to carry shear loading. The applied displacement of the circular column was also well beyond that of the hypothetical ultimate deflection of 2.59 cm by a factor of 2.81.

Table 6-1: Final Measurement Comparison for Shear Columns

Column Type	Maximum Load	Maximum Displacement
Circular Experimental	979 kN	7.28 cm
Circular Theoretical	511 kN	2.59 cm
Circular As-Built	560 kN	2.85 cm
Square Experimental	467 kN	9.71 cm
Square Theoretical	256 kN	4.16 cm
Square As-Built	358 kN	3.30 cm

The retrofitted square column showed a 182% increase in the column's ability to carry shear loading. The applied displacement of the square column was also well beyond that of the

hypothetical ultimate deflection of 4.16 cm by a factor of 2.33, emphasizing the enhancement of overall response through use of the novel jacketing system.

Table 6-2: Ductility Comparison for Shear Columns

Ductility Comparisons	Circular Shear		Square Shear	
	μ_Δ	μ_ϕ	μ_Δ	μ_ϕ
As-Built	2.58	3.92	2.62	4.00
Measured	7.24	12.56	6.42	11.04
Factor of Increase	2.81	3.20	2.45	2.76

Table 6-2 provides a summary of the increased ductility each of these columns as a result of the application of the composite jacket. It should be noted that the HITEC protocol requires a 2.0 increase in curvature ductility and a 1.5 times increase in displacement ductility. Each retrofitted column was able to surpass the HITEC criteria of the 2 fold increase in curvature and a 1.5 fold increase in displacement ductility.

Although each of the columns performed well in terms of increases in ductility, the circular shear column did not fail in the predicted failure mode. The circular shear column failed in a brittle manner, rather than in the ductile mode which was expected. It is noted that even with the increase in ductility, the composite jacket did not provide enough shear enhancement to change the as-built column's failure mode of shear failure to a ductile one. This mode of unexpected failure did not meet the final criterion of the HITEC protocol that a test specimen should fail in a pretest predicted failure mode [11], and can be linked to the lack of well prepared joints in the composite jacket sections.

When the retrofitted columns are compared to other composite jacketing systems, such as those in the ''The HITEC Evaluation Program for Composite Column Wrap Systems for Seismic Retrofit'' [11] there is a significant reduction in the ductility factor from the tested columns and those columns presented in the paper by D. Reynaud, V. M. Karbhari, and F. Seible. Table 6-3

provides a summary of the novel experimental jacketing system with the previously tested composite jackets presented in the paper.

Table 6-3: Comparison for Shear Columns with Other Composite Jacket Systems

Column Type	Maximum Displacement	Displacement Ductility Factor of Increase	Curvature Ductility Factor of Increase
Circular Experimental	*7.28 cm*	*2.8*	*3.2*
Circular Example 1	13.35 cm	3.9	7.2
Circular Example 2	10.64 cm	4.5	5.1
Square Experimental	*9.71 cm*	*2.5*	*2.8*
Square Example 1	11.44 cm	3.6	4.4
Square Example 2	10.97 cm	5.2	3.3

Comparing the experimental novel jacketing system with that of previously tested composite jacketing system, there is a difference in the factor of increased ductility. In a few cases the difference in increase is a magnitude of more than 2 fold as with the square Example 2 displacement ductility of 5.2 to the experimental square column with displacement ductility of 2.5.

The experimental jacketing system did behave similarly to other tested composite jackets such that their load displacement curves displayed a non-linear relationship to failure. When compared to the a steel jacketed column [4], as shown in Figure 6-2 and Figure 6-3, with its bilinear load to displacement relationship, the increase in load capabilities at the same displacement level is evident. Unlike the steel jacket which increases its load carry capability with each level of ductility, there is a visible decrease in the composite jacketing systems ability to carry the same or increased load at each ductility level once a maximum load is achieved. However, it is stressed that the load level is higher and failure is more gradual.

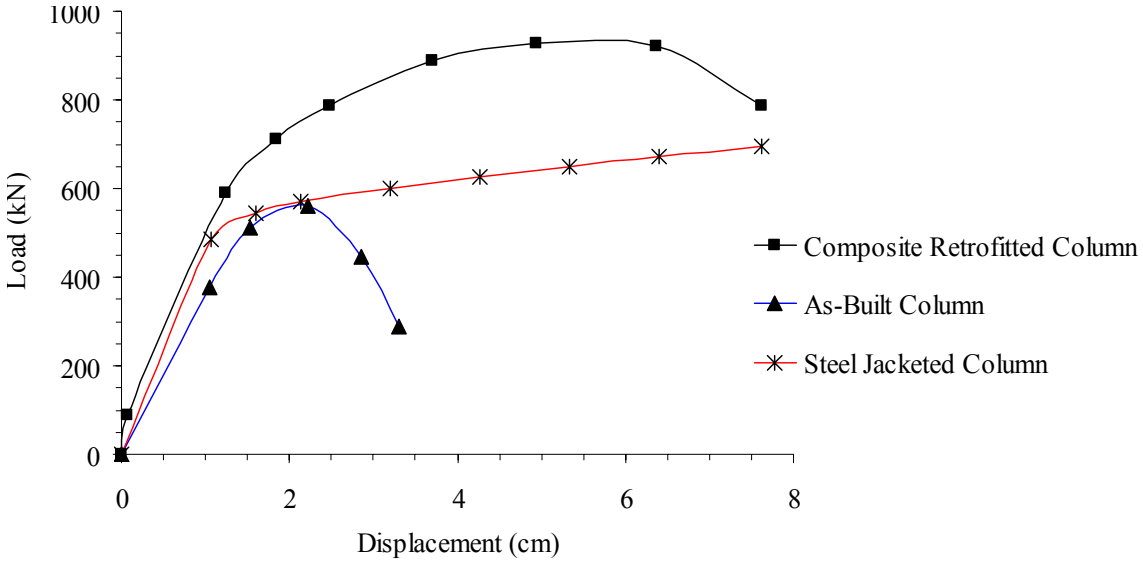

Figure 6-2: Comparison of Tested Circular Shear Column Lateral Load-Displacement Curves

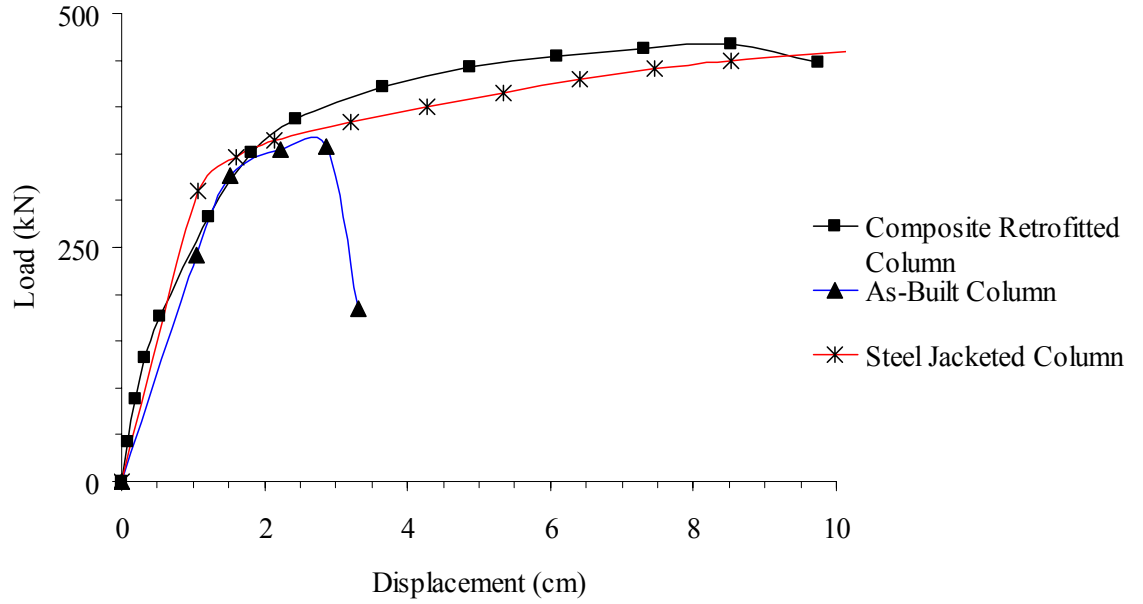

Figure 6-3: Comparison of Tested Square Shear Column Lateral Load-Displacement Curves

The review of the flexural columns was combined to compare how the lapped splice clamping pressure and concrete confinement reinforcement of the jacket compared side by side in

a circular and square column layout. Figure 6-4 is given to show how each of the flexure column's load-displacement curves compared with each other.

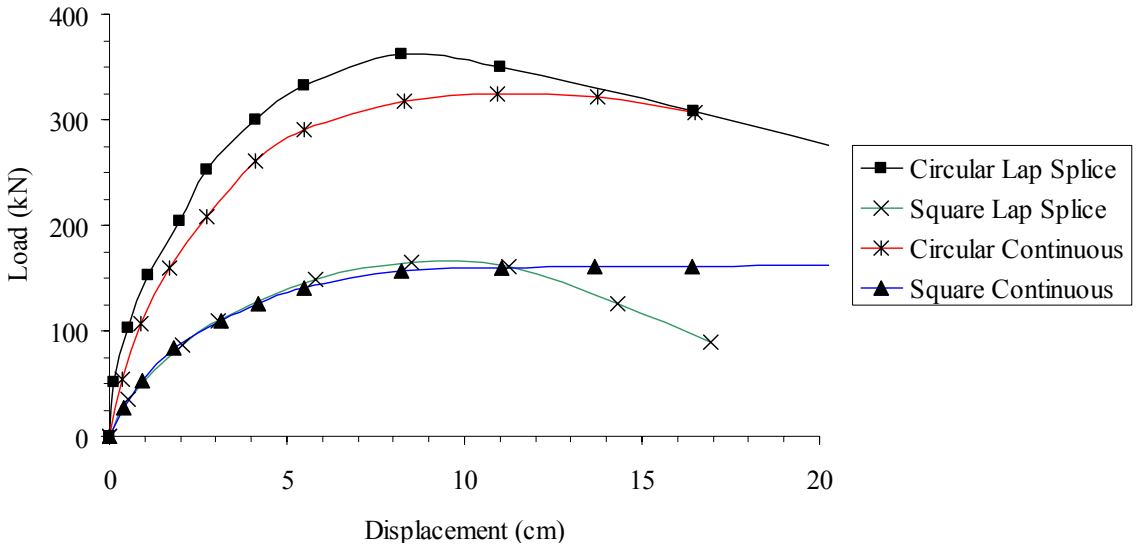

Figure 6-4: Comparison of Tested Flexural Column Lateral Load-Displacement Curves

Each of the circular columns performed similarly with the lap splice reinforced column reaching a higher maximum load before the clamping pressure of the column began to give way causing a quick decrease in load carrying ability. This difference in maximum load achieved by the retrofitted lap spliced reinforced column in comparison to the continuously reinforced column could be due to the differences in concrete strength, the quality of the composite jacketing system construction and/or the difference in the theoretical as-built ductilities. The counter-intuitive difference in load carrying abilities of the columns is most likely explained by jacket construction due to the lack of early jacket failure in the lap spliced reinforced column which the continuously reinforced column experienced.

Table 6-4: Final Measurement Comparison for Flexural Columns

Column Type	Maximum Experimental Load	Theoretical As-Built Load Capacity, V_i	Maximum Experimental Displacement	Theoretical As-Built Displacement
Continuous Circular	323 kN	307 kN	16.55 cm	5.56 cm
Continuous Square	162 kN	178 kN	21.93 cm	8.82 cm
Lap Spliced Circular	361 kN	347 kN	16.83 cm	5.89 cm
Lap Spliced Square	163 kN	197 kN	16.94 cm	10.11 cm

In Table 6-4 lists the final test loads and displacements for each of the flexural columns and shows a comparison of test results with those of the theoretical values for the as-built columns. As seen in Table 6-5, the lapped circular column as-built ductility was not greater than that of the continuous circular column. So even with greater final load and displacement values, the lapped circular column saw an 11% smaller ductility increase than compared to the continuously reinforced column. This shows the effect of each column's as-built ductilities on jacketing performance.

The square retrofitted columns also behaved similarly. The inability of the circular jacketing system on a square column to produce adequate lap splice clamping is evident in the early failure of the column when compared to the continuously reinforced column. This minimal clamping pressure produced by the jacket was expected, but the lower than needed level of ductility increase is problematic and would require additional evaluation if the jacketing system is to be used for a non-circular lap spliced reinforced column.

Table 6-5: Ductility Comparison for Flexural Columns

Ductility Comparisons	Continuous Circular		Lap Spliced Circular		Continuous Square		Lap Spliced Square	
	μ_Δ	μ_ϕ	μ_Δ	μ_ϕ	μ_Δ	μ_ϕ	μ_Δ	μ_ϕ
As-Built	2.39	3.58	2.62	4.00	2.22	3.25	2.56	3.88
Measured	7.13	12.35	6.42	11.04	5.51	9.35	4.31	7.13
Factor of Increase	2.98	3.45	2.45	2.76	2.48	2.88	1.68	***1.84***

Table 6-4 numerically shows that load and displacement values for each of the square columns were alike. There was less than a 1% difference in load from the lapped splice reinforcement to the continuously reinforced and 29% increase in applied displacement. These results would imply that the jacketing system was able to provide additional column confinement but not as much lap splice clamping pressure on the lapped square column. This is supported in previous research as well [41]. As seen in Table 6-5, as-built ductility of the lapped square column was an average 52% lower than that of the continuous circular column. The continuously reinforced square column was able to meet all aspects of the HITEC protocol criteria for a structurally sound retrofit system; however the lapped spliced reinforced column fell below the required curvature ductility requirement increase of a two-fold increase. The limited clamping pressure provided by the circular composite jacket on the square column was not enough to provide enough additional column ductility.

The experimental retrofitted flexural column data evaluated against previously tested composite jacketing systems showed that there is an analogous column performance relationship present for relating the retrofitted ductility factors of the flexural columns (in contrast to the retrofitted shear columns). Both of the experimental continuously reinforced and lapped reinforced retrofitted columns are compared to the existing test data of composite retrofitted columns in ‘‘The HITEC Evaluation Program for Composite Column Wrap Systems for Seismic Retrofit’’ paper [11] in Table 6-6.

Comparison of the experimental novel jacketing system of continuously reinforced column provided very similar ductility increase factors for both the circular and square columns. In fact, the experimental jacketing system had the same or better ductility increase factors as the existing composite retrofit systems. The experimental circular lap spliced retrofitted column performed better than other composite jacketing systems in displacement ductility but not in curvature ductility. This could be due to the crushing of the jacketing against the base of the

column, hampering the experimental columns range of motion but did not limit the allowable displacement at the top of column. Comparison of the experimental retrofitted square lap splice column to the existing composite jacket data showed that low curvature ductility is not comparable to existing composite systems. Each of the tested composite jackets averaged a 4.3 fold increase in curvature ductility compared to the 1.8 curvature ductility increase of the experimental jacketing system. The lower level of ductility of the experimental jacketing system would be critical if choosing a retrofit system for providing a higher level of ductility capacity.

Table 6-6: Comparison for Flexure Columns with Other Composite Jacket Systems

Flexural Column Type	Maximum Displacement	Displacement Ductility Factor of Increase	Curvature Ductility Factor of Increase
Circular Continuously Experimental	*16.55 cm*	*2.9*	*3.5*
Circular Example 1	39.03 cm	2.4	4.6
Square Continuous Experimental	*16.83 cm*	*2.5*	*2.9*
Square Example 1	16.76 cm	2.0	1.8
Square Example 2	21.34 cm	2.5	2.3
Circular Lapped Experimental	*21.93 cm*	*2.5*	*2.8*
Circular Example 1	9.05 cm	1.4	6.0
Circular Example 2	24.77 cm	2.2	5.1
Square Lapped Experimental	*16.94 cm*	*1.7*	*1.8*
Square Example 1	19.63 cm	2.4	8.7
Square Example 2	15.44 cm	1.9	6.8

The experimental jacketing system did behave similarly to other tested composite jackets such that their load displacement curves displayed a non-linear relationship to failure. When compared to the a steel jacketed column [4], as shown in Figure 6-5 and Figure 6-6, with its linear load to displacement relationship, the increase in load capabilities at the same displacement level is evident. Unlike the steel jacket which increases its load carry capability with each level of

ductility, there is a visible decrease in the composite jacketing system ability to carry the same or increased load at each ductility level once a maximum load is achieved.

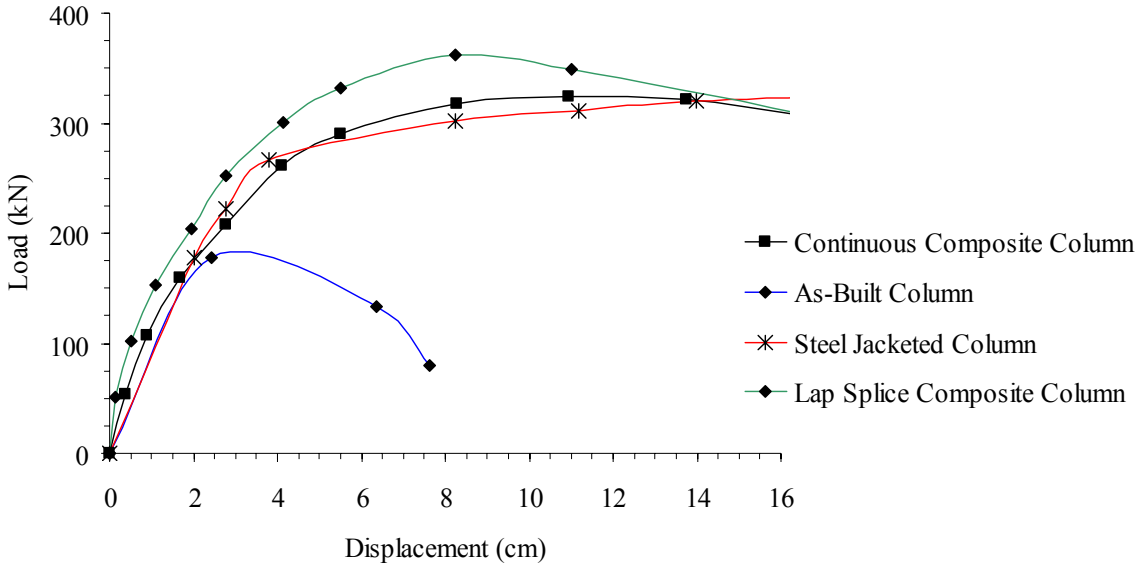

Figure 6-5: Comparison of Tested Circular Flexural Columns Lateral Load-Displacement Curves

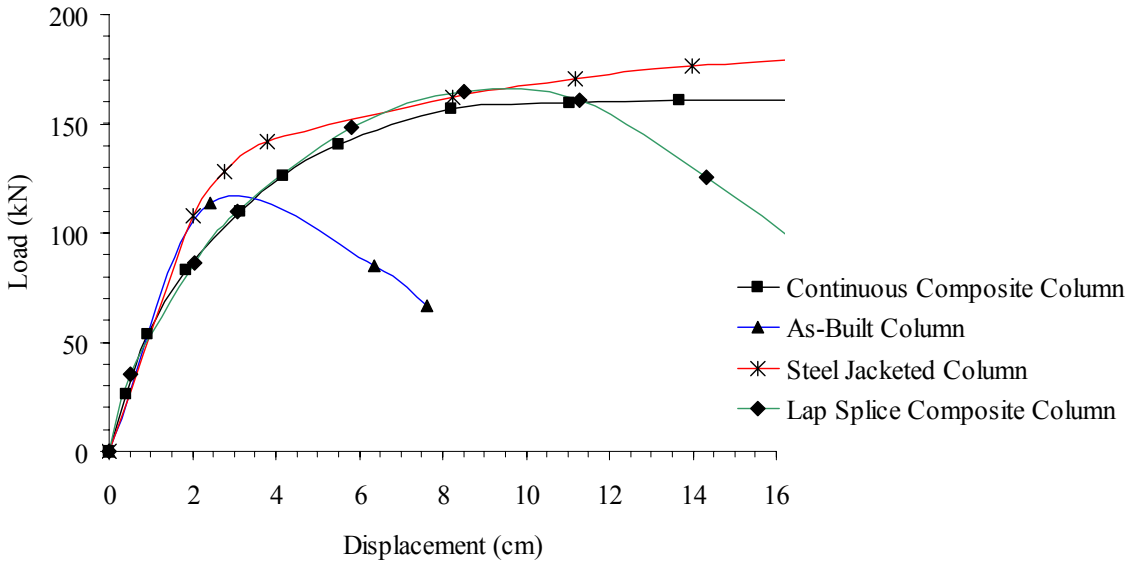

Figure 6-6: Comparison of Tested Square Flexural Column Lateral Load-Displacement Curves

The steel jacket data correlates with the lateral load displacement curves of the square columns more than the composite retrofitted circular columns. This is seen with the grouping of the retrofitting columns until ductility level 4 where each of the curves begins to disperse. This also can allow for the interpretation that the experimental jacketing system can provide the similar level of retrofit ability as that of a steel jacketing system.

The matrix in Table 6-5 is given to clarify which of the HITEC criteria each test column passed. Both of the continuously reinforced columns, circular and square, passed all the requirements set in the protocol as did the square shear column. The circular shear column did not pass the predicted failure mode criterion and the square lapped spliced reinforced column did not meet the established curvature ductility enhance factor criterion.

Table 6-7: HITEC Criteria for Retrofit Strengthening System [11]

Column Type	1.5 μ_Δ Increase	2.0 μ_ϕ Increase	Predicted Failure Mode	Exceeded Design Displacement
Circular Shear	X	X		X
Square Shear	X	X	X	X
Circular Continuous	X	X	X	X
Circular Lapped	X	X	X	X
Square Continuous	X	X	X	X
Square Lapped	X		X	X

6.2 Strengths of the Proposed Composite Jacketing System

As a new and novel strengthening jacket system, the performance represented through testing of the (6) six retrofitted concrete columns showed that the new retrofit procedure has potential as a viable option. The following aspects may be advantageous in comparison with other existing systems:

- The use of a sandwich structure comprising of in-situ formed high performance foam may in some cases result in decreased cost due to the need for less carbon fabric layers. The economics, though, were not assessed in this study.
- The use of an expansive foam results in a higher degree of compaction of fabric and hence higher efficiency of use.
- The ability for closed processing may offer advantages related to clean-up, quality control and environmental aspects of resin use.
- Minimal equipment is needed for installation beyond the use of a portable mold, mixing & measuring equipment.
- Quick installation. A column can be wrapped and cured within a 24 hour period thereby decreasing disruption time to a minimum.

6.3 Weaknesses of the Proposed Composite Jacketing System

While there appear to be a number of potential advantages, improvements also need to be made to the proposed jacketing system in order to enable more reliable performance, as below:

- Application of the inner carbon jacket to the concrete column may benefit from the preparation of the concrete prior to lay-up. Power-washing of the concrete has been noted in prior research as a mechanism of roughening the substrate to enhance the bonding of the composite material with the concrete.
- Improvement of the installation process by means of creating a jacketing mold that is easier and lighter to handle and maneuver. The heavy steel jacket mold was tricky to place on the column and required the use of an overhead crane to lift in place. For field use this need for a crane is an additional expense in comparison to other composite strengthening jacket systems. However, the use of a rigid composite or sheet steel mold or even a rigid polymer mold, would work just as well.

- Improvement of the jacket construction to enhance the performance of the jacket seams. This was the location on the jackets where the first signs of failure began on each of the columns except for the square lapped splice specimen.
- Increasing the gap at the bottom of each jacket. The jackets on each of the columns showed initiation of crushing at the lower ends under the cyclic loading. All the columns demonstrated audible noises associated with cracking of foam and the composite under force loading as the jacket began crushing against the column footing base.

6.4 Conclusions

With the completion of testing of each of the six retrofitted column and analyzing applicability of the experimental composite sandwich panel jacketing system for use as a retrofit option, the proposed jacketing system was found to have provided increased ductility on each of the six columns tested. All of the columns, with the exception of the square lapped reinforced column, would provide a structurally sound retrofit option. The square lap spliced reinforced column jacket, due to the sub-par curvature ductility increase, should be re-evaluated before being used on existing as-built columns constructed with lapped splice reinforcement.

In conclusion, the proposed composite jacketing system was found to be a possible retrofit choice in lieu of the multiple layered composite jacketing systems or steel jacketing. Understanding the extent of public and private structures in danger of failure with a strong seismic event, economical means to provided retrofit system is critical. The experimental jacketing system has the capabilities required to offer a cost effective solution. The unique in-situ application was found to be a novel approach to forming a composite sandwich panel outside of a manufacturing setting. The problematic overlapping of the panel seams during construction created a drawback to the application and performance.

Improving the construction of the jacketing system opens the opportunity to further refine and advance the performance capabilities of the system. Looking at alternative mean of jacket construction, such as a stay in place mold or providing a means to stitch the fabric seams together, offer additional avenues for improving the system to provide a consistent means of increased ductility performance. Analysis as to whether the location of the retrofit jacket seams on the column effect the ductility performance may provide additional potential area of study.

References

1. Merriam Webster Website, 2005. www.merriam-webster.com/dictionary/retrofit

2. P.C. Jennings, (editor), *Engineering Features of the San Fernando Earthquake of February 9, 1971*, California Institute of Technology Report EERL 71-02, 1971.

3. Federal Highway Administration website, 2004 http://www.fhwa.dot.gov/bridge/

4. M.J.N. Priestley, F Seible, G.M. Calvi, *Seismic Design and Retrofit of Bridges*. 1996, New York: John Wiley & Sons, Inc.

5. KOERI website, 2006 of the May 01, 2003 Bingol, Turkey Earthquake http://www.koeri.boun.edu.tr/depremmuh/eqspecials/bingol/bingol_eq.htm

6. M.A. Haroun, M. Feng, H. Bhatia, K. Baird, H. Elsanadedy, *Structural Qualification Testing of Composite-Jacketed Circular and Rectangular Bridge Columns* - Report No. RTA-59A0005. University of California, Irvine: October 1999.

7. Federal Emergency Management Agency (FEMA). (1997) "NEHRP Guidelines for Seismic Rehabilitation of Buildings", FEMA Publication 273, Washington D.C.

8. U.S. Geological Survey Website, 2008. http://gldims.cr.usgs.gov/nshmp2008/viewer.htm

9. F. Seible, G. Hegemier, M.J.N. Priestley, D. Innamorato, *Seismic Retrofit of RC Columns with Continuous Carbon Fiber Jackets,* Journal of Composites for Construction. May 1997: 52-62.

10. Y.H. Chai, M.J.N. Priestley, and F. Seible, *Seismic Retrofit of Circular Bridge Columns for Enhanced Flexural Performance,* ACI Structural Journal. Volume 88: No 5, pp 484-572.

11. D. Reynaud, V.M. Karbhari, and F. Seible, (1999) "The HITEC evaluation program for composite wrap systems for seismic retrofit" *Proc., Int. Composites Exposition,* Composites Institute, Washington D.C., 4A/1-6.

12. M.J.N. Priestley, F Seible, G.M. Calvi, *Seismic Design and Retrofit of Bridges*. 1996, New York: John Wiley & Sons, Inc.

13. D. Innamorato, V.M. Karbhari, *FRP Composite Wrap Durability Evaluation: Volume 2- Structural Test Results Summary* - Report No. TR-2001/11. University of California, San Diego: La Jolla, April 2002.

14. C. Pantelides., J. Gergely, L. Reaveley, V. Volnyy, *Retrofit of RC Bridge Pier with CFRP Advanced Composites,* Journal of Structural Engineering. October 1999: 1094-1099.

15. C. Pantelides, J. Gergely, *Carbon Fiber Reinforced Polymer Seismic Retrofit of RC Bridge Bent: Design and In Situ Validation*, Journal of Composites for Construction. February 2002: 52-60.

16. J.G. Teng, L. Lam, *Behavior and Modeling of Fiber reinforced Polymer-Confined Concrete,* Journal of Structural Engineering. November 2004: 1713-1723.

17. California Department of Transportation Website, 2004 http://www.dot.ca.gov/hq/LocalPrograms/lam/prog_g/g07seism.pdf

18. California Department of Transportation Website, 2006 http://www.dot.ca.gov/baybridge/1Q2006Reportv09.pdf

19. Applied Technology Council (ATC). (1996) "The Seismic Evaluation and Retrofit of Concrete Building", ATC Rep. 40, Redwood City, California.

20. K. Kawashima, *Seismic Retrofit Design and Retrofit of Bridges,* Tokyo Institute of Technology, 2004. http://seismic.civ.titech.ac.jp

21. Federation Internationale du Beton (FIB). (2001) "Management, maintenance, and strengthening of concrete structures" Technical Rep., Bulletin No 17, Lausanne, Switzerland.

22. Canadian Standards Association (CSA). (2006) CAN/CSA-S6-06 Canadian Highway Bridge Design Code, Ontario, Canada.

23. J. Kelly, *Base Isolation: Origins and Development,* EERI News. Volume 12: No 1, January 1991, pp 2.

24. DIS, Inc. website, 2006. http://www.dis-inc.com

25. San Francisco Exploratorium Center Website, 2005. www.exploratorium.edu/faultline/engineering/retrofit.html

26. FIB – TG 7.4 Committee for Seismic Design and Assessment of Procedures for Bridges, "Structural Solutions for Bridge Seismic Design and Retrofit – Chapter 11", 2006. http://seismic.civ.titech.ac.jp/committee/FIB/PDF/5-Chapter11.pdf

27. Wikipedia, Online Encyclopedia, 2004. http://en.wikipedia.org/wiki/Seismic_retrofit

28. G. Hegemier, FRP in Civil Structures - Course Notes, 2004.

29. Y. Chhabra, *Bridge Rehabilitation Techniques,* Master Builder Feb 2004, pp 10-12.

30. Caltrans Memorandum to Designers 20-4. Attachment B: Composite Column Casing and Standard Specification, I.48-AENC.DOC, California Department of Transportation; 1996.

31. American Concrete Institute (ACI). (2008) "Guide for the design and construction of externally bonded FRP system for strengthening concrete structures", *ACI Committee 440 Rep.*, Detroit.

32. A. Kaw, *Mechanics of Composite Materials*. 1997, Boca Raton, Florida: CRC Press LLC

33. Y. Xiao, R. Ma, *Seismic Retrofit of RC Circular Columns Using Prefabricated Composite Jacketing,* Journal of Structural Engineering. October 1997: 1357-1364.

34. Y. Xiao, H. Wu, G.R. Martin, *Prefabricated Composite Jacketing of RC Columns for Enhanced Shear Strength,* Journal of Structural Engineering. March 1999: 255-264.

35. J.S. Zhang, V.M. Karbhari, L. Wu, D. Reynaud, *Field exposure based durability assessment of FRP column wrap systems,* Composites Part B: Engineering. Volume 34, Issue 1, January 2003, pp 41-50.

36. M.K. Thompson, J.O. Jirsa, J.E. Breen, R.E. Klingner, *Anchorage Behavior of Headed Reinforcement* - Research Report 1855-1. University of Texas, Austin, May 2002.

37. National Geophysical Data Center Website, 2004. http://www.ngdc.noaa.gov

38. R. Englekirk, *Seismic Deisgn of reinforced and Precast Concrete Buildings.* 2003, New Jersey: John Wiley & Sons, Inc.

39. ACI Committee 318, *ACI 318-05: Building Code Requirements for Structural Concrete*. 2005, Michigan: American Concrete Institute

40. D. Val, Reliability of Fiber-Reinforced Polymer-Confined Reinforced Concrete Columns, Journal of Structural Engineering. August 2003: 1122-1130.

41. M.A. Haroun, H.M. Elsanadedy, *Fiber-reinforced Plastic Jackets for Ductility Enhancement of Reinforced Concrete Bridge Columns with Poor Lap Splice Detailing,* Journal of Bridge Engineering. November/December 2005: 749-757.

42. ACI 440 Committee, *Guide for the Design and Construction of Externally Bonded FRP Systems for Strengthening Concrete Structures*. ACI 440, Michigan: American Concrete Institute

43. M.N. Fardis, H.H. Khalili, (1982) *FRP Encased Concrete as a Structural Material,* Magazine of Concrete Research, 34 (121), 191-202.

44. D. Cusson, P. Paultre, (1995) *Stress-strain Model for Confined High Strength Concrete*, Journal of Structural Engineering. 121 (3), 468-477.

45. V.M. Karbhari, Y. Gao, Composite Jacketed Concrete Under Uniaxial Compression-Verification of Simple Design Equations, Journal of Materials in Civil Engineering. November 1997, 468-477.

46. AC125, *Interim Criteria for Concrete and Reinforced and Un-Reinforced Masonry Strengthening Using Fiber-Reinforced (FRP) Composite Systems,* ICC Evaluation Service, Inc, June 2007.